

UC Riverside

UC Riverside Electronic Theses and Dissertations

Title

Emissions and Their Implications From Heavy-Duty Diesel Vehicles and Marine Engines

Permalink

<https://escholarship.org/uc/item/4fj6h1v7>

Author

Jiang, Yu

Publication Date

2018

Copyright Information

This work is made available under the terms of a Creative Commons Attribution License, available at <https://creativecommons.org/licenses/by/4.0/>

Peer reviewed|Thesis/dissertation

UNIVERSITY OF CALIFORNIA
RIVERSIDE

Emissions and Their Implications From Heavy-Duty Diesel Vehicles and Marine Engines

A Dissertation submitted in partial satisfaction
of the requirements for the degree of

Doctor of Philosophy

in

Chemical and Environmental Engineering

by

Yu Jiang

June 2018

Dissertation Committee:

Dr. David R. Cocker III, Chairperson

Dr. Kent C. Johnson

Dr. Tom D. Durbin

Dr. Kelley Barsanti

Copyright by
Yu Jiang
2018

The Dissertation of Yu Jiang is approved:

Committee Chairperson

University of California, Riverside

Acknowledgements

I would like to thank many individuals for making this dissertation possible. I would like to thank my advisor Dr. David R. Cocker for his endless support throughout the PhD program. I also appreciate Dr. Cocker for inviting me to the thanksgiving dinner at his home for the last couple years. I would like to thank Dr. Kent Johnson for giving me opportunity to join the emission and fuel research group and training me throughout my PhD program. I would like to thank Dr. Tom Durbin for his invaluable advice and providing me opportunities to work on a wide array of projects for making this dissertation possible. I would like to thank Dr. Kelley Barsanti for her guidance during my PhD program. I would like to thank Dr. Wayne Miller for all of his advice and help with several projects. I would like to thank Dr. Georgios Karavalakis and Dr. Heejung Jung for their guidance.

I would also like to thank Mr. Don Pacocha for his continued help and support with the entire emissions field testing. I am also very grateful to Mr. Edward O'Neil, Mr. Mark Villela, Mr. Daniel Gomez, Ms. Lauren Aycock, Mr. Daniel Sandez, Mr. Kurt Bumiller and Mr. Joe Valdez for their help with all of the field study test.

I thank Jiacheng Yang and Dr. Weihua Li as my best friends for all of their help and support. I would also like to thank former and current graduate students, Dr. Tanfeng Cao, Dr. Poornima Dixit, Dr. Nick Gysel, Dr. Emmanuel Fofie, Dr. Chia-Li Chen, Dr. Mary Kacarab, Dr. Chengguo Li, Paul Van Rooy, Yue Lin, Cavan McCaffery, Jinwei Zhang and Hanwei Zhu all of the undergraduate students for all of their help.

I would like to recognize the funding sources including Engine Manufacturers Association (EMA), California Air Resources Board (CARB) and International Council on Clean Transportation (ICCT) for the projects that made this dissertation possible.

The text of Chapter 2 of this dissertation, in part or in full, is reprinted from Science of The Total Environment, Volume 619; Yu Jiang, Jiacheng Yang, David Cocker, Georgios Karavalakis, Kent C Johnson, Thomas D Durbin; Characterizing emission rates of regulated pollutants from model year 2012+ heavy-duty diesel vehicles equipped with DPF and SCR systems, Pages 765-771, Copyright (2018), with permission from Elsevier. The text of Chapter 5 of this dissertation, in part or in full, is reprinted from Atmospheric Environment, Volume 182; u Jiang, Jiacheng Yang, Stéphanie Gagné, Tak W Chan, Kevin Thomson, Emmanuel Fofie, Robert A Cary, Dan Rutherford, Bryan Comer, Jacob Swanson, Yue Lin, Paul Van Rooy, Akua Asa-Awuku, Heejung Jung, Kelley Barsanti, Georgios Karavalakis, David Cocker, Thomas D Durbin, J Wayne Miller, Kent C Johnson; Sources of variance in BC mass measurements from a small marine engine: Influence of the instruments, fuels and loads, Pages 128-137, Copyright (2018), with permission from Elsevier.

Dedication

I dedicate this work to my parents Renfang Jiang and Yulian Sun, for their love, encouragement, and support all through my life.

ABSTRACT OF THE DISSERTATION

Emissions and Their Implications From Heavy-Duty Diesel Vehicles and Marine Engines

by

Yu Jiang

Doctor of Philosophy, Graduate Program in Chemical and Environmental Engineering
University of California, Riverside, June 2018
Dr. David R. Cocker III, Chairperson

This dissertation evaluated emissions from heavy-duty diesel vehicles (HDDVs) and marine engines under a variety of different conditions. This dissertation characterizes the NO_x emissions of five 2010 and newer, low-mileage, HDDVs equipped with diesel particulate filters (DPFs) and selective catalytic reduction (SCR) systems were evaluated over test cycles representing urban, highway, and stop-and-go driving on a chassis dynamometer. This information can be used to develop “zero mile” emission rates (ZMRs) for emissions inventory modes.

It is important to investigate and understand the differences between certification and in-use emission rates and to understand the factors contributing to these differences and discrepancies. This dissertation evaluated two 2010-compliant HDDVs using an engine-dynamometer, a chassis-dynamometer, and on-road. The results showed that in-use NO_x emissions over urban driving cycles of chassis dynamometer, on-road testing and

engine dynamometer tests were above the 0.2 g/bhp-hr certification level for both vehicles, with higher emissions for the on-road and chassis dynamometer testing. The differences between the tailpipe NO_x emissions could be attributed to several factors, including differences in SCR inlet temperatures and engine out NO_x emissions. The SCR efficiencies were found to be impacted by the SCR inlet temperature. The SCR efficiencies were as a function of load, especially for the manufacturers B truck. The Not to Exceed (NTE) analysis shows that the NTE method has the limitation that it represents only a small percent of real-world operation.

The implementation of an enhanced heavy-duty (HD) Inspection and Maintenance (I/M) program could be a critical element in ensuring the emissions performance of HDDVs over their full useful life. A prototype HD I/M pilot study was conducted where the emissions of 47 vehicles were measured before and after repair. The vehicles showed good reductions post-repair for NO_x for some of the higher emitting vehicles, but not significant PM reductions. Based on a review of the potential methods, a comprehensive HD I/M program was proposed with OBD as the primary methodology, remote sensing for validation testing, and mini-PEMS for dispute resolution.

It is important to understand black carbon (BC) emission factors from ships from human health and environmental perspectives. A study of instruments measuring BC and fuels typically used in marine operation was carried out on a small marine engine with and without a sampling condition (SC) system. Six analytical methods measured the BC emissions in the exhaust of the marine engine operated at two load points while burning three fuels. The results showed that both higher engine loads and higher sulfur fuels

contributed to higher BC emission factors with engine load having the biggest impact on BC emissions. There was a spread of about a factor of two in the BC emissions measured by the 6 different methods. The SC system improved the comparability of some BC measurements, but only slightly.

Table of Contents

1. Introduction.....	1
1.1. Testing Methodologies for Heavy-Duty and Marine Diesel Engines	5
1.2. Studies of Model Year 2010 and Newer Heavy-Duty Diesel Vehicles	7
1.3. Issues of Current Testing Methodologies for Heavy-Duty and Marine Diesel Engines.....	9
1.4. California Heavy-duty On-Road Vehicle Inspection and Maintenance.....	10
1.5. Black Carbon Emissions	11
1.6. Outline of Dissertation	12
1.7. References	15
2. Characterizing Emission Rates of Regulated Pollutants from Model Year 2012+ Heavy-Duty Diesel Vehicles Equipped with DPF and SCR Systems	20
2.1. Abstract	20
2.2. Introduction	21
2.3. Materials and Methods	24
2.3.1. Test Vehicles and Fuels	24
2.3.2. Test Cycles.....	25
2.3.3. Emission Measurements	26
2.4. Results and Discussion.....	27

2.4.1.	NO _x Emissions	27
2.4.1.1.	NO _x emission rates	27
2.4.1.2.	SCR temperature.....	34
2.4.2.	Other Regulated Pollutants	37
2.4.2.1.	PM mass	37
2.4.2.2.	THC emissions	37
2.4.2.3.	CO emissions	38
2.4.3.	CO ₂ Emissions and Fuel Economy	38
2.4.3.1.	CO ₂ emissions.....	38
2.4.3.2.	Fuel Economy.....	39
2.5.	Conclusions	40
2.6.	Acknowledgements	42
2.7.	References	43
3.	Certification and In-Use Compliance Testing for Heavy-Duty Diesel Engines to Understand High In-Use NO_x Emissions	46
3.1.	Abstract	46
3.2.	Introduction	47
3.3.	Materials and Methods	50
3.3.1.	Test Vehicles and Fuels	50

3.3.2.	Test Cycles, Test Matrix, and Test Methods	50
3.3.3.	Emission Measurements	54
3.4.	Results and Discussion	54
3.4.1.	NO _x Emissions	54
3.4.1.1.	NO _x Emission rates.....	55
3.4.1.2.	UDDS NO _x emission differences between the different testing conditions	59
3.4.1.3.	Average SCR efficiency by Test Cycle.....	66
3.4.1.4.	SCR efficiency as a function of SCR temperature	68
3.4.1.5.	SCR efficiency as a function of load	71
3.4.2.	NTE Analysis.....	74
3.4.2.1.	NTE analysis.....	74
3.4.2.2.	NTE Activity Analysis	76
3.4.2.3.	NTE compliance results.....	81
3.4.3.	Modified NTE Analysis	83
3.4.4.	MAW Analysis	85
3.4.4.1.	Modified MAW Analysis with CF of 2.25	89
3.4.4.2.	Modified MAW Analysis with temperature criteria.....	90

3.4.5.	Potential Improvements for Heavy-Duty In-Use Compliance Testing	
	Procedures.....	91
3.5.	Conclusions	93
3.6.	Acknowledgements	96
3.7.	References	97
3.8.	Supporting Information	103
4.	Heavy-duty On-Road Vehicle Inspection and Maintenance Program	105
4.1.	Abstract	105
4.2.	Introduction	106
4.3.	Literature Review	110
4.3.1.	Tailpipe Emissions Measurements.....	111
4.3.2.	On-Board Diagnostics.....	112
4.4.	Materials and Methods	113
4.4.1.	Test Vehicles.....	113
4.4.2.	Overall Flow Chart for the Pilot Program.....	115
4.4.3.	Test methods	116
4.5.	Results and Discussion.....	117
4.5.1.	NOx Emissions	118
4.5.2.	PM emissions	123

4.6.	Emission Impact Rates	128
4.6.1.	Emission Impact Rates from Pilot Study	128
4.6.2.	Repair Frequencies.....	130
4.6.3.	Emission Impact Rates	132
4.6.4.	Discussion of Emissions Impact Rates in the Context of the Available Literature	133
4.7.	Discussions	135
4.7.1.	OBD as the Primary Methodology of HD I/M	135
4.7.2.	Coupling of an OBD-based HD I/M with roadside monitoring with a remote sensing methodology	137
4.7.3.	A comprehensive HD I/M program with OBD as the primary methodology, remote sensing for validation testing, and mini-PEMS for dispute resolution	138
4.8.	Conclusions and Recommendations	140
4.9.	Acknowledgements	141
4.10.	References	142
4.11.	Supporting Information	149
5.	Sources of Variance in BC Mass Measurements from a Small Marine Engine: Influence of the Instruments, Fuels and Loads	151
5.1.	Abstract	151

5.2.	Introduction	152
5.3.	Experimental Approach.....	155
5.3.1.	Test Engine	155
5.3.2.	Test Fuels	156
5.3.3.	Test Loads.....	158
5.3.4.	Measurement Methods	158
5.3.4.1.	Instruments	158
5.3.4.2.	Experimental Layout.	161
5.4.	Results and Discussion.....	163
5.4.1.	BC Emission Factors (g/kg fuel).....	163
5.4.2.	BC Instrument Comparisons.	169
5.4.3.	Particle Size Distributions (PSD).....	175
5.5.	Conclusions and Implications	178
5.6.	Acknowledgements	180
5.7.	References	181
5.8.	Supporting Information	187
6.	Black Carbon Measurements from a Marine Engine with Various Fuels: Impacts of Sample Conditioning on Black Carbon Measurement Instruments ...	199
6.1.	Abstract	199

6.2.	Introduction	200
6.3.	Experimental Approach.....	204
6.3.1.	Test Engine	204
6.3.2.	Test Fuels and Loads.....	204
6.3.3.	Measurement Methods	204
6.3.3.1.	Instruments	204
6.3.3.2.	Experimental Layout	206
6.4.	Results and Discussion	207
6.4.1.	SC Performance and Particle Loss in SC	207
6.4.2.	PM Emission Factors (g/kg fuel)	209
6.4.3.	BC Emission Factors (g/kg fuel).....	210
6.4.4.	BC Instrument Correlations	214
6.4.5.	BC Morphology	219
6.4.6.	Particle Size Distributions.....	221
6.5.	Conclusion.....	222
6.6.	Acknowledgements	223
6.7.	References	224
6.8.	Supporting Information	229
7.	Conclusions	233

List of Figures

Figure 2-1 Comparisons of NOx emission rates over the UDDS from this study, CARB retesting of some of the vehicles from this study, and the CARB study that was used to develop EMFAC2014 emission factors for SCR-equipped 2010+ vehicles; D1* represents the UDDS emission level found after retesting the manufacturer D1 truck after a regeneration; A2** and B** represents results from CARB retest.	32
Figure 2-2 Average SCR inlet temperature.....	36
Figure 3-1 In-use Testing Route	51
Figure 3-2 Average NOx Emissions on a g/bhp-hr Basis for the urban cycles for the manufacturer A truck (top) and the manufacturer b truck (bottom)	57
Figure 3-3 Cumulative NOx emissions for the UDDS Cycle of the first Chassis dynamometer testing (top) and the engine dynamometer testing (bottom) for the manufacturer A truck	61
Figure 3-4 Cumulative NOx emissions for the UDDS Cycle of the first Chassis dynamometer testing (top) and the engine dynamometer testing (bottom) for the manufacturer B truck	62
Figure 3-5 Comparison of engine out and SCR out NOx emission on a PPM basis from ECM of UDDS chassis dynamometer and engine dynamometer test of the manufacturer B truck.....	64
Figure 3-6 Integrated of engine out and SCR out NOx emissions and SCR efficiencies for the UDDS chassis dynamometer and on-road cycles for the manufacturer A truck (top) and the manufacturer b truck (bottom)	66

Figure 3-7 Average NO _x penetration by test cycles of the manufacturer A truck (Top) and the manufacturer B truck (Bottom)	68
Figure 3-8 SCR efficiency as a function of SCR inlet temperature for the manufacturer A (Top) and the manufacturer B (Bottom)	70
Figure 3-9 SCR efficiency as a function of load for the manufacturer A truck (Top) and the manufacturer B truck (Bottom)	73
Figure 3-10 NO _x emission rates of NTE zone, valid NTE events and non NTE zone	76
Figure 3-11 NTE Activity Analysis of the manufacturer A truck (top) and the manufacturer B truck (bottom)	79
Figure 3-12 NTE NO _x breakdown Analysis of the manufacturer A truck (top) and the manufacturer B truck (bottom)	80
Figure 3-13 Comparison of activity analysis with standard NTE criteria and modified NTE criteria.....	85
Figure 3-14 Comparison of Standard MAW (CF≤1.5) and Modified MAW (CF≤2.25).	89
Figure 3-15 Comparison of Standard MAW (with temperature criteria) and Modified MAW (without temperature criteria)	91
Figure 4-1 Overall flow chart for pilot demonstration program	115
Figure 5-1 Schematic of the Experimental Layout with Dilution Factor (DF) and Instruments.....	163
Figure 5-2: Summary of BC Emissions Factors (g/kg fuel) at 25% Load	168
Figure 5-3 Summary of BC Emissions Factors (g/kg fuel) at 75% Load	168

Figure 5-4 Various Instrument Responses with respect to PAS Mass Concentration	171
Figure 5-5 Correlations between Two TOA Methods	175
Figure 5-6 Particle Size Distributions for Various Engine Loads and Fuels on a logarithmic scale	176
Figure 6-1 Schematic depiction of the planned experimental layout.....	207
Figure 6-2 PM _{2.5} Composition (based on TOA-Integrated) on a percent of total PM mass basis.....	210
Figure 6-3 Instrument Response as a Function of PAS Mass Concentration for the SC Measurements	216
Figure 6-4 Effect of SC on BC Particles.....	220
Figure 6-5 Particle Size Distributions from SMPS for the SC Mode	222

List of Tables

Table 2-1 Engine/Vehicle specifications	25
Table 2-2 Description of test cycles.....	26
Table 2-3 Emission rates of regulated pollutants on a distance-specific unit and fuel economy	30
Table 3-1 Engine/Vehicle specifications	50
Table 3-2 Description Test Cycles of Chassis Dynamometer, On-Road and Engine Dynamometer.....	53
Table 3-3 NTE Requirements with Measurement Allowance	83
Table 3-4 NTE Requirements with Measurement Allowance	88
Table 4-1 List of ECM Trouble Codes identified and the repairs for each vehicle	114
Table 4-2 Pre- and post-repair for NOx emissions for the MGT5 for each vehicle on a g/bhp-hr basis.....	120
Table 4-3 Pre- and post-repair for NOx emissions for the MGT5 for each vehicle on a g/bhp-hr basis (continued)	121
Table 4-4 Pre- and post-repair for NOx emissions for the MGT5 for each vehicle on a g/bhp-hr basis (continued)	122
Table 4-5 Pre- and post-repair for opacity for each vehicle	126
Table 4-6 Pre- and post-repair for opacity for each vehicle (continued)	127
Table 4-7 Emissions Benefits for Vehicles with Check Engine Light On Pre-Repair and Vehicles with DM1=1 on Pre-Repair	130
Table 4-8 Emission Impact Rates Based on Pilot Study.....	133

Table 4-9 EIRs and TMM Frequencies for Disabled and Leaking DPFs for EMFAC2014 and EMFAC2017	135
Table 5-1 Selected Fuel Properties	157
Table 5-2 Black Carbon Measurement Instruments and Associated Measurement Principles.....	160
Table 6-1 BC Measurement Instruments Principles	205
Table 6-2 BC Associated Measurement Principles.....	205
Table 6-3 Particle loss and SC removal efficiencies (based on TOA-Integrated)	209
Table 6-4 BC Emission Factors in the SC Mode for the Marine Engine on a g/kg fuel basis.....	213
Table 6-5 Slopes and Intercepts of Instrument Response as a Function of PAS Mass Concentration	215

Acronyms and Abbreviations

ANOVA.....	An analysis of variance
ARB.....	Air Resources Board
BAR.....	Bureau of Automotive Repair
BC.....	black carbon
bhp.....	brake horse power
bhp-hr.....	brake horse power – hour
BP.....	Bypass
C.....	Carbon
CAA.....	Clean Air Act
CAFEE.....	West Virginia University Center for Alternative Fuels Engines and Emissions Laboratory
CAI.....	California Analytical Instruments
CARB.....	California Air Resources Board
CBD.....	Central Business District
CCAI.....	Calculated Carbon Aromaticity Index
CE-CERT.....	College of Engineering-Center for Environmental Research and Technology (University of California, Riverside)
CFR.....	Code of Federal Regulations
CH ₄	methane
CI.....	compression-ignition
CIMAC.....	International Council on Combustion Engines
CO.....	carbon monoxide
CO ₂	carbon dioxide
CO ₂	carbon dioxide
CPC.....	condensation particle counter
CS.....	Catalytic Stripper
CVS.....	constant volume sampling
DEF.....	diesel emissions fluid
DI.....	direct injection
DMA.....	distillate marine fuel
DOC.....	diesel oxidation catalyst
DPF.....	diesel particulate filter
Dp.....	particle diameter
DTP.....	Drayage Truck Port
eBC.....	equivalent black carbon
ECAs.....	Emissions Control Areas

EC.....	elemental carbon
ECL.....	Emissions Control Label
ECM.....	engine control module
EDAR.....	Emission Detecting and Reporting
EGR.....	exhaust gas recirculation
EFs.....	emission factors
EMA.....	Truck and Engine Manufacturers Association
EMFAC.....	EMission FACtors inventory model
EPA.....	United States Environmental Protection Agency
FID.....	flame ionization detector
FSN.....	Filter Smoke Number
FTP.....	Federal Test Procedure
g/mi.....	grams per mile
HDVIP.....	Heavy-Duty Vehicle Inspection Program
HDDE.....	heavy-duty diesel engine
HDDV.....	heavy-duty diesel vehicle
HDIUC.....	heavy-duty in-use compliance
HEAT.....	Hager Environmental & Atmospheric Technologies
HFO.....	Heavy Fuel Oil
HSHFO.....	high sulfur heavy fuel oil
lbs.....	pounds
ICCT.....	International Council on Clean Transportation
I/M.....	Inspection and maintenance
IMO.....	International Maritime Organization
LA.....	light absorption
LD.....	Light-duty
LII.....	Laser Induced Incandescence
LLSP.....	Laser Light Scattering Photometry
LSFs.....	Low Sulfur Fuels
LSHFO.....	low sulfur heavy fuel oil
MAAP.....	Multi-Angle Absorption Photometer
MARPOL.....	International Convention for the Prevention of Pollution from Ships
MAW.....	Moving Averaging Window
MEL.....	CE-CERT's Mobile Emissions Laboratory
MGO.....	marine gas oil
MIL.....	Malfunction Indicator Light
mpg.....	miles per gallon
Mph.....	Miles per Hour
m/s ²	meters per second squared
MSS.....	Micro Soot Sensor

MY	Model Year
NDIR	non-dispersive infrared detector
nm.....	nanometer
NRTC	nonroad transient cycle
NMHC.....	non-methane hydrocarbons
NO.....	Nitric Oxide
NO ₂	Nitrogen Dioxide
NO _x	oxides of nitrogen
NTE.....	Not to Exceed
O ₂	Oxygen
OBD	On-Board Diagnostics
OC	
OEM.....	Original Equipment Manufacturer
OHMS	On-road Heavy-duty vehicle emissions monitoring system
OIS	OBD Inspection System
OGVs.....	ocean going vessels
PAS	Photoacoustic Spectroscopy
PEAQS	Portable Emissions AcQuisition System
PEMS	portable emissions measurement systems
PM.....	particulate matter
PN.....	particle number
PSD	Particle Size Distributions
PSIP.....	Periodic Smoke Inspection Program
R ²	Coefficient of Determination
rBC.....	refractory black carbon
RDD	rotating disk dilutor
RDE.....	real driving emissions
DF.....	dilution factor
RSD.....	Remote Sensing Devices
SC.....	Sampling Conditioning
SI.....	spark-ignition
SIM.....	Subscriber Identification Module
SCAQMD.....	South Coast Air Quality Management District
SCR.....	Selective Catalytic Reduction
SHED	Streamlined Heavy-Duty Emissions Determination
SMPS.....	Scanning Mobility Particle Sizer
SET.....	Supplemental Emissions Test
TEM	Transmission Electron Microscopy
THC.....	total hydrocarbons
TM&M	tampering, mal-maintenance, and malfunction
TOA.....	Thermal-Optical-Analysis

UCR.....	University of California, Riverside
UDDS	Urban Dynamometer Driving Schedule
ULSD.....	ultralow sulfur diesel
USEPA	United States Environmental Protection Agency
VIN.....	Vehicle Identification Number
VOC.....	volatile organic compounds
VSP.....	Vehicle Specific Power
WTO.....	World Trade Organization
ZMR	zero mile emission rates

1. Introduction

Diesel engines, known as a compression-ignition or CI engines, are one of the most important sources of power generation. CI engines have higher fuel efficiencies and produce more torque for a given displacement than spark-ignition (SI) engines (Heywood, J.B., 1988). A variety of configurations and designs of diesel engines are used in a wide range of applications, including marine, locomotive, stationary generator, automobile, trucks, non-road diesel equipment, and small diesel machines (Heywood, J.B., 1988). The need for diesel powered engines is also expected to grow into the future, as projections have shown the demand of diesel fuel will continue to grow and is anticipated to surpass gasoline by 2020 (ExxonMobil, 2018).

Heavy-duty diesel trucks (HDDTs) and shipping are two important applications of diesel engines. HDDTs and marine shipping, as the major components of the global freight system, transport materials and goods worth trillions of dollars, which are a driver of economic growth (World Trade Organization (WTO), 2016). HDDTs are used to distribute significant volumes of domestic goods (International Council on Clean Transportation [ICCT], 2018). They are responsible for moving over 40% of cargo in the United States (U.S.) (Corbett and Winebrake, 2008). HDDTs consume around one-third of the transportation related oil, and this demand is projected to increase close to 50 percent by 2040 (ExxonMobil, 2018). Marine shipping is also one of the key components of international trade. In particular, over 90% of global merchandise is carried at some point

by ships (ICCT, 2018). Marine shipping, as a low-cost and efficient means of transportations, helps to distribute food, technology, medicine, and other things all over the world, and serves as a backbone of global trade and the global economy (United Nations, 2016).

Diesel engines are a significant contributor to oxides of nitrogen (NO_x) emissions from mobile sources as a consequence of high combustion temperatures and lean burn combustion (Heywood, J.B., 1988; Miller et al., 2013; Carder et al., 2014; Misra et al., 2015; Dixit et al., 2017). NO_x emissions can increase the risk of respiratory diseases by itself and it also react with volatile organic compounds (VOC) to form ground level ozone (Jerrett et al., 2009). HDDTs emit high levels of NO_x and have become a dominant source of mobile related NO_x emissions over the past decade. Diesel and gasoline vehicles together account for 60% of total NO_x emissions for the national emissions inventory in the U.S. (EPA, 2008). This is a particularly critical issue in regions such as the greater LA basin, where it is estimated that large reductions in diesel NO_x are needed to meet 2023 and 2030 ozone standards.

Diesel engines also emit significant amounts of particulate matter (PM) emissions as a result of inhomogeneous mixing that creates fuel-rich zones during combustion. This PM is also largely PM_{2.5} (aerodynamic diameters less than 2.5 μm), which can penetrate more deeply into the lungs. Exposure to PM_{2.5} increases the risk of chronic illnesses, such as lung cancer and cardiopulmonary disease. PM_{2.5} suspended in the air can also reduce visibility in urban areas. Black Carbon (BC), which is an important component of PM, also has specific adverse impacts on health, including contributing to cardiovascular and

chronic lung diseases (Janssen et al., 2012; Winebrake et al., 2009). BC emissions also have climatic effects that include direct and indirect radiative forcing, influencing cloud formation, and melting of snow, glaciers, and sea ice, especially in the highly sensitive Arctic (Bond et al., 2013; Corbett et al., 2010a; Lack and Corbett, 2012).

HDDTs can emit high levels of PM_{2.5}, especially older model years that are not equipped with diesel particle filters (DPFs). Mobile sources together contribute over 10% of total primary PM_{2.5} emissions to the national emission inventory in the U.S. (EPA, 2008). Over 370 tons PM were emitted by HDDTs national widely per day before complying with DPF system (Dallmann and Harley, 2010). Marine ships have also been identified to be significant sources of PM emissions. Marine shipping, in particular, contributes to have high levels of PM emissions due to the use of heavy fuel oil (HFO) with a high sulfur content. Overall, shipping emissions contribute 2% of the global BC inventory from all sources (Azzara et al., 2015; Bond et al., 2013).

The United States Environmental Protection Agency (US EPA) has set a series of regulations to archive progressive reductions in NO_x and PM emissions from HDDTs over the last forty years. The NO_x emission standards were implemented starting in 1974, and were last made more stringent in 2007 and 2010. Those rules have required that emissions of NO_x be reduced from an estimated unregulated emission level of 16 g/bhp-hr to 0.20 g/bhp-hr. The combination of selective catalytic reduction (SCR) and exhaust gas recirculation (EGR), along with other engine design changes, were used to meet the NO_x 2010 standard. Recently, the California Air Resources Board (CARB) adopted optional low NO_x standards, which targeted an additional order of magnitude reduction in NO_x

emissions (from 0.2 to 0.02 g/bhp-hr) for the model year of 2015 and newer HDDTs. Regulations of PM emissions have remained static since 2007, when the PM was reduced from 0.1 to 0.01 g/bhp-hr. The diesel engines were equipped with DPFs to remove particles to meet the 2007 PM standards.

Historically, the emission regulations of marine engines have been less stringent. Emissions standards of ships are defined by the International Maritime Organization (IMO), or specifically, the International Convention for the Prevention of Pollution from Ships (MARPOL) Annex VI. The first round of standards were implemented in 2005 by setting the limits on the sulfur content (4.5% and less) in marine fuels and by setting NO_x emission standards. The regulations got more stringent in 2012 by designating emission control areas (ECAs) around the U.S. and Canadian shorelines. Ships are required to switch to lower sulfur fuels (LSFs) (10,000 ppm and less) in designated ECAs since high sulfur, heavy fuel oil (HFO) has been found to lead to significant PM mass emissions (Wall et al., 1988; Khan et al., 2012). IMO has announced further limits on the use of high sulfur marine fuels in ECAs, which will limit fuel sulfur content below 1,000 ppm. Marine diesel engines installed on U.S. vessels have also been required to comply with off-road engine emission standards from the U.S. EPA since 2000. Off-road engines are divided into three categories based on displacement per cylinder and the emissions standards are set based on the categories. The emissions regulated include CO, NO_x plus total hydrocarbon (THC) and PM emissions.

1.1. Testing Methodologies for Heavy-Duty and Marine Diesel Engines

A variety of methods can be used to measure emissions of diesel engines, including engine dynamometer testing, chassis dynamometer testing, and in-use testing. The primary method for measuring emissions and performance of diesel engines over the years has been an engine dynamometer. The dynamometer is used to apply a load to the engine and control its power output. Currently, certification tests of on-highway heavy-duty diesel engines (HDDEs) are conducted on an engine-dynamometer over the Federal Test Procedure (FTP) cycle, which was developed to be representative of real-world heavy-duty diesel vehicle (HDDV) driving patterns. The certification test procedures were augmented in the late 1990s as part of the consent decree to incorporate a wider range of operating conditions. This included the addition of a Supplemental Emissions Test (SET), which was a multi-mode test covering a range of steady state operating conditions. The SET cycle was put in place for engines meeting U.S. EPA standards for 2004 and later emissions standards. Nonroad diesel engines were originally certified on an engine-dynamometer over a steady-state test cycle, such as the C1 cycle, the G2 cycle and the E3 cycle. A nonroad transient cycle (NRTC) cycle was added as a certification cycle in 2011 to evaluate emissions during transient operations.

Chassis dynamometers are becoming increasingly more important in characterizing emissions of heavy-duty vehicles, however, as it is important to understand how engines that are certified on an engine dynamometer perform under typical driving conditions. Chassis dynamometers include a roll or rollers that the vehicle is positioned on during a simulated driving schedule. The dynamometer rolls apply a load to the vehicle tires based

on the type of driving that is being simulated and measure the power being delivered by the drive wheels. A variety of test cycles have been utilized to characterize various types of driving or typical operation for various types of vehicles, such as buses or refuse haulers. The driving cycles include the Urban Dynamometer Driving Schedule (UDDS), the Central Business District (CBD) cycle, the California Air Resources Board (CARB) – Heavy Heavy-Duty Diesel Truck (HHDDT) schedule, the Drayage Truck Port (DTP) cycle, and the Refuse Truck Cycles.

In-use testing was developed to evaluate emissions from real-world driving conditions, as dynamometer testing alone has been insufficient to characterize the emissions that are seen under the full range of typical in-use driving conditions. In-use testing has been incorporated into the in-use HDDV Not-To-Exceed (NTE) emission limits and testing requirements in the U.S. and the real driving emissions (RDE) testing requirements in Europe. NTE and RDE testing don't involve a specific driving cycle of any specific length (mileage or time). NTE operation involves driving of any type that could occur within the bounds of the *NTE control area*, including operation at over 30% of maximum power and under varying ambient conditions. RDE testing is performed on-road and is evaluated in accordance to the Moving Averaging Window (MAW) method based on the CO₂ mass or the work from the certification cycle. Portable emissions measurement systems (PEMS) are used for both NTE and RDE testing. PEMS is designed to provide the capability of measuring emissions typically measured in the laboratory for in-use testing, but in a more compact package that can be installed in a vehicle or on a piece

of equipment so that measurements can be made while the vehicle or piece of equipment is being operated.

1.2. Studies of Model Year 2010 and Newer Heavy-Duty Diesel Vehicles

Characterizing emission rates of model year 2010 and newer HDDVs is important, as these vehicles are expected to represent the majority of the in-use fleet going into the future. There are extensive data on the emission rates of HDDEs equipped with DPF and SCR systems over certification test cycles run in engine dynamometer laboratories, while data on in-use emissions from modern diesel engines are scarce. Since the HDD engines are certified to meet emission standards before the engines are integrated into a vehicle chassis, it is important to characterize in-use emissions of HDDVs from a broad range of applications for commercial uses. Additionally, understanding in-use emissions from on-road heavy-duty trucks is also an important element of developing accurate emissions inventory estimates. For example, the California Air Resources Board (CARB) has been utilizing emissions testing results from chassis dynamometer studies in the development of emissions factors for its Emission FACTors inventory model (EMFAC) for a number of years (California Air Resources Board (CARB), 2015a, 2015b). For the EMFAC2017 model (CARB, 2017), a greater emphasis was placed on developing emission factors for vehicles equipped with newer PM and NO_x aftertreatment control devices. Emissions data from chassis dynamometer testing with 2010 and newer engines/vehicles were the primary data source for EMFAC2017 model.

A variety of studies have been conducted to evaluate the emissions from 2010 and newer engines and vehicles. This includes studies using chassis dynamometers, PEMS

systems and remote sensing methods. Chassis dynamometer studies include a South Coast Air Quality Management District in-use chassis dynamometer study and CARB chassis dynamometer studies (Miller et al., 2013; Carder et al., 2014; CARB2015a, 2015b; CARB, 2017). Chassis dynamometer studies have shown that NO_x emissions vary considerably from cycle to cycle and for different vehicles/engines. NO_x emissions are typically lowest for higher speed cruise cycles, where the higher exhaust temperatures provide more optimal SCR performance. More moderate cycles, such as the UDDS, tend to show higher emissions, with these emissions often higher than the typical certification values when characterized on a g/bhp-hr basis. NO_x emissions for lower load cycles, such as the HHDDT creep or the near dock DPT cycles, tend to show even higher emissions, since the exhaust temperature for the SCR is typically below 250°C, where the SCR is not effective in reducing NO_x emissions (Miller et al., 2013; Carder et al., 2014).

Several PEMS studies conducted by West Virginia University (WVU) and CARB have evaluated the emissions of 2010 and newer trucks on the open road (Carder et al., 2014; Misra et al., 2013; Misra et al., 2016; O’Cain et al., 2016; Tu et al., 2016; O’Cain et al. 2018). This includes studies conducted in Northern California, in Southern California, and for a cross country trip. Information is also starting to become available from the manufacturer heavy-duty in-use compliance (HDIUC) program and through some associated investigations being conducted by CARB (CARB, 2017). The incorporation of NO_x sensors in SCR-equipped trucks has provided an additional source of emissions information (Tan et al., 2018a, 2018b; Spears et al. 2018). Other methodologies have been developed for roadside measurements of emissions from HDDV’s, such as remote sensing,

an on-road heavy-duty measurement system (OHMS) (Bishop et al., 2013) and a portable emissions acquisition system (PEAQS) (CARB, 2017).

1.3. Issues of Current Testing Methodologies for Heavy-Duty and Marine Diesel Engines

Several studies have indicated that there are differences between NO_x emission measurements under certification conditions on an engine dynamometer in comparison with in-use testing conditions on a chassis dynamometer or on-road using the same engines. This includes recent studies that have shown that NO_x emissions measured from 2010 in-use HDDVs on chassis-dynamometers over the UDDS cycle are substantially higher than the certification standard of 0.2 g/bhp-hr NO_x (Miller et al, 2014; CARB2015a, 2015b). Although the UDDS on a chassis dynamometer does not replicate the FTP on an engine dynamometer, the UDDS is designed to be comparable to the FTP engine-dynamometer cycle.

Results of on-road testing have shown emissions higher than engine certification values under a variety of conditions, especially under low load conditions. CARB has conducted in-use testing on a total of 23 vehicles so far as part of its in-use testing verification program (O’Cain, 2016; O’Cain, 2018; Tu et al. 2016). These tests focused on evaluating emissions in the NTE zone of operation, which includes criteria such as being at more than 30% of the maximum engine power and having SCR temperatures higher than 250 °C for at least 30 seconds. The results showed that a large fraction of the operation was not in the NTE zone or do not represent valid NTE events. Misra et al. (2013, 2016) of CARB also found that NO_x emissions are generated disproportionately under lower load

operation and that NO_x emissions for different types of driving can often be higher than certification NO_x levels.

1.4. California Heavy-duty On-Road Vehicle Inspection and Maintenance

Another potential issue with the high in-use emission rates for HDDVs could be the deterioration of vehicles. Emission deterioration of HD trucks, including tampering, mal-maintenance, and malfunction (TM&M), can result in high in-use NO_x emissions. While engines meeting the newest emissions standards continue to penetrate into the in-use fleet, it is also important to ensure that the emissions from these vehicles do not significantly deteriorate over the course of the lifetime of the vehicle. This is important because heavy-duty engines tend to have relatively long lifetimes, both in terms of years of service as well as miles of travel or hours of engine life.

Inspection and maintenance (I/M) programs can be effective in preventing excessive emissions from in-use vehicles. Such programs have been extensively implemented for light-duty vehicles throughout the U.S. For California's current roadside HD vehicles, the inspection program includes opacity testing, and checks for emission control labels and tampering. The fleet inspection program requires California-based fleets with two or more heavy-duty vehicles to conduct annual opacity testing. Neither program includes inspections for NO_x emissions control from the in-use fleet, nor have they kept pace with advances in diesel engine technology, such as aftertreatment for PM and NO_x control, and the use of on-board diagnostics (OBD). In order to better ensure that modern diesel engines are maintained and repaired to continue to meet emissions performance requirements in-use, California is now in need of a more comprehensive HD I/M program.

It is expected that such a program could also be implemented in other “Section 177” states that are allowed to follow and tend to adopt California environmental regulations.

1.5. Black Carbon Emissions

BC emission factors (EFs) for marine engines and fuels are not well characterized due to the challenges of measuring BC emissions and a dearth of scientific studies to estimate marine BC EFs. The International Council on Combustion Engines (CIMAC) reported BC EFs varied more than ten-fold (0.1 to 1 g/kg fuel) in various studies of marine engine emissions (CIMAC, 2012; Lack et al., 2008; Corbett et al., 2010b). The report also indicated that BC depended non-linearly on loads and fuel properties, and that switching to a distillate fuel may not result in reduced black carbon emissions from large engines. Having such a wide range of BC emission factors makes it difficult to evaluate the climate impacts of BC from shipping with confidence and has raised concern during international discussions relating to marine BC standards.

Engine load, fuel properties, and measurement methods all contribute to uncertainties in BC EFs. Lack and Corbett (2012) found that BC emission factors increased by an average factor of 3 in going from 100 to 25% load, with increases of up to a factor of 6.5 for loads below 25%. Marine fuel properties are also known to be important parameters driving PM mass emission factors (Wall et al., 1988; Khan et al., 2012). However, the effect of fuel quality on BC emissions is not clear (Lack and Corbett, 2012). Some studies have suggested that switching to low sulfur heavy fuel oil (LSHFO) could reduce BC emissions due to reductions in aromatics and long chain hydrocarbon components in the fuel, resulting in lower concentrations of BC particle nuclei (Lack et al.,

2011; Lack and Corbett, 2012; Buffaloe et al., 2014). However, several authors have found that LSHFO increased BC emissions, while lowering sulfate aerosols, which could be due to metal oxides present in the high sulfur heavy fuel oil (HSHFO) (CIMAC, 2012; Aakko-Saksa et al., 2016a; Sippula et al., 2014). There are also many potential methodologies and instruments for measuring BC based on different BC properties, such as light absorption methods, laser induced incandescence, and thermal-optical analysis (TOA). It is important to understand the different methods for measuring BC emissions because data is reported from a wide range of instruments in the literature.

1.6. Outline of Dissertation

Chapter 2 presents in-use NO_x emissions and other pollutants from five HHDVs with 2012 and newer model years. The goal of this work was to obtain emission data on Class 8 trucks equipped with the newest emission control strategies and operated over in-use cycles on a heavy-duty chassis dynamometer. A particular emphasis was on gathering data that can be used to improve estimates of “zero mile” emission rates (ZMRs) for 2010 and later model year heavy-duty engines/trucks. The implications of these results in developing and analyzing emissions inventory models utilized at different levels of the regulatory process are discussed, particularly for CARB’s EMFAC2017 model.

A number of studies have shown that NO_x emission rates of urban driving cycles tested by a chassis dynamometer are higher than the typical certification values based on engine dynamometer testing. Chapter 3 presents a study comparing NO_x emission rates for the same engines on an engine dynamometer, in a vehicle on a chassis dynamometer, and in a vehicle on the road. The objectives were 1) understand the differences between

certification and in-use operating conditions and 2) evaluate current and proposed in-use compliance procedures. Emissions testing included a chassis-dynamometer test, an over the road test, an engine-dynamometer test, and a final chassis-dynamometer test to provide a comparison with the initial chassis test conducted prior to removing the engine. Emission measurements included both PEMS and CE-CERT's Mobile Emission Laboratory (MEL) to gather information on the comparability of PEMS to constant volume sampling (CVS) testing.

Deterioration can have a significant impact on NO_x emission rates from HHDVs equipped DPFs and SCR systems. It is important to ensure that the emissions from these vehicles do not significantly deteriorate over the lifetime of the vehicle. Chapter 3 focuses on the development of an I/M program for HD on-road vehicles. The objective of this study is to develop, evaluate, and assess the potential emissions benefit impacts of a HD vehicle I/M program. A total of 47 vehicles with emission related issues were tested before and after repair on a chassis dynamometer using I/M grade instruments. The emission benefits from the repairs and the overall emissions impact rates are discussed in this chapter.

Chapter 4 and chapter 5 discuss the influence of different instrument methodologies, fuels, loads and sample conditioning (SC) on BC mass measurements from a small marine engine. Six analytical methods, based on different operating principles, were used to measure the BC emission factors in the exhaust of a marine diesel engine, including a Micro Soot Sensor (MSS), a filter smoke number (FSN), a multi-angle absorption photometer (MAAP), a laser induced incandescence (LII), and an integrated and a continuous TOA. The engine was operated at two load points (25% and 75%) while

burning a distillate marine (DMA), a low-sulfur, residual marine (RMB-30) and a high-sulfur residual marine (RMG-380). A system including a catalytic stripper (CS) and sulfur absorber unit (S-absorber) was used to evaluate the impacts of sample conditioning on the measurement of marine engine BC emissions.

1.7. References

- Aakko-Saksa, P., Murtonen, T., Vesala, H., Koponen, P., Nyyssönen, S., Puustinen, H., Lehtoranta, K., Timonen, H., Teinilä, K., Hillamo, R., Karjalainen, P., Kuittinen, N., Simonen, P., Rönkkö, T., Keskinen, J., Saukko, E., Tutuianu, M., Fischerleitner, R., Pirjola, L., Brunila, O., Hämäläinen, E., 2016b. SEA-EFFECTS BC Black carbon measurements from ship engine when using different marine fuels. Presented at the ICCT's 3rd and final Workshop on Marine Black Carbon Emissions: BC Control Strategies, Vancouver, Canada, September.
- Azzara, A., Minjares, R., Rutherford, D., 2015. Needs and opportunities to reduce black carbon emissions from maritime shipping. *Assessment*. 118, 5380-5552.
- Bishop, G.A., Schuchmann, B.G., Stedman, D.H., 2013. Heavy-Duty Truck Emissions in the South Coast Air Basin of California. *Environ. Sci. Technol.* 47, 9523–9529.
- Bond, T.C., Doherty, S.J., Fahey, D.W., Forster, P.M., Berntsen, T., DeAngelo, B.J., Flanner, M.G., Ghan, S., Kärcher, B., Koch, D., Kinne, S., 2013. Bounding the role of black carbon in the climate system: A scientific assessment. *J. Geophys. Res.* 118, 5380-5552.
- Buffaloe, G.M., Lack, D.A., Williams, E.J., Coffman, D., Hayden, K.L., Lerner, B.M., Li, S. M., Nuaaman, I., Massoli, P., Onasch, T.B., Quinn, P.K. 2014. Black carbon emissions from in-use ships: a California regional assessment. *Atmos. Chem. Phys.* 14, 1881-1896.
- California Air Resources Board, 2015a. Mobile Source Emissions Inventory and Assessment. Los Angeles. <http://www.arb.ca.gov/msei/msei.htm> (access 16.10.05).
- California Air Resources Board, 2015b. EMFAC2014 Volume III Technical Documentation. <https://www.arb.ca.gov/msei/downloads/emfac2014/emfac2014-vol3-technical-documentation-052015.pdf> (access 16.10.05).
- California Air Resources Board, 2017. EMFAC2017 An update to California On-road Mobile Source Emission Inventory. https://www.arb.ca.gov/msei/downloads/emfac2017_workshop_june_1_2017_final.pdf (access 17.07.05).
- Carder, D. K., Gautam, M., Thiruvengadam, A., Besch, M. C., 2014. In-Use Emissions Testing and Demonstration of Retrofit Technology for Control of On-Road Heavy-Duty Engines. Final Report by West Virginia University to the South Coast Air Quality Management District under contract No. 11611, July.

- CIMAC - International Council on Combustion Engines. 2012. Background information on black carbon emissions from large marine and stationary diesel engines-definition, measurement methods, emission factors and abatement technologies, Main, Germany, http://www.cimac.com/cms/upload/workinggroups/WG5/black_carbon.pdf (access 16.12.15).
- Corbett, J.J. and Winebrake, J., 2008. The Impacts of Globalisation on International Maritime Transport Activity: Past Trends and Future Perspectives. Paper read at Global Forum on Transport and Environment in a Globalising World, at Guadalajara, Mexico.
- Corbett, J.J., Lack, D. A., Winebrake, J.J., Harder, S., Silberman, J.A., Gold, M., 2010b. Arctic shipping emissions inventories and future scenarios. *Atmos. Chem. Phys.* 10, 9689-9704.
- Corbett, J.J., Winebrake, J.J., Green, E.H., 2010a. An assessment of technologies for reducing regional short-lived climate forcers emitted by ships with implications for Arctic shipping. *Carbon Manage.* 1, 207-225.
- Dallmann, T.R. and Harley, R.A., 2010. Evaluation of mobile source emission trends in the United States. *Journal of Geophysical Research: Atmospheres*, 115(D14).
- Dixit, P., Miller, J.W., Cocker III, D.R., Oshinuga, A., Jiang, Y., Durbin, T.D. and Johnson, K.C., 2017. Differences between emissions measured in urban driving and certification testing of heavy-duty diesel engines. *Atmospheric Environment*, 166, pp.276-285.
- ExxonMobil, 2018. 2018 Outlook for Energy: A View to 2040. <http://corporate.exxonmobil.com/en/energy/energy-outlook/a-view-to-2040> (access 18.05.01).
- Heywood, J.B., 1988. *Internal combustion engine fundamentals*.
- Lack, D.A., Corbett, J.J., 2012. Black carbon from ships: a review of the effects of ship speed, fuel quality and exhaust gas scrubbing. *Atmos. Chem. Phys.* 12, 3985-4000.
- Lack, D., Lerner, B., Granier, C., Baynard, T., Lovejoy, E., Massoli, P., Ravishankara, A.R., Williams, E. 2008, Light absorbing carbon emissions from commercial shipping. *Geophys. Res. Lett.* 35, L13815.
- Lack, D.A., Cappa, C.D., Langridge, J., Bahreini, R., Buffaloe, G., Brock, C., Cerully, K., Coffman, D., Hayden, K., Holloway, J., Lerner, B., 2011. Impact of fuel quality regulation and speed reductions on shipping emissions: implications for climate and air quality. *Environ. Sci. Technol.* 45, 9052-9060.

- Lack, D.A., Corbett, J.J., 2012. Black carbon from ships: a review of the effects of ship speed, fuel quality and exhaust gas scrubbing. *Atmos. Chem. Phys.* 12, 3985-4000.
- Lee, A., O’Cain, J., Avila, J., Lemieux, S., Karim, Sahay, K., Berdahi, S., Sahay, K., Na, K., Chang, O., and Macias, K., 2018. Findings from carb’s heavy-duty in-use compliance testing program. Presentation at 28th CRC Real World Emissions Workshop, Garden Grove, CA, March.
- International Council on Clean Transportation (ICCT), 2018. <https://www.theicct.org/publications/barriers-adoption-fuel-saving-technologies-trucking-sector> (access 18. 04. 25).
- International Council on Clean Transportation (ICCT), 2018. Marine Programs <https://www.theicct.org/marine> (access 18. 04. 25).
- International Maritime Organization (IMO), 2018. Emission Control Areas (ECAs) designated under regulation 13 of MARPOL Annex VI. [http://www.imo.org/en/OurWork/Environment/PollutionPrevention/AirPollution/Pages/Emission-Control-Areas-\(ECAs\)-designated-under-regulation-13-of-MARPOL-Annex-VI-\(NOx-emission-control\).aspx](http://www.imo.org/en/OurWork/Environment/PollutionPrevention/AirPollution/Pages/Emission-Control-Areas-(ECAs)-designated-under-regulation-13-of-MARPOL-Annex-VI-(NOx-emission-control).aspx) (access 18. 04. 25).
- International Maritime Organization (IMO) Website, 2017. [http://www.imo.org/en/OurWork/environment/pollutionprevention/airpollution/pages/sulphur-oxides-\(sox\)---regulation-14.aspx](http://www.imo.org/en/OurWork/environment/pollutionprevention/airpollution/pages/sulphur-oxides-(sox)---regulation-14.aspx) (access 17.05.10).
- Janssen, N.A., Hoek, G., Simic-Lawson, M., Fischer, P., Van Bree, L., Ten Brink, H., Keuken, M., Atkinson, R.W., Anderson, H.R., Brunekreef, B., Cassee, F. R. 2012. Black carbon as an additional indicator of the adverse health effects of airborne particles compared with PM10 PM 2.5. *Environ. Health Perspect.* 119, 1691-1699.
- Jerrett, M., Burnett, R.T., Pope III, C.A., Ito, K., Thurston, G., Krewski, D., Shi, Y., Calle, E. and Thun, M., 2009. Long-term ozone exposure and mortality. *New England Journal of Medicine*, 360(11), 1085-1095.
- Khan, M.Y., Giordano, M., Gutierrez, J., Welch, W.A., Asa-Awuku, A., Miller, J.W., Cocker III, D.R. 2012. Benefits of two mitigation strategies for container vessels: cleaner engines and cleaner fuels. *Environ. Sci. Technol.* 46, 5049-5056.
- Miller, W., Johnson, K.C., Durbin, T., P. Dixit., 2013. In-Use Emissions Testing and Demonstration of Retrofit Technology for Control of On-Road Heavy-Duty Engines. Final Report by University of California, Riverside to the South Coast Air Quality Management District under contract no. 11612, September.

- Misra, C., Collins, J. F., Herner, J. D., Sax, T., Krishnamurthy, M., Sobieralski, W., Burntitzki, m., Chernich, D., 2013. In-Use NOx Emissions from Model Year 2010 and 2011 Heavy-Duty Diesel Engines Equipped with Aftertreatment Devices. *Environmental Science & Technology*, 47(14), 7892-7898.
- Misra, C., Yoon, S., Collins, J., Chernich, D., Herner, J., 2016. Evaluating In-Use SCR Performance: Older vs. Late MY Engines. Presentation at 26th CRC Real World Emissions Workshop, Newport Beach, CA, March.
- O’Cain, J., Lemieux, S., Karim, J., Sahay, K., Chang, O., Lee., D. and Sardar, S., 2016. Heavy-duty in-use compliance pilot program. Presentation at 26th CRC Real World Emissions Workshop, Newport Beach, CA, March.
- Sippula, O., Stengel, B., Sklorz, M., Streibel, T., Rabe, R., Orasche, J., Lintelmann, J., Michalke, B., Abbaszade, G., Radischat, C., Groger, T., 2014. Particle emissions from a marine engine: chemical composition and aromatic emission profiles under various operating conditions. *Environ. Sci. Technol.* 48, 11721-11729.
- Tan, Y., Collins, J., Yoon, S., Herner, J., Henderick, P., Montes, T., Ham, W., Howard, C., Hu, S., Johnson, K., Scora, G., Sandez, D., Durin, T., 2018. NOx Emission Estimates from the Activity Data of On-Road Heavy-Duty Diesel Vehicles. Presentation at 28th CRC Real World Emissions Workshop, Garden Grove, CA, March.
- Tan, Y., Collins, J., Yoon, S., Herner, J., Henderick, P., Montes, T., Johnson, K., Scora, G., Sandez, D., Durin, T., 2018. Evaluation of a NOxTracking Concept Using Heavy-Duty Truck OBD Data. Presentation at 8th PEMS Conference, Riverside, CA, March.
- Tu, J., Berdahl, S., Tran, T., O’Cain, J., Karim, J., Sardar, S., Lemieux, S., Huai, T., 2016. Study of heavy-duty vehicle emissions during in-use compliance testing. Presentation at 26th CRC Real World Emissions Workshop, Newport Beach, CA, March.
- Spears, M., 2018. Needs and Opportunities for Reducing Real World NOx Emissions from Heavy-Duty On-Highway Engines. Presentation at 28th CRC Real World Emissions Workshop, Garden Grove, CA, March.
- United Nations, 216. <https://www.un.org/press/en/2016/sgsm18129.doc.htm> (access 18. 04. 25).
- United States Environmental Protection Agency (US EPA). EPA Emission Standards for Heavy-Duty Highway Engines and Vehicles. <https://www.epa.gov/emission-standards-reference-guide/epa-emission-standards-heavy-duty-highway-engines-and-vehicles> (access 18. 04. 25).

- United States Environmental Protection Agency (US EPA). National Emissions Inventory (NEI). <https://www.epa.gov/air-emissions-inventories/2008-national-emissions-inventory-nei-data> (access 18. 04. 25).
- United States Environmental Protection Agency (US EPA). EPA Emission Standards for Nonroad Engines and Vehicles. <https://www.epa.gov/emission-standards-reference-guide/epa-emission-standards-nonroad-engines-and-vehicles> (access 18. 04. 25).
- Wall, J.C., Shimpi, S.A., Yu, M.L. 1988. Fuel sulfur reduction for control of diesel particulate emissions. SAE Tech. Pap. No. 872139. DOI: 10.4271/2006-11- 872139.
- Winebrake, J.J., Corbett, J.J., Green, E.H., Lauer, A., Eyring, V. 2009. Mitigating the health impacts of pollution from oceangoing shipping: an assessment of low -sulfur fuel mandates. *Environ. Sci. Technol.* 43, 4776-4782.
- World Trade Organization (WTO), 2016. World Trade Statistical Review. https://www.wto.org/english/res_e/statis_e/wts2016_e/wts2016_e.pdf (access 18. 04. 25)

2. Characterizing Emission Rates of Regulated Pollutants from Model Year 2012+ Heavy-Duty Diesel Vehicles Equipped with DPF and SCR Systems

2.1. Abstract

The regulated emissions of five 2012 and newer, low-mileage, heavy-duty Class 8 diesel trucks equipped with diesel particulate filters (DPFs) and selective catalytic reduction (SCR) systems were evaluated over test cycles representing urban, highway, and stop-and-go driving on a chassis dynamometer. NO_x emissions over the Urban Dynamometer Driving Schedule (UDDS) ranged from 0.495 to 1.363 g/mi (0.136 to 0.387 g/bhp-hr) for four of the normal emitting trucks. For those trucks, NO_x emissions were lowest over the cruise (0.068 to 0.471 g/mi) and high-speed cruise (0.067 to 0.249 g/mi) cycles, and highest for the creep cycle (2.131 to 9.468 g/mi). A fifth truck showed an anomaly in that it had never regenerated throughout its relatively short operating lifetime due to its unusual, unladed service history. This truck exhibited NO_x emissions of 3.519 g/mi initially over the UDDS, with UDDS NO_x emissions decreasing to 0.39 g/mi after a series of parked regenerations. PM, THC, and CO emissions were found to be very low for most of the testing conditions, due to the presence of the DPF/ SCR aftertreatment system, and were comparable to background levels in some cases.

2.2. Introduction

Heavy-duty diesel trucks (HDDTs) are a significant source of oxides of nitrogen (NO_x) and particulate matter (PM) emissions in urban areas. In order to reduce emissions of NO_x and PM from HDDTs, a series of regulations for heavy heavy-duty diesel engines (HDDE) were implemented starting in 1974, and were last made more stringent in 2007 and 2010. Those rules have required that emissions of NO_x and PM be reduced from an estimated unregulated emission level of 16 g/bhp-hr to 0.20 g/bhp-hr, and from 1.0 g/bhp-hr to 0.01 g/bhp-hr, respectively. Current-technology diesel engines are now equipped with diesel particulate filters (DPFs) to meet the PM standards for 2007 and newer engines, and selective catalytic reduction (SCR) systems to meet the NO_x standards for 2010 and newer engines.

While there are extensive data on the effectiveness of DPF and SCR systems over certification test cycles run on an engine-dynamometer, data on in-use emissions from modern diesel engines are scarce and show some variation depending on the type of truck tested and the testing conditions (Miller et al., 2013; Carder et al., 2014; Misra et al., 2015; California Air Resources Board 2015a, b; Quiros et al., 2017). The need for in-use emissions data is particularly important because HDD engines are certified to meet emission standards before the engines are integrated into a vehicle chassis for commercial use, which can span a broad range of applications. The Coordinating Research Council's (CRC) E-55/59 program was the first chassis dynamometer study to acquire in-use emissions data from a vast number of HDDTs and evaluate the impacts of different cycles on in-use emissions (Clark et al., 2004, 2006, 2007). A study conducted under funding by

the South Coast Air Quality Management District (SCAQMD) collected chassis dynamometer emissions test data from twenty-four 2007-2012 model year (MY) HDDTs (Miller et al., 2013; Carder et al., 2014). The California Air Resources Board (ARB) also has initiated a pilot truck and bus surveillance program that includes chassis dynamometer testing from randomly selected trucks representing a range of manufacturers and mileages (Quiros et al., 2017; CARB., 2017). Some on-road studies using portable emissions measurement systems (PEMS) also have been conducted on 2007 and newer trucks equipped with DPF and/or SCR systems (Carder et al., 2014; Lee, et al., 2017; Tu et al., 2016; Misra et al., 2013, 2016).

The ARB has been utilizing in-use emissions testing results in the development of emissions factors for its Emission FACtors inventory model (EMFAC) model for a number of years (California Air Resources Board, 2015a, 2015b). Those emissions factors are developed from “zero-mile” emissions rates (ZMRs) that can be adjusted to account for engine deterioration with age and for variations in vehicle speed. For the EMFAC2007 and EMFAC2011 model, in-use emissions data were primarily obtained from the CRC E-55/59 study (Clark et al., 2006, 2007), which was limited to 2003 and older vehicles, coupled with estimates for 2007 and newer model year vehicles.

For the EMFAC2014 model, a greater emphasis was placed on developing emission factors for vehicles equipped with newer PM and NO_x aftertreatment control devices, and incorporating in-use emissions data from 2007 and newer engines/vehicles. Those data were derived from studies conducted by the CARB (2015a, 2015b) and testing associated with the SCAQMD study (Miller et al., 2013; Carder et al., 2014). Those studies included

some chassis dynamometer testing and some over-the-road testing with a PEMS. While this represented an important step in better quantifying emissions from 2007-2009 and 2010 and later model year vehicles, the data were still relatively scarce to serve as the basis for making important emissions inventory projections out to 2020 and beyond. In particular, for the 2010 and later model year technology engines, only 5 vehicle/engines were included in the CARB/SCAQMD studies, with all the engines being in the 2010-2011 model year range, which only covers the earliest implementation years for advanced NOx control strategies. More importantly, of those 5 engines, only 2 were certified to the 0.20 g/bhp-hr NOx standard, and both of those engines were from the same manufacturer. Additionally, 2 of the 5 engines utilized only exhaust gas recirculation (EGR) for NOx control, an approach that had a very limited production run.

The goal of this study is to provide additional information regarding emission rates of modern heavy-duty diesel vehicles equipped with the newest emission control strategies for reducing NOx. Testing was conducted on 5 HDDTs with model year 2012 to 2015 engines equipped with DPF and SCR systems. The vehicle matrix included 5 engines from heavy-duty engine manufacturers representing the majority of trucks operating in California, with two engines being from the same manufacturer. The engines/vehicles were certified to a 0.20 g/bhr-hp NOx emission limit, with the exception of one credit-using engine that was certified to a 0.35 g/bhr-hp NOx standard. Each vehicle was tested on the University of California at Riverside's (UCR's) heavy-duty chassis dynamometer over the four phases of ARB's Heavy Heavy-Duty Diesel Truck (HHDDT) cycle (i.e., idle, creep, transient, and cruise), the HHDDT-short or HHDDT-S cycle (which is a high-speed cruise

cycle), and the Urban Dynamometer Driving Schedule (UDDS) (which is a cycle considered to be the chassis dynamometer equivalent of the engine dynamometer transient test). The results obtained from this study can augment the data being used in the development of future emissions inventory model that are relied on throughout the regulatory process by the CARB and other governmental agencies.

2.3. Materials and Methods

2.3.1. Test Vehicles and Fuels

Five heavy-duty Class 8 diesel vehicles were tested in this program and selected from four heavy-duty engine manufacturers representing the majority of trucks operating in California. All of the vehicles had model year 2012 and newer engines with the mileages less than 30,000 miles. They were equipped with the latest generation of emissions control technology, including a DPF and a SCR system. The engines were certified to a 0.20 g/bhr-hp NO_x emission limit, with the exception of one engine that was certified to a 0.35 g/bhr-hp NO_x standard. The test fuel was the California No. 2 diesel. A description of the vehicles/engines is provided in Table 2-1.

Table 2-1 Engine/Vehicle specifications

Manufacturer	A1	A2	B	C	D
Model Year	2014	2015	2014	2014	2012
Displacement	14.9 L	14.9 L	12.8 L	12.4 L	12.8 L
Horsepower	400 HP	550 HP	450 HP	450 HP	415 HP
Vehicle Mileage	28611	2924	15914	7686	12640
Aftertreatment	DOC/DPF/SCR				
Standard/FEL Level	NOx:0.35	NOx:0.20	NOx:0.20	NOx:0.20	NOx:0.20
(g/bhp-hr)	PM:0.01	PM:0.01	PM:0.01	PM:0.01	PM:0.01
Certification Level	NOx:0.22	NOx:0.18	NOx:0.17	NOx:0.12	NOx:0.12
(g/bhp-hr)	PM:0.001	PM:0.000	PM:0.004	PM:0.003	PM:0.003

2.3.2. Test Cycles

There were six different driving cycles in this program, including four phases of ARB's HHDDT cycle (i.e., idle, creep, transient, and cruise) (Gautam et al., 2002), the HHDDT-S cycle (Clark et al., 2004), and the UDDS (U.S. Environmental Protection Agency, 2005). The characteristics of each test cycle are provided in Table 2-2. The preconditioning for the cycles was designed to be consistent with the procedures utilized in the earlier testing program the ARB (2015b) conducted to update its emission factors for EMFAC2014. Different numbers of replicates of each driving cycle were utilized in order to ensure that a sufficient mass of PM was collected for weighing. Duplicate tests were conducted for each driving cycle on each vehicle.

Table 2-2 Description of test cycles

Schedule	Time (s)	Avg Speed (mph)	Distance (mi)	Number of Iterations	Description
UDDS	1060	18.86	5.55	3	FTP surrogate
HHDDT Idle	900	0	0	3	Idle of vehicle
HHDDT Creep	256	1.7	0.124	10	Stop and go modes
HHDDT Transient	688	14.9	2.9	4	Local street driving
HHDDT Cruise	2083	39.9	23.1	1	Freeway driving
HHDDT-Short	760	49.9	10.5	2	High speed driving

2.3.3. Emission Measurements

The vehicles were tested on the chassis dynamometer with the inertial weight of 65,000 lbs. The emissions measurements were made using UCR's Mobile Emissions Laboratory (MEL). A detail description of MEL was provided by Cocker et al. (2004a, 2004b). For all tests, standard emissions measurements included total hydrocarbons (THC), non-methane hydrocarbons (NMHC), methane (CH₄), carbon monoxide (CO), NO_x, carbon dioxide (CO₂), and PM. Fuel consumption was derived from the CO₂, CO, and THC emissions by the carbon balance method, using typical densities and carbon weight fractions for California ULSD.

The mass concentrations of PM were obtained by analysis of particulates collected through an impactor with a 50% cutoff particle diameter of 2.5 μm on 47 mm diameter 2 μm pore Teflon filters (Whatman brand). The filters were measured for net gains using a UMX2 ultra precision microbalance with buoyancy correction in accordance with the weighing procedure guidelines set forth in the Code of Federal Regulations (CFR).

Sampling for PM was done cumulatively over the entire duration of the cycles due to the very low mass levels expected for PM.

Engine brake power was calculated using engine control module (ECM) broadcast J1939 standardized information, including the engine speed in revolutions per minute (rpm), ECM broadcast actual torque in (%) estimated using engine speed and instantaneous fuel flow, ECM broadcast friction torque in (%), and ECM broadcast reference torque in (ft-lb). Those signals are the same signals used for in-use compliance testing according to the test procedures in 40 CFR Part 1065.

2.4. Results and Discussion

The emission test results are presented in this section. Table 2-3 shows the emission rates of regulated pollutants on a g/mi basis for each vehicle /cycle combination based on the average of tests conducted on that particular test combination. Emissions on a g/bhp-hr basis are discussed at various points in the text of this section, and are shown in graphs in the supplementary material.

2.4.1. NO_x Emissions

2.4.1.1. NO_x emission rates

NO_x emissions for the test trucks are shown on a mass emitted per distance-traveled (grams/mile or g/mi) units in Table 2-3. NO_x emissions varied depending on the test cycle and the test truck. The manufacturer D truck was an outlier with noticeably higher NO_x emissions relative to the other vehicles. Therefore, this truck is discussed separately from other trucks. For the manufacturer A1, manufacturer A2, manufacturer B and manufacturer C engine-powered trucks, NO_x emissions ranged from 0.495 to 1.363 g/mi [0.308 to 0.847

g/km] over the UDDS (the cycle most relevant to ZMRs), from 2.131 to 9.468 g/mi [1.323 to 5.883 g/km] over the Creep cycle, from 0.803 to 3.252 g/mi [0.499 to 2.020 g/km] over the Transient cycle, from 0.068 to 0.471 g/mi [0.042 to 0.293 g/km] over the Cruise cycle, and from 0.067 to 0.249 g/mi [0.042 to 0.155 g/km] over the HHDDT-S. The lowest NO_x emissions were recorded over the Cruise and HHDDT-S cycles, which produced the highest speeds, loads, and exhaust temperatures. Under those conditions, SCR catalysts are expected to operate at temperatures (>250 °C) where NO_x conversion efficiencies are robust, leading to relatively low tailpipe NO_x emission (Misra et al., 2013), even though engine-out NO_x levels are likely highest. Higher emissions were observed over the other cycles, which include more transient and lower average speed operation, with different vehicles showing higher or lower emissions depending on the vehicle and cycle. The Creep cycle showed the highest NO_x emissions since it is comprised of short, low-speed accelerations between periods of idle that yield lower loads and exhaust temperatures (134~179 °C), and that cover a very short distance. It also should be noted that while the NO_x emissions on a per mile or per unit of work basis are considerable higher for the Creep, the differences between the Creep and other cycles is less significant in terms of absolute NO_x emissions.

The manufacturer D vehicle had poor NO_x conversion efficiencies relative to the other vehicles. Upon further investigation, it was found that this specific vehicle had served its entire life as a dealer demonstrator, and as such rarely or ever operated with a loaded trailer, and spent a considerable amount of time operating in an idle mode. This type of low-temperature, high proportion idle operation is known to cause significant exposure of

the aftertreatment system to unburned hydrocarbons in the exhaust stream. An examination of the logged electronic history revealed no OBD faults or other indications of failure or system malfunction. A clear anomaly, however, was that due to its unusual, unladed service history and duty cycle, the engine had never undergone a regeneration event, despite having been in service for approximately 2.5 years (albeit with only 12,000 miles on the odometer). A series of conventional parked regenerations were performed. After further operation, there was a significant recovery of the aftertreatment NO_x-conversion efficiency, as revealed through PEMS measurements. The regeneration intervention was believed to have been fully effective in driving off the accumulated unburned hydrocarbons that were hindering catalytic reaction. Additional chassis dynamometer testing of the manufacturer D vehicle was conducted at the West Virginia University (WVU) Center for Alternative Fuels Engines and Emissions (CAFEE) Laboratory, replicating the testing that had been performed at UCR, with the exception of a 70,000 lbs. [as opposed to UCR's 65,000 lbs. test weight]. The results of that testing indicated a NO_x emission rate of 0.39 g/mi over the UDDS cycle, near the lower end of the NO_x emission rates found in the current study. This example suggests that longtime non-regeneration could lead to poor SCR catalyst performance and high NO_x emission rates.

Table 2-3 Emission rates of regulated pollutants on a distance-specific unit and fuel economy

Engine	Trace	NO _x	CO ₂	THC	CO	PM	Fuel Economy	Conversion Factor
		g/mi						mi/gallon (mpg)
A1	UDDS	0.99 ± 0.38	1865 ± 51	0.017 ± 0.022	0.162 ± 0.069	0.006 ± 0.004	5.41 ± 0.14	3.40
	Creep	5.28 ± 4.16	4148 ± 330	0.391 ± 0.214	0.467 ± 0.287	0.004 ± 0.001	2.44 ± 0.19	
	Trans	1.82 ± 0.42	2260 ± 38	0.010 ± 0.038	0.088 ± 0.060	0.005 ± 0.003	4.46 ± 0.08	
	Cruise	0.07 ± 0.04	1160 ± 10	0.006 ± 0.006	0.024 ± 0.033	0.012 ± 0.001	8.69 ± 0.07	
	HHDDT-S	0.07 ± 0.04	1450 ± 12	0.003 ± 0.005	0.120 ± 0.056	0.010 ± 0.000	6.95 ± 0.06	
A2	UDDS	1.36 ± 0.30	2063 ± 176	0.000 ± 0.029	0.002 ± 0.000	0.002 ± 0.001	4.91 ± 0.37	3.52
	Creep	6.02 ± 4.29	3351 ± 1492	0.263 ± 0.155	0.003 ± 0.001	0.016 ± 0.022	2.11 ± 0.07	
	Trans	3.25 ± 1.66	2580 ± 101	- ± 0.030	0.003 ± 0.001	0.001 ± 0.002	3.91 ± 0.15	
	Cruise	0.12 ± 0.01	1327 ± 51	- ± 0.012	0.002 ± 0.001	0.002 ± 0.000	7.60 ± 0.29	
	HHDDT-S	0.08 ± 0.05	1707 ± 22	0.007 ± 0.007	0.002 ± 0.000	0.007 ± 0.005	5.91 ± 0.08	
B	UDDS	0.50 ± 0.22	2006 ± 58	0.026 ± 0.011	0.174 ± 0.028	0.003 ± 0.001	5.03 ± 0.14	3.63
	Creep	9.47 ± 6.48	3707 ± 288	0.239 ± 0.071	0.864 ± 0.579	0.006 ± 0.003	2.73 ± 0.19	
	Trans	0.80 ± 0.21	2436 ± 118	0.019 ± 0.007	0.105 ± 0.051	0.002 ± 0.000	4.15 ± 0.19	
	Cruise	0.17 ± 0.05	1264 ± 6	0.007 ± 0.004	0.101 ± 0.002	0.002 ± 0.000	7.97 ± 0.04	
	HHDDT-S	0.25 ± 0.15	1587 ± 14	0.003 ± 0.001	0.090 ± 0.025	0.002 ± 0.000	6.35 ± 0.06	
C	UDDS	0.81 ± 0.30	2128 ± 42	0.034 ± 0.004	0.079 ± 0.050	0.004 ± 0.002	4.74 ± 0.09	3.14
	Creep	2.13 ± 0.88	5095 ± 346	0.375 ± 0.105	2.447 ± 2.536	0.005 ± 0.002	1.99 ± 0.14	
	Trans	1.31 ± 0.44	2607 ± 151	0.024 ± 0.008	0.143 ± 0.056	0.012 ± 0.004	3.88 ± 0.21	
	Cruise	0.47 ± 0.03	1232 ± 2	0.003 ± 0.000	0.058 ± 0.033	0.010 ± 0.002	8.18 ± 0.01	
	HHDDT-S	0.22 ± 0.15	1646 ± 29	- ± 0.007	0.069 ± 0.032	0.033 ± 0.006	6.13 ± 0.11	
D	UDDS	3.52 ± 0.76	2219 ± 144	0.026 ± 0.014	0.178 ± 0.083	0.001 ± 0.000	4.56 ± 0.27	3.64
	Creep	22.50 ± 9.53	4850 ± 185	0.457 ± 0.210	5.042 ± 4.039	0.003 ± 0.002	2.08 ± 0.08	
	Trans	6.27 ± 2.02	2625 ± 47	0.014 ± 0.023	0.246 ± 0.228	0.002 ± 0.001	3.84 ± 0.07	
	Cruise	0.66 ± 0.22	1443 ± 1	0.009 ± 0.006	0.057 ± 0.005	0.003 ± 0.001	6.98 ± 0.00	
	HHDDT-S	0.75 ± 0.14	1744 ± 9	0.006 ± 0.003	0.059 ± 0.003	0.003 ± 0.000	5.78 ± 0.03	

The results of this study can also be compared to the emission factors being used in the EMFAC2014 model. For engines certified to the 0.20 g/bhp-hr NO_x level, EMFAC2014 utilizes a ZMR of 1.89 g/mi. This ZMR is adjusted by a fuel correction factor of 0.93 to account for the clean CARB diesel fuel used in California, such that a ZMR of 1.76 g/mi was used for the comparisons in this study for the 0.20 g/bhp-hr NO_x engines. The two vehicles used to develop those estimates are shown by the two bars on the right hand side of Figure 2-1. The results of this study, utilizing the post-DPF regeneration data for the manufacturer D1 (the four bars on the left side of Figure 2-1), can be readily compared with the data for the 0.20 g/bhp-hr engines that were used in developing the EMFAC2014 ZMR. The results of additional tests that were conducted on a subset of vehicles in the present study by the CARB at their heavy-duty chassis dynamometer facility in Los Angeles are also included in Figure 2-1 (the two middle bars). Significantly, average UDDS value for the current study for the 0.20 g/bhp-hr NO_x trucks are 0.77 g/mi utilizing the post-regeneration results for the manufacturer D1 truck.

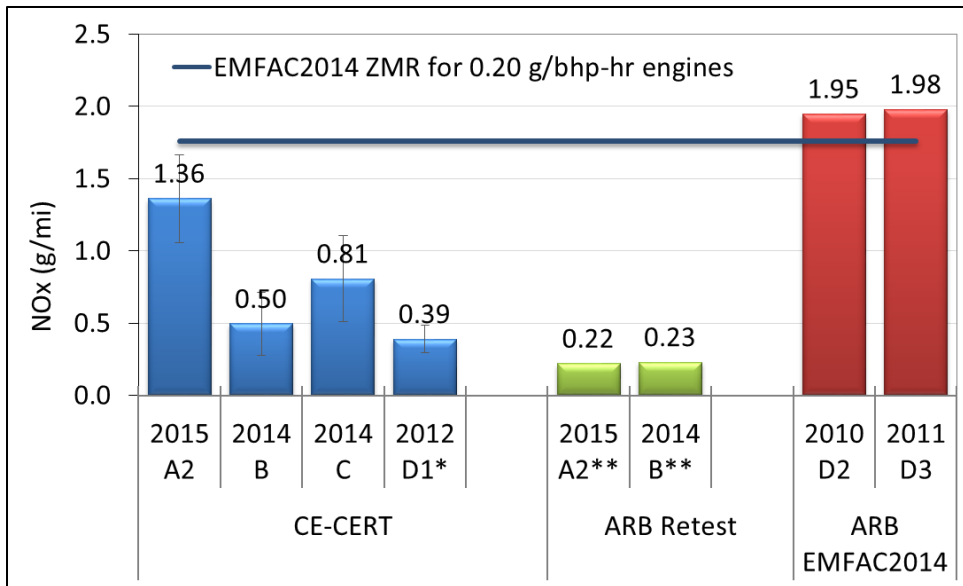


Figure 2-1 Comparisons of NOx emission rates over the UDDS from this study, CARB retesting of some of the vehicles from this study, and the CARB study that was used to develop EMFAC2014 emission factors for SCR-equipped 2010+ vehicles; D1* represents the UDDS emission level found after retesting the manufacturer D1 truck after a regeneration; A2 and B** represents results from CARB retest.**

The results of this study also can be compared to results from previous and on-going studies. Other studies have shown vehicles with emission rates similar to those seen in the current study. UCR measured UDDS NOx emission rates for trucks equipped a manufacturer A 8.3 liter engine, a manufacturer A 11.9 liter engine, and a manufacturer D 12.8 liter engine, which were found to be 1.07, 0.25, and 1.27 g/mi, respectively (Miller et al., 2013). In a related study, WVU found slightly higher UDDS NOx emissions of 1.98 g/mi for the same manufacturer D vehicle (D4) (Carder et al., 2015), which were more comparable with the manufacturer D vehicle results from CARB EMFAC2014 study (CARB, 2015a, 2015b). More recent information from a Truck and Bus Surveillance study being conducted by the CARB also found some of the vehicles with emission rates

comparable to the 0.2 g/bhp-hr standard over the UDDS (ARB, 2017; Quiros et al., 2017), while others were not, as discussed below.

Other information has indicated that some heavy-duty vehicles have higher emission rates. Those studies have included higher mileage vehicles or vehicles with emission levels high enough to suggest either major issues with their SCR systems or largely dysfunctional SCR systems, as the NO_x emissions are near what might be expected for engine out levels.” In the CARB Truck and Bus Surveillance study, a range of heavy-duty vehicles from 8 different engine families with model years ranging from 2010 to 2014 and mileages from 59,000 to 594,000 miles were tested (Quiros et al., 2017). Although some of the vehicles from the Quiros et al. study had emission rates comparable to the 0.2 g/bhp-hr standard, as discussed above, a number of vehicles had emission rates ranging from 1 to over 2 g/bhp-hr, considerably higher than those found in the present study. Thiruvengadam et al. (2015) also found emission rates of 6.11 and 9.39 g/mi over the UDDS for two 2010 SCR-equipped trucks.

Clearly, there is a significant range between the emission values of lower mileage or otherwise properly functioning heavy-duty vehicles, as tested in our study, and the higher emission rates from certain other studies that indicate significant SCR issues. The vehicles from this study, by design, represent low mileage vehicles that are well maintained and checked for any evidence of tampering, which may best represent the true emission rates for vehicles with mileages near zero. The ZMRs for heavy-duty vehicles for EMFAC incorporate a much wider range of vehicles with higher mileages, potentially different levels of deterioration, and SCR systems with functionality issues, and hence tend to be

higher than the values found in the current study. The most recent CARB estimates that have incorporated data from additional heavy-duty vehicles, including those from this study and other studies discussed above have suggested a ZMR of 2.40 g/mi for a baseline pre-CARB diesel fuel and 2.23 g/mi for a CARB diesel fuel for the 0.20 g/bhp-hr NO_x engines (CARB, 2017). Overall, understanding the relative populations of heavy-duty vehicles in different states of operating condition will be important in continuing to improve emission inventories going forward.

2.4.1.2. SCR temperature

For SCR-equipped vehicles, NO_x emissions are typically strongly correlated to the SCR temperature. Specifically, a minimum exhaust temperature is needed to promote hydrolysis of urea into ammonia (NH₃), which then reduces NO_x into nitrogen (N₂) and water (H₂O) (Majewski, 2006), with the SCR being most effective at temperatures above 250°C (CARB, 2015b). The average SCR inlet temperature for all vehicles in this study is provided in Figure 2-2. Note that the emissions for the Creep cycle are divided by 5 to allow the emissions over all 5 cycles to be more clearly presented on the same graph. The results show that the average SCR inlet temperature is at or above 250°C for the Cruise and HHDDT-S cycles for all of the vehicles. The SCR inlet temperature sensor for the manufacturer A2 vehicle was not working when the Cruise cycle was run. Note that although the SCR inlet temperature was not available for the manufacturer A2 engine, the SCR outlet temperature for that engine over the HHDDT-S cycle was above 250°C, indicating that the average SCR inlet would be above 250°C, as the inlet temperature was higher than the outlet temperature for all test combinations. NO_x emissions were lowest in

most cases for the Cruise and HHDDT-S cycles, consistent with the effective conversion rate of NO_x when the SCR has reached its effective operational temperature, with the increased NO_x reduction efficiency more than making up for the increased NO_x engine out emissions at high speed, high load operation. For the UDDS and Transient cycles, the average SCR inlet temperature was in the range of 213 to 261°C. This suggests that the SCR is at or above its operational temperature for only part of those cycles, which is consistent with the higher average NO_x emissions observed over the UDDS and Transient cycles compared to the two Cruise mode cycles. The lowest temperature was found over the Creep cycle, where the average SCR inlet temperature ranged from approximately 124 to 174°C. At those lower temperatures, the SCR would not be reducing NO_x emissions as effectively and the denominators in term of g/mi would be very low, so that is the cycle where the highest g/mi NO_x emissions were observed.

The average measured NO_x emissions are also shown in Figure 2-2 to provide an additional comparison between NO_x emissions and SCR inlet temperature. Overall, the results do not show significant trends in SCR inlet temperature vs. NO_x emissions beyond the general trends observed between the cycles discussed above. There are some slight differences in NO_x emissions that could be attributed to differences in SCR inlet temperature. For the UDDS, the manufacturer B truck had the lowest NO_x emissions and the highest average SCR inlet temperature, while the manufacturer A2 vehicle had the lowest average SCR inlet temperature and highest NO_x emissions of the trucks, other than the outlier manufacturer D truck. The manufacturer C truck had the highest SCR inlet temperature and corresponding lower NO_x emissions over the Creep cycle. On the other

hand, the manufacturer D truck engine did not have appreciably lower SCR inlet temperatures, suggesting that inlet temperature was not the primary factor in its higher NOx emissions (which were determined to be related to an absence of any regeneration event). Overall, although SCR temperature helps explain the difference in NOx emissions between cycles, the results suggest that other factors beyond just SCR temperature are likely responsible for the differences in the trends in NOx emissions for the different vehicles over the same test type. Additional comparisons between the real-time NOx emissions and the SCR temperatures are provided in the supplementary material for each vehicle over the UDDS.

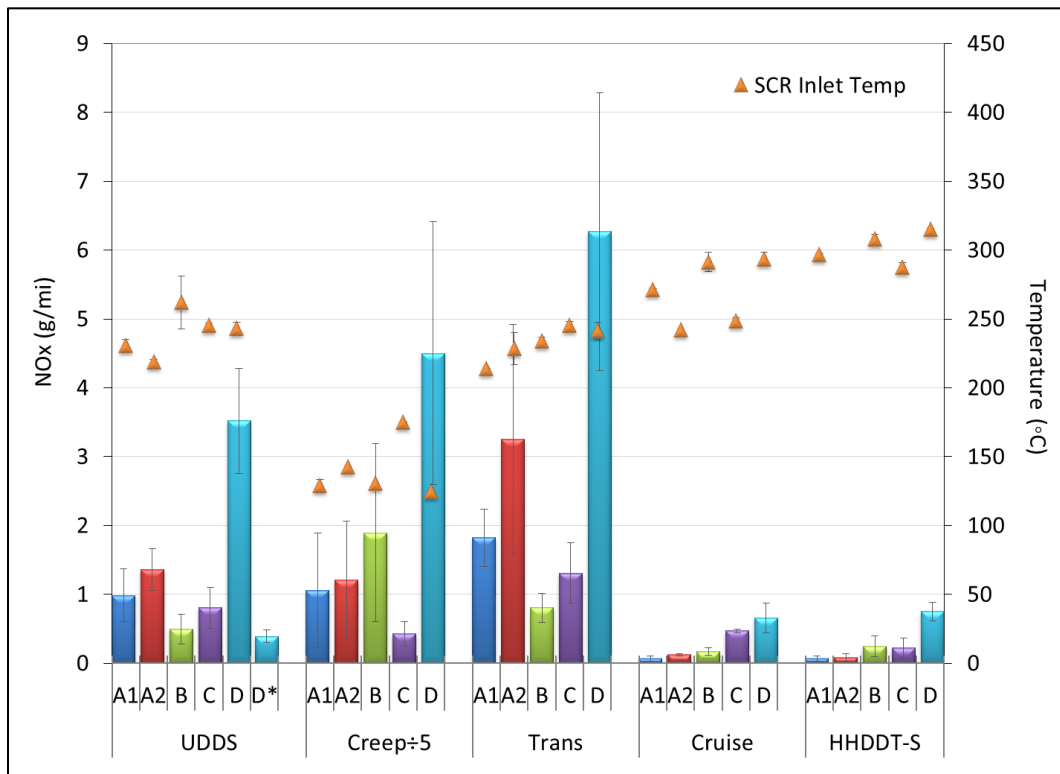


Figure 2-2 Average SCR inlet temperature

2.4.2. Other Regulated Pollutants

The emission rates of THC, CO and PM are shown on a distance-specific basis in Table 2-3. Overall, the values of those regulated pollutants were very low for most of the test cycles, due to the presence of the DOC/DPF/SCR aftertreatment system, and are comparable to background levels in some cases. Separate discussions of those pollutants are provided below.

2.4.2.1. PM mass

PM mass emissions were very low for most of the test cycles. PM emissions were below 0.015 g/mi [0.009 g/km] for all vehicles over all cycles, except for the manufacturer C truck over the HHDDT-S cycle and the manufacturer A2 truck over the Creep cycle. The PM levels are significantly below the 0.01 g/bhp-hr [0.013 g/kW-hr] PM standard under all test conditions, except the manufacturer C truck over the HHDDT-S cycle. The HHDDT-S PM data for manufacturer C were examined and it does not appear that any regenerations occurred during these outlier tests. It should also be noted that even these PM levels were comparable to the 0.01 g/bhp level, and were below the NTE limits, which are 1.5 x standard.

2.4.2.2. THC emissions

As expected, THC emissions were very low for most of the test cycles, due to the presence of the DOC/DPF/SCR aftertreatment system, and are comparable to background levels in some cases, as indicated by the negative values for some tests. THC emissions were below 0.034 g/mi [0.021 g/km] for all test vehicles over the UDDS, Transient, Cruise, and HHDDT-S cycles, and were below 0.458 [0.285 g/km] g/mi for all vehicles over all

test cycles. The Creep cycle did show considerably higher THC emissions on a per-mile basis, ranging from 0.241 to 0.458 g/mi [0.150 to 0.285 g/km] due its short, low-speed accelerations and longer idle periods.

2.4.2.3. CO emissions

CO emissions were very low for most of the test cycles. CO emissions were below 0.2 g/mi [0.12 g/km] for all vehicles over all cycles, except over the Creep cycle and the manufacturer D truck over the Transient cycle. Emissions over the Creep cycle ranged from 0.004 to 5.042 g/mi [0.02 to 3.133 g/km] and from 0.001 to 1.011 g/bhp-hr [0.001 to 1.356 g/kW-hr]. Overall, the CO emission rates were considerably below the 15.5 g/bhp-hr [20.8 g/kW-hr] and 14.0 g/bhp-hr [18.8 g/kW-hr] standards established by EPA and CARB, respectively, for all vehicles and cycles.

2.4.3. CO₂ Emissions and Fuel Economy

2.4.3.1. CO₂ emissions

CO₂ emissions for the five test trucks are shown in units of g/mi in Table 2-3. CO₂ emissions over the UDDS cycle ranged from 1864 to 2219 g/mi [1159 to 1379 g/km]. CO₂ emissions over the Transient cycle were similar to those over the UDDS, ranging from 2260 to 2624 g/mi [1404 to 1631 g/km]. CO₂ emissions over the Cruise and HHDDT-S cycles were slightly lower on a g/mi basis. CO₂ emissions ranged from 1160 to 1443 g/mi [721 to 897 g/km] and 1450 to 1743 g/mi [901 to 1084 g/km] for the Cruise cycle and the HHDDT-S cycle, respectively. CO₂ emissions were highest over the Creep cycle, where loads were lowest, ranging from 3351 to 5095 g/mi [2082 to 3166 g/km].

The ranges of CO₂ emissions observed in the current study are comparable to ranges found in other studies in the literature. In comparison, CO₂ emissions as measured in the earlier CARB study ranged from 1831 to 2964 g/mi over the UDDS, from 2034 to 2432 g/mi over the Transient cycle, from 1014 to 1558 g/mi over the Cruise cycle, from 1310 to 1898 g/mi for the High Speed Cruise cycle, and from 3805 to 5006 g/mi over the Creep cycle (CARB, 2015a, 2015b). For the previous UCR-SCAQMD study (Miller et al., 2013), CO₂ emissions for the Class 8 diesel trucks ranged from 2379 to 3117 g/mi over the hot UDDS cycle. For the previous WVU-SCAQMD study (Carder et al., 2014), CO₂ emissions for 2009 model year and newer Class 8 goods-movement diesel trucks ranged from 2115 to 2757 g/mi over the UDDS cycle. Note that some of the differences between those various studies could be due to differences in test weight loading, as the CARB study used a weight of 56,000 lbs., the SCAQMD study used a test weight of 69,500 lbs, and the present study used 65,000 lbs. It should also be noted that the range in CO₂ emissions for trucks tested over the same cycle in those two earlier studies is similar to that found in the current study.

2.4.3.2. Fuel Economy

Fuel economy for the five test trucks is shown in Table 2-3. Fuel economy was similar over the UDDS and Transient cycles. Fuel economy over the UDDS ranged from 4.56 to 5.41 mi/gal [1.94 to 2.30 km/l], while fuel economy over the Transient ranged from 3.84 to 4.46 mi/gal [1.63 to 1.90 km/l]. Fuel economy over the Cruise and HHDDT-S cycles was slightly better, ranging from 6.98 to 8.69 mi/gal [2.97 to 3.69 km/l] for the Cruise cycle, and from 5.78 to 6.95 mi/gal [2.46 to 2.96 km/l] for the HHDDT-S cycle. The lowest fuel economy was found over the Creep cycle, and ranged from 1.98 to 2.73

mi/gal [0.84 to 1.16 km/l], due to the slow speeds and stop-and-go nature of the cycle. Again, it should be noted that some of the differences in fuel economy between different vehicles for the same cycle at the same test weight could be more a function of the differences in the dynamometer loading between trucks due to different frontal areas, as opposed to differences in engine technologies/manufacturers. A more detailed discussion of the CO₂ emissions, as a surrogate for fuel economy, is provided in the supplementary material.

2.5. Conclusions

This study tested five heavy-duty Class 8 diesel trucks equipped with DPFs for PM emissions control and SCR systems for NO_x emissions control. The vehicles tested ranged in model year from 2012 to 2015, and were certified to a 0.20 g/bhp-hr [0.27 g/kW-hr] NO_x emissions standard, with the exception of one engine that was certified to a 0.35 g/bhp-hr [0.47 g/kW-hr] standard. Each vehicle was tested on UCR's heavy-duty chassis dynamometer over the four phases of CARB's HHDDT cycles, the HHDDT-S cycle, and the UDDS. The conclusions of this study are summarized below.

NO_x emissions varied depending on the test cycle and the test truck. For the manufacturer A1, manufacturer A2, manufacturer B and manufacturer C trucks, NO_x emissions over the UDDS cycle ranged from 0.495 to 1.363 g/mi (0.136 to 0.387 g/bhp-hr) [0.308 to 0.847 g/km (0.182 to 1.341 g/kW-hr)]. On a bhp-hr basis, those emission levels are comparable to or below the 0.20/0.35 NO_x [0.268/0.469 g/kW-hr] level for three of the four vehicles, while one vehicle was higher than the certification standard at 0.387 g/bhp [0.519 g/kW-hr]. NO_x emissions over the CARB chassis dynamometer transient

cycle were slightly higher than for the UDDS (0.803 to 3.252 g/mi [0.499 to 2.020 g/km]). The lowest emissions were found over the two cruise cycles, with NO_x emissions ranging from 0.067 to 0.249 g/mi [0.042 to 0.155 g/km g/km] for the HHDDT-S and from 0.068 to 0.471 g/mi [0.042 to 0.293 g/km] for the Cruise cycle. The highest NO_x emissions were seen for the Creep cycle, which showed NO_x emission ranging from 2.131 to 9.468 g/mi [1.323 to 5.883 g/km g/km].

The manufacturer D truck was an outlier with noticeably higher NO_x emissions relative to the other vehicles. In this study, on a g/mi basis, its NO_x emissions were 3.519 [2.187 g/km] over the UDDS. Subsequent to the initial testing of this vehicle, it was found that the engine had never undergone a regeneration event, due to its unusual, unladed service history and duty cycle. After a series of conventional parked regenerations were performed, additional chassis dynamometer testing showed a NO_x emission rate of 0.39 g/mi [0.24 g/km] over the UDDS cycle, near the lower end of the NO_x emission rates found in the current study.

The NO_x results of this study and other recent studies suggest that there is a wide range of NO_x emission levels in the in-use fleet. The results of this study, by design, best represent low mileage, well maintained heavy-duty vehicles, while other studies have shown higher NO_x emission rates for higher mileage vehicles or vehicles that appear to have SCR system issues. The ZMRs for heavy-duty vehicles for EMFAC incorporate a wide range of vehicles with higher mileages, potentially different levels of deterioration, and SCR systems with functionality issues, and hence tend to be higher than the values found in the current study. Understanding the relative populations of heavy-duty vehicles

in different states of condition will be important in continuing to improve emission inventories going forward.

PM, THC, and CO emissions were found to be very low under most of the testing conditions. PM emissions were below 0.015 g/mi [0.009 g/km] for nearly all vehicle/cycle combinations. THC emissions were below 0.05 g/mi [0.03 g/km] for all test cycles except the Creep cycle, which showed THC emissions ranging from 0.241 to 0.458 g/mi [0.150 to 0.285 g/km]. CO emissions were below 0.2 g/mi [0.12 g/km] for almost all vehicles and cycles, except over the Creep cycle. Fuel economy ranged from 3.84 to 8.69 mi/gal [1.63 to 3.69 km/l] for the non-Creep cycles, with higher fuel economies found for the cycles representing driving at highway cruising speeds.

2.6. Acknowledgements

The authors thank the following organizations and individuals for their valuable contributions to this project. We acknowledge funding from the Truck and Engine Manufacturers Association, Chicago, Illinois. We acknowledge the participation of the California Air Resources Board (ARB) in this program, including involvement in the development of the test plan, the selection of the test vehicles, and their own chassis dynamometer testing of three of the five selected vehicles. We acknowledge Mr. Don Pacocha, Mr. Eddie O'Neal, and Mr. Joe Valdez of the University of California, Riverside for their contributions in conducting the emissions testing for this program.

2.7. References

- Bartley, G.J., Kostek, T., 2012. SCR Deactivation Study for OBD Applications. SAE Technical Paper No. 2012-01-1076. Society of Automotive Engineers, Warrendale, PA.
- California Air Resources Board, 2015a. Mobile Source Emissions Inventory and Assessment. Los Angeles. <http://www.arb.ca.gov/msei/msei.htm> (access 16.10.05).
- California Air Resources Board, 2015b. EMFAC2014 Volume III Technical Documentation. <https://www.arb.ca.gov/msei/downloads/emfac2014/emfac2014-vol3-technical-documentation-052015.pdf> (access 16.10.05).
- California Air Resources Board, 2017. EMFAC2017 An update to California On-road Mobile Source Emission Inventory. https://www.arb.ca.gov/msei/downloads/emfac2017_workshop_june_1_2017_final.pdf (access 17.07.05).
- Carder, D. K., Gautam, M., Thiruvengadam, A., Besch, M. C., 2014. In-Use Emissions Testing and Demonstration of Retrofit Technology for Control of On-Road Heavy-Duty Engines. Final Report by West Virginia University to the South Coast Air Quality Management District under contract No. 11611, July.
- Clark, N. N., Gautam, M., Wayne, W. S., Lyons, D. W., Thompson, G., Zielinska, B., 2007. Heavy-duty vehicle chassis dynamometer testing for emissions inventory, air quality modeling, source apportionment and air toxics emissions inventory, E-55/59 all phases. Final Report by West Virginia University to the Coordinating Research Council, August. Available at <www.crao.com>.
- Clark, N. N., Gautam, M., Wayne, W. S., Thompson, G. J., Lyons, D. W., 2004. California heavy heavy-duty diesel truck emissions characterization for project E-55/E-59 phase 1.5. Final Report by West Virginia University to the Coordinating Research Council.
- Clark, N., Gautam, M., Wayne, W. S., Thompson, G. J., Nine, R. D., Lyons, D. W., Buffamonte, T., Xu, S., Maldonado, H., 2006. Regulated emissions from heavy heavy-duty diesel trucks operating in the south coast air basin. SAE Technical Paper No. 2006-01-3395. Society of Automotive Engineers, Warrendale, PA.
- Code of Federal Regulations, 2010. Control of Emissions from New and In-Use Highway Vehicles and Engines. 40 CFR Part § 86.
- Couch, P., Leonard, J., 2011. Characterization of Drayage Truck Duty Cycles at the Port of Long Beach and Port of Los Angeles. Final Report prepared by TIAX for the Ports of Long Beach and Los Angeles, March.

- Federal Highway Administration, 2000. Table III-4, Comprehensive Truck Size and Weight Study. <http://www.fhwa.dot.gov/reports/tswstudy/Vol3-Chapter3.pdf> (access 16.09.11).
- Gautam, M., Clark, N., Riddle, W., Nine, R., Wayne, W. S., Maldonado, H., Agrawal, A., Carlock, M., 2002. Development and initial use of a heavy-duty diesel truck test schedule for emissions characterization. SAE Technical Paper No. 2002-01-1753. Society of Automotive Engineers, Warrendale, PA.
- Gieshoff, J., Schäfer-Sindlinger, A., Spurk, P.C., Van Den Tillaart, J.A.A., Garr, G., 2000. Improved SCR systems for heavy duty applications. SAE Technical Paper No. 2000-01-0189. Society of Automotive Engineers, Warrendale, PA.
- Khan, A. S., Clark, N. N., Thompson, G. J., Wayne, W. S., Gautam, M., Lyon, D. W., Hawelti, D., 2006. Idle emissions from heavy-duty diesel vehicles: review and recent data. *Journal of the Air & Waste Management Association*, 56(10), 1404-1419.
- Khair, M. K., Majewski, W. A., 2006. Diesel emissions and their control. Society of Automotive Engineers, Warrendale, PA.
- Lee, D-H., O’Cain, J.E., Avila, J., Lemieux, S.C., Karim, J., Berdahl, S., Sahay, K., Na, K., Chang, O., Sardar, S., Macias, K.A., 2017. Heavy-duty In-Use Compliance Testing Program Results. Presentation at 27th CRC Real World Emissions Workshop, Newport Beach, CA, March.
- Li, Y., Xue, J., Johnson, K., Durbin, T., Villela, M., Pham, L., Hosseini, S., Zheng, Z., Short, D., Karavalakis, G., Asa-Awuku, A., 2014. Determination of suspended exhaust PM mass for light-duty vehicles. SAE Technical Paper No. 2014-01-1594. Society of Automotive Engineers, Warrendale, PA.
- Littera, D., Besch, M., Cozzolini, A., Carder, D., Thiruvengadam, A., Sayres, A., Kappanna, H., Gautam, M., Oshinuga, A., 2011. Fresh and Aged SCRT Systems Retrofitted on a MY 1998 Class-8 Tractor: Investigation on In-use Emissions. SAE Technical Paper No. 2011-24-0175.
- Miller, W., Johnson, K.C., Durbin, T., P. Dixit., 2013. In-Use Emissions Testing and Demonstration of Retrofit Technology for Control of On-Road Heavy-Duty Engines. Final Report by University of California, Riverside to the South Coast Air Quality Management District under contract no. 11612, September.
- Misra, C., Collins, J. F., Herner, J. D., Sax, T., Krishnamurthy, M., Sobieralski, W., Burntizki, m., Chernich, D., 2013. In-Use NOx Emissions from Model Year 2010 and 2011 Heavy-Duty Diesel Engines Equipped with Aftertreatment Devices. *Environmental Science & Technology*, 47(14), 7892-7898.

- Misra, C., Yoon, S., Collins, J., Chernich, D., Herner, J., 2016. Evaluating In-Use SCR Performance: Older vs. Late MY Engines. Presentation at 26th CRC Real World Emissions Workshop, Newport Beach, CA, March.
- Misra, C.H., Pournazeri, S., Zhou, L., and Hughes, V., 2017. Updates to MY2010+ Heavy-Duty Emissions in EMFAC. Presentation at the 27th CRC Real World Emissions Workshop, Long Beach, CA, March.
- Nova, I., Ciardelli, C., Tronconi, E., Chatterjee, D., Bandl-Konrad, B., 2006. NH₃-NO/NO₂ chemistry over V-based catalysts and its role in the mechanism of the fast SCR reaction. *Catalysis Today*, 114(1), 3-12.
- Quiros, D.C., Ham, W.A., Ianni, R., Smith, J.D., Sobieralski, W., Chernich, D.J., Hu, S., Huai, T., 2017. Assessing Emission Control System Durability using ARB's Pilot Heavy-Duty Truck and Bus Surveillance Program. Presentation at the 27th CRC Real World Emissions Workshop, Long Beach, CA, March.
- Schaefer, M., Hofmann, L., Girot, P., Rohe, R., 2009. Investigation of NO_x-and PM-reduction by a Combination of SCR-catalyst and Diesel Particulate Filter for Heavy-duty Diesel Engine. *SAE International Journal of Fuels and Lubricants* No. 2009-01-0912.
- Tu, J., Berdahl, S., Tran, T., O'Cain, J., Karim, J., Sardar, S., Lemieux, S., Huai, T., 2016. Study of heavy-duty vehicle emissions during in-use compliance testing. Presentation at 26th CRC Real World Emissions Workshop, Newport Beach, CA, March.
- U.S. Environmental Protection Agency, 2015. Heavy Trucks, Buses, and Engines. <http://www.epa.gov/otaq/hd-hwy.htm#regs>.

3. Certification and In-Use Compliance Testing for Heavy-Duty Diesel Engines to Understand High In-Use NO_x Emissions

3.1. Abstract

Given the importance of achieving actual oxides of nitrogen (NO_x) emissions over the road, it is important to investigate and understand the differences between certification and in-use emission rates and to understand the factors contributing to these differences and discrepancies. For this program, two 2010-compliant HDDV engines equipped with diesel particulate filter (DPF) and selective catalytic reduction (SCR) technologies were evaluated using an engine-dynamometer, a chassis-dynamometer, and on-road. The results showed that in-use NO_x emissions over the urban driving cycles of chassis dynamometer, on-road and engine dynamometer tests were above the 0.2 g/bhp-hr level for both vehicles with the highest emissions for the chassis dynamometer testing. For the freeway/steady state testing, the results were much lower compared with the results of urban driving cycles. For the UDDS, the differences between the tailpipe NO_x emissions could be attributed to several factors, including differences in SCR inlet NO_x temperatures, and engine out NO_x emissions. The cycle average SCR efficiencies for both vehicles ranged from 68 to 98%, with the SCR efficiencies for the cruise and hi-speed cruise cycles being higher than those for the urban driving cycles. For the on-road testing, the results from the Not to Exceed (NTE) analysis showed that the manufacturer A truck passed the NTE criteria for 7 of 9

tests, while the manufacturer B truck passed for only 3 of 9 tests. The current NTE has the limitation of low coverage of activity. Using modified NTE criteria, where the criteria for excluding data was lowered to below 10% maximum power and torque, only a small increase in the percentage of activity covered was found. The activity analysis of Moving Averaging Window (MAW) showed a significant improvement of the amount of data that was included. The emissions were found to fail the MAW test for a majority of the routes.

3.2. Introduction

The State of California has a number of regions that are out of compliance with national air quality standards for both ozone and particulate matter (PM) emissions. Although considerable progress has been made in reducing the contributions of vehicle emissions to the emissions inventory and in improving air quality, further reductions in oxides of nitrogen (NOx) emissions are still needed to achieve future air quality goals. Heavy-duty diesel vehicles (HDDVs) and heavy-duty diesel engines (HDDEs) are the largest sources of NOx emissions, and as such have been the source of a number of regulations. The implementation of new emissions beginning in 2010 for new HDDEs were designed to provide 90 percent reductions in NOx emissions, which have generally been met by selective catalytic reduction (SCR) aftertreatment control strategies in combination with other engine design changes. California also has an In-use Truck and Bus regulation designed to accelerate fleet turnover such that by the 2023 nearly all trucks operating in California will have engines complying with the 2010 emissions standards.

In order to achieve air quality goals, it is important that the levels of reductions anticipated with the implementation of more stringent emissions standards can be achieved

during typical operating conditions on the road. Currently, HDD engines are certified to meet emission standards before the engines are integrated into a vehicle chassis for commercial use. HDDE certification tests are conducted on an engine-dynamometer over the Federal Test Procedure (FTP) cycle that was developed to be representative of real-world HDDV driving patterns. This is due in part to the wide range of applications that particular engine might be used for, and the expense/complexity of testing vehicles from a wide range of applications on a heavy-duty chassis dynamometer. HDDEs integrated into a vehicle chassis for commercial use also need to comply with in-use HDDV Not-To-Exceed (NTE) emission limits and testing requirements (US EPA). The NTE regulations are intended to ensure that in-use HDDV emissions are controlled over a wide range of speed and load, especially during sustained high load, steady-state operations. The NTE requires monitoring of emissions under in-use conditions for a subset of engines sold in different engine families for a give engine manufacturer.

While significant steps have been taken to reduce NO_x emissions from HDDVs, it is still uncertain how effective these changes have been in reducing in-use NO_x emissions. The NTE regulations, were designed primarily to prevent off-cycle emissions from high-speed high-load line-haul operation on freeways, but a substantial fraction of vehicle activity and NO_x emissions are not subjected to in-use emission limits, especially at low-speed low-load stop-and-go HDDV operations. Additionally, chassis dynamometer and on-road testing are showing smaller reductions in NO_x emissions than would be expected based on the emissions standards. This includes recent studies that have shown that NO_x emissions measured from 2010 in-use HDDV on chassis-dynamometers over the Urban

Dynamometer Driving Schedule (UDDS) cycle are substantially higher than the certification standard of 0.2 g/bhp-hr NO_x (Miller et al, 2014). Although the conditions for the UDDS on a chassis dynamometer do not replicate the FTP on an engine dynamometer, the UDDS is designed to be compared to the FTP engine-dynamometer cycle and the engine torque and RPM values experienced over the UDDS cycle are similar to the torque and RPM values from the FTP engine dynamometer cycle.

Given the importance of achieving actual NO_x emissions over the road, it is important to investigate and understand the differences between certification and in-use emission rates and to understand the factors contributing to these differences and discrepancies. For this program, a minimum of two 2010-compliant HDDV engines equipped with diesel particulate filter (DPF) and selective catalytic reduction (SCR) technologies will be evaluated using an engine-dynamometer, a chassis-dynamometer, and on-road. This study will include an evaluation of the emissions as well as the activity differences between the different methods. Testing will be conducted over a number of different cycles or driving conditions to evaluate a wide range of engine and vehicle operations. Test data collected from all measurement methods will be analyzed and compared with each other. The differences between the different test methods will also be evaluated in term of the theoretical principles, purposes, and characteristics of the different methods. Based on findings from this study, the effectiveness of current HDDE certification procedures and HDDV in-use compliance procedures will be assessed and possible enhancements or alternatives to those procedures will be evaluated.

3.3. Materials and Methods

3.3.1. Test Vehicles and Fuels

Two 2010-compliant HDDVs that are certified to the 0.20 g/bhp-hr NO_x standard were recruited for the testing. The two vehicles had different makers with a model year of 2013 for the manufacturer A truck and a model year of 2014 for the manufacturer B truck. The latest generation of emissions control technology (SCR system) were equipped for both vehicles. The displacements were 12.8 liter of both vehicles with the manufacturer B truck having a higher rated power (500 hp) than the manufacturer A truck (405 hp). The test fuel was the California No. 2 diesel. The specifications were provided in Table 3-1

Table 3-1 Engine/Vehicle specifications

Maker	Model Year	Engine size	Rated Power	Mileage	Aftertreatment	NO _x Standard
A	2014	12.8L	405 @1700 rpm	135,000	DOC/DPF/SCR	0.20 g/bhp-hr
B	2013	12.8L	500@1800 rpm	226,000	DOC/DPF/SCR	0.20 g/bhp-hr

3.3.2. Test Cycles, Test Matrix, and Test Methods

Chassis Dynamometer Testing. Each vehicle was tested over the four phases of the Heavy Heavy-Duty Diesel Truck (HHDDT) schedule developed by the California Air Resources Board (i.e., idle, transient, and cruise), with the exception of the creep cycle, the HHDDT short or (HHDDT-S) cycle, which high speed cruise schedule, and the UDDS. The characteristics of each test cycle are provided in Table 3-2. Three tests were conducted on each of the cycles. The pre-conditioning was one UDDS cycle of hot start UDDS cycle

and cruise at a speed of 45mph for 15 minutes of other hot start cycles such that the engine remains warm.

On-Road Testing. The on-road tests were conducted over portions of a test route that has been used by the ARB in-use testing studies. To provide a comparison with in-use testing studies that have been conducted by the ARB, this study utilized a route that goes from the Riverside to Hesperia, from Hesperia to Indio, and then from Indio returning to the Riverside. This route is shown in Figure 3-1. The Riverside to Hesperia test route is uphill driving and needs higher load on the engine, while the Hesperia to Indio route includes considerable downhill driving and require less load. The Indio to Riverside route is also uphill driving, but less gradient and smoother compared with the Hesperia to Indio route.



Figure 3-1 In-use Testing Route

The on-road version of UDDS cycles was also conducted in this study in order to compare the difference in emission rates between chassis dynamometer, engine dynamometer and on-road. A section of road near Thermal, California in the Palm Springs

area were selected to conduct the UDDS cycle. This section of road is located at an elevation near sea level and has an approximately 2 mile stretch of road without a stop sign, and where traffic is light and sparse minimizing the potential need for stopping. Although the road provides significant advantages, the length of the road was still too short for the duration of an entire UDDS test cycle. As such, sampling was split into three separate testing sections that need to be integrated to get the total mass emission rates. Note that in previous studies, comparison of the on-road UDDS, split into sub-segments, showed good correlation with test results from the same vehicle on a chassis dynamometer. The special segmented UDDS cycle driving trace was programmed into a driver's aid computer that the driver can follow over the course of the cycle under the condition of no safety risk while conducting the testing.

Engine Dynamometer Testing. The test cycles included two standard engine-dynamometer cycles (the FTP and the ramped modal cycle - supplemental emissions test, RMC-SET) that were developed based on the CFR specifications. The engine versions of the CARB 4-mode cycles also were used, including the CARB-transient, CARB-cruise, and CARB-high-speed cruise. The characteristics of each test cycle are provided in Table 3-2. An engine dynamometer version of the UDDS also was developed. This UDDS cycle was developed by translating relevant engine operational data from the chassis dynamometer testing, including the engine torque, rpm, and power for each specific engine. A separate UDDS cycle was constructed for each of the test vehicles/engines. Preliminary tests with each test cycle were conducted with each engine to insure the proper operation

of the engine over the cycle prior to beginning the testing. This also included setting the idle point and running engine maps to map out the operational conditions.

Chassis Dynamometer Retesting. Under this task, the two test vehicles were retested on the chassis dynamometer. The vehicles were tested over the same five driving cycles, namely the UDDS, CARB-creep, CARB-transient, CARB-cruise, and CARB-high-speed cruise. Testing was consistency with the initial chassis dynamometer testing. A description of the test sequence for each vehicle is provided in Table 3-2.

Table 3-2 Description Test Cycles of Chassis Dynamometer, On-Road and Engine Dynamometer

Laboratory	Test Cycle	Time	Avg Speed (mph)	Distance (mi)
First and Second Chassis Dynamometer	Cold-start UDDS	1061s	18.86	5.55
	UDDS	1061s	18.86	5.55
	HHDDT Transient	668s	14.9	2.9
	HHDDT Cruise 55	2083s	39.9	23.1
	HHDDT Cruise 65	760s	49.9	10.5
On-Road	UDDS	1061s	18.86	5.55
	UDDS M1	529	11.4	1.69
	UDDS M2	289	41.5	3.3
	UDDS M3	242	7.94	0.53
	CE-CERT-Hesperia	49 mins		47
	Hesperia-Indio	1h 41mins		110
	Indio-CE-CERT	1h 15mins		77
Engine	Cold-start FTP	1200s		
	FTP	1200s		
	UDDS	1061s		
	RMC	2380s		
	HHDDT Transient	668s		
	HHDDT Cruise 55	2083s		
	HHDDT-S Cruise 65	760		

3.3.3. Emission Measurements

The primary emissions measurements were collected with CE-CERT's Mobile Emissions Laboratory (MEL). The MEL measures criteria pollutants, and particulate matter (PM) with a constant volume sampling (CVS) system meeting 40 CFR Part 1065 requirements (Cocker et al., 2004a) for both chassis dynamometer testing and engine dynamometer testing in this study. For all tests, standard emissions measurements of total hydrocarbons (THC), carbon monoxide (CO), oxides of nitrogen (NO_x, NO, NO₂), carbon dioxide (CO₂), and particulate matter (PM), were measured.

In addition to the primary emissions measurements, additional emissions measurements were also made with a PEMS system for gaseous and PM emissions. The PEMS measurements were included to provide an independent confirmation of emission differences between chassis and engine dynamometer testing and to gather information on the comparability of PEMS to CVS testing. The emissions measurements were conducted using the PEMS system for the chassis dynamometer testing, on-road testing and engine dynamometer testing. The PEMS system measured NO_x, CO, CO₂, THC and PM emissions.

3.4. Results and Discussion

3.4.1. NO_x Emissions

The NO_x emissions test results are presented in this section. Emissions were measured with both MEL and PEMS systems for most testing combinations, with the exception of the on-road without MEL and the final chassis dynamometer testing without PEMS. The error bars on the figures are the standard deviation for each test combination.

3.4.1.1. NO_x Emission rates

NO_x emissions for the manufacturer A truck and manufacturer B truck are shown on a g/bhp-hr in Figure 3-2 for the urban driving cycles, including the CS-UDDS, UDDS, CS-FTP, FTP and HHDDT-transient cycles. These figures include the results for the initial and final Chassis dynamometer tests, the on-road tests, and the engine dynamometer tests. The average SCR inlet temperature for each cycle is also included in these figures. The results for the manufacturer A truck and the manufacturer B truck are shown in the top and bottom panels, respectively, of each figure.

The NO_x emissions ranged from 0.16 to 1.1 g/bhp-hr over all of the urban test conditions for both vehicles. In comparing the results for the different test cycles between the different testing conditions (i.e., chassis dynamometer, on-road, and engine dynamometer), the results showed mixed trends, depending on the vehicle and test cycle. The manufacturer A truck for the UDDS showed the highest emissions for the chassis dynamometer testing, followed by the on-road testing, and then with the lowest emissions for the engine dynamometer testing. For the manufacturer A truck, discussion with the manufacturer indicated that the engine was running in a cold-start mode during the engine dynamometer testing due to the absence of vehicle dash cluster communication. In this mode, the fuel injection timing was retarded, leading to lower NO_x emissions for the engine dynamometer testing. The transient test for the manufacturer A truck were comparable between the chassis dynamometer and engine dynamometer tests. The manufacturer B truck also showed the highest UDDS results for the chassis dynamometer testing, with comparable results for the on-road and engine dynamometer UDDS results.

The manufacturer B truck showed opposite results for the transient cycle, however, with lower emissions for the chassis dynamometer testing compared to the engine dynamometer testing results.

The results for the freeway/steady state tests were generally lower than those for the urban cycles. For the manufacturer A truck, the cruise results were on the order of 0.1 g/bhp-hr, while the high-speed cruise results were 0.3 g/bhp-hr or less. For the manufacturer B truck, the cruise and high speed cruise results were on the order of 0.3 g/bhp-hr or less based on the MEL results. Although there were some differences between the initial and final Cruise and Hi-Speed Cruise cycles, there were not any consistent differences between the initial and final testing. In comparing the results for the different test cycles between the different testing conditions for the freeway/steady state tests, the results were more consistent than those of urban cycles.

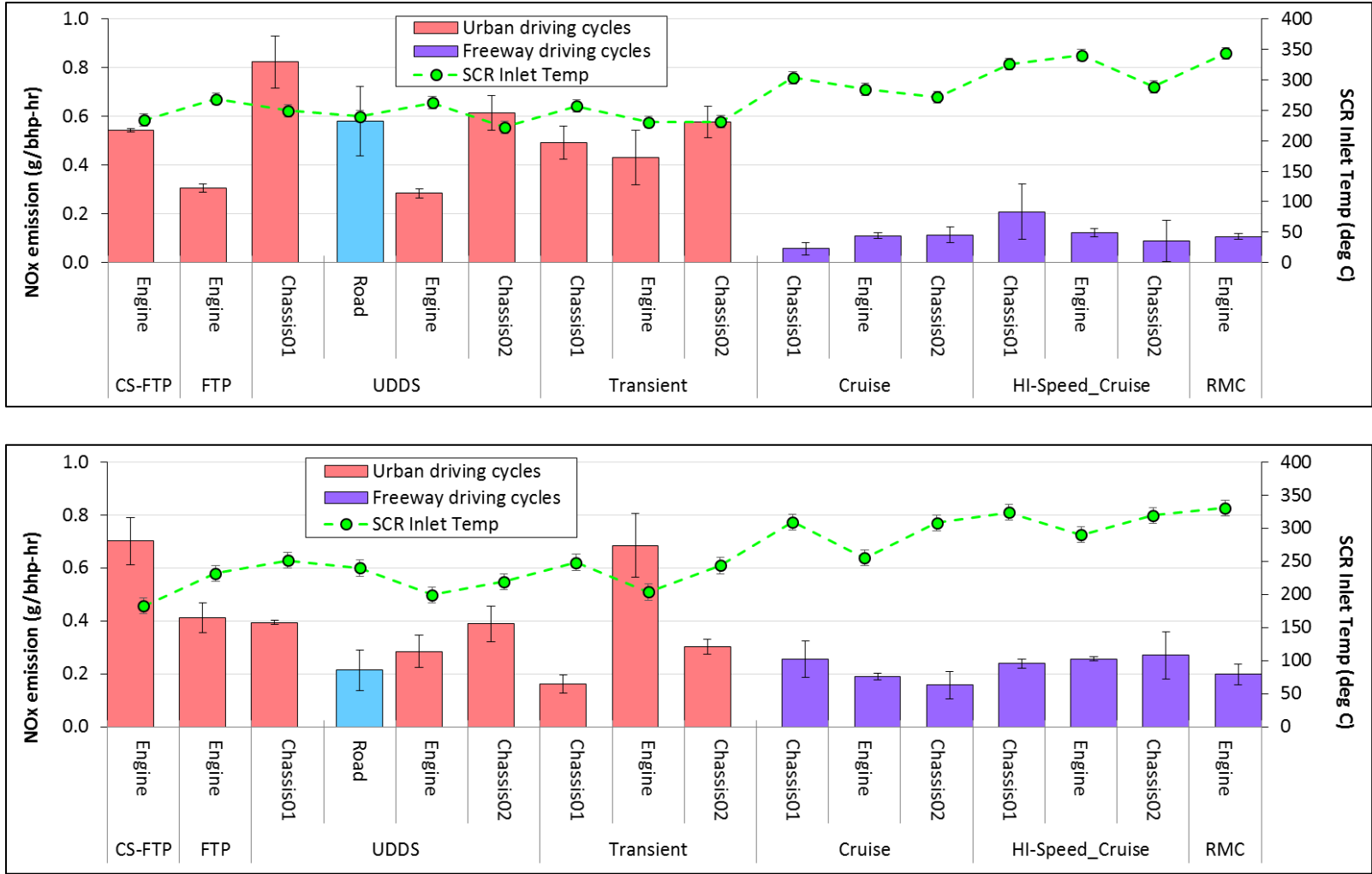


Figure 3-2 Average NOx Emissions on a g/bhp-hr Basis for the urban cycles for the manufacturer A truck (top) and the manufacture B truck (bottom)

The results of this study can also be compared to results from previous and on-going studies. Jiang et al. (2018) measured UDDS NO_x emission rates for four MY 2012 or newer HDDVs with the low mileages (<30,000miles). The NO_x emissions ranged from 0.14 and 0.39 g/bhp-hr over the UDDS cycle, which was consistent with the 0.39 g/bhp-hr emission rate of the manufacturer B vehicle tested in this study. The UDDS NO_x emission rates of 0.82 g/bhp-hr for the manufacturer A vehicle was much higher than the range reported by the EMA study. Other studies have indicated that some heavy-duty vehicles have higher emission rates. Thiruvengadam et al, (2015) found slightly higher UDDS NO_x emissions of 1.28 and 2.07 g/bhp-hr for two SCR equipped HDDVs. More recently, CARB has collected information from a range of different trucks as part of a Truck and Bus Surveillance study. This included data on 20 trucks that was used to update the Emission FACTors inventory model 2017 (EMFAC 2017) (CARB, 2018). The vehicles from this study showed a with range of emission rates, with some comparable to the 0.2 g/bhp-hr standard over the UDDS, but with many vehicles with higher emission rates ranging from 1 to over 2 g/bhp-hr (CARB, 2017; Quiros et al., 2017).

For SCR-equipped vehicles, NO_x emissions are typically strongly correlated to the SCR temperature. Specifically, a minimum exhaust temperature is needed to promote hydrolysis of urea into ammonia (NH₃), which then reduces NO_x into nitrogen (N₂) and water (H₂O) (Majewski, 2006). That requisite conversion temperature is typically around 250°C. The SCR inlet temperatures for all vehicles in this study is provided in Figure 3-2. For the urban driving cycles for the manufacturer A truck, all the hot start cycles had average SCR inlet temperatures above 250°C, except for the UDDS cycle for the second

chassis dynamometer test, on-road UDDS and the transient cycles for the engine dynamometer and the second chassis dynamometer tests. The average SCR inlet temperatures for the cold start cycles ranged from 217 to 240°C were comparable to the range of 222 to 269°C of the hot start UDDS and FTP cycles for both chassis dynamometer testing and engine dynamometer testing for the manufacturer A truck. For the urban driving cycles of the manufacturer B truck, only the hot start UDDS cycles of the first chassis dynamometer testing had average SCR temperatures above 250°C. The average SCR inlet temperatures of the cold start cycles ranged from 165 to 182°C, which was much lower than the range of 199 to 275°C of the hot start UDDS cycles for the chassis dynamometer testing for the manufacturer B truck. For the freeway driving cycles, the results show that the average SCR inlet temperature is at or above 250°C for the Cruise, HHDDT-S cycles, on-road driving cycles, and RMC cycles of the engine dynamometer testing for both vehicles.

3.4.1.2. UDDS NO_x emission differences between the different testing conditions

Cumulative NO_x emissions. In order to understand the differences in NO_x emission between the first Chassis dynamometer testing and the engine dynamometer testing, plots of cumulative NO_x emissions and real-time SCR inlet temperature for the UDDS chassis dynamometer and engine dynamometer cycles are shown in Figure 3-3 for the manufacturer A truck and Figure 3-4 for the manufacturer B truck. For SCR-equipped vehicles, NO_x emissions are typically strongly correlated to the SCR temperature. A number of studies have shown that the freeway driving cycles with the higher average SCR temperatures had much lower NO_x emission rates compared to the transient cycles, such

as the UDDS and CARB-transient, which was also consistent with the results of our study (CARB, 2017; Quiros et al., 2017; Jiang et al., 2018). For both vehicles, the results show very similar NO_x emissions between the initial chassis dynamometer testing and the engine dynamometer testing for the first 350 seconds. The primary differences in NO_x emissions for the UDDS occur between 350 and 700 seconds. During this time period, the NO_x emissions were considerably higher for the chassis dynamometer testing for both vehicles, even though the SCR inlet temperatures for the chassis dynamometer testing were above 250°C for the manufacturer A truck and above 230°C for the manufacturer B truck. As discussed above, for the manufacturer A truck, the lower emissions for the engine dynamometer testing was attributed to the engine running in a cold-start mode, which resulted in retarded injection timing.

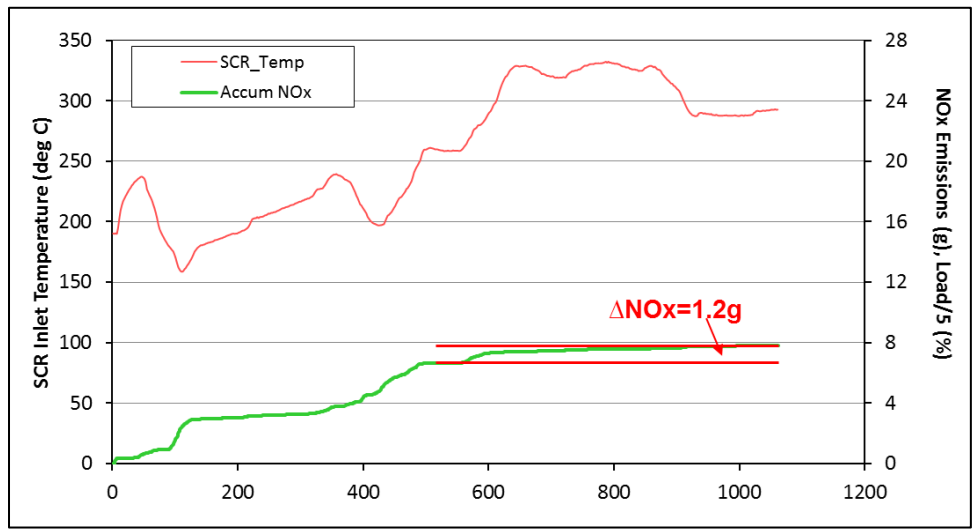
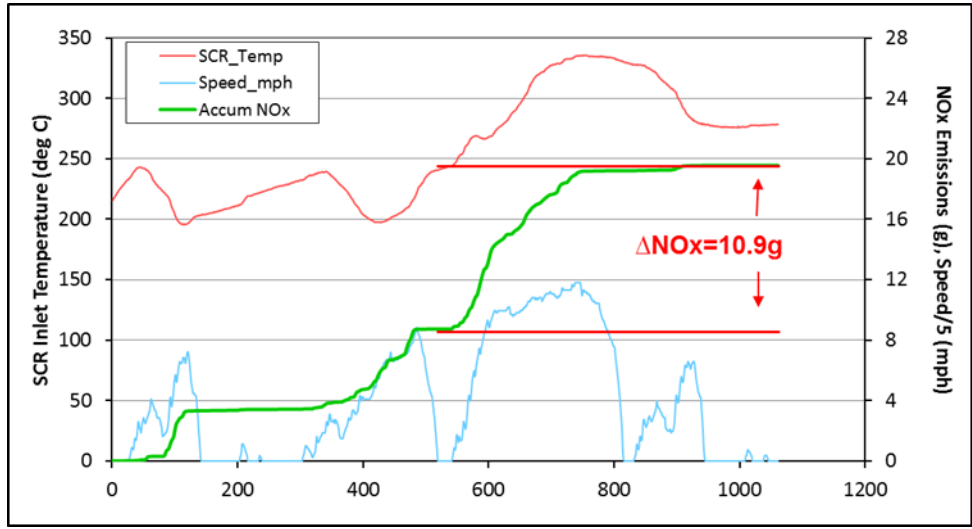


Figure 3-3 Cumulative NOx emissions for the UDDS Cycle of the first Chassis dynamometer testing (top) and the engine dynamometer testing (bottom) for the manufacturer A truck

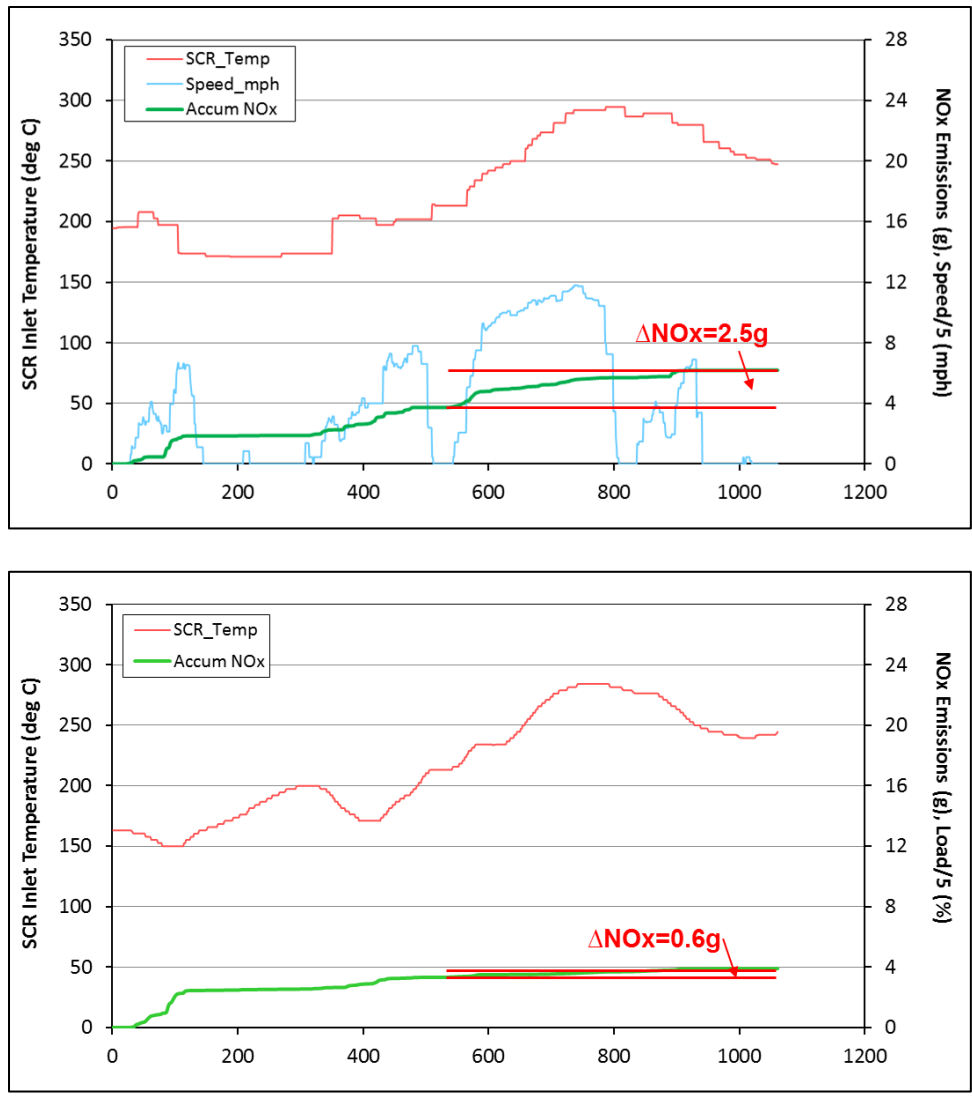


Figure 3-4 Cumulative NOx emissions for the UDDS Cycle of the first Chassis dynamometer testing (top) and the engine dynamometer testing (bottom) for the manufacturer B truck

As discussed, SCR inlet temperature is typically an important indicator for NOx emissions. When examining the NOx emission differences between the different laboratories in this study, although the impacts from the SCR temperature can explain some results, it is more likely that other factors beyond just SCR temperature are also responsible

for some of the differences in the trends in NO_x emissions for the different laboratories over the same test cycle.

Engine out NO_x emission impact. In order to further analyze the factors that may be responsible for the differences in NO_x emissions between chassis dynamometer and engine dynamometer testing for the manufacturer B truck. Figure 3-5 show a comparison of engine out and SCR out UDDS NO_x emissions on a concentration basis between two laboratories for the manufacturer B truck. As the rpm and torque for the engine dynamometer version UDDS were obtained from one of the three initial chassis dynamometer UDDS tests. It was expected the performance of the engine was similar between two tests. However, much higher engine out NO_x emissions were found for the chassis dynamometer test than the engine dynamometer test for both vehicles, especially between 500 to 800 seconds, which was the high-speed portion of UDDS cycle. The SCR out NO_x emissions of chassis dynamometer test was also observed to be higher than those of engine dynamometer test. As discussed before, the largest difference in cumulative NO_x emissions between the chassis and engine dynamometer testing was from NO_x emissions generated around 500 to 800 seconds (Figure 3-5), where higher concentrations of engine out and SCR out NO_x were also observed for chassis dynamometer testing.

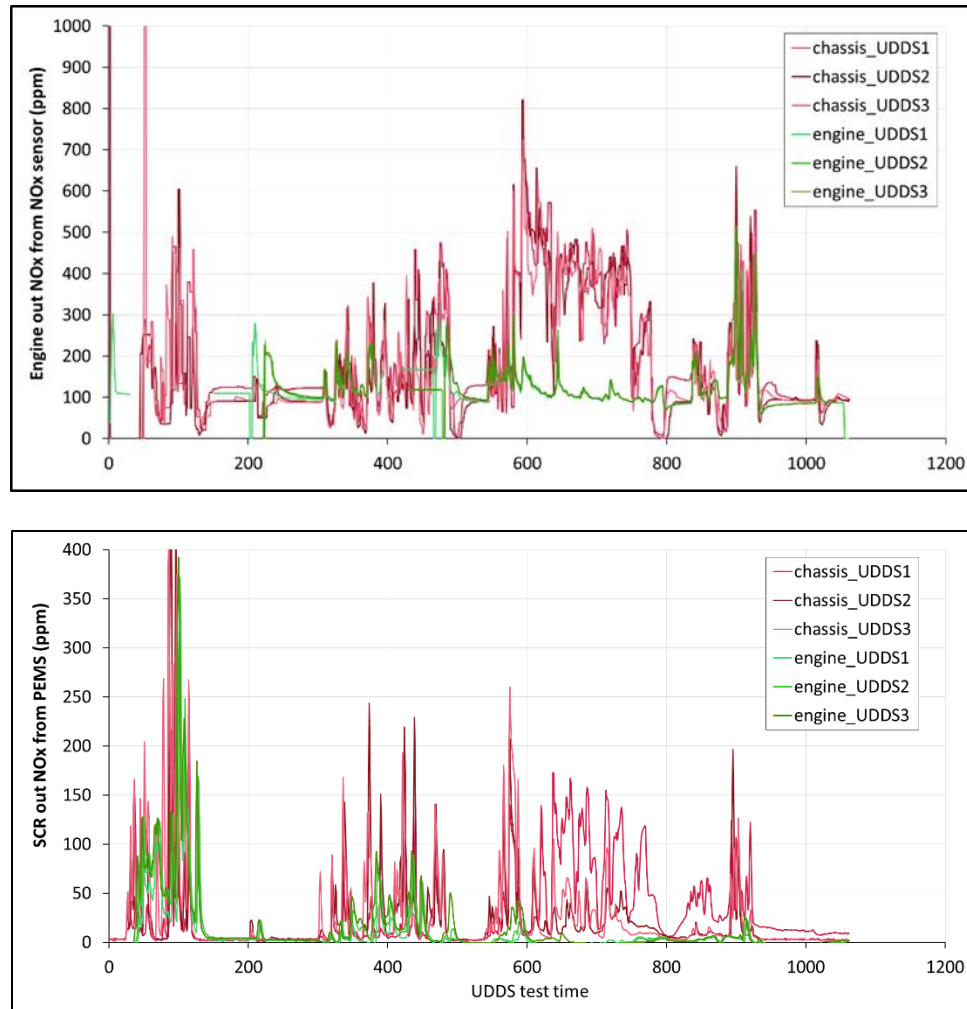


Figure 3-5 Comparison of engine out and SCR out NOx emission on a PPM basis from ECM of UDDS chassis dynamometer and engine dynamometer test of the manufacturer B truck

UDDS NOx emission differences between the chassis dynamometer and on-road testing. The NOx emissions for the chassis dynamometer and on-road tests can also be compared. For both trucks, NOx emissions for the on-road testing were also lower than those of chassis dynamometer, as shown in Figure 3-7 for both vehicles. Note that the on-road UDDS was not a continuous test. Three segments of on-road testing were not in the same order as in the chassis UDDS. The order was shown in the Figure 3-1 (M2-M1-M3).

In order to further understand the differences in NO_x emission between the first Chassis dynamometer and the on-road testing, integrated of engine out and SCR out NO_x emissions and SCR efficiencies for the UDDS chassis dynamometer and on-road cycles are shown in Figure 3-7 for both vehicles. For the manufacturer A truck, the on-road UDDS had lower engine out NO_x than for the chassis dynamometer UDDS, although similar SCR efficiencies were observed between two test conditions. Higher engine out NO_x is the main reason for the higher NO_x emissions for the chassis dynamometer testing results compared to the on-road UDDS testing results for the manufacturer A truck. For the manufacturer B truck, on the other hand, similar engine out NO_x emissions were found between the on-road and chassis dynamometer tests, while the SCR inlet temperature for the chassis dynamometer testing was lower than that for the on-road testing. The SCR temperatures contributed to associated SCR efficiencies for the manufacturer B truck for the chassis dynamometer testing, leading to higher tailpipe NO_x emissions for the chassis dynamometer compared to the on-road testing.

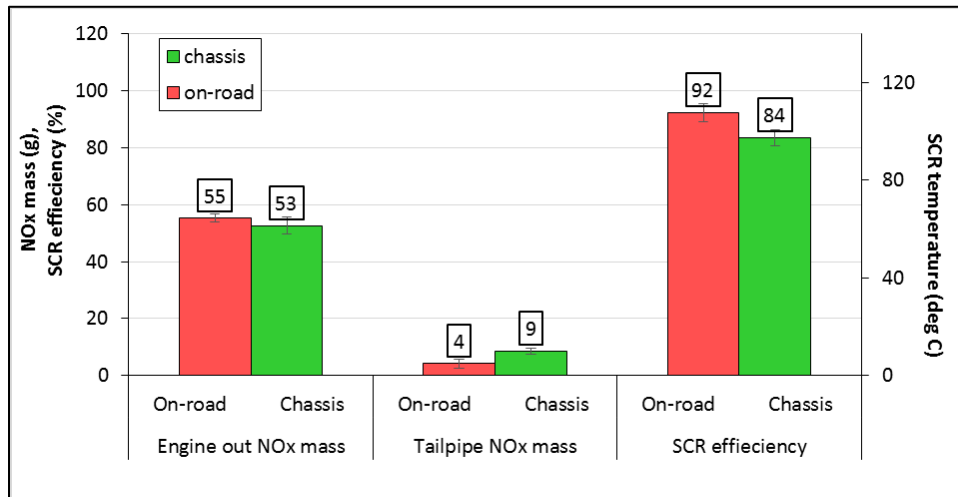
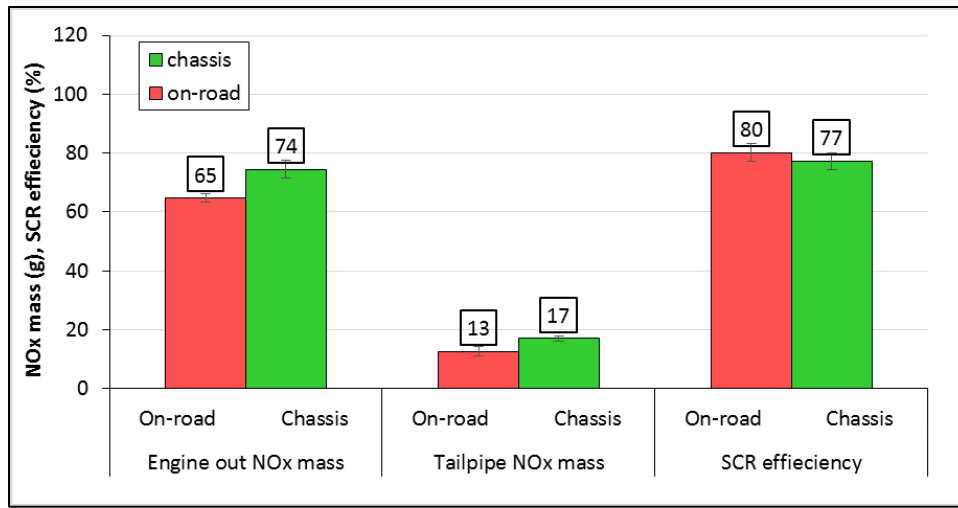


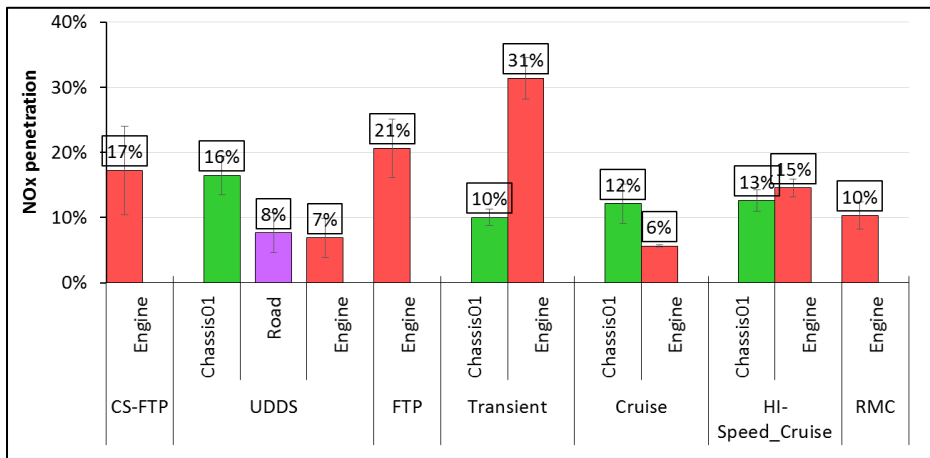
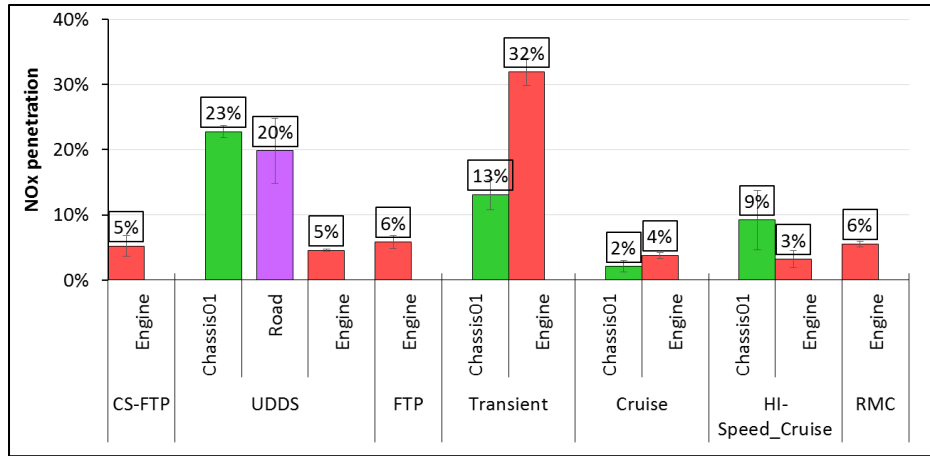
Figure 3-6 Integrated of engine out and SCR out NOx emissions and SCR efficiencies for the UDDS chassis dynamometer and on-road cycles for the manufacturer A truck (top) and the manufacturer b truck (bottom)

3.4.1.3. Average SCR efficiency by Test Cycle

Figure 3-7 shows the NOx penetration for all the test cycles of both vehicles, based on the readings from engine out NOx sensor and tailpipe PEMS measurements. It should be noted that the SCR efficiency values in Figure 3-7 did not represent values over the whole cycles, as valid data from the engine out NOx sensor at the beginning of each cycle

was not available, due to as the NOx sensors do not provide readings until the temperatures have reached the temperature threshold of 190°C.

NOx penetration rates ranged from 2 to 32% for all the test cycles for both vehicles, with the NOx penetration for the cruise and hi-speed cruise cycles being lower than those for the urban driving cycles. The cold start cycles had relatively low to moderate NOx penetration rates because the engine out NOx sensor only provided values for the last portion of the cold start cycle. The NOx penetration rates for the UDDS on the engine dynamometer were found to be lower for both vehicles than those for the chassis dynamometer and on-road tests, except for the on-road testing of the manufacturer B truck, while the transient cycle showed the opposite trend. For the freeway driving and set cycles, the NOx penetration rates were lower than 10% for all the cycles for the manufacturer A truck and ranged from 6 to 17% for the manufacturer B truck.



Note that the SCR efficiency was calculated based on engine out NOx sensor and PEMS measurement. The portions of cycle that engine out NOx sensor didn't work were excluded from calculation.

Figure 3-7 Average NOx penetration by test cycles of the manufacturer A truck (Top) and the manufacturer B truck (Bottom)

3.4.1.4. SCR efficiency as a function of SCR temperature

Figure 3-8 show SCR efficiency for the chassis dynamometer, on-road and engine dynamometer testing as a function of SCR temperature for both the manufacturer A and manufacturer B trucks. All the test data of each test was divided into three groups based on SCR inlet temperatures: SCR inlet temperatures < 200°C, 200°C ≤ SCR inlet temperatures < 250°C and SCR inlet temperatures ≥ 250°C. The SCR efficiencies for each group were calculated based the integrated engine out NOx mass from the engine out NOx

sensors and the integrated tailpipe NO_x mass from the PEMS. The SCR inlet temperatures were the average values of each group. The SCR efficiency values didn't represent the values over the whole cycles, as valid data from the engine out NO_x sensor at the beginning of each cycle was not available due to the 190°C temperature threshold.

SCR efficiencies were above 80% for both vehicles for all the test conditions when the SCR inlet temperatures were above 250°C with efficiencies remaining constant as the temperature increasing for the manufacturer A truck and dropping slightly as the temperature increasing to 350°C for the manufacturer B truck. In terms of different test conditions, for the manufacturer A truck, the engine dynamometer testing showed the highest SCR efficiency (>90%) with the SCR temperatures above 250°C and chassis had the lowest SCR efficiency, which was consistent with the observation of lower SCR inlet temperature. For the manufacturer B truck, there is no significant difference in SCR efficiency between different test conditions when the SCR temperatures were above 250°C. When the SCR temperatures were below 250°C, the SCR efficiency dropped significantly for both vehicles. The lowest SCR efficiency was around 40% for the manufacturer A truck for both the chassis and on-road testing, under conditions where the SCR temperature was lower than 200°C. The lowest SCR efficiencies for the manufacturer B truck were around 50% to 60% for all the test conditions where the SCR temperature was lower than 200°C.

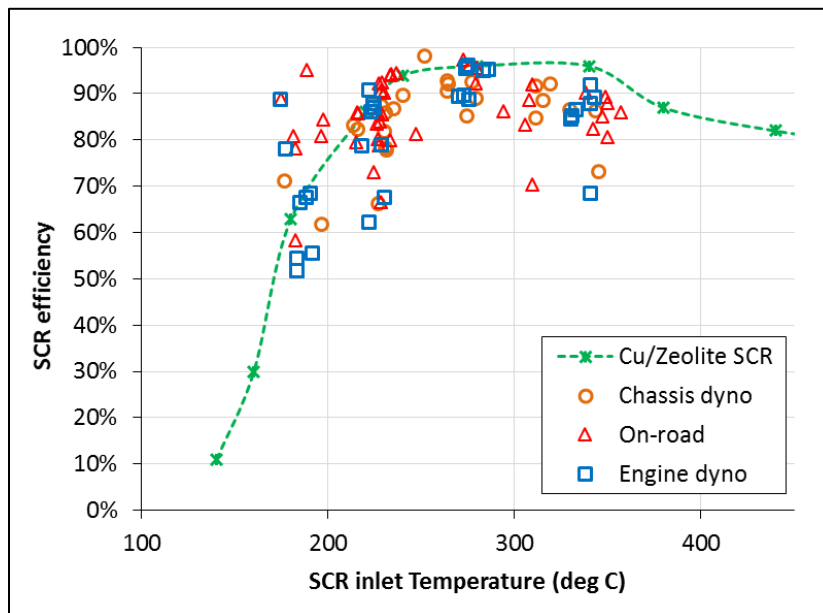
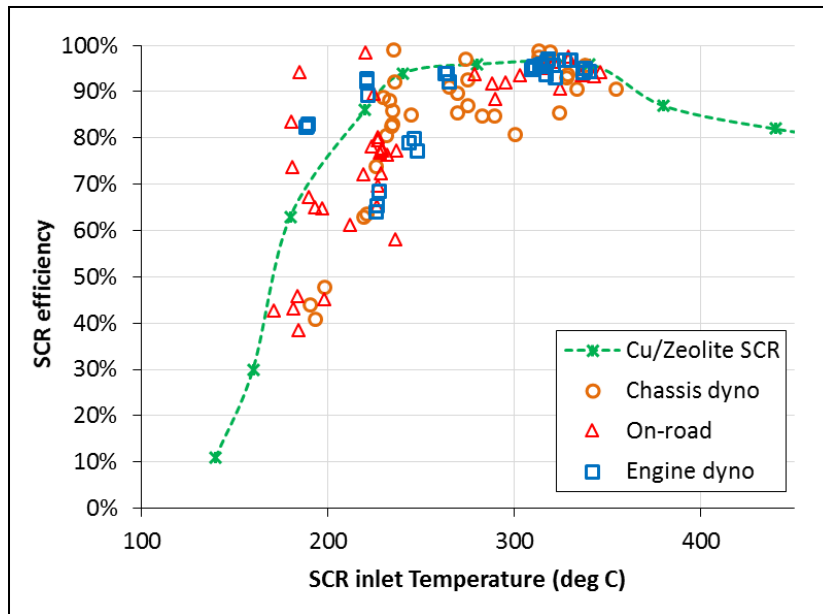


Figure 3-8 SCR efficiency as a function of SCR inlet temperature for the manufacturer A (Top) and the manufacturer B (Bottom)

The SCR conversion efficiency in this study can also be compared that to experimental values in Figure 3-8 (Cavataio et al., 2007), as both vehicles were equipped with Cu/Zelite based SCR. Their experimental data showed that SCR efficiencies were

above 90% when the SCR inlet temperatures were higher than 250°C, which was higher than the values seen in the present study for both vehicles, except for the engine dynamometer testing for the manufacturer A truck. The SCR efficiency started to drop as the SCR inlet temperatures went above 350°C for the experimental data, which was consistent with the results for the manufacturer B truck. The experimental data also showed that SCR efficiency was temperature dependent for SCR inlet temperatures below 200°C, which is consistent with the results for both vehicles.

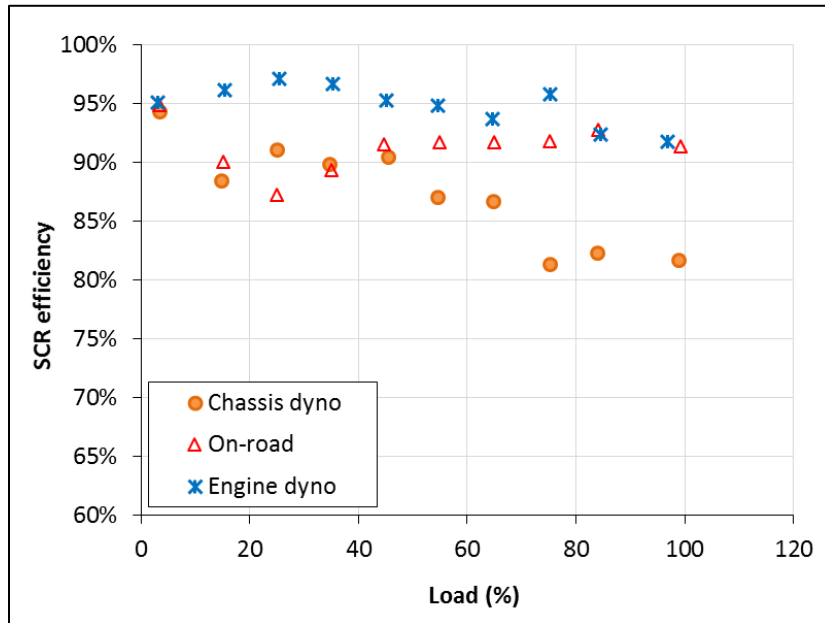
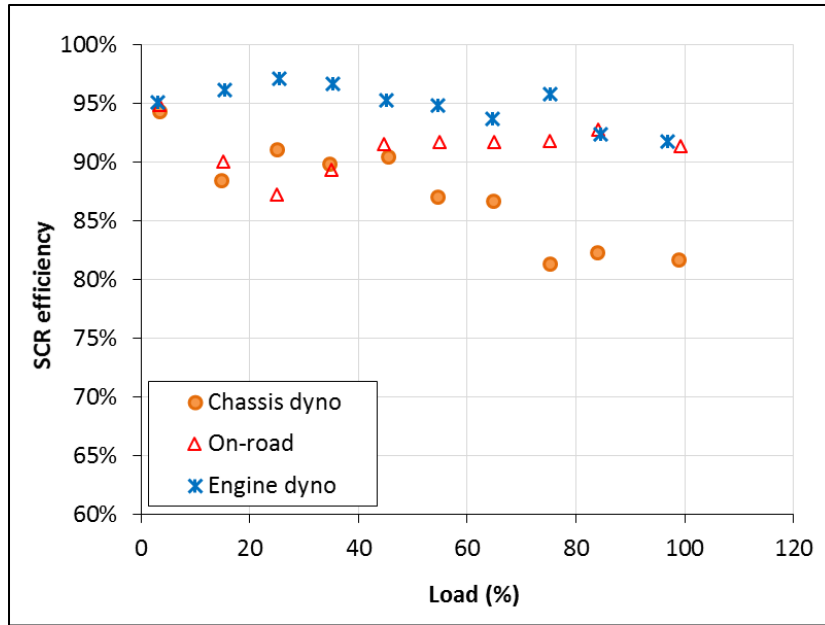
3.4.1.5. SCR efficiency as a function of load

Figure 3-9 show SCR efficiencies for chassis dynamometer, on-road and engine dynamometer testing as a function of load for both the manufacturer A and manufacturer B truck. The test data was divided into ten groups based on load, representing 10% increments in load. The SCR efficiency for each group was calculated based on the integrated engine out NOx mass from engine out NOx sensors and the integrated tailpipe NOx mass from the PEMS. The SCR efficiency values did not represent the values over the whole cycles, as valid data from the engine out NOx sensor at the beginning of each cycle was not available due to the temperature threshold of 190°C.

For the manufacturer A truck, the overall SCR efficiency was above 80% for all the load points. The highest SCR efficiency was observed between 30 to 60% load with the efficiency higher than 90%, except for the 30 to 40% load of on-road testing. The lowest SCR efficiencies were found between 10-30% load for the chassis dynamometer and on-road testing due to the lower SCR temperatures at these lower loads, although this trend was not found for the engine dynamometer testing. The SCR efficiency also dropped at the

high load operations for the chassis and engine dynamometer testing, but not for on-road testing. This was because the chassis and engine dynamometer testing had higher fractions of transient operations than the on-road testing. Also, high load operations for chassis and engine dynamometer typically occurred during accelerations, while the high load operations for the on-road testing were typically under cruise conditions.

For the manufacturer B truck, the overall SCR efficiency was above 70% for all the load points. The highest SCR efficiency was observed between 10 to 40% load, with the efficiencies higher than 90%, except for 30 to 40% load of chassis testing. The SCR efficiency did not drop into the 10-30% load range, as might be expected for lower load operation with lower SCR temperatures. However, the SCR efficiency dropped as the load increased in the middle load range, and the SCR efficiency remained lower under high load conditions for all the test conditions, even for the on-road where most of the high load operation was under cruise conditions.



Note that engine dynamometer had extra cycles compared with Chassis dynamometer.

Figure 3-9 SCR efficiency as a function of load for the manufacturer A truck (Top) and the manufacturer B truck (Bottom)

3.4.2. NTE Analysis

This section discusses and analyzes emissions data and activity data over the different routes using the NTE in-use compliance test methodology. The analyses were conducted separately for the three on-road driving segments, including Riverside to Hesperia, Hesperia to Indio, and Indio to Hesperia, and are discussed in this section.

3.4.2.1. NTE analysis

The NTE analysis is based on driving where the engine is operating in the NTE control area or zone. This includes operation at over 30% of maximum power and under conditions where the SCR temperature is higher than 250°C for at least 30 seconds. For regulatory requirements, operation in the NTE zone for a period of at least 30 seconds is required to create a valid NTE event. For 2010 and newer trucks, the passing criteria for the NTE test is that at least 90% of time-weighted NTE pass events should be below a threshold of 0.45 g/bhp-hr for NO_x, based on 1.5 times the 0.2 g/bhp-hr certification standard plus 0.15 g/bhp-hr (PEMS accuracy margin). A summary of NO_x emission rates for the full route, for operation in the NTE zone, for valid NTE events, and for operation not in the NTE zone is provided in Figure 3-10.

NO_x emission rates for the whole trip ranged from 0.24 to 0.50 g/bhp-hr of three test routes for both vehicles. Similar values from 0.19 to 0.43 g/bhp-hr were seen for the overall activity in the NTE zone, and from 0.19 to 0.41 g/bhp-hr for valid NTE events. NO_x emission rates for valid NTE events were lower to those of overall activity in the NTE zone for the manufacturer A truck, but were comparable for the manufacturer B truck. Overall, typical emissions were higher than the 0.2 g/bhp-hr certification limit, but were

below the 0.45 b/bhp-hr NTE limit. NO_x emission rates for the whole trip, the NTE zone and the valide NTE events generally were lower for the manufacturer A truck than the manufacturer B truck. Figure 3-10 also shows that NO_x emissions outside the NTE zone of both vehicles (ranging from 0.60 to 1.46 g/bhp-hr) were significantly higher than both the threshold of 0.45 g/bhp-hr and also those in the NTE zone (ranging from 0.24 to 0.5 g/bhp-hr). NO_x emissions the failed NTE events (ranging from 0.71 to 1.12 g/bhp-hr) were considerably higher than those valid NTE events (ranging from 0.19 to 0.14 g/bhp-hr).

Previous PEMS studies have also reported that in-use NO_x emission rates were higher than certification level. Misra et al. (2013, 2016) undertook a study to characterize the in-use emissions of model year (MY) 2010 or newer diesel engines and found that NO_x emissions are generated disproportionately under lower load operation and that NO_x emissions for different types of driving can often be higher than certification NO_x levels. As part of a HDIUC validation program, O’Cain et al. (2013, 2016) found that average NTE NO_x emissions were 0.59 and 1.02 g/bhp-hr for the two selected engine families over routes similar to those used in the present study, which was considerably higher than the threshold of 0.45 g/bhp-hr of in-use compliance. The average NTE NO_x emissions (0.26 g/bhp-hr) for this study were lower than the values above, while the average NO_x emission (0.83 g/bhp-hr) for failing NTE events was comparable to from failing NTE events in O’Cain et al.’s study. WVU characterized emissions from a 2011 heavy-duty diesel truck and the results showed that the brake specific NO_x emissions were higher than certification standards by an order of magnitude at high altitudes due to engine protection strategies (Carder et al., 2014). The altitude of test routes in this study was generally lower than 1200

m (3900 ft), as shown in Figure 3-1, and the NOx emission rates of the higher attitude route (Riverside to Hesperia) were also comparable to those of the other two routes. However, the NOx emission rates under lower load operation (outside NTE zone) were found significant higher than the certification standard, which was consistent with Misra’s study.

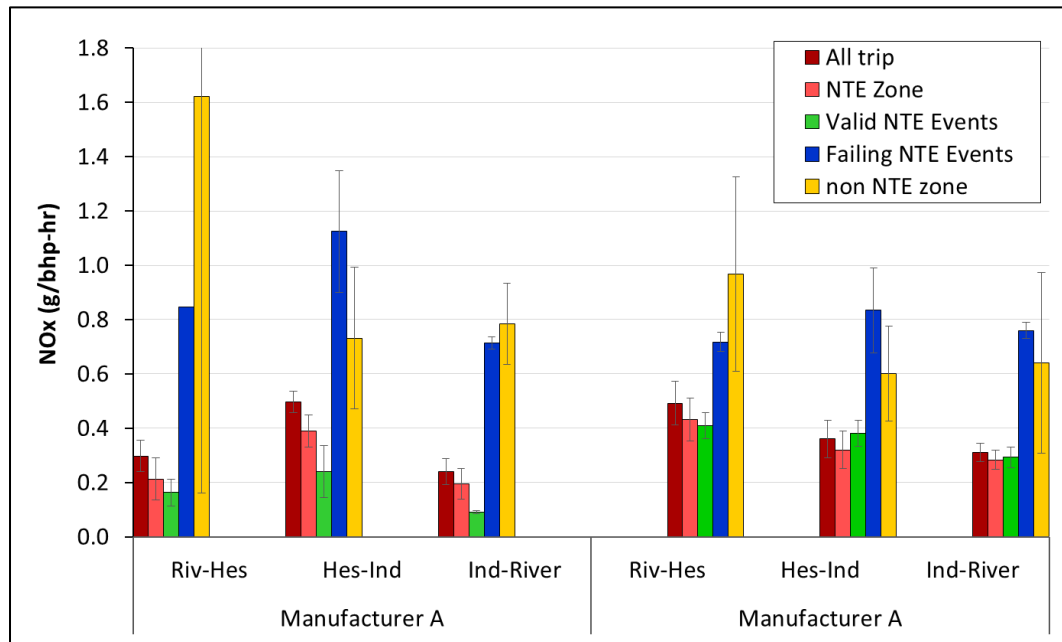


Figure 3-10 NOx emission rates of NTE zone, valid NTE events and non NTE zone

3.4.2.2. NTE Activity Analysis

A summary of the activity statistics for the three routes is provided in Figure 3-11 and a summary of the NOx breakdown for different types of activity is provided in Figure 3-12 for both vehicles. The results of the basic NTE analyses are provided in Table 3-3.

The activity analyses are provided in Figure 3-11a for the manufacturer A truck and Figure 3-11b for the manufacturer B truck. The results showed similar trends between the different routes with the manufacturer B truck did having a slightly higher fraction of operation in the NTE zone. The Indio to Riverside had the highest percentage of activity

in the NTE zone (53 to 57%), compared to 52% for the Riverside to Hesperia route for both vehicles, and less than 35% for the Hesperia to Indio route for both vehicles. The Indio to Riverside and Riverside to Hesperia route had a higher percentage of activity (higher than 30%) spent in valid NTE events, compared to less than 15% for the Hesperia to Indio route for both vehicles.

The breakdown of NO_x emissions for different types of activity is provided in Figure 3-12a for the manufacturer A truck and Figure 3-12b for the manufacturer B truck. For both vehicles, a majority of NO_x was generated during driving in the NTE zone, with values ranging from 50 to 79% for both vehicles. However, in terms of valid NTE events, only 15 to 30% and 41 to 61% of NO_x was generated during valid NTE events for the manufacturer A truck and for the manufacturer B truck, respectively. For the manufacturer A truck, significant amount of the NO_x (40 to 62%) came from NTE zone operation that did not qualify as an NTE event due to temperature <250°C or the duration being < 30 seconds, while that fraction (13 to 30%) was much lower for the manufacturer B truck. There was also a significant fraction of NO_x generated under cold operation for both vehicles, representing 7 to 21% of the total.

The breakdown of NO_x emissions between the NTE and non-NTE operation also varied between the different routes for both vehicles. In terms of NO_x emissions generated for different test routes, The highest fraction of NO_x generated during NTE zone was for the Indio to Riverside route (higher than 70% for both vehicles), followed by the Riverside to Hesperia routes (57 to 72 %), with Hesperia to Indio having the lowest fraction (50 to 66%). Note that both the Riverside to Hesperia and Indio to Riverside test routes are

predominantly uphill driving that puts a higher load on the engine, is more likely to generate NTE events. The Indio to Riverside route for the manufacturer B truck also had more than 60% of NO_x generated during valid NTE events, while the fraction was only 27% for the manufacturer A truck due to the high fraction of the NO_x (45%) coming from NTE zone operation that did not qualify as an NTE event due to temperature <250°C or the duration being < 30 seconds. The Hesperia to Indio route showed the lowest fraction of NO_x generated during valid NTE events with 15% for the manufacturer A truck and 41% for the manufacturer B truck. This is due to the fact that the Hesperia to Indio route includes considerable downhill driving, where the load on the engine is relatively low, and these low load operations are more likely to be outside the NTE zone.

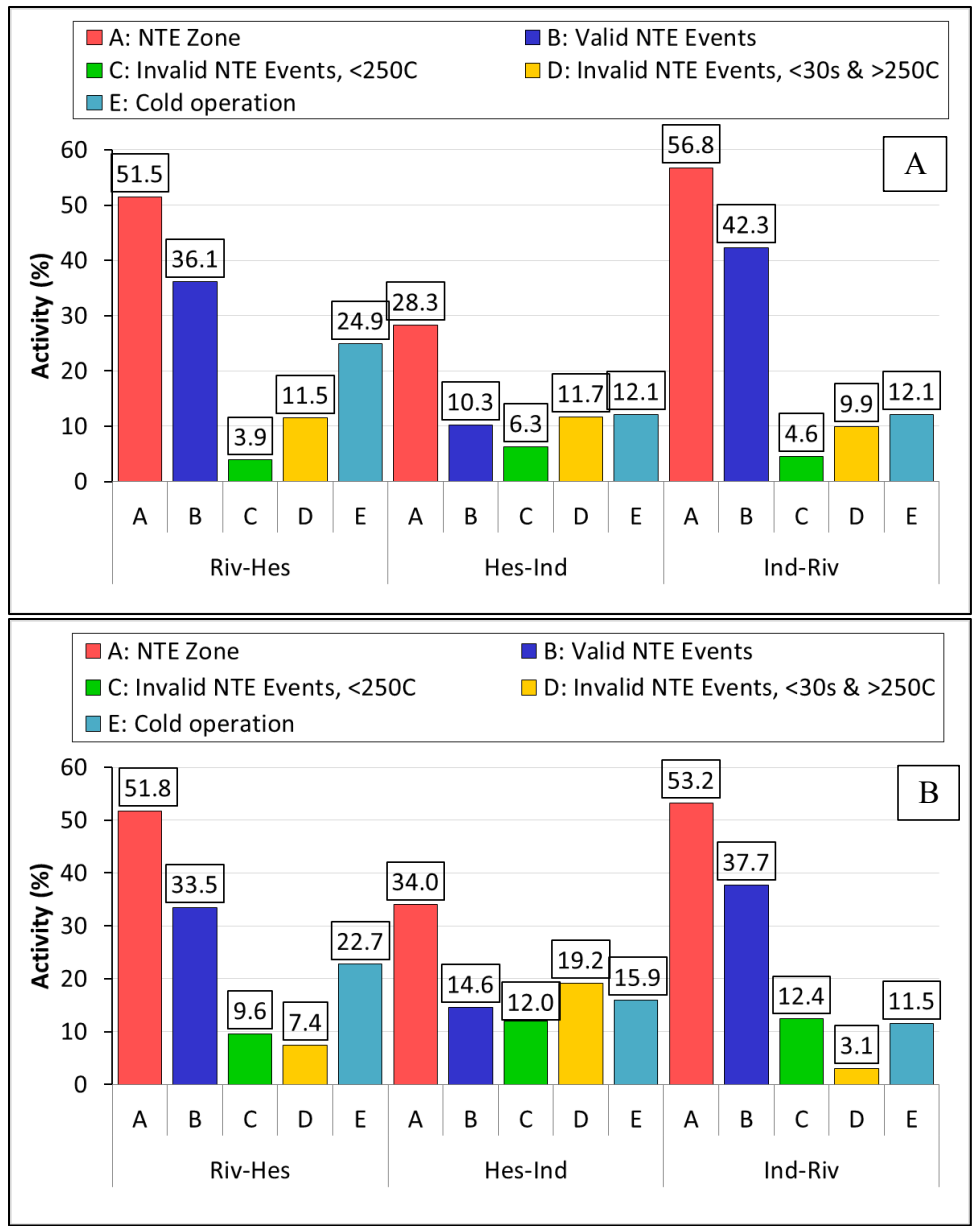


Figure 3-11 NTE Activity Analysis of the manufacturer A truck (top) and the manufacturer B truck (bottom)

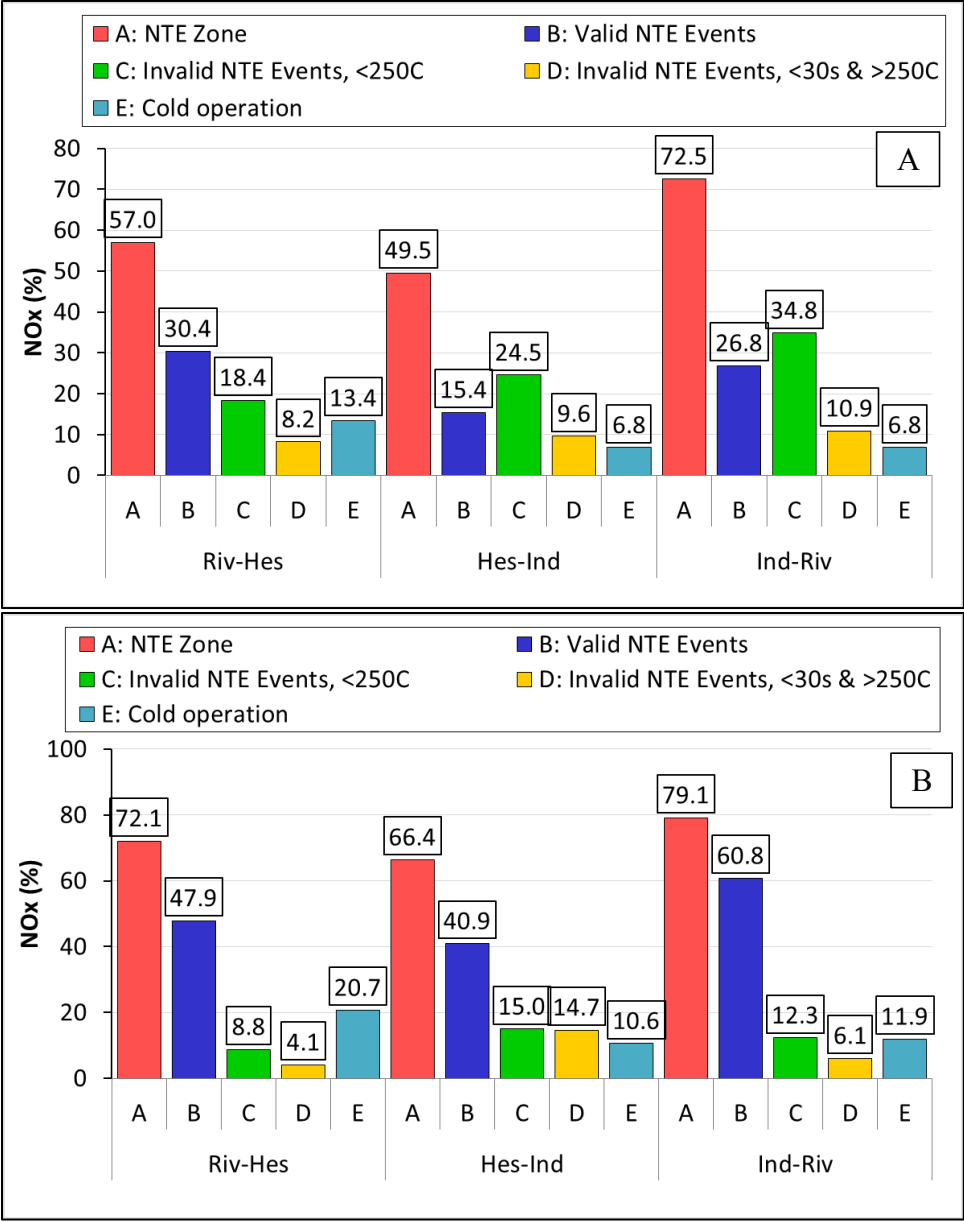


Figure 3-12 NTE NOx breakdown Analysis of the manufacturer A truck (top) and the manufacturer B truck (bottom)

The results of the NTE analyses can be compared to other studies of heavy-duty in-use emissions. CARB is in the process of conducting in-use testing for a range of different manufacturers (O’Cain, 2018). The routes used for the CARB testing are very similar to those used in the current study, in that the CARB route goes from El Monte to Hesperia to

Indio and then back to El Monte. Similar to the results of our study, the CARB testing is showing that a large fraction of the operation over this route is not in the NTE zone or does not represent valid NTE events. In earlier results from this work, Tu et al. (2016) showed approximately 16 percent of operation being in the NTE zone and typically 9 percent of operation being in valid NTE events over the route. This is lower than the average of 47% of three routes of two vehicles in our study. It should be noted that the CARB routes were longer compared with our study due to the extra distance between El Monte to Riverside, where very few NTE events are generated. Bartholome et al. (2018) conducted analysis of manufacturer derived HDIUC data, which should be more representative of a broader range of driving. They found that only 5% of this data was valid NTE events, and that 24% of the tests did not have any valid NTE events. Yoon et al. (2016) conducted additional analyses of CARB's study and found that 94% of the total trip NO_x emissions were not generated in the NTE zone and that the activity meeting the criteria for an NTE event only contributed 5% of the total trip NO_x emissions. The percentage of NO_x emissions generated in the NTE zone (66%) and for valid NTE events (37%) in this study were greater compared to CARB's study.

3.4.2.3. NTE compliance results

The NTE emission results were also evaluated in terms of compliance with the in-sue testing requirements with the passing criteria being that 90% of the time weighted NTE emission are below the 0.45 g/bhp-hr. NTE analyses were conducted separately for the three main on-road driving segments, including Riverside to Hesperia, Hesperia to Indio, and Indio to Hesperia. The results of the basic NTE analyses are provided in Table 3-3.

The manufacturer A truck passed the NTE criteria for 7 of 9 tests, while the manufacturer B truck passed for only 3 of 9 tests. The number of NTE events was greater for the Riverside to Hesperia (7 to 17) and the Indio to Riverside (11 to 27) route, as these routes include a steep uphill climb, compared to the Hesperia to Indio route (4 to 16).

CARB have conducted in-use testing for three engine families over similar routes. O’Cain et al. found that 6 of 10 vehicles were found to be noncompliant with the NTE for one engine family, with an average NTE emission rate of 0.59 g/bhp-hr, 8 of 10 vehicles were found to be noncompliant for a second engine family, with an average NTE emission rate of 1.02 g/bhp-hr, and 3 of 3 vehicles have been found to be noncompliant for a third engine family. The percentage of failing NTE events was 60%, 80%, and 100%, respectively, for the three manufacturers (O’Cain, 2018). The passing ratio over the 9 tests per vehicle in this study was 7/9 for the manufacturer A truck and 3/9 for the manufacturer B truck. It should be noted that the analyses for the O’Cain study were based on the full route from El Monte to Hesperia to Indio and back, whereas the analyses in our study were conducted separately for each route segment. The NO_x emission rates of the valid NTE events of our study was 0.18 g/bhp-hr for the manufacturer A truck and 0.41 for the manufacturer B truck, which were lower than the values above.

Table 3-3 NTE Requirements with Measurement Allowance

Manufacturer A truck							
Route	Route ID	All event		Pass event		Pass/Fail Ratio	
		Numbers	Duration	Numbers	Duration		
Riv-Hes	1	17	1470	15	1346	0.92	Pass
	2	7	656	7	656	1.00	Pass
	3	13	1494	12	1456	0.97	Pass
Hes-Ind	1	19	1234	14	1024	0.83	Fail
	2	4	281	4	281	1.00	Pass
	3	11	646	10	573	0.89	Fail
Ind-Riv	1	27	2707	26	2677	0.99	Pass
	2	18	2665	17	2532	0.95	Pass
	3	22	2390	22	2390	1.00	Pass
Manufacturer B truck							
Route	Route ID	All event		Pass event		Pass/Fail Ratio	
		Numbers	Duration	Numbers	Duration		
Riv-Hes	1	14	1558	5	825	0.53	Fail
	2	17	1694	6	371	0.22	Fail
	3	8	891	3	420	0.47	Fail
Hes-Ind	1	9	520	7	360	0.69	Fail
	2	23	1379	16	923	0.67	Fail
	3	15	1048	14	955	0.91	Pass
Ind-Riv	1	25	2705	23	2509	0.93	Pass
	2	11	1197	9	1115	0.93	Pass
	3	20	2516	17	2235	0.89	Fail

3.4.3. Modified NTE Analysis

To evaluate the impact of NTE exclusion criteria on the data coverage in the NTE zone, the NTE analysis was repeated with the NTE criteria modified to have exclusions only below 10% Max power and 10% Max Torque, as opposed to requiring all operation to be above the 30% level. The ratio of modified NTE results divided by standard NTE results are presented in Figure 3-13. Overall, there were no significant differences in activity results between the standard NTE criteria and the modified NTE criteria. The modified NTE criteria showed an increase of 1% in passing rate for Manufacturer A truck

and 11% for the manufacturer B truck. In terms of data coverage, the modified NTE criteria on average increased the amount data within the NTE zone by 12% for the manufacturer A truck and 6% for the manufacturer B truck. The fraction of non-NTE activity decreased 22% for the manufacturer A truck and 14% for the manufacturer B truck. Even though the modified NTE criteria improved data coverage in the NTE zone, no significant change in NO_x emission rates was found comparing with those with the original NTE criteria. The fraction of NO_x generated in the NTE zone increased 12% for the manufacturer A truck and did no change for the manufacturer B truck.

Bartholome et al. (2018) of CARB conducted some more extensive analysis of manufacturer derived HDIUC data. They modified different exclusion criteria for valid NTE operation, including changing the torque criteria from 30% to 10% Max torque, changing power from 30% to 10% Max power, and deleting some of the temperature criteria. With the modified NTE criteria, they found that the percent of operation within valid NTEs increased to 28%, that the fraction of tests with no valid NTE events decreased to only 3.4%, and that the fraction of passing NTE events decreased to 71%. The modification of the NTE criteria in the Bartholome et al. study showed greater impact than observed in the present study, where modifying the NTE criteria to 10% of maximum power and torque only increased the fraction of valid NTEs by less than 5%. This is because the HDIUC data is drawn from vehicles operating under a broader range of operating conditions and loads. This is as opposed to the routes used in the present study, which include significant uphill driving designed to generate greater number of NTE events.

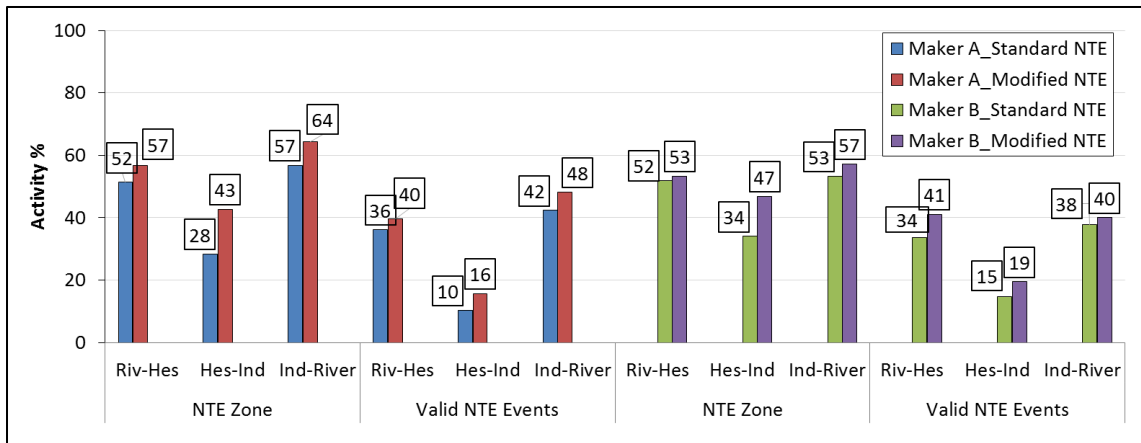


Figure 3-13 Comparison of activity analysis with standard NTE criteria and modified NTE criteria

3.4.4. MAW Analysis

The results for the MAW analysis are presented in Table 3-4 for both vehicles. The passing criteria for the NTE test is that at least 90% of time-weighted NTE pass events should be below a threshold of 1.5 times the certification limit, or 0.3 g/bhp-hr for NO_x. So the MAW method has a lower emissions threshold level for failure. The MAW also differs from the NTE method in that all operation over period of time is included, with the provision that the period of time represents the same amount of work that the engine uses over a certification cycle, which in this case was a typical FTP test. For the MAW methodology, several criteria are utilized to determine if the test is acceptable. For the windows calculated over the course of the route, at least 50% should be valid MAW windows, which requires that the average power should be at least 10% of the maximum power. Additionally, the MAW method does not have an exclusion for operation below 250°C, hence it includes more operation where NO_x emissions could potentially be higher.

In terms of passing/failing the MAW test, the majority of tests were failed for both vehicles with only two tests for the Riverside to Hesperia route passing for the manufacturer A truck. The percent of MAW windows <1.5 times the conformity factor varied for different test routes and test vehicles, with the percent being higher for the manufacturer A truck. The Riverside to Hesperia route had the highest percentage of the windows <1.5 times the conformity limit for the manufacturer A truck, while it had the lowest percentage for the manufacturer B truck, indicating the results of MAW significantly depended on the test vehicles. For the Riverside to Hesperia route, 79 and 93% of the windows for the manufacture A truck passed the 1.5 times criteria, compared to 6 to 26% of the windows for the manufacture B truck. The Hesperia to Indio route had between 36 and 42% of the windows being <1.5 times the conformity limit for the manufacturer A truck and between 22 and 55% for the manufacturer B truck. The Indio to Riverside route showed the highest percentage of the windows being <1.5 times the conformity limit for the manufacturer B truck (44 to 80%), while the percent ranged from 63 to 73% for the manufacturer A truck.

Bartholome et al. (2018) evaluated the HDIUC data with the MAW method and found that the MAW method captures a greater percentage of in-use operation and emissions during real-world operation compared with both the current and modified NTE methods. With the MAW criteria, they found that the percent of operation within valid windows increased to 60%, that 62% of the total trip NO_x was included in the analysis, and that the fraction of passing windows events decreased to 11.6%. In terms of the MAW method, the activity analysis of this study also show a significant improvement in the

amount of data coverage, as 100% of activity was in a valid window for both the manufacturer A truck and the manufacturer B trucks for the MAW analysis. The fail rate was almost 100% for both vehicles, consistent failure rate (88.4%) found by Bartholome et al.

Table 3-4 NTE Requirements with Measurement Allowance

Manufacturer A truck									
Route	Route ID	All MAW		MAW Valid (%)		CF Total	CF <= 1.5	CF <=1.5 (%)	Pass/Fail
		Windows	NOx (g/bhp-hr)	Windows	Valid Test				
Riv-Hes	1	2984	0.244	100	Valid Test	2984	2367	79.3	Fail
	2	2911	0.186	100	Valid Test	2911	2667	91.6	Pass
	3	2287	0.181	100	Valid Test	2287	2125	92.9	Pass
Hes-Ind	1	6801	0.497	100	Valid Test	6801	2432	35.8	Fail
	2	6563	0.505	100	Valid Test	6563	2735	41.7	Fail
	3	6316	0.482	100	Valid Test	6316	2305	36.5	Fail
Ind-Riv	1	5597	0.244	100	Valid Test	5597	3582	64.0	Fail
	2	6048	0.260	100	Valid Test	6048	3814	63.1	Fail
	3	5088	0.179	100	Valid Test	5088	3721	73.1	Fail
Manufacturer B truck									
Route	Route ID	All MAW		MAW Valid (%)		CF Total	CF <= 1.5	CF <=1.5 (%)	Pass/Fail
		Windows	NOx (g/bhp-hr)	Windows	Valid Test				
Riv-Hes	1	3311	0.471	100	Valid Test	3311	206	6.2	Fail
	2	2383	0.489	100	Valid Test	2383	385	16.2	Fail
	3	2343	0.379	100	Valid Test	2343	604	25.8	Fail
Hes-Ind	1	4994	0.588	100	Valid Test	4994	1091	21.8	Fail
	2	7062	0.351	100	Valid Test	7062	2553	36.2	Fail
	3	6049	0.310	100	Valid Test	6049	3306	54.7	Fail
Ind-Riv	1	4922	0.228	100	Valid Test	4626	3436	74.3	Fail
	2	4395	0.363	100	Valid Test	4395	1937	44.1	Fail
	3	5802	0.248	100	Valid Test	5802	4638	79.9	Fail

3.4.4.1. Modified MAW Analysis with CF of 2.25

Since the threshold for the MAW (0.3 g/bhp-hr) is lower than that for the NTE (0.45 g/bhp-hr), further analysis was conducted to evaluate the impacts of emission threshold. This analysis looked at the impacts of utilizing a threshold of 0.45 g/bhp-hr for the MAW method. The comparison of MAW analysis with CF of 1.5 and CF of 2.25 criteria is provided in Figure 3-14. The overall pass rate changed from two to three test segments for the manufacturer A truck and from zero to two for the manufacturer B truck, which indicated that the threshold was part of reason that the majority of the routes failed the MAW method, although it was not the entire the reason. The fraction of data CF increased significantly (higher than 25%) for the manufacturer B truck, especially for the Riverside to Hesperia and the Hesperia to Indio routes. The fraction of below the CF increased up to 19% for the manufacturer A truck.

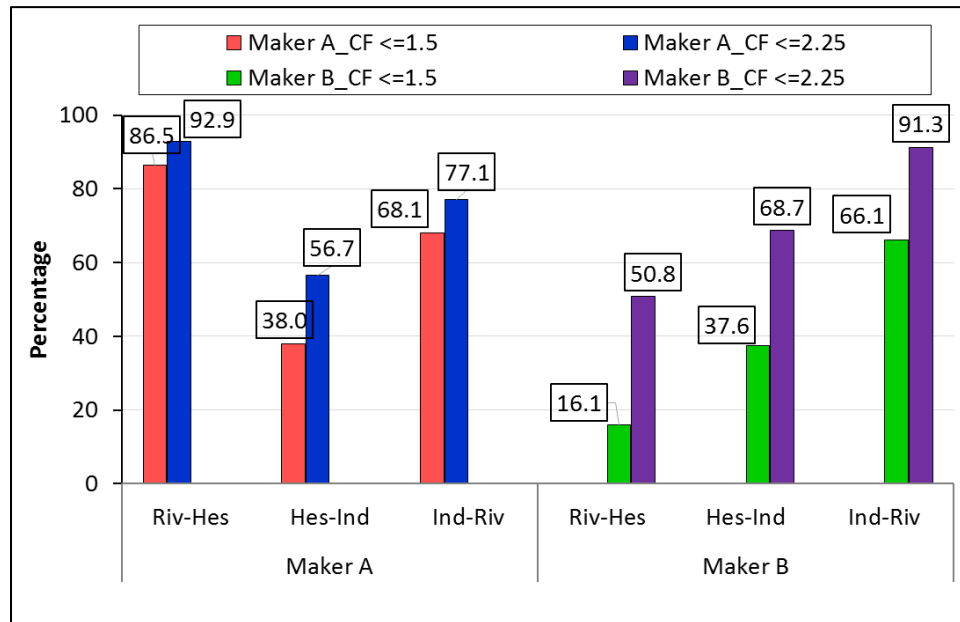


Figure 3-14 Comparison of Standard MAW (CF≤1.5) and Modified MAW (CF≤2.25).

3.4.4.2. Modified MAW Analysis with temperature criteria

The NTE criteria also excludes test data where the SCR temperature is lower than 250°C, as NO_x conversion efficiencies are relatively lower at these lower temperatures, while the MAW method does not have such a temperature criteria. Figure 3-15 in the supporting information shows the conformity factors and average SCR temperatures for one test route for the manufacturer A and B trucks. The results showed that a large number of windows with CFs higher than 1.5 had average SCR temperatures lower than 250°C for the manufacturer A truck. Only a small fraction of failing windows for the manufacturer B truck had SCR temperatures below 250°C. This is consistent with the fact that the average SCR temperatures of the manufacturer B truck were higher than those for Manufacturer A for all the on-road routes.

Further analysis of the impacts of adding a temperature criteria requiring the average window SCR temperature to be higher than 250°C was conducted for the MAW method. This analysis was only conducted for the manufacturer A truck, as only a small fraction of windows for the manufacturer B truck had average window SCR temperatures lower than 250°C. A comparison of MAW analysis without and with the temperature criteria is provided in Figure 3-15. Although the overall pass rate didn't change by eliminating data points with low SCR efficiency operation, the fraction of CF higher than 1.5 increased 14% for the Hesperia to Indio route and 10% for the Indio to Riverside route. The coverage of valid windows decreased after applying the temperature criteria, but the overall coverage was still higher than 59%.

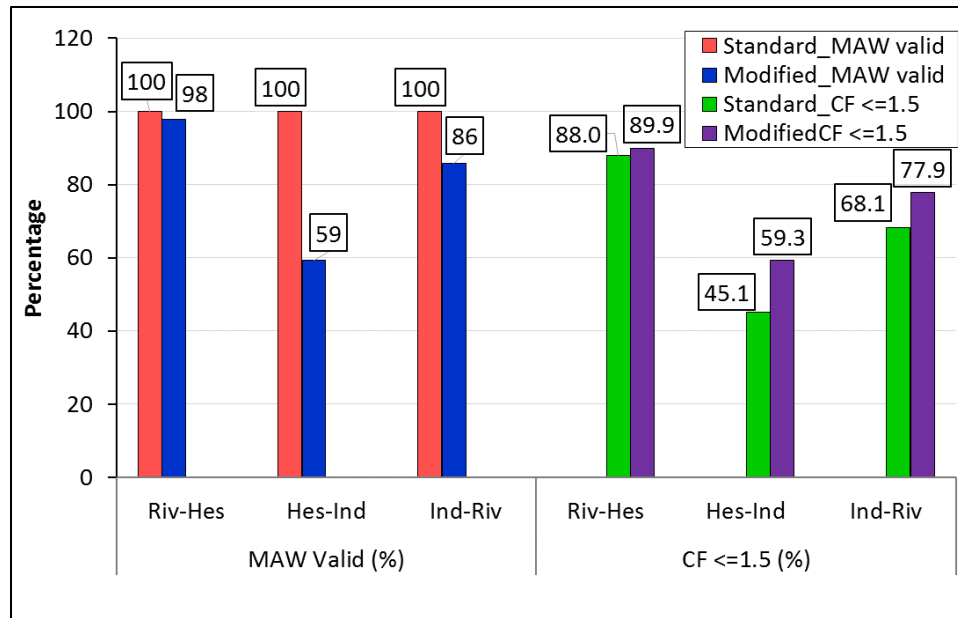


Figure 3-15 Comparison of Standard MAW (with temperature criteria) and Modified MAW (without temperature criteria)

3.4.5. Potential Improvements for Heavy-Duty In-Use Compliance Testing Procedures

CARB is currently evaluating potential alternatives to the present in-use compliance testing. The main issue with the current NTE procedure is that the NTE procedure excludes a large percentage of operation. As the original NTE procedures was targeted more for long haul operation, the criteria in terms of power levels excludes a considerable fraction of lower load operation. The requirement for NTE event durations of at least 30 seconds also excludes a large amount of operation.

Improvements to the in-use compliance procedures have focused primarily on developing methodologies to cover a wider range of operation, and to ensure that areas of operation where disproportionate amounts of NO_x are formed are also covered. As discussed above, Bartolome et al. found that the fraction of operation covered during in-

use testing could be increased from 5% for NTE operation to 30 by broadening the NTE criteria to 60% using a MAW method. Correspondingly, the percent of NO_x generated during testing increased from 6% for the NTE operation to 33% by broadening the NTE criteria to 62% using a MAW method.

The results of our testing show similarly that the use of a MAW methodology would increase the percentage of operation covered as part of an in-use testing procedure. For the manufacturer A truck, the percentage of operation covered by the NTE procedure represented approximately 45% with an average emission rate of 0.27 g/bhp-hr. The operation excluded by the NTE represented approximately 16 percent of the emissions at a typical emissions rate of 0.94 g/bhp-hr. Similarly for the manufacturer B truck, the percentage of operation covered by the NTE procedure represented approximately 46% with an average emission rate of 0.34 g/bhp-hr. The operation excluded by the NTE represented approximately 13 percent of the emissions at a typical emissions rate of 0.74 g/bhp-hr. For the MAW analysis, the percentage of operation included increased to 85% for the manufacturer A truck and 92% for the manufacturer B truck. The average emission rate for the operation in the MAW was 0.23 g/bhp-hr for the manufacturer A truck and 0.37 g/bhp-hr for the manufacturer B truck, while the average emission rate for operation outside of the MAW was 0.74 g/bhp-hr for the manufacturer A truck and 0.43 g/bhp-hr for the manufacturer B truck.

There were also limitations for the MAW procedure in terms of data coverage. Even though 100% of the activity in our study was in valid MAW control areas, this was due to the freeway driving conditions. For other normal daytime traffic conditions, Yoon et al.

(2016) found only about 50% of the MAWs were valid. The NO_x emission rates of the invalid MAW areas were found to generate more NO_x emission than those of the valid MAWs. The data coverage could also be even worse during the urban low-power truck operations.

3.5. Conclusions

NO_x emissions results of urban driving cycles (CS-UDDS, CS-FTP, UDDS, FTP and CARB-transient) and the freeway and SET cycles (CARB-cruise, CARB-high-speed cruise, on-road routes and RMC) are presented in this study. The results showed that in-use NO_x emissions over the most of urban driving cycles of chassis dynamometer, on-road and engine dynamometer tests were above the 0.2 g/bhp-hr level for both vehicles. The NO_x emissions ranged from 0.16 to 1.1 g/bhp-hr over all of the urban test conditions for both vehicles. The results for the freeway/steady state tests were generally lower than those for the urban cycles. For the manufacturer A truck, the cruise results were on the order of 0.1 g/bhp-hr, while the high-speed cruise results were 0.3 g/bhp-hr or less. For the manufacturer B truck, the cruise and high-speed cruise results were on the order of 0.3 g/bhp-hr or less. The on-road testing results were higher for the both trucks, compared with the cruise and hi-speed cruise cycle results from the engine and chassis dynamometer testing.

In comparing the UDDS results between the different testing conditions (i.e., chassis dynamometer, on-road, and engine dynamometer), the manufacturer A truck showed the highest emissions for the chassis dynamometer testing, followed by the on-road testing, and then with the lowest emissions for the engine dynamometer testing for

the urban driving cycles. The manufacturer B truck also showed the highest results for the chassis dynamometer testing, with comparable results for the on-road and engine dynamometer results for the urban driving cycles. The differences between the tailpipe NOx emissions could be attributed to several factors, including differences in SCR inlet NOx temperatures and engine out NOx emissions.

The cycle average SCR efficiencies for both vehicles ranged from 68 to 98%. For inlet SCR temperatures higher than 250°C, the SCR conversion efficiencies remained consistently high (>80%). At temperatures below 250°C, the SCR efficiencies were generally lower, although this varied from cycle to cycle. The SCR efficiencies were also found as a function of load, especially for the manufacturer B truck. The highest SCR efficiencies (>90%) were observed between 30 to 60% load for the Volvo truck and 10 to 40% load for the manufacturer B truck. The SCR efficiency of the manufacturer B truck also dropped as the load increased into the middle load range, and the SCR efficiency remained lower under high load conditions for all the testing conditions.

For the on-road testing, the results from the NTE analysis showed that the manufacturer A truck passed the NTE criteria for 7 of 9 tests, while the manufacturer B truck passed for only 3 of 9 tests. The current NTE has the limitation of low coverage of activity. Using modified NTE criteria, where the criteria for excluding data was lowered to below 10% maximum power and torque, only a small increase in the percentage (12%) of activity covered was found. The activity analysis of MAW showed a significant improvement of the amount of data that was included. The emissions were found to fail the MAW test for a majority of the routes.

The results of this study indicate that in-use NO_x emissions are above the 0.2 g/bhp-hr level for a wide range of operation, and that there are higher emitting trucks that also can contribute disproportionately to the NO_x inventory. It is likely that a combination of expanded certification criteria, tightened certification limits, and expanded in-use compliance procedures will be needed to provide greater control of in-use NO_x emissions.

In terms of certification procedures, a reduction of the certification standard to 0.02 g/bhp-hr is currently under consideration. CARB is conducting on-going studies to evaluate different methodologies to achieve such emissions levels at the Southwest Research Institute. These include heated dosing, gaseous dosing, and supplemental heat addition devices, thermal management strategies, and supplemental exhaust heat addition devices which have shown success in reducing cold start emissions. Additional provisions will also likely be needed to reduce emissions for vocations that operate under low load conditions, where the SCR efficiency can be much lower. This could include the development of additional cycles that would better characterize operation under low load conditions. Such cycles could potentially be added to the certification procedure to better ensure that low NO_x levels could be maintained under such low load operating conditions.

The current procedures for in-use compliance testing also have limitations that can make it difficult to identify the full range of operations conditions and vehicles contributing to higher NO_x emissions. The current exclusion criteria for NTE testing eliminates a large fraction of in-use operation. The modification of NTE exclusion criteria, such as reducing the power requirement to 10% or reducing the temperature exclusions for aftertreatment systems, could broaden the amount of operation covered by the in-use compliance test, but

even with such modifications, the NTE methodology appeared to have limitations. The MAW methodology, currently being used in Europe, provided improved coverage of in-use operation, and could provide a better methodology for capturing NOx emissions under a full range of operating conditions. It is also possible that greater control of in-use NOx emissions could be obtained by placing a greater emphasis on in-use compliance testing through the use of sensors that could be utilized to track emissions performance on a continuous basis.

3.6. Acknowledgements

The authors thank the following organizations and individuals for their valuable contributions to this project. We acknowledge funding from the California Air Resources Board (CARB) under contract 15RD001. We acknowledge Mr. Mark Villa, Mr. Don Pacocha, and Mr. Edward O'Neil of the University of California, Riverside for their contributions in conducting the emissions testing for this program.

3.7. References

- Bishop, G.A., Schuchmann, B.G., Stedman, D.H., Lawson, D.R., 2012. Emission Changes Resulting from the San Pedro Bay, California Ports Truck Retirement Program. *Environ. Sci. Technol.* 46, 551–558.
- Bishop, G.A., Schuchmann, B.G., Stedman, D.H., 2013. Heavy-Duty Truck Emissions in the South Coast Air Basin of California. *Environ. Sci. Technol.* 47, 9523–9529.
- Brown, J.E., Clayton, M.J., Harris, D.B., King, F.G., 2000, Comparison of the Particle Size Distribution of Heavy-Duty Diesel Exhaust Using a Dilution Tailpipe Sampler and an In-Plume Sampler during On-Road Operation; *J. Air & Waste Manage. Assoc.* 50, 1407-1416.
- Brown, J.E., King Jr, F.G., Mitchell, W.A., Squier, W.C., Harris, D.B., and Kinsey, J.S., 2002, On-Road Facility to Measure and Characterize Emissions from Heavy-Duty Diesel Vehicles, *Journal of the Air & Waste Management Association*, 52:4, 388-395, DOI: 10.1080/10473289.2002.10470797.
- Burgard, D.A., Bishop, G.A., Stedman, D.H., Gessner, V.H., Daeschlein, C., 2006, Remote sensing of in-use heavy-duty diesel trucks. *Environ. Sci. Technol.* 40, 6938–6942.
- California Air Resources Board. 2013. Presentation entitled Mobile Source Emissions Inventory and Assessment Updates. October.
- Carder, D., Gautam, M., Thiruvengadam, A., Besch, M., 2014. "In-Use Emissions Testing and Demonstration of Retrofit Technology for Control of On-Road Heavy-Duty Engines." Final Report by West Virginia University for the South Coast Air Quality Management District.
- Clark, N. N., Gautam, M., Wayne, W. S., Lyons, D. W., Thompson, G. J., 2007. Heavy-duty vehicle chassis dynamometer testing for emissions inventory, air quality modeling, source apportionment, and air toxics emissions inventory. CRC Report No. E55/59.
- Clark, N. N., Gautam, M., Wayne, W. S., Thompson, G. J., Lyons, D. W., 2004. California heavy heavy-duty diesel truck emissions characterization for project E-55/E-59 phase 1.5. CRC Report No. E55/59. Final Report for the Coordinating Research Council.
- Clark, N. N., Gautam, M., Wayne, W. S., Thompson, G. J., Nine, R. D., Lyons, D. W., Buffamonte T., Xu S., Maldonado H., 2006. Regulated emissions from heavy heavy-duty diesel trucks operating in the south coast air basin. Soc. SAE Paper 2006-01-3395.
- Clark, N.N., M. Gautam, M., W.S. Wayne, D. Lyons, W. F. Zhen, C. Bedick, R.J. Atkinson, and D.L. McKain. 2007a. Creation of the “Heavy Heavy-Duty Diesel Engine

- Test Schedule” for representative Measurement of Heavy-Duty Engine Emissions, CRC Report No. ACES-1, CRC Website at crcao.org, July.
- Clark, N.N., F. Zhen, C. Bedick, M. Gautam, W. Wayne, G. Thompson, and D. Lyons, 2007b. Creation of the 16-Hour Engine Test Schedule from the Heavy Heavy-Duty Diesel Engine Test Schedule, CRC Report No. ACES-1-a, CRC Website at crcao.org, July.
- Cocker III, D. R., Shah, S., Johnson, K., Miller, J. W., Norbeck, J., 2004a. Development and Application of a Mobile Laboratory for Measuring Emissions from Diesel Engines. I Regulated Gaseous Emissions, *Environ. Sci. & Technology*. 38, 2182-2189.
- Cocker, D.R.; Shah, S.D.; Johnson, K.J.; Zhu, X; Miller, J.W.; Norbeck, J.M., 2004b, Development and Application of a Mobile Laboratory for Measuring Emissions from Diesel Engines. 2. Sampling for Toxics and Particulate Matter, *Environ. Sci. & Technology*, 38, 6809-6816.
- Code of Federal Regulations CFR, 2007. Supplemental emission test; test cycle and procedures. Office of the Federal Register National Archives and Records Administration. CFR Title 40 Part § 86.1360,2007.
- Code of Federal Regulations CFR, 2007. Not-To-Exceed test procedures, Office of the Federal Register National Archives and Records Administration. CFR Title 40 Part § 86.1370, 2007.
- Code of Federal Regulations CFR, 2011. Emission standards and supplemental requirements for 2007 and later model year diesel heavy-duty engines and vehicles, Office of the Federal Register National Archives and Records Administration. CFR Title 40 Part § 86.007, 2007.
- Dallmann, T.R. and Harley, R.A., 2010, Evaluation of mobile source emission trends in the United States. *J. Geophys. Res.* 115, D14305.
- Dallmann, T.R., Harley, R.A., and Kirchstetter, T.W., 2011, Effects of diesel particle filter retrofits and accelerated fleet turnover on drayage truck emissions at the Port of Oakland, *Environ. Sci. Technol.*, 45, 10773–10779, doi:10.1021/es202609q.
- Dallmann, T.R., DeMartini, S.J., Kirchstetter, T.W., Herndon, S.C., Onasch, T.B., Wood, E.C., Harley, R.A., 2012, On-road measurement of gas and particle phase pollutant emission factors for individual heavy-duty diesel trucks. *Environ. Sci. Technol.* 46, 8511–8518.
- Dallmann, T.R., Kirchstetter, T.W., DeMartini, S.J., and Harley, R.A., 2013, Quantifying On-Road Emissions from Gasoline-Powered Motor Vehicles: Accounting for the

- Presence of Medium- and Heavy-Duty Diesel Trucks, *Environ. Sci. Technol.*, 47, 13873–13881
- Dallmann, T.R., Onasch, T.B., Kirchstetter, T.W., Worton, D.R., Fortner, E.C., Herndon, S.C., Wood, E.C., Franklin, J., Worsnop, D.R., Goldstein, A.G., Harley, R.A., 2014, Characterization of particulate matter emissions from on-road gasoline and diesel vehicles using a soot particle aerosol mass spectrometer, *Atmos. Chem. Phys. Discuss.*, 14, 4007–4049
- Dallmann, T.R., Kirchstetter, T.W., DeMartini, S.J., and Harley, R.A., 2014, Quantifying on-road emissions from gasoline-powered motor vehicles: accounting for the presence of medium and heavy-duty diesel trucks, *Environ. Sci. Technol.*, 47, 13873–13881, 25 doi:10.1021/es402875u, 2014.
- Durbin, T.D., K. Johnson, D.R. Cocker, J.W. Miller, H. Maldonado, A. Shah, C. Ensfield, C. Weaver, M. Akkard, N. Harvey, J. Symon, T. Lanni, W.D. Bachalo, G. Payne, G. Smallwood, M. Linke, 2007. Evaluation and Comparison of Portable Emissions Measurement Systems and Federal Reference Methods for Emissions from a Back-up Generator and a Diesel Truck Operated on a Chassis Dynamometer. *Environ. Sci. & Technol.*, vol. 41, 6199-6204.
- EPA, 2002. Update Heavy-Duty Engine Emission Conversion Factors for MOBILE6: Analysis of BSFCs and Calculation of Heavy-Duty Engine Emission Conversion Factors. EPA420-R-02-005, January.
- European Commission - DG ENTR (Enterprise), 2002, Study on Emission Control Technology For Heavy Duty Vehicles, "In-use Conformity Testing of Emissions Control Devices", May. http://ec.europa.eu/enterprise/automotive/pagesbackground/emission_control/vol_5-in-use_conformity_testing.pdf.
- Gautam, M., Thompson, G.J., Carder, D.K., Clark, N.N., Shade, B.C., Riddle, W.C., and Lyons, D.W., 2001, Measurement of In-Use, On-Board Emissions from Heavy-Duty Diesel Vehicles: Mobile Emissions Measurement System, SAE Technical Paper No. 2001-01-3643.
- Gautam, M., N. N. Clark, W. Riddle, R. Nine, W. S. Wayne, H. Maldonado, A. Agrawal, and M., Carlock. 2002. Development and initial use of a heavy-duty diesel truck test schedule for emissions characterization. In Proceedings of Society of Automotive Engineers (SAE) Fuels and Lubricants Meeting; SAE Paper 2002-01-1753. SAE: Warrendale, PA.
- Harris, D.B., King, F.G., and Brown, J.E., Development of On-Road Emission Factors for Heavy-Duty Diesel Vehicles Using a Continuous Sampling System; EPA-600/A-98-

- 125 (NTIS PB99-106296). Presented at the A&WMA Emission Inventory: Programs and Progress Conference, Research Triangle Park, NC, October 10–13, 1995.
- Herner, D. J.; Hu, S.; Robertson, H. W.; Huai, T.; Collins, F. J.; Dwyer, H.; Ayala, A., 2000. Effect of advanced after treatment for PM and NO_x control on heavy-duty diesel truck emissions. *Environ. Sci. Technol.* 43, 5928–5933.
- Huai T.; Durbin T. D.; Miller J. W.; Pisano J.T.; Sauer C. G.; Rhee S. H.; et al. 2003, Investigation of the formation of NH₃ emissions as a function of vehicle load and operating condition. *Environ. Sci. Technol.* 37, 4841-4847.
- Jiang, Y., Yang, J., Cocker, D., Karavalakis, G., Johnson, K.C. and Durbin, T.D., 2018. Characterizing emission rates of regulated pollutants from model year 2012+ heavy-duty diesel vehicles equipped with DPF and SCR systems. *Science of the Total Environment*, 619,765-771.
- Johnson, D., 2002, ROVER – Real-time On-road Vehicle Emissions Reporter. Presentation for the Mobile Source Technical Review Committee, February.
- Johnson, K.C., T.D. Durbin, D.R. Cocker III, J.W. Miller, R.J. Agama, N. Moynahan, G. Nayak, 2008. On-Road Evaluation of a PEMS for Measuring Gaseous In-Use Emissions from a Heavy-Duty Diesel Vehicle. *SAE Int. J. Commer. Veh.*, 1, 200-209.
- Johnson, K.C., Durbin, T.D., Cocker III, D.R., Miller, J.W., Bishnu D.K., Maldonado H., Moynahan N., Ensfield C., Laroo C.A.. 2009. On-Road Comparison of a Portable Emission Measurement System with a Mobile Reference Laboratory for a Heavy Duty Diesel Vehicle. *Atmospheric Environment*. Vol. 43, pp. 2877-2883.
- Johnson, K.C., Durbin, T.D., Jung, H., Cocker III, D.R., Giannelli, R., Bishnu, D., 2010. Quantifying In-Use PM Measurements for Heavy Duty Diesel Vehicles. *Environ. Sci. Technol.*, Vol. 45, pp. 6073-6079.
- Khalek I., Bougher, T., Merritt P., and Zielinska B., 2011. Regulated and Unregulated Emissions from Highway Heavy-Duty Diesel Engines Complying with U.S. Environmental Protection Agency 2007 Emissions Standards *Journal of Air and Waste Management Assoc.* Vol 61, pages??.
- Khalek, I. Blanks, M., Merritt, P., 2013, Phase 2 of The Advanced Collaborative Emissions Study, Final Report Project 03.17124, November. www.crao.org/reports/recentstudies2013/.
- Khan, M.Y., Johnson, K.C., Durbin, T.D., Jung, H., Cocker III, D., Bishnu, D., and Giannelli, R. 2012. Characterization of PM-PEMS for In-Use Measurements –

- Validation Testing for the PM-PEMS Measurement Allowance Program. *Atmospheric Environment*, 55, 311-318.
- Miller, J. W., Johnson, C. K., Durbin, T., Dixit, P., 2013. In-Use Emissions Testing and Demonstration of Retrofit Technology for Control of On-Road Heavy-Duty Engines. Final Report by the University of California at Riverside to the South Coast Air Quality Management District under Contract No. 11612.
- Misra, C., Collins, J.F., Herner, J.D., Sax, T., Krishnamurthy, M., Sobieralski, W., Burntizki, M., and Charnich, D. 2013. In-Use NOx Emissions from Model Year 2010 and Heavy-Duty Diesel Engines Equipped with Aftertreatment Devices, *Environ. Sci. Technol.* 47, 7892–7898.
- Misra, C., Yoon, S., Collins, J., Chernich, D., Herner, J., 2016. Evaluating In-Use SCR Performance: Older vs. Late MY Engines. Presentation at 26th CRC Real World Emissions Workshop, Newport Beach, CA, March.
- San Pedro Bay Ports Clean Air Action Plan Technical Report (CAAP), The Port Of Long Beach and Los Angeles, 2006.
- Sawyer, R. F.; Harley, R. A.; Cadle, S. H.; Norbeck, J. M.; Slott, R.; Bravo, H. A., 2000, Mobile Sources Critical Review. *Atmos. Environ.* 34, 2161–2181.
- Shah, S., Johnson, C. K., Miller, J. W., Cocker, R. D., 2006. Emission rates of regulated pollutants from on-road heavy-duty diesel vehicles. *Atmos. Environ.* 40, 147–153.
- Sharp, C. A., Webb, C. C., Neely, G. D., Smith, I., 2017. Evaluating technologies and methods to lower nitrogen oxide emissions from heavy-duty vehicles by Southwest Research Institute to the California Air Resources Board under Contract No. 13-312.
- Strots, O. V.; Santhanam, S.; Adelman, J. B.; Griffin, A. G.; Derybowski, M. E., 2009. Deposit formation in urea-SCR systems. SAE Technical Paper 2009-01–2780, 2009.
- Texas A&M Transportation Institute, 2013, Heavy-Duty Diesel Inspection and Maintenance Pilot Program.
- Thiruvengadam, A, Besch, M. C., Thiruvengadam, P., Pradhan S., Carder, D., Kappanna, H., Gautam, M., 2015. Emission Rates of Regulated Pollutants from Current Technology Heavy-Duty Diesel and Natural gas goods, movement Vehicles. *Environ. Sci. Technol* 49 (8), 5236-5244.
- Thiruvengadam, A, Besch, M. C., Thiruvengadam, P., Pradhan S., Carder, D., Kappanna, H., Gautam, M., 2015. Emission Rates of Regulated Pollutants from Current

- Technology Heavy-Duty Diesel and Natural gas goods, movement Vehicles. Environ. Sci. Technol 49 (8), 5236-5244.
- Thiruvengadam, A., Saroj, Pradhan, S., Demirgok, B., Besch, M., Carder, D., Quiros, D., Hu, S., Tao, Huai, Oshinuga, A., Chernich, D., Gautam, M., 2016, In-use Emissions from Current Model Year Heavy-duty Diesel and Natural Gas Trucks – Evaluation of NTE vs. Alternative Metrics. Presentation at 26th CRC Real World Emissions Workshop, Newport Beach, CA, March
- TIAX, 2011. Development of a Drayage Truck Chassis Dynamometer Test Cycle, Report for the Port of Long Beach/Contract HD-7188 Port of Los Angeles/Tetra Tech, September.
- Tu, J., Berdahl, S., Tran, T., O’Cain, J., Karim, J., Sardar, S., Lemieux, S., Huai, T., 2016. Study of heavy-duty vehicle emissions during in-use compliance testing. Presentation at 26th CRC Real World Emissions Workshop, Newport Beach, CA, March.
- U.S. Environmental Protection Agency; Heavy Trucks, Buses, and Engines; Regulations and Related Documents; see <http://www.epa.gov/otaq/hd-hwy.htm#regs>.
- U.S. Environmental Protection Agency, 2004. Working Group On Off- Cycle Emissions, "EPA Answers to Questions from March 22nd 2004 NTE Presentation". <http://www.oica.net/htdocs>.
- Zhao., Y., Hu, J., Hua, L., Shuai, S., Wang, J. 2011. Ammonia Storage and Slip in a Urea Selective Catalytic Reduction Catalyst under Steady and Transient Conditions. IE&C, 50, 11863–11871.
- Yoon, S., Berdahl, S., O’Cain, J., Bishnu, D., Misra, C., Collins, J., Chernich, D., Karim, J., Herner, J., 2016. Comparison of Heavy-Duty In-Use Engine Compliance Methods for Controlling NOx Emissions. Presentation at 26th CRC Real World Emissions Workshop, Newport Beach, CA, March.

3.8. Supporting Information

Another important consideration in understanding NO_x emissions is the SCR efficiency over the course of a test cycle. SCR efficiency was calculated based on the differences between engine-out and tailpipe NO_x. In conjunction with this analysis, some comparisons between the sensor and PEMS NO_x tailpipe values were made. Figure S1 provides a comparison of NO_x emissions between SCR out NO_x sensor and PEMS measurements in order to add confidence in the measurement from NO_x sensor for both vehicles. For the manufacturer A truck, the SCR NO_x sensor had a good correlation to the PEMS with the slope of 1.06 and R² of 0.89, indicating the manufacturer A NO_x sensor measurement was comparable to the PEMS. For the manufacturer B truck, the SCR NO_x sensor didn't perform as well, with data being more scattered around the parity line. This could be due to the frequency of manufacturer B NO_x sensor being around 0.3 Hz. The slope of the correlations between the manufacturer B SCR out NO_x sensor and tailpipe PEMS NO_x was 1 with an R² of 0.72.

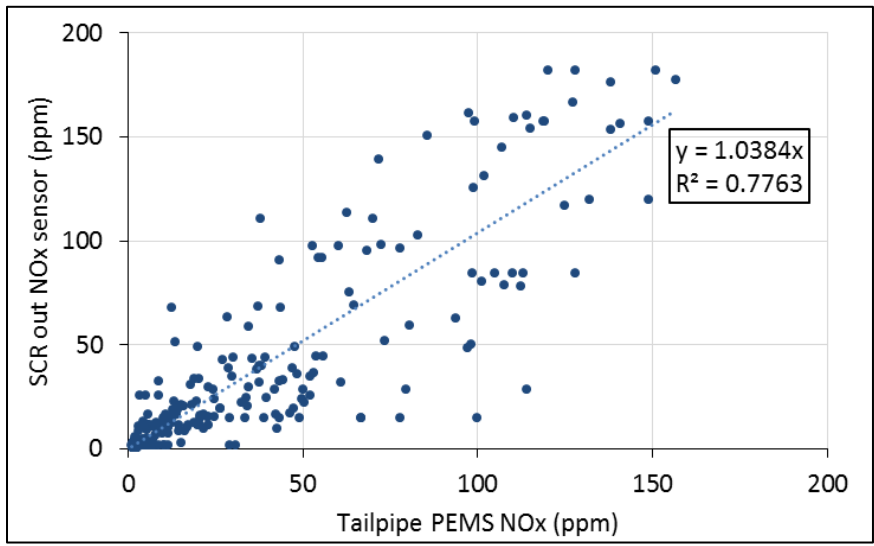
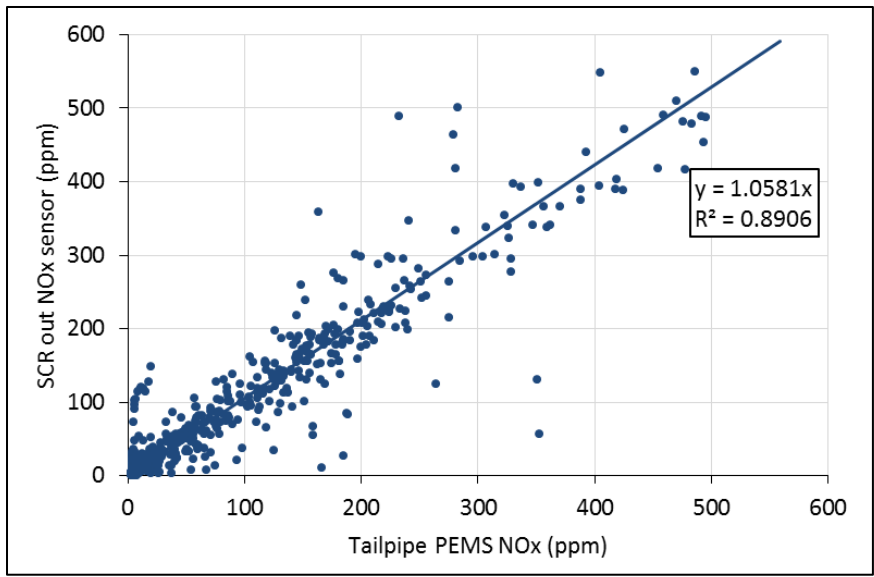


Figure S1 SCR out sensor vs tailpipe PEMS for the manufacturer A truck and the manufacturer B truck

4. Heavy-duty On-Road Vehicle Inspection and Maintenance Program

4.1. Abstract

The implementation of an enhanced heavy-duty (HD) Inspection and Maintenance (I/M) program could be a critical element in ensuring the emissions performance of HD diesel vehicles over their full useful life. The objective of this study was to evaluate and assess alternatives for a more comprehensive HD I/M program that could be implemented in California. A prototype HD I/M pilot study was conducted where the emissions of 47 vehicles were measured before and after repair. The vehicles showed good reductions post-repair for NO_x for some of the higher emitting vehicles, especially for some of the vehicles with the highest emissions. The pre-repair NO_x emissions results showed that a number of vehicles had emissions higher than the 2010 NO_x standard for both the initial 30 and 50 mph tests. The repairs did not appear to have a significant impact on reducing post-repair PM emissions. The pre-repair opacity were generally low for most vehicles (5% or less). This suggests that most of the vehicles tested did not have significant DPF failures at the level where they might be targeted for an I/M program.

Based on a review of the potential methods, OBD was selected as the primary methodology of HD I/M, coupled with roadside monitoring with a remote sensing device (RSD). A mini-PEMS could potentially also be incorporated into a HD I/M program as a verification of the pass/fail determinations.

4.2. Introduction

Emissions from on-road heavy-duty vehicles are major contributors to poor air quality in California. Although heavy-duty (HD) vehicles represent a relatively small portion of the total population of vehicles on the road, (only two percent by count), they produce a disproportionate amount of the emissions generated from on-road motor vehicles. The problem is complicated by the large number of heavy-duty vehicles, registered in other states that travel in and out of California transporting various goods. Heavy-duty vehicles and engines have been the subject of progressively more stringent emissions regulations over the past several decades. This has led to significant reductions in emissions from newer diesel engines over the years, with the latest generation of regulations requiring exhaust aftertreatment for the control of both oxides of nitrogen (NO_x) and particulate matter (PM) emissions. At this time, the truck fleets include those with urea-SCR NO_x reduction, those with exhaust gas recirculation (EGR) NO_x reduction, and earlier models with in-cylinder combustion control for NO_x reduction. Despite these significant reductions, HD vehicles still represent 33% of NO_x emissions and 26% of PM emissions. As trucks represent only 8% of greenhouse gas (GHG) emissions from motor vehicles, this suggests that the fuel-specific emissions of NO_x and PM are substantially above the motor vehicle fleet average.

While engines meeting the newest emissions standards continue to penetrate into the in-use fleet, it is also important to ensure that the emissions from these vehicles do not significantly deteriorate over the course of the lifetime of the vehicle. This is important because heavy-duty engines tend to have relatively long lifetimes, both in terms of years

of service as well as miles of travel or hours of engine life. Inspection and maintenance (I/M) programs are one of the most important measures put in place to prevent excessive emissions from in-use vehicles. Although I/M programs for light-duty vehicles have been extensively implemented throughout the United States (U.S.), I/M programs for heavy-duty vehicles are more limited in number and in scope. Most HD I/M programs focus predominantly on controlling smoke or opacity emissions (Texas A&M Transportation Institute, 2013; NYSDEC 2008, 2013; St. Dennis et al., 2005). California has an existing HD vehicle I/M program that includes several different types of inspections or programs that are implemented by the California Air Resources Board (CARB, 2015). The Heavy-Duty Vehicle Inspection Program (HDVIP) and Periodic Smoke Inspection Program (PSIP) have been in place since the late 1980s. The HDVIP requires HD trucks and buses to be inspected for excessive smoke and tampering, and engine certification label compliance. These inspections can be administered at various locations, including weigh stations and border crossings, and include Snap and Idle testing with a smoke meter to measure the opacity of the exhaust. The PSIP requires diesel truck and bus fleet owners to conduct their own annual smoke opacity inspections, and repair those vehicles with excessive smoke emissions to ensure compliance. There is also an Emissions Control Label (ECL) Inspection Program that requires all vehicles operating in the State to have an ECL showing that the engine met the required federal emission standards applicable for the model year of the engine. Newer trucks are also subject to in-use testing with portable emissions measurement systems (PEMS), although this testing is only for a very small portion of the actual vehicles that are out on the road and not over the full lifetime of the

vehicle. While these programs provide some important benefits in maintaining emission levels of HD vehicles, the existing program does not include significant controls for NO_x emissions from the in-use fleet and also may not be adequate to control emissions from newer HD vehicles that are equipped with exhaust aftertreatment. In order to better ensure that in-use engines continue to meet emissions performance requirements, California still needs a more comprehensive HD I/M program.

Given the importance of controlling in-use emissions from heavy-duty trucks, there has been increased emphasis on studies characterizing in-use emissions, such as the UC Riverside, Mobile Emissions Laboratory (MEL) (Durbin et al., 2007; Johnson et al., 2010, 2009, 2008; Khan et al., 2012; Miller et al., 2014; West Virginia University 2003, 2004). While the number of vehicles that can be tested utilizing these more comprehensive laboratory techniques is relatively limited. There have also been a number of studies designed to characterize emissions from larger populations of vehicles, and in particular heavy-duty vehicles, using a variety of techniques, including remote sensing (Burgard et al., 2006; Bishop et al., 2012; Envirotec Canada, 2013; Stanard et al. 2012), tunnel or probe studies (Dallmann et al., 2012; Kuwayama et al., 2013; McDonald et al., 2014), and more recently studies utilizing tents that vehicles are driven through (Bishop et al., 2013, 2015; Texas A&M Transportation Institute, 2013). Several of these studies have suggested that such techniques could provide value if implemented in a HD I/M program. A Texas A&M Transportation Institute study suggested that using a tent, or On-road Heavy-duty Emissions Measurement System (OHMS) potentially used in combination with remote sensing and/or a chassis dynamometer could be beneficial in I/M applications, while a

study in Vancouver suggested the possible benefits of using remote sensing for an I/M program. Other methods that have been investigated for HD I/M include the use of chassis dynamometers (Chernich, 2003) or the use of On-Board Diagnostics (OBD), as this becomes more readily implemented into the in-use HD fleet.

Although these studies have suggested the potential benefits of using a variety of different methods in an enhanced HD I/M program, a number of questions must be answered before these methods could be implemented in a full scale I/M program in California, including how effective the program might be in identify high vs. low emitters and in reducing the emissions of high emitters. Another difficulty in developing an I/M test is that the emissions of the vehicle can vary with the way in which the vehicle is operated, its duty cycle (Clark et al., 2002), and the thermal condition of the engine and aftertreatment (Clark et al., 2011). Moreover, the exhaust aftertreatment can cause the instantaneous emissions to be less strongly related to the immediate engine behavior than was the case for older engines. Also, while light-duty I/M programs are comparatively mature and in the U.S., they address primarily gasoline vehicles that employ stoichiometric combustion. Equipment failures or deterioration leading to high emissions levels for light-duty vehicles are well understood and differ substantially from high emissions causes in diesel vehicles. So, while some light duty measurement methods and I/M philosophies could translate to HD diesel vehicles, it is important to consider the differences between LD gasoline and HD diesel vehicles in developing a HD I/M program.

The objective of this study is to develop, evaluate, and assess emissions benefit impacts of alternatives for a more comprehensive HD vehicle I/M program prototype for

a total number of 47 vehicles over 14,000 pounds gross vehicle weight rating (GVWR), and provide recommendations for the implementation of a full-scale program. The vehicles were procured from two local repair facilities based on the need for emissions related repairs. Emissions measurements using I/M grade emissions analyzers were used to evaluate the emissions benefits from various repairs based on a comparison of the before and after emissions measurements. For vehicles so equipped, the OBD system was monitored before and after the repair to evaluate the effectiveness of the OBD in identifying emissions related issues and what benefits are obtained from OBD based repairs. The study results will inform the design of an improved HD I/M program expected for the Air Resources Board's (ARB or Board) consideration in 2018 or 2019, and support the ARB's State Implementation Plan development to achieve national ambient air quality targets in California. California still needs a more comprehensive HD I/M program.

4.3. Literature Review

The main emphasis of the literature review was to evaluate potential methodologies and instruments that could be utilized for a HD I/M program and propose a framework for a prototype HD I/M program that could be evaluated as part of this study. The International Council on Clean Transportation (ICCT) has recently completed a comprehensive evaluation of heavy-duty I/M methodologies and this provided key information for the literature survey to be performed in this study (ICCT, 2015). They evaluated two main testing methods, the free acceleration smoke (FAS) test and the lug down smoke test, as well as a number of newer measurement technologies and testing methods that could be

utilized to improve I/M programs, including the use of OBD, RSD, and the On-road Heavy Duty Vehicle Emissions Monitoring system (OHMS). The Texas Department of Transportation has also recently completed a heavy-duty diesel I/M pilot program which included an assessment of OBD, opacity measurement, idle testing, ASM testing, IM240 testing, RSD, PM filter sampling and chassis dynamometer testing using PEMS (Texas A&M – Texas Department of Transportation, 2013). Additionally, heavy-duty I/M programs being conducted in California as well as other states were also evaluated. CARB evaluated the potential of using chassis dynamometer testing in an inspection and maintenance program as part of their State Implementation Plan measure M17 (Chernich, 2003). The program envisioned portable dynamometers setup at roadside locations where trucks would be pulled over to undergo a short dynamometer test. A total of 91 vehicles was tested over a sequence that included a power curve test, a 60 mph steady-state test at three loads, an idle test and a snap acceleration test.

4.3.1. Tailpipe Emissions Measurements

Tailpipe emission measurement methodologies that were evaluated included chassis dynamometer emissions measurements, portable emissions measurement systems (PEMS), and remote sensing devices (RSD).

Dynamometer testing represents one of the most comprehensive methods that could be utilized for heavy-duty I/M programs, and provides the best potential to correlate with laboratory grade emission measurements, but the implementation of a dynamometer based inspection system would require a level of testing that is probably too extensive and expensive to be implemented for the full HD fleet.

PEMS can include both fully 1065-compliant PEMS, which represent laboratory grade measurement accuracy, and smaller mini-PEMS that are designed to provide good quality measurements without meeting full laboratory grade requirements. The cost and level of intrusion on the HD vehicle operator is still an issue with fully compliant and mini-PEMS, putting limitations on more widespread implementation. PEMS may determine the emissions levels in brake-specific or fuel-specific terms, depending on the sophistication of the equipment.

RSD has the advantage of being non-invasive, having the ability to capture the emissions of vehicles as they are driven by the owner/operator under real-world conditions. Although like dynamometer and PEMS based testing, all vehicles would need to be screened to find those likely to fail, RSD does not require that trucks be taken out of service in order to perform such testing. RSD typically determines the emissions levels in fuel-specific terms, and does not control precisely the load on the vehicle's engine during the sensing.

4.3.2. **On-Board Diagnostics**

OBD monitors all emissions critical devices and systems, stores diagnostic trouble code(s) (DTC) and illuminates a malfunction indicator light (MIL) when a problem is detected, as required by law. A key advantage of OBD is that the vehicle's emission control system is continuously monitored as the vehicle is driven under real-world conditions. An OBD based I/M program requires monitoring the entire fleet, but the test itself is relatively quick, convenient to the owner operator, and the per test costs are considerably lower than the dynamometer or PEMS based alternative.

4.4. Materials and Methods

4.4.1. Test Vehicles

47 heavy-duty over-the-road tractors were selected as candidate vehicles for evaluation in the pilot program. Candidate vehicles were selected from those arriving at two repair facilities based on whether they fell into specific model year ranges (~80% of the test vehicles were MY2013+, 20% were MY2010-2012) and on the nature of their emissions related malfunction. The objective of the selection process was to evaluate a distribution representative of the 2025 fleet and its probable emissions related maintenance issues, as this represents a timeframe when the program may be into full implementation. Trucks were procured with the assistance of local repair facilities with the objective of collectively assembling a fleet equipped with emission control technologies and displaying malfunctions which are typical for in-use heavy-duty trucks. The vehicle procured through these repair facilities were all in need of repairs or corrective maintenance. As such, the expense related with repairs are borne by the fleet operator/vehicle owner and the accuracy of diagnosis and resulting change in emissions due to repairs are reflective of the actual abilities of heavy-duty engine mechanics. The target repair test matrix that was used for this project, and actual number of identified vehicles needing each of the corresponding repairs. These repairs categories were selected based on the component or system malfunctions that are expected to cause excessive emissions of different pollutants. The test matrix was developed based on information about the frequency at which the repairs were expected to occur, based on the local repair facility repair records, coupled with estimates of the expected emissions increases for different failures, based on EMFAC2014

estimates and durability demonstration vehicle (DDV) report analyses. During the vehicle recruitment, candidate was identified based on vehicles being diagnosed for repairs, which were typically diagnosed based on the OBD-codes and coupled with additional diagnoses by a repair technician. Table 4-1 lists the target repair test matrix that was used for this project, and actual number of identified vehicles needing each of the corresponding repairs.

Table 4-1 List of ECM Trouble Codes identified and the repairs for each vehicle

No.	Part/Repair	Targeted # of Test Vehicles	# Identified Test Vehicles
1	DPF filter cleaning	3	3
2	DPF filter	6	3
3	exhaust pressure sensor	2	2
4	oxidation catalyst	2	0
5	injector doser	4	5.5
6	EGR valve/cooler/system	4	4.5
7	DEF filter, fluid & parts	2	5
8	turbocharger	2	2
9	boost pressure sensor	2	0
10	inlet or outlet NOx sensor	2	7.5
11	charge air cooler	2	0
12	ammonia sensor	2	1
13	SCR	2	3
14	temperature sensor	6	2
15	fuel injector	2	1
16	fuel system components	2	3
17	Engine control module (ECM)	2	3
18	lambda(O2) sensor	2	0
19	crankcase filter		2
20	crankcase pressure sensor		1
21	crank position sensor		1
22	air filter	1	1
	aborted vehicles		3 (Count as half vehicle)
	total number of vehicles	50	50.5

4.4.2. Overall Flow Chart for the Pilot Program

A generalized flow chart of the sequences for the pilot program is provided below. This provides an overview of the methodology that was utilized for the pilot program, with specific elements of the testing being discussed in greater detail below.

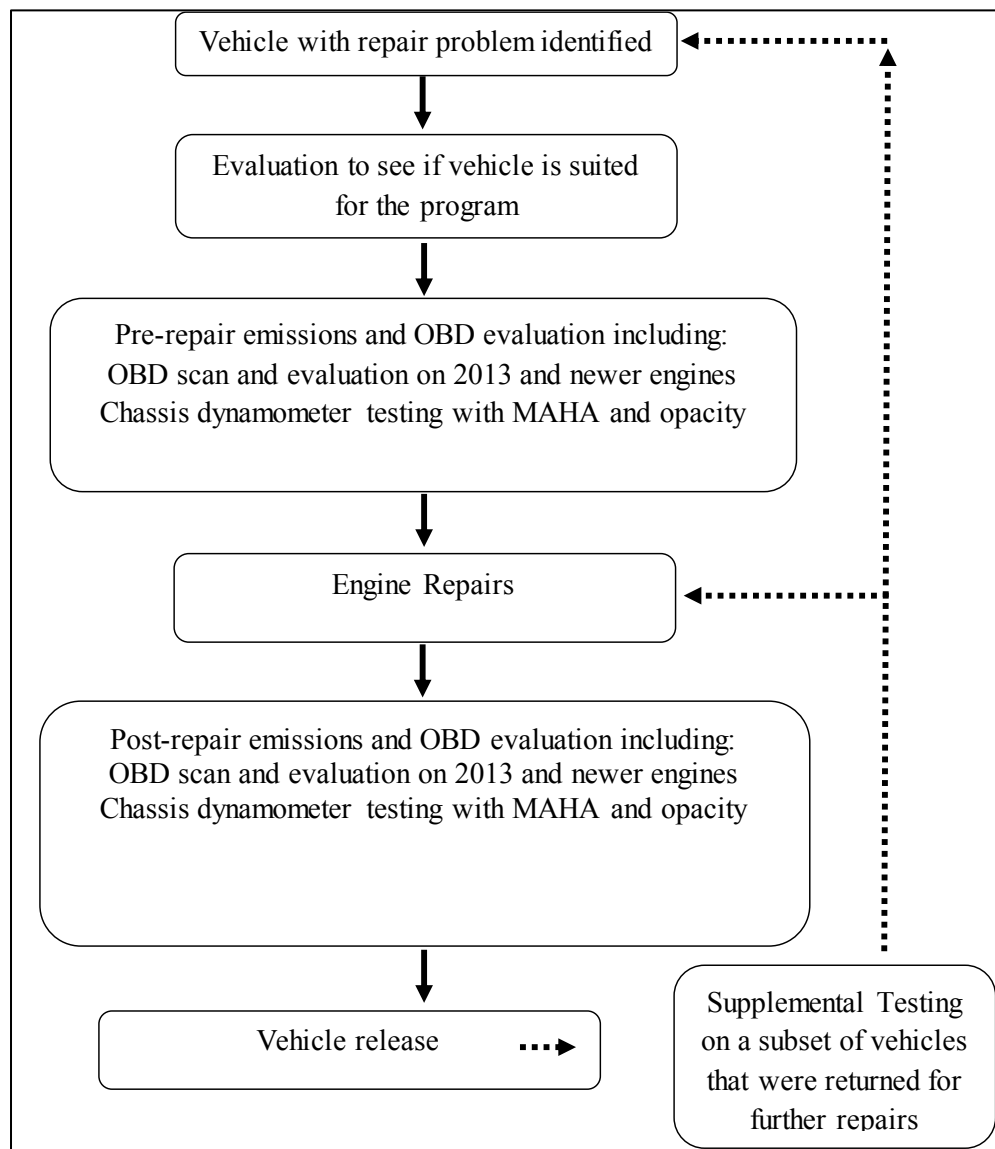


Figure 4-1 Overall flow chart for pilot demonstration program

4.4.3. Test methods

Chassis Dynamometer Testing. For this study, dynamometer testing with a repair grade dynamometer is being used as the reference method or gold standard around which the effectiveness of the prototype I/M program was evaluated. Both repair facilities maintain repair-grade eddy current chassis dynamometers on site.

There was a warm up sequence before emissions measurements being collected. The vehicle was initially warmed by driving the vehicle until the engine coolant temperature reached ~140°F. The vehicle was then driven to its maximum speed with no load and a lug down test was conducted, where a load was applied until the vehicle reached its maximum horsepower and then started to drop. The vehicle speed reached approximately 60-65 miles per hour (mph) during this segment. This is the standard test done at the repair facilities to evaluate the performance of the engine, and appeared to sufficiently warm up the engine and aftertreatment systems.

Following this warm up sequence, the vehicle's speed was then dropped back down to 50 mph and the dynamometer load was adjusted until it reached approximately 200 hp. The emissions testing was conducted for a period of approximate 2 minutes when the vehicle operation was reasonably stable. The vehicle speed was then dropped to 30 mph, and the dynamometer load was adjusted until it reached approximately 100 hp. The emissions testing was conducted for a period of approximate 2 minutes. For each speed, the hp levels were selected to represent hp that would be representative of typical driving on the road with a loaded trailer at the respective speeds. For the 50 mph point in particular, the hp was typically near the peak torque point on the power curve. Opacity measurements

were then made that included 3 clean out snap accelerations, followed by the 3 snaps accelerations for main opacity readings.

Emission Measurements. A MAHA MGT 5 Emissions Tester, a MAHA MPM4 Particle Analyzer and an opacity meter were used in conjunction with the chassis dynamometer measurements. These instruments were capable of collecting emissions of HC, CO, NO_x, CO₂, and PM.

OBD Measurements. OBD measurements were another important aspect of this study. As discussed above, 80% of the test vehicles were equipped with engines with model years (MYs) of 2013 or newer, so a majority of the vehicles recruited were equipped with OBD. For vehicles equipped with OBD, information was obtained on-site during testing by directly interfacing with the OBD system. A HEM data logger was also used during the course of the chassis dynamometer testing to obtain data on engine parameters as the tests are being conducted.

4.5. Results and Discussion

Pre- and post-repair chassis dynamometer tests were conducted on a total of 47 vehicles, with three of these vehicles requiring a second or third visit to resolve their repair issue. The results for PM and NO_x emissions are presented for the 30 and 50 mph tests in this subsection. The results are typically presented normalized on a g/bhp-hr basis. This allows the pre- and post-test results to be more readily compared by normalizing out any variations in load that might be seen within the tests itself. For the tests where engine ECU data was not available, i.e., such that bhp-hr information was not available from the ECU,

a linear regression was used to determine the g/bhp-hr values based on the emission concentrations.

4.5.1. NO_x Emissions

Pre- and Post-repair NO_x emissions were separated by repair category for the 30 and 50 mph tests, as presented in Table 4-2 to Table 4-4. Overall, the pre-repair NO_x emissions results showed that a number of vehicles had emissions higher than the 2010 NO_x standard for both the initial 30 and 50 mph tests, although it is acknowledged that the standard is set for a specific transient test that was not performed. This included 4 vehicles (J&R01, 17, 22 and Cum02) with particularly high NO_x emissions, which had problems that included injector dosers, DPF replacement, and exhaust pressure sensors. All these vehicles showed significant reductions in NO_x emission after repair, with reductions of greater than 83% after repair for all test conditions. Vehicles with other problems, including DEF system issues and SCR inlet and outlet NO_x sensors, showed mixed trends in comparing the pre- and post-repair NO_x emissions.

The NO_x emissions results for 30 and 50 mph were examined for any trends based on different types of repairs. Repair issues such as those associated with the EGR, DEF, or SCR systems, or NO_x sensors are ones that could have an impact on NO_x emissions. A total of 15 vehicles (Cum01, J&R01, 05, 06, 12, 15, 17, 19, 22 second visit, 27, 28, 30, 31, 37 and 40 second visit) had issues associated with the DEF system. Eight of these vehicles (Cum01, J&R01, 12, 17, 19 first visit, 28, 30, and 37) showed lower NO_x emissions readings after fixing the DEF associated issues. Other vehicles showed opposite trends between the 30 mph and 50 mph, while J&R15 and the second visit for J&R 40 showed

increases in NO_x emissions. There were 10 vehicles (J&R10, 11, 13, 17, 20, 22 second visit, 31, 42, 46 and 47) where either the SCR inlet or outlet NO_x sensors were replaced. Of these 10 vehicles, only J&R10, 11, 17 and 20 showed NO_x emission reductions after the repair, while J&R13, 46 and 47 showed higher NO_x emissions post-repair, and the remaining test vehicles showed mixed trends between the 30 and 50 mph driving conditions. J&R31 was the only vehicle where the SCR system was completely replaced, it is expected that this vehicle might show significant NO_x reductions. J&R31 did show decreases in NO_x emissions from 4.4 ppm to <0.01 ppm for the 30 mph driving condition, but slightly increased NO_x emissions for the 50 mph driving condition. J&R37 showed the largest NO_x emission reductions (from 68 ppm to 0.3 ppm) after replacing the EGR cooler and valve. J&R41, on the other hand, showed similar NO_x emissions before and after changing the EGR valve. Other vehicles that showed post-repair NO_x emission reductions include, J&R03, 04 and 25 after replacing temperature sensors, except for J&R25 under for the 50 mph test. J&R38, 39 and 42 had higher NO_x emissions after updating or calibrating the ECM. J&R45 showed NO_x emission reductions after replacing the fuel injectors. J&R48 was a 2013 Maxforce engine that was not equipped with an SCR system and was certificated to a 0.5 g/bph-hr NO_x standard. The NO_x emissions for this vehicle were much higher compared with other engine manufacturers in same model year range under the same test conditions. The NO_x emissions of this truck were found to increase after replacing the intake air manifold.

Table 4-2 Pre- and post-repair for NOx emissions for the MGT5 for each vehicle on a g/bhp-hr basis

part/repair	total	Vehicle NO.	Pre-repair NOx Emissions (g/bhp-hr)		Post-repair NOx Emissions (g/bhp-hr)		DM1=1
			30 mph	50 mph	30 mph	50 mph	
DPF filter cleaning	3	J&R_23	0.52	1.79	0.00	0.86	Yes
		J&R_09	1.13	2.05	0.31	0.15	
		J&R_21	0.09	0.49	0.01	0.40	
		ave	0.58	1.44	0.11	0.47	
DPF filter	3	J&R_01	7.24	4.64	1.09	0.13	Yes
		Cum_02	3.65	1.87	0.17	0.21	
		J&R_44	0.13	1.06	0.05	0.91	
		ave	3.67	2.52	0.44	0.41	
exhaust pressure sensor	2	J&R_32	0.00	2.16	0.05	1.25	
		J&R_33	0.00	0.00	0.00	0.00	
		ave	0.00	1.08	0.02	0.63	
injector doser	6.5	J&R_06	0.59	0.35	0.06	0.69	Yes
		J&R_15	0.54	0.49	2.91	1.15	
		J&R_17	4.02	6.18	0.15	0.64	
		J&R_27	0.15	1.00	0.00	2.34	
		J&R_30	0.79	0.60	0.00	0.45	
		J&R_40	0.02	0.00	0.00	0.00	Yes
		J&R_40_Secon d visit	0.00	0.00	0.00	0.20	
ave	0.87	1.23	0.45	0.78			
EGR valve/cooler /system	4.5	J&R_22	4.13	2.87	0.07	0.24	Yes
		J&R_37	0.02	3.72	0.00	0.00	
		J&R_41	0.00	0.37	0.02	0.07	Yes
		J&R_48	2.07	2.24	5.93	5.09	
		ave	1.56	2.30	1.50	1.35	

Table 4-3 Pre- and post-repair for NOx emissions for the MGT5 for each vehicle on a g/bhp-hr basis (continued)

part/repair	total	Vehicle NO.	Pre-repair NOx Emissions (g/bhp-hr)		Post-repair NOx Emissions (g/bhp-hr)		DM1=1
			30 mph	50 mph	30 mph	50 mph	
DEF filter, fluid & parts	5	Cum_01	0.41	0.27	0.40	0.26	Yes
		J&R_05	0.00	0.50	0.37	0.38	
		J&R_19	1.02	1.99	0.03	0.23	
		J&R_28	0.02	0.67	0.00	0.00	
		J&R_19_Second visit ave	0.03	0.23	0.02	0.19	
turbocharger	2	J&R_07	0.75	1.27	0.45	1.18	
		J&R_16	0.66	0.52	0.07	1.13	
		ave	0.70	0.89	0.26	1.16	
inlet or outlet NOx sensor	7.5	J&R_10	0.00	0.03	0.00	0.00	Yes
		J&R_11	1.41	0.64	1.25	0.34	Yes
		J&R_12	0.33	1.63	0.15	2.12	Yes
		J&R_13	0.00	0.00	0.19	0.19	Yes
		J&R_20	0.00	0.01	0.00	0.00	
		J&R_46	0.00	0.00	0.00	0.44	
		J&R_47	0.13	0.30	0.89	2.27	
		J&R_22_Second visit ave	0.05	0.19	0.00	0.86	
ave	0.24	0.35	0.31	0.78			
ammonia sensor	1	J&R_03	0.07	0.20	0.04	0.16	
SCR	2	J&R_31	0.22	0.00	0.00	0.09	Yes
		J&R_39	0.00	0.01	0.00	0.26	Yes
		ave	0.11	0.01	0.00	0.17	

Table 4-4 Pre- and post-repair for NOx emissions for the MGT5 for each vehicle on a g/bhp-hr basis (continued)

part/repair	total	Vehicle NO.	Pre-repair NOx Emissions (g/bhp-hr)		Post-repair NOx Emissions (g/bhp-hr)		DM1=1
			30 mph	50 mph	30 mph	50 mph	
temperature sensor	2	J&R_04	0.37	1.46	0.06	0.95	
		J&R_25	1.27	0.04	0.68	0.19	
		ave	0.82	0.75	0.37	0.57	
fuel injector	1	J&R_45	0.01	0.10	0.00	0.00	
fuel system components	3	J&R_26	0.02	0.04	0.00	0.00	Yes
		J&R_34	0.00	0.00	0.00	0.20	
		J&R_40_3rd visit	0.01	0.21	0.00	0.00	Yes
		ave	0.01	0.08	0.00	0.07	
ECM	3	J&R_38	0.02	0.00	0.13	0.06	
		J&R_42	0.00	0.38	0.00	0.01	
		J&R_43	0.00	0.00	0.00	0.00	
		ave	0.01	0.13	0.04	0.02	
crankcase filter	2	J&R_14	0.70	0.87	0.85	1.25	
		J&R_29	0.11	0.02	0.09	0.04	
		ave	0.41	0.44	0.47	0.65	
crankcase pressure sensor	1	J&R_35	0.08	0.74	0.00	0.37	
crank position sensor	1	J&R_36	0.58	0.84	0.10	0.85	
air filter	1	J&R_18	0.00	0.25	0.05	0.07	

4.5.2. PM emissions

Pre- and Post-opacity measurements for all of the vehicles were separated by repair category, as presented in Table 4-5. The pre- and post-repair PM emissions normalized on a g/bhp-hr basis are shown in the supporting information. Overall, the MAHA PM and opacity measurements were generally low for most vehicles. The pre-repair opacity values were 5% or less for all but 8 vehicles. Similarly, the MAHA pre-repair PM emission rates were generally on the order of 0.001 g/bhp-hr, as shown in the supporting information, approximately 1/10 of the actual standard, which is fairly typical of a properly functioning DPF, at least in terms of reduction effectiveness. This suggests that most of the vehicles tested did not have significant DPF failures at the level where they might be targeted for an I/M program. The repairs for some of the higher PM emitters included DEF, NOx sensors, ECM updates, and an intake air manifold. Of the vehicles with pre-repair opacity readings that were above 5%, 6 of the 8 vehicles showed reductions in opacity to below the 5% level for the post-repair tests. Overall, the repairs did not appear to have a significant impact on reducing post-repair PM emissions for the 30 and 50 mph tests, even for a vehicle that had major DPF repairs.

Some vehicles had higher opacity readings after the repair, however. J&R019 and 48 had opacity readings over 5% for the pre-repair tests, and had higher opacity readings for the post-repair tests. This is plausible because DPF filtration efficiency may vary with operation and with particle loading. In addition, two other vehicles with pre-repair opacity readings below 5% showed increases in opacity to levels above 5% for the post-repair tests

(J&R23 and 26). Interestingly, J&R19 with the highest opacity readings for both pre- and post-tests during the first visit, did not have any fault codes associated with the DPF system.

Repairs such as DPF cleaning, and replacing DPF associated sensors and aftertreatment fuel injectors could potentially impact opacity readings. A total 12 vehicles in this study (J&R01, 06, 09, 11, 15, 17, 21, 23, 27, 31, 37 and 44) had a DPF cleaning performed as part of the repair process. Most of the vehicles showed lower opacity readings after the DPF cleaning, except for J&R06, 23 and 27. J&R32, 33 and 44 showed decreases in post-repair opacity readings after changing the differential pressure sensor. J&R06 had slightly higher opacity readings after the changing the DPF temperature sensor, but they were still below the 5% level. Four vehicles (J&R26, 27, 34 and 40 third visit) had the aftertreatment fuel injector or valve, which was part of the DPF regeneration system, replaced. Of these vehicles, three of the 4 showed comparable or lower pre- and post-repair opacity readings, while J&R26 showed an increase in opacity levels to above 5%.

Besides the vehicles discussed above, 13 vehicles had issues associated with DEF and/or NOx sensors (Cum01, J&R05, 10, 12, 13, 19, 20, 22 second visit, 28, 30, 40, 46 and 47). These vehicles showed lower opacity readings for the post-repair tests, except for J&R19 and 28 after repairing the DEF harness and J&R22 after replacing the NOx sensor and DEF filter during the second visit. Both J&R07 and J&R16 had lower opacity readings after repairing turbo-related issues. J&R03 and J&R 04 showed higher opacity readings after replacing the temperature sensor, while J&R25 showed the opposite trend with the same issue. J&R14 and J&R18 showed increases in opacity after replacing the crankcase filter and air filter, while J&R29 had lower opacity readings after replacing the crankcase

filter. J&R22 showed increases in opacity after replacing the exhaust pressure sensor, however, J&R35 showed opposite results after replacing the crankcase pressure sensor. Besides replacing parts, an updated ECM calibration lead to lower opacity readings for Cum01, J&R38, 39 and 43, but not for J&R41, which had the EGR valve changed in addition to an ECM update.

Table 4-5 Pre- and post-repair for opacity for each vehicle

part/repair	total	Vehicle NO.	Pre-repair Opacity (%)	Post-repair Opacity (%)
DPF filter cleaning*	3	J&R_23	3.33	6.38
		J&R_09	4.81	2.46
		J&R_21	3.15	2.29
		ave	3.76	3.71
DPF filter	3	J&R_01	11.30	4.54
		Cum_02	1.20	1.60
		J&R_44	0.00	0.00
		ave	4.17	2.05
exhaust pressure sensor	2	J&R_32	0.00	0.00
		J&R_33	2.15	0.00
		ave	1.08	0.00
injector doser	6.5	J&R_06	0.00	2.33
		J&R_15	9.69	0.00
		J&R_17	12.30	0.00
		J&R_27	0.00	0.74
		J&R_30	0.00	0.00
		J&R_40	3.03	1.46
		J&R_40_Second visit	1.46	0.00
ave	3.78	0.65		
EGR valve/cooler/system	4.5	J&R_22	0.76	3.69
		J&R_37	2.18	0.00
		J&R_41	0.00	3.73
		J&R_48	6.96	9.21
		ave	2.48	4.16
DEF filter, fluid & parts	5	Cum_01	1.00	0.90
		J&R_05	4.40	0.00
		J&R_19	7.53	12.10
		J&R_28	0.00	3.96
		J&R_19_Second visit	12.10	1.81
ave	5.01	3.75		
turbocharger	2	J&R_07	2.69	0.00
		J&R_16	0.00	0.00
		ave	1.35	0.00

Table 4-6 Pre- and post-repair for opacity for each vehicle (continued)

part/repair	total	Vehicle NO.	Pre-repair Opacity (%)	Post-repair Opacity (%)
inlet or outlet NOx sensor	7.5	J&R_10	5.30	1.29
		J&R_11	0.00	0.00
		J&R_12	0.70	0.24
		J&R_13	5.74	0.00
		J&R_20	0.00	0.00
		J&R_46	0.00	0.00
		J&R_47	0.00	0.00
		J&R_22_Second visit ave	3.69 1.93	4.52 0.76
ammonia sensor	1	J&R_03	0.85	2.10
SCR	2	J&R_31	0.00	0.00
		J&R_39	0.00	0.00
		ave	0.00	0.00
temperature sensor	2	J&R_04	0.00	0.76
		J&R_25	6.40	0.00
		ave	3.20	0.38
fuel injector	1	J&R_45	1.54	1.49
fuel system components	3	J&R_26	3.84	6.05
		J&R_34	1.59	2.53
		J&R_40_3rd visit ave	0.00 1.81	0.00 2.86
		ave	1.81	2.86
ECM	3	J&R_38	4.45	2.02
		J&R_42	n/a	n/a
		J&R_43	0.00	0.00
		ave	2.23	1.01
crankcase filter	2	J&R_14	4.18	4.45
		J&R_29	0.00	0.00
		ave	2.09	2.23
crankcase pressure sensor	1	J&R_35	0.55	0.00
crank position sensor	1	J&R_36	4.16	0.00
air filter	1	J&R_18	0.00	1.03

4.6. Emission Impact Rates

Additional analyses were conducted on the pilot study information to evaluate the emissions impacts and repair frequencies. The analyses from this section form the basis for the emissions inventory assessments.

4.6.1. Emission Impact Rates from Pilot Study

Determining the emissions impacts of the repairs in a broader sense was an important part of the data analysis of the pilot study. The emissions benefit for each vehicle repair was determined in g/bhp-hr units for 30 and 50 mph.

Two scenarios were then developed to represent different potential implementation plans for an I/M program. The first scenario included all vehicle that were tested as part of the pilot study that were recruited with the check engine light on, where the check engine light was subsequently turned off by the repair performed. This essentially included most of the vehicles in the test program. In examining the results for the test vehicles, it was noted that two vehicles were equipped with Navistar engines that did not utilize SCR aftertreatment and that showed emissions increases in the post-repair results compared to the pre-repair results. Since the HD I/M emissions inventory estimates are based on time periods of 2025 and beyond, it is estimated that the fraction of Navistar non-SCR engines in the fleet will represent a very small fraction of the fleet. Additionally, the likelihood of having a category of vehicles that will consistently show increases in emissions upon repair is unlikely. As such, it was decided that these two Navistar vehicles should be removed from the sample for the subsequent analyses.

Since the OBD systems for heavy-duty vehicles provide different levels of information on the failure condition of the vehicle, an additional scenario was evaluated that included only those vehicles where the DM1 code had value of 1. This provides a stronger indication that a problem that is beyond typical maintenance is occurring with the vehicle that could be emissions related. Of the vehicles tested, a total of 27 vehicles had the DM1=1 in either the pre-repair OBD scan, or in the data logger information. Of the remaining vehicles, 20 had DM1 = 0 or 3, while the DM1 status was not available for an additional 3 vehicles.

The results for the emissions repair benefits for both the vehicles in the broader category of having their check engine light and for the vehicle that all had DM1=1 in the pre-repair OBD scan are provided in Table 4-7. Note that both tables excluded the Nativstar vehicles J&R15 and J&R48, as discussed above. The results show fleet average NO_x emissions reductions of 292% at 30 mph and 88% at 50 mph and average PM emissions reductions of 45% at 30 mph and 72% at 50 mph for the vehicles with a check engine light on before repairs. For the vehicles with DM1=1, the fleet average NO_x emissions reductions of 436% at 30 mph and 112% at 50 mph and average PM emissions reductions of 42% at 30 mph and 47% at 50 mph.

Table 4-7 Emissions Benefits for Vehicles with Check Engine Light On Pre-Repair and Vehicles with DM1=1 on Pre-Repair

Emissions Benefits	Vehicles with Check Engine Light On Pre-Repair				Vehicles with DM1=1 On Pre-Repair			
	NOx		PM		NOx		PM	
	30 mph	50 mph	30 mph	50 mph	30 mph	50 mph	30 mph	50 mph
Simple Average	292%	88%	45%	72%	436%	112%	42%	47%

4.6.2. Repair Frequencies

In attempting to predict the failure rate in the future heavy-duty fleet, an analysis was performed on the repair records obtained from the J&R facility. Specifically, the analysis focused on the J&R mechanic's comments recorded on each repair order which stated the reasons for repair. As the proposed method of identifying potentially high emitting trucks in I/M is through an assessment of the trucks' on-board diagnostic systems, the coded comments for a total of 2,784 model-year 2010 and newer trucks were examined.

The clearest indication that repairs were emissions related and prompted by the OBD system was a notation by the mechanic that the Check Engine Light was on when the vehicle was initially brought in for service. However, vehicles were also counted as potential failures if mechanics noted they had found stored fault codes. These notations were considered less reliable because the OBD system may have been queried in the course of investigating other problems rather than being primary reason for seeking repair. As an example, the operator of a truck may seek repair because of loss of power. While the Check Engine light may not be illuminated, the mechanic may seek insight into the problem by querying the OBD system for stored codes.

Yet another subset of vehicle owners were advised by the J&R mechanics that the Check Engine Light was on and that emissions related repair were needed, however the owners/operators declined service believing that the needed repairs could/should be performed under warranty. It is important to note that J&R is not authorized by engine manufacturers to perform warranty work and the emission reductions related to repairs performed under warranty cannot be attributed to I/M at the risk of double counting. It is also important to note that the vehicles undergoing emissions related repairs at the J&R facility were doing so in the absence of I/M.

A total of 723 vehicles, or 26% of the 2010 and newer model year vehicles were identified as potential failures under the proposed I/M criteria relating to the check engine light. The average mileage of the J&R fleet was about 522,000 miles. The corresponding failure rates from the J&R fleet are estimated at 27% and 24%, respectively for 2010 to 2012, and 2013 and newer trucks after half a million miles of travel. CARB assumes linear growth in the incidence of tampering and mal-maintenance and reports fleet failure rate at 1,000,000 miles for the EMFAC model. Extrapolating these rates to 1,000,000 miles, the failures rates become 52% and 46%, respectively, for 2010-2012 and 2013 and newer vehicles.

Failure rate frequencies were also estimated for DM1=1 vehicles. As the J&R repair records do not provide information related to the status of the DM1 MIL, failure rates were obtained through a combination of the J&R repair records and the pilot study data. As discuss above in section 3.2.2, the DM1 was set to 1 for 27 of 51 repair visits for the pilot. This is further broken down to be 5 of 11 2010-12 vehicles (45%), and 22 of 40 2013 and

newer vehicles (55%). Thus, the check engine light on was a criteria for recruitment for the pilot study, it was assumed that the fraction of check engine light on vehicles that would also have DM1=1 would be the fraction identified in the pilot study. As such, the failure rates for the DM1=1 vehicles at 1,000,000 miles were $52\% \times 45\% = 23\%$ for 2010-2012 vehicles and $46\% \times 55\% = 21\%$ for 2013 and newer vehicles.

4.6.3. Emission Impact Rates

Emissions impact rates (EIRs) are a critical input used in determining the deterioration rates in the EMFAC model, which is utilized to determine the emissions inventory benefits in section 5. The EIRs used in EMFAC based on estimated emissions reductions in specific repair categories multiplied by their relative frequencies, and then are ultimately derived via an equation developed by the Radian equation. As data was limited for typical repair categories used in the Radian equation, estimated EIRs were obtained from the simple averages obtained from section 4 and supporting information. Since the EIRs in EMFAC are based on the average UDDS of 19 mph, the pilot study results for the lower 30 mph test point were used. As such, the emission reductions were 292% for the vehicles with the check engine light and 439% for the DM1=1 vehicles. The emissions reductions are multiplied by the corresponding frequencies for the all check engine lights and the DM1=1 categories, to obtain the EIRs for each pollutant and vehicle category.

The resulting EIRs obtained from the pilot study are provided in Table 4-8 based a mileage accrual of 1,000,000. For NO_x, the EIRs were 152% and 134% for 2010-2012 and 2013+ for vehicles with check engine light vehicles, and 101% and 110% for 2010-2012

and 2013+ for vehicles with DM1=1 vehicles. For PM, the EIRs were 23% and 21% for 2010-2012 and 2013+ for vehicles with check engine light vehicles, and 11% and 12% for 2010-2012 and 2013+ for vehicles with DM1=1 vehicles.

Table 4-8 Emission Impact Rates Based on Pilot Study

Failure Category	Model Year	Pollutant	Emission Impact	Frequency (at 1,000,000 miles)	Emission Impact Rate (%)
Check Engine Lights	2010-12	NOx	292%	52%	152%
Check Engine Lights	2013+	NOx	292%	46%	134%
Check Engine Lights	2010-12	PM	45%	52%	23%
Check Engine Lights	2013+	PM	45%	46%	21%
DM1=1	2010-12	NOx	439%	23%	101%
DM1=1	2013+	NOx	439%	25%	110%
DM1=1	2010-12	PM	47%	23%	11%
DM1=1	2013+	PM	47%	25%	12%

4.6.4. Discussion of Emissions Impact Rates in the Context of the Available Literature

The EIRs and other pilot studies emission results can be compared to other analyses and information in the literature. The EIRs can be directly compared with the 1,000,000 mile EIRs from EMFAC, as shown in Table 4-9. The EIRs for NOx for the check engine light vehicles from this work are slightly lower than those in EMFAC2017 for 2013+ vehicles, but are in a similar range at 134% compared to 170%. Larger differences are seen

in the EIRs for the 2010-2012 check engine light vehicles, with a value of 152% vs. 272% for EMFAC2017. The 2010-2012 model year group will be less important going into the future, as the fraction of these vehicles relative to the 2013+ will continue to decline over time, particularly moving into the 2025 and beyond timeframe. The EIRs for the DM1=1 vehicles are below those for both the check engine light and EMFAC values since this condition represents a smaller subset of vehicles with definitive emissions related issues that could potentially be targeted in an I/M program.

The EIRs for the PM emissions show greater differences with the EMFAC values. In examining the derivation of the EIRs for EMFAC, these EIR are based on a combination of tampering, mal-maintenance, and malfunction (TM&M) frequencies of between 6.7 and 10% for 2010+ vehicles, as shown in Table 4-9, coupled with the corresponding values for emissions increases for the DPF leaking. In this regard, it should be noted that the DPF disabled category has been eliminated in the most recent EMFAC2017 model, as no distinction could be made between leaking and disabled DPFs in recent roadside studies. The corresponding emissions increase for the DPF leaking category is based on an assumed emission rate of 0.07 g/bhp-hr for leaking DPFs. The corresponding base emissions level for 2010+ vehicles, on the other hand, is based on a base emission rate of approximately 0.001 g/bhp-hr. Although this level is approximately 10 times below certification standard, this is the level that is typically found during certification testing of engines equipped with modern DPF systems. The overall emissions increase thus assumed to be 5200%.

Table 4-9 EIRs and TMM Frequencies for Disabled and Leaking DPFs for EMFAC2014 and EMFAC2017

EIRs		EMFAC2014		EMFAC2017	
		2010-12 MY	2013+MY	2010-12 MY	2013+MY
Pollutant	NOx	357%	220%	272%	170%
	PM	288%	193%	579%	375%
DPF Related TM&M	DPF Leaking	37.6%	26.3%	10%	6.7%
	DPF Disabled	2%	1.3%	0%	0%

To the extent that the pilot EIRs were lower than those in EMFAC, it is possible that the pilot study fleet may not adequately represent the fraction of high emitters in the fleet. In comparing with larger J&R repair record database, for example, only a single vehicle identified through the pilot study had a full DPF replacement, whereas 3-6% of the 2010+ vehicles in the J&R database had full DPF replacements.

4.7. Discussions

Based on a review of the potential methods, it is proposed that a revised HD I/M incorporate both OBD and tailpipe methods.

4.7.1. OBD as the Primary Methodology of HD I/M

HD OBD II systems were designed in anticipation of statewide I/M. Phased in beginning with 2010 model year engines, OBD is required on all 2013 and newer model year heavy-duty vehicles. The advantages of the use of these systems in an enhanced I/M program are numerous. All emissions critical components are monitored continuously by OBD while the vehicles are in service, as such the vehicles and engines are by definition being tested under “real world” driving conditions. An OBD-based test would be relatively

quick, convenient to the owner operator, and the pre-test costs are considerably lower than the dynamometer or PEMS-based alternatives. The algorithms used to illuminate the MIL are intrinsic to the vehicle and are based upon its certified level of emissions thus eliminating the need to establish either representative driving cycles or pass/fail cut-points. OBD also has the greatest potential for shortening the interval between emission control system malfunction, detection, and vehicle repair. In contrast to alternative strategies, OBD provides diagnostic and repair information which should prove invaluable to the repair and maintenance community compared to reports of levels of pollutant that they may not be familiar with. It should also be noted that the use of OBD minimizes the potential liability borne by the state associated with dynamometer testing, requiring a vehicle to be driven over a uniform route, or the installation and removal of portable emissions measurement equipment on privately owned vehicles by agents of the state.

Given that the state owns and operates weigh stations strategically located throughout the state and that CARB has the existing authority to conduct testing at these stations, it is suggested that site-based OBD information collection systems be installed at these locations. In as much the same manner that light-duty kiosks have been established in some states for periodic inspection of the fleet, trucks would be automatically scanned when passing through or by the weigh stations. The cost per transaction (communication from the vehicle to the reader) is estimated be pennies per vehicle and would not represent additional owner/operators cost or inconvenience given existing requirements to visit the scales. It is suggested that site-based remote OBD readers be considered for deployment at other strategic locations including major cargo terminals and border crossings. Aftermarket

“plug-in” remote OBD devices are currently commercially available for less than \$100/unit which utilize either blue-tooth or SIM based technology for communications purposes. This technological choice would be ideal for monitoring out-of-state vehicles and those that may routinely avoid control locations. CARB should consider requiring the incorporation of blue-tooth and/or SIM based communication capability in its next generation of OBD regulations.

Particular concerns regarding enhanced statewide HD I/M include the monitoring of out-of-state vehicles, and vehicles that can perform their normal operations without reporting to a designated point of control such as a weigh station, terminal, or border crossing. It is also anticipated that a significant portion of the heavy-duty fleet will be OBD II equipped when enhancements to HD I/M are anticipated to be enacted. In each of these instances, the use of remotely monitored OBD should be considered. Another potential issue with OBD is that it has been shown in previous analyses that some HDVs can emit excessive levels of pollutants without illuminating the MIL. For these reasons, it will be important to have a validation testing element as a supplement to OBD within a comprehensive HDV I/M program, such as remote sensing devices, roadside pullovers, or other monitoring systems such as a Portable Emissions Acquisition System (PEAQS).

4.7.2. Coupling of an OBD-based HD I/M with roadside monitoring with a remote sensing methodology

Given the potential that some problems contributing to excessive emissions would be missed in an OBD-only HD I/M program and that some portion of the fleet will not be equipped with OBD, it will be important to have a validation testing element as a

supplement to OBD within a comprehensive HDV I/M program. It is suggested that one component of a HD I/M program include the implementation of RSD at weigh stations throughout the state. The advantages of RSD include the fact that the devices are non-invasive, and have the ability to capture emissions of vehicles as they are driven by the owner/operator under real-world conditions. To eliminate the need for trucks to report to a centralized facility, RSD or OHMS could be set up at truck weighing stations throughout the state. This would include the 51 weigh stations at 37 locations that the state currently owns. An RSD system that can be operated at a low cost and largely unmanned for extended hours would be key for this implementation. Mini-PEMS and OMHS systems could also be more widely implemented at weigh stations, but the costs and complication of operation would be greater than that of RSD. The RSD system should provide the potential to measure HC, NO_x, PM, CO, and CO₂, speed information, and vehicle identification information. One disadvantage of RSD, however, is that it only evaluates over the limited operating conditions that occur while the HDV is passing through the system, which could lead to conditions where some high emission failures would be missed, while the HDV might also be operated in a manner that might trigger high emissions that would not otherwise be seen under typical operations.

4.7.3. A comprehensive HD I/M program with OBD as the primary methodology, remote sensing for validation testing, and mini-PEMS for dispute resolution

Although the coupling of OBD with remote sensing will provide for a relatively comprehensive HD I/M program, there are some conditions that may still require additional resolution beyond what would be captured in a pure OBD+remote sensing program. This

could include situations where high emissions don't trigger the OBD MIL and are also not detectable at the limited conditions evaluated by RSD. This could also include situations where an issue is identified under conditions utilized for RSD testing that would not be present under typical operating conditions. As such, HDV owners might challenge the validity of the test findings. Mini-PEMS could be used on a more limited basis to verify emissions readings or the effectiveness of RSD in identifying high emitters. Mini-PEMS could be utilized at weigh stations or in fleets similar to the PSIP for this purpose, and could provide significant advantages in sensitivity compared to current opacity testing with a similar cost basis. It is expected that over the next 8 years that mini-PEMS technology will continue to improve, and that such mini-PEMS would be able to provide sufficient accuracy to distinguish between failing and non-failing vehicles in this capacity. Vehicle owners would be allowed to schedule an appointment at the nearest weigh station for confirmatory testing by PEMS (and query of the OBD system). It is expected that approximately 10-20 would need to be purchased, maintained, and deployed with related personnel for this type of validation testing.

Chassis dynamometer and fully 1065-compliant PEMS methods were also considered in this capacity, but were determined to be too burdensome to implement due to the need for vehicles to be taken out of service to report to a centralized location, as well as the greater cost in terms of time and money associated with test setup and conduct. Chassis dynamometer and 1065-compliant PEMS would, however, continue to play an important role in terms of in-use surveillance testing and in-use regulatory testing of manufacturer trucks.

4.8. Conclusions and Recommendations

A pilot heavy-duty I/M study was conducted to evaluate emissions measurement methods that might be used and the potential emissions benefits of HD I/M repairs. The exploratory pilot program consisted of testing 47 vehicles before and after repair on a chassis dynamometer. The testing included I/M grade emissions analyzers and OBD read outs.

The PM and opacity measurements were generally low for most vehicles. The pre-repair opacity were 5% or less for all but 8 vehicles. This suggests that most of the vehicles tested did not have significant DPF failures at the level where they might be targeted for an I/M program. Overall, the repairs did not appear to have a significant impact on reducing post-repair PM emissions for the 30 and 50 mph tests, even for a vehicle where the DPF was replaced.

The pre-repair MAHA NO_x emissions results showed that a number of vehicles had emissions higher than the 2010 NO_x standard for both the initial 30 and 50 mph tests, although it is acknowledged that the standard is set for a specific transient test that was not performed. The results for some vehicles with the highest emissions showed significant reductions in NO_x emission after repair. The mini-PEMS showed relatively high NO_x emissions for some of the same vehicles that showed high NO_x emissions for the I/M grade instruments.

Based on a review of the potential methods, it is proposed that a revised HD I/M incorporate both OBD and tailpipe methods. As proposed, OBD is primary method, unmanned RSD devices and automated diagnostic and repair code readers would be

deployed at state operated weigh stations, border crossings, cargo terminals and other strategic locations ensuring full coverage of the fleet including gasoline and diesel powered vehicles and those without or equipped with OBD. The deployment of the combination of on-site RSD and OBD provides advantages in terms of both comprehensiveness and cost effectiveness in terms of monitoring the fleet as these vehicles are operated under real world conditions. Mini-PEMS could potentially also be incorporated into a HD I/M program as a verification of the pass/fail determinations, in a manner comparable that of opacity testing in the current California program, either on a limited basis for confirmatory roadside testing or for fleets under a PSIP type of program.

4.9. Acknowledgements

We acknowledge funding from the California Air Resources Board under contract 15RD022.

4.10. References

- Anyon P, Brown S, Pattison D, Beville-Anderson J, Walls G, Mowle M, 2000, Proposed Diesel Vehicle Emissions National Environment Protection Measure Preparatory Work, In-Service Emissions Performance - Phase 2: Vehicle Testing, Prepared for the National Environment Protection Council by Parson, Inc., November.
- Bell, F., Boettcher, M., Chee, J., Fitzpatrick, J., Harding, S., Henderson, B., Lippoth, D., Phee, M., Sorensen, L., Wang, V., Woo L.Y., R. F. Novak and J. H. Visser, 2016, Development of Novel NO_x Sensors and System Integration with Alumina Heater Elements, PEMS Workshop 2016, UC Riverside, Riverside, CA, March.
- Bilby, D., Kubinski, D., Maricq, M., 2016, Investigating the operating principle of the Emisense PMTrac sensor, PEMS Workshop 2016, UC Riverside, Riverside, CA, March.
- Bishop, G.A., Schuchmann, B.G., Stedman, D.H., Lawson, D.R., 2012. Emission Changes Resulting from the San Pedro Bay, California Ports Truck Retirement Program. *Environ. Sci. Technol.* 46, 551–558.
- Bishop, G.A., Schuchmann, B.G., Stedman, D.H., 2013. Heavy-Duty Truck Emissions in the South Coast Air Basin of California. *Environ. Sci. Technol.* 47, 9523–9529.
- Burgard, D.A., Bishop, G.A., Stedman, D.H., Gessner, V.H., Daeschlein, C., 2006, Remote sensing of in-use heavy-duty diesel trucks. *Environ. Sci. Technol.* 40, 6938–6942.
- Burnette, A.D., Sandeep Kishan, S., and DeFries, T.H., 2008, Evaluation of Remote Sensing for Improving California's Smog Check Program, Final Report by Eastern Research Group for the California Air Resources Board and California Bureau of Automotive Repair, March.
- California Air Resources Board, 2007, Tables for Emission Reduction and Cost-Effectiveness Calculations, Carl Moyer Program Workshop, November.
- California Air Resources Board, 2017, Update on Truck Field Enforcement Activities and New Screening Technologies for High Emitting Vehicles, CARB Board Meeting, April 27.
- Carder, D., Gautam, M., Thiruvengadam, A., Besch, M., 2014. "In-Use Emissions Testing and Demonstration of Retrofit Technology for Control of On-Road Heavy-Duty Engines." Final Report by West Virginia University for the South Coast Air Quality Management District.

- Chen, X., Schmid, N.A., Wang, L., and Clark, N.N., "Regression-Based Oxides of Nitrogen Predictors for Three Diesel Engine Technologies," *Journal of the Air and Waste Management Association*, Vol. 60 No. 1, January 2010, pp. 72-90.
- Chernich, D., J., 2003, Development of a Chassis Based Inspection and Maintenance Program for Heavy-Duty Diesel Powered Vehicles, 13th CRC On-Road Vehicle Emissions Workshop, San Diego, CA.
- Clark N.N., Tehranian, A., Nine, R.D., and Jarrett, R., 2002. Translation of Distance-Specific Emissions Rates between Different Chassis Test Cycles using Artificial Neural Networks, SAE Spring Fuels and Lubricants Meeting, Reno, NV, SAE Paper 2002-01-1754.
- Clark, N. N., Gautam, M., Wayne, W. S., Thompson, G. J., Lyons, D. W., 2004. California heavy heavy-duty diesel truck emissions characterization for project E-55/E-59 phase 1.5. CRC Report No. E55/59. Final Report for the Coordinating Research Council.
- Clark, N. N., Gautam, M., Wayne, W. S., Thompson, G. J., Nine, R. D., Lyons, D. W., Buffamonte T., Xu S., Maldonado H., 2006. Regulated emissions from heavy heavy-duty diesel trucks operating in the south coast air basin. Soc. SAE Paper 2006-01-3395.
- Clark, N. N., Gautam, M., Wayne, W. S., Lyons, D. W., Thompson, G. J., 2007. Heavy-duty vehicle chassis dynamometer testing for emissions inventory, air quality modeling, source apportionment, and air toxics emissions inventory. CRC Report No. E55/59.
- Clark N.N., McKain, D.L., Wayne, W.S., Carder, D., and Gautm, M. 2011. Chassis Dynamometer Emissions Characterization of a Urea-SCR Transit Bus, Society of Automotive Engineers Paper 2011-01-2469.
- Clean Air Act Advisory Committee, Mobile Source Technical Review Subcommittee. 2010. Recommended Guidance for Remote OBD I/M Programs.
- Code of Federal Regulations CFR, 2007. Supplemental emission test; test cycle and procedures. Office of the Federal Register National Archives and Records Administration. CFR Title 40 Part § 86.1360,2007.
- Code of Federal Regulations CFR, 2007. Not-To-Exceed test procedures, Office of the Federal Register National Archives and Records Administration. CFR Title 40 Part § 86.1370, 2007.
- Code of Federal Regulations CFR, 2011. Emission standards and supplemental requirements for 2007 and later model year diesel heavy-duty engines and vehicles,

- Office of the Federal Register National Archives and Records Administration. CFR Title 40 Part § 86.007, 2007.
- Dallmann, T.R. and Harley, R.A., 2010, Evaluation of mobile source emission trends in the United States. *J. Geophys. Res.* 115, D14305.
- Dallmann, T.R., Harley, R.A., and Kirchstetter, T.W., 2011, Effects of diesel particle filter retrofits and accelerated fleet turnover on drayage truck emissions at the Port of Oakland, *Environ. Sci. Technol.*, 45, 10773–10779, doi:10.1021/es202609q.
- Dallmann, T.R., DeMartini, S.J., Kirchstetter, T.W., Herndon, S.C., Onasch, T.B., Wood, E.C., Harley, R.A., 2012, On-road measurement of gas and particle phase pollutant emission factors for individual heavy-duty diesel trucks. *Environ. Sci. Technol.* 46, 8511–8518.
- Dallmann, T.R., Kirchstetter, T.W., DeMartini, S.J., and Harley, R.A., 2013, Quantifying On-Road Emissions from Gasoline-Powered Motor Vehicles: Accounting for the Presence of Medium- and Heavy-Duty Diesel Trucks, *Environ. Sci. Technol.*, 47, 13873–13881
- Dallmann, T.R., Onasch, T.B., Kirchstetter, T.W., Worton, D.R., Fortner, E.C., Herndon, S.C., Wood, E.C., Franklin, J., Worsnop, D.R., Goldstein, A.G., Harley, R.A., 2014, Characterization of particulate matter emissions from on-road gasoline and diesel vehicles using a soot particle aerosol mass spectrometer, *Atmos. Chem. Phys. Discuss.*, 14, 4007–4049
- Dallmann, T.R., Kirchstetter, T.W., DeMartini, S.J., and Harley, R.A., 2014, Quantifying on-road emissions from gasoline-powered motor vehicles: accounting for the presence of medium and heavy-duty diesel trucks, *Environ. Sci. Technol.*, 47, 13873–13881, 25 doi:10.1021/es402875u, 2014.
- DeFries, T.H., 2016, Evaluation of EDAR for Measurement of Simulated Exhaust Emissions, Memorandum from ERG, January.
- Envirotest Canada, 2013, Remote Sensing Device Trial for Monitoring Heavy-Duty Vehicle Emissions.
- Federal Reserve Bank of St. Louis and U.S. Federal Open Market Committee, FOMC Summary of Economic Projections for the Personal Consumption Expenditures less Food and Energy Inflation Rate, Central Tendency, Midpoint [JCXFECTM], retrieved from FRED, Federal Reserve Bank of St. Louis; <https://fred.stlouisfed.org/series/JCXFECTM>, March 28, 2018.

- Gautam, M., Thompson, G.J., Carder, D.K., Clark, N.N., Shade, B.C., Riddle, W.C., and Lyons, D.W., 2001, Measurement of In-Use, On-Board Emissions from Heavy-Duty Diesel Vehicles: Mobile Emissions Measurement System, SAE Technical Paper No. 2001-01-3643.
- Gautam, M., N. N. Clark, W. Riddle, R. Nine, W. S. Wayne, H. Maldonado, A. Agrawal, and M., Carlock. 2002. Development and initial use of a heavy-duty diesel truck test schedule for emissions characterization. In Proceedings of Society of Automotive Engineers (SAE) Fuels and Lubricants Meeting; SAE Paper 2002-01-1753. SAE: Warrendale, PA.
- Hager, J.S., Study of EDAR using a Portable Emissions Measurement System (PEMS), Memorandum by HEAT LLC, Knoxville, TN.
- Ham, W., Smith, J.D., Burnitzki, M., Downey, S., Quiros, D., Hu, S., Chernich, D., Huai, T., Benjamin, M., and Sax, T., 2017, Development of CARB's Portable Emissions Acquisition System (PEAQS), presentation at 27th CRC Real World Emissions Workshop, March.
- Hart, C., Hawkins, D., Fulper, C., Stanard, A., DeFries, T., Kishan, S., Glinsky, G., Reek, A., Hager, J.S., 2015, Canister Degradation Study, 25th CRC On-Road Vehicle Emissions Workshop, San Diego, CA, March.
- International Council on Clean Transportation (ICCT). Review of Current Practices and New Developments in Heavy-Duty Vehicle Inspection and Maintenance Programs, August, 2015.
- Jiang, Y., Johnson, K.C., Durbin, T.D., and Yang, J., 2016, Evaluation of NTK Compact Emission Meter (NCEM), PEMS Workshop 2016, UC Riverside, Riverside, CA, March.
- Johnson, K.C., T.D. Durbin, D.R. Cocker III, J.W. Miller, R.J. Agama, N. Moynahan, G. Nayak, 2008. On-Road Evaluation of a PEMS for Measuring Gaseous In-Use Emissions from a Heavy-Duty Diesel Vehicle. SAE Int. J. Commer. Veh., 1, 200-209.
- Johnson, K.C., Durbin, T.D., Cocker III, D.R., Miller, J.W., Bishnu D.K., Maldonado H., Moynahan N., Ensfield C., Laroo C.A.. 2009. On-Road Comparison of a Portable Emission Measurement System with a Mobile Reference Laboratory for a Heavy Duty Diesel Vehicle. Atmospheric Environment. Vol. 43, pp. 2877-2883.
- Johnson, K., Durbin, T.D., Jung, H., Cocker, D.R., Yusuf Khan, M. 2010a. Validation Testing for the PM-PEMS Measurement Allowance Program. Final Report by UC Riverside to the California Air Resources Board under Contract No. 07-620, November.

- Johnson, K.C., Durbin, T.D., Jung, H., Cocker III, D.R., Giannelli, R., Bishnu, D., 2010b. Quantifying In-Use PM Measurements for Heavy Duty Diesel Vehicles. Environ. Sci. Technol., Vol. 45, pp. 6073-6079.
- Khalek, I.A., and Premnath, V., 2016, Spark-Plug Sized Exhaust Particle Sensors for OBD and Emissions Monitoring, 6th International PEMS Conference and Workshop, UC Riverside, Riverside, CA, March.
- Khan, M.Y., Johnson, K.C., Durbin, T.D., Jung, H., Cocker III, D., Bishnu, D., and Giannelli, R. 2012. Characterization of PM-PEMS for In-Use Measurements – Validation Testing for the PM-PEMS Measurement Allowance Program. Atmospheric Environment, 55, 311-318.
- Knoema (2018) <https://knoema.com/kyaewad/us-inflation-forecast-2017-2018-and-up-to-2060-data-and-charts>.
- Lyons, A. and McCarthy, M. 2009. Transitioning Away from Smog Check Tailpipe Emission Testing in California for OBD II Equipped Vehicles.
- Miller, J. W., Johnson, C. K., Durbin, T., Dixit, P., 2013. In-Use Emissions Testing and Demonstration of Retrofit Technology for Control of On-Road Heavy-Duty Engines. Final Report by the University of California at Riverside to the South Coast Air Quality Management District under Contract No. 11612.
- Misra, C., Collins, J.F., Herner, J.D., Sax, T., Krishnamurthy, M., Sobieralski, W., Burntitzki, M., and Charnich, D. 2013. In-Use NOx Emissions from Model Year 2010 and Heavy-Duty Diesel Engines Equipped with Aftertreatment Devices, Environ. Sci. Technol. 47, 7892–7898.
- Misra, C., Yoon, S., Collins, J., Chernich, D., Herner, J., 2016. Evaluating In-Use SCR Performance: Older vs. Late MY Engines. Presentation at 26th CRC Real World Emissions Workshop, Newport Beach, CA, March.
- Ropkins, K., Li, H., and Andrew Burnette, A., 2016, Next Generation (Smaller, Lower Cost, Lower Energy Consumption) Portable Emissions Measurement Systems, PEMS Workshop 2016, UC Riverside, Riverside, CA, March.
- San Pedro Bay Ports Clean Air Action Plan Technical Report (CAAP), The Port Of Long Beach and Los Angeles, 2006.
- Saukko, E., Järvinen, A., Wihersaari, H., Rönkkö, T., Janka, K., and Keskinen, J., 2016, Expanded Capabilities of Dual Pegasor PPS-M Sensor in PEMS Measurements Beyond PN, PM and Particle Size, PEMS Workshop 2016, UC Riverside, Riverside, CA, March.

- St. Denis, M.J., Budd, R., Hager, S., Hager, Y., 2015, Connecticut Vehicle Inspection Program: 2014 On-Road Vehicle Survey, Final report by Revecorp and Hager Environmental & Atmospheric Technologies (HEAT) for Applus and the State of Connecticut Department of Motor Vehicles, February.
- Texas A&M Transportation Institute, 2013, Heavy-Duty Diesel Inspection and Maintenance Pilot Program.
- TSI Incorporated, 2015, Nanoparticle Emissions Tester Model 3795 brochure and website, www.tsi.com/NPET.
- Tu, J., Berdahl, S., Tran, T., O’Cain, J., Karim, J., Sardar, S., Lemieux, S., Huai, T., 2016. Study of heavy-duty vehicle emissions during in-use compliance testing. Presentation at 26th CRC Real World Emissions Workshop, Newport Beach, CA, March.
- U.S. Environmental Protection Agency; Heavy Trucks, Buses, and Engines; Regulations and Related Documents; see <http://www.epa.gov/otaq/hd-hwy.htm#regs>.
- U.S. Environmental Protection Agency, 2002. Update Heavy-Duty Engine Emission Conversion Factors for MOBILE6: Analysis of BSFCs and Calculation of Heavy-Duty Engine Emission Conversion Factors. EPA420-R-02-005, January.
- U.S. Environmental Protection Agency, 2004. Working Group On Off- Cycle Emissions, "EPA Answers to Questions from March 22nd 2004 NTE Presentation". <http://www.oica.net/htdocs/WWH/Off%20cycle/7th%20meeting/Informal%20Doc%20No%2014%20-%20EPA%20answers%20to%20NTE%20Questions%20from%206th%20E2%80%A6.pdf>.
- Vescio, N., Full, G., Fraser, J., Balon, T., Grumet, S., Lowell, D., McClintock, M., 2006, Cross Border In-Use Emissions Study for Heavy Duty Vehicles, Nogales, AZ – Final Report. Prepared for the Arizona DEQ and EPA. September 8.
- Virginia DEQ, 2006: <http://www.deq.virginia.gov/Portals/0/DEQ/LawsAndRegulations/2007.on.road.emissions.testing.program.status.report.pdf>
- Weaver, C.S., and Klausmeier, R.F., 1988, Final reports by Radian for the California Air Resources Board under contract no. A4-151-32, May.
- Heavy-Duty Vehicle Inspection and Maintenance - Final Report Volume I – Summary Report.

Heavy-Duty Vehicle Inspection and Maintenance - Final Report Volume II – Quantifying the Problem.

Heavy-Duty Vehicle Inspection and Maintenance - Final Report Volume III – Development and Validation of I/M Test Procedures.

Heavy-Duty Vehicle Inspection and Maintenance - Final Report Volume IV – I/M Program Design and Cost Effectiveness Analysis.

U.S. Environmental Protection Agency, 2015. Heavy Trucks, Buses, and Engines. <http://www.epa.gov/otaq/hd-hwy.htm#regs>.

4.11. Supporting Information

Table S1 Pre- and post-repair for PM emissions for the MPM4 for each vehicle on a g/bh-hr basis

Vehicle No.	Engine Year & Make	50 km/h	80 km/h	50 km/h	80 km/h	DM1=1
		Pre-repair PM Emissions (g/bhp-hr)	Pre-repair PM Emissions (g/bhp-hr)	Post-repair PM Emissions (g/bhp-hr)	Post-repair PM Emissions (g/bhp-hr)	
J&R01	2011 Cummins	0.001	0.002	0.000	0.000	YES
J&R03	2013 Cummins	0.024	0.025	0.017	0.015	NO
J&R04	2013 Volvo	0.004	0.006	0.004	0.003	N/A
J&R05	2012 Cummins	0.029	0.021	0.028	0.011	NO
J&R06	2015 Cummins	0.031	0.023	0.013	0.004	NO
J&R07	2014 Volvo	0.002	0.004	0.001	0.001	N/A
J&R09	2012 Cummins	0.051	0.103	0.024	0.003	NO
J&R10	2011 Cummins	0.034	0.024	0.019	0.017	YES
J&R11	2013 Cummins	0.017	0.012	0.027	0.015	YES
J&R12	2011 Volvo	0.005	0.004	0.006	0.006	YES
J&R13	2013 Cummins	0.020	0.005	0.030	0.012	NO
J&R14	2010 DDC	0.000	0.000	0.004	0.013	NO
J&R15	2010 Navistar					NO
J&R16	2010 Mack	0.009	0.056	0.001	0.008	NO
J&R17	2011 Cummins					YES
J&R18	2014 Cummins	0.011	0.017	0.024	0.018	NO
J&R19	2015 Cummins	0.024	0.030	0.016	0.024	YES
J&R19 Second visit		0.016	0.024	0.006	0.012	YES
J&R20	2011 Cummins	0.014	0.017	0.002	0.004	YES
J&R21	2013 Cummins	0.006	0.009	0.000	0.000	NO
J&R22	2013 Cummins	0.046	0.031	0.005	0.009	YES
J&R22 Second visit		0.004	0.007	0.000	0.000	YES
J&R23	2013 Cummins	0.018	0.020	0.000	0.000	YES
J&R25	2013 Cummins	0.005	0.002	0.020	0.018	NO
J&R26	2013 Paccar	0.017	0.019	0.003	0.005	NO
J&R27	2014 Volvo	0.002	0.004	0.006	0.001	YES
J&R28	2013 Cummins					NO
J&R29	2014 Cummins	0.013	0.009	0.021	0.023	NO
J&R30	2013 Cummins	0.004	0.003	0.000	0.001	YES

Table S2 Pre- and post-repair for PM emissions for the MPM4 for each vehicle on a g/bh-hr basis (continued)

Vehicle No.	Engine Year & Make	50 km/h	80 km/h	50 km/h	80 km/h	DM1=1
		Pre-repair PM Emissions (g/bhp-hr)	Pre-repair PM Emissions (g/bhp-hr)	Post-repair PM Emissions (g/bhp-hr)	Post-repair PM Emissions (g/bhp-hr)	
J&R31	2013 Cummins	0.012	0.007	0.027	0.022	YES
J&R32	2013 Volvo	0.001	0.003	0.001	0.001	YES
J&R33	2015 Cummins	0.001	0.000	0.002	0.002	NO
J&R34	2015 Volvo	0.001	0.001	0.002	0.003	YES
J&R35	2014 Volvo	0.000	0.000	0.001	0.001	YES
J&R36	2013 Volvo	0.001	0.009	0.001	0.003	YES
J&R37	2016 DDC	0.002	0.003	0.000	0.001	YES
J&R38	2013 Cummins	0.001	0.001	0.004	0.003	NO
J&R39	2013 Cummins	0.011	0.011	0.020	0.018	YES
J&R40	2013 Cummins	0.031	0.029	0.018	0.017	YES
J&R40 Second visit		0.000	0.000	0.000	0.000	NO
J&R40 Third visit		0.000	0.000	0.000	0.000	YES
J&R41	2014 Paccar	0.008	0.008	0.011	0.007	NO
J&R42	2013 Cummins	0.003	0.002	0.002	0.002	YES
J&R43	2014 Cummins	0.001	0.001	0.004	0.003	YES
J&R44	2014 Volvo	0.002	0.002	0.003	0.001	YES
J&R45	2013 Cummins	0.007	0.002	0.004	0.004	NO
J&R46	2013 Cummins	0.001	0.000	0.004	0.004	YES
J&R47	2013 Volvo	0.000	0.000	0.002	0.002	YES
J&R48	2013 Maxxforce	0.035	0.025	0.037	0.025	NO
Cum01	2015 Cummins	0.022	0.022	0.030	0.019	NO
Cum02	2010 Cummins	0.091	0.004	0.001	0.000	N/A

5. Sources of Variance in BC Mass Measurements from a Small Marine Engine: Influence of the Instruments, Fuels and Loads

5.1. Abstract

Knowledge of black carbon (BC) emission factors from ships is important from human health and environmental perspectives. A study of instruments measuring BC and fuels typically used in marine operation was carried out on a small marine engine. Six analytical methods measured the BC emissions in the exhaust of the marine engine operated at two load points (25% and 75%) while burning one of three fuels: a distillate marine (DMA), a low sulfur, residual marine (RMB-30) and a high-sulfur residual marine (RMG-380). The average emission factors with all instruments increased from 0.08 to 1.88 gBC/kg fuel in going from 25 to 75% load. An analysis of variance (ANOVA) tested BC emissions against instrument, load, and combined fuel properties and showed that both engine load and fuels had a statistically significant impact on BC emission factors. While BC emissions were impacted by the fuels used, none of the fuel properties investigated (sulfur content, viscosity, carbon residue and CCAI) was a primary driver for BC emissions. Of the two residual fuels, RMB-30 with the lower sulfur content, lower viscosity and lower residual carbon, had the highest BC emission factors. BC emission factors determined with the different instruments showed a good correlation with the PAS values with correlation coefficients $R^2 > 0.95$. A key finding of this research is the relative BC

measured values were mostly independent of load and fuel, except for some instruments in certain fuel and load combinations.

5.2. Introduction

Black Carbon (BC) emissions have important implications on health effects and air quality (Corbett et al., 2007; Buffaloe et al., 2014; Khan et al., 2012; Lack et al., 2008). The health effects of BC include cardiovascular and chronic lung diseases, which are linked with particulate matter (PM) (Janssen et al., 2012; Winebrake et al., 2009). BC can make up a significant component of PM. BC emissions also have climatic effects that include direct and indirect radiative forcing, influencing cloud formation, and melting of snow, glaciers, and sea ice, especially in the highly sensitive Arctic (Bond et al., 2013a; Corbett et al., 2010a; Lack and Corbett, 2012). BC emitted from marine traffic in the Arctic in particular has a nearly five-times greater surface warming effect than BC emitted at mid-latitudes (Sand et al., 2013). BC is the second largest anthropogenic contributor to global warming after CO₂, due to its strong light absorbing properties (Fuglestvedt et al., 2008).

Marine transportation is estimated to contribute significantly to the global BC load. Overall, shipping emissions contribute 2% of the global black carbon (BC) inventory from all sources and 8-13% of BC emissions from diesel sources (Azzara et al., 2015; Bond et al., 2013). Previous investigations reported a range of BC emission factors from ships, varying from 0.1 to 1 g/kg fuel (International Council on Combustion Engines (CIMAC), 2012; Lack et al., 2008; Corbett et al., 2010b). Having such a wide range of BC emission factors makes it challenging to evaluate the climate impacts of BC from shipping and has raised concern during international discussions of the need for BC control measures.

Modeling and inventory studies have utilized a value of 0.324 g/kg fuel, with several BC inventories using 0.34 g/kg fuel (Comer et al., 2017) or 0.35 g/kg fuel (Corbett et al., 2010b; Peters et al., 2011; Winther et al., 2014). While these emission factors are within the range of reported values, they have a high degree of uncertainty. In particular, if the full uncertainty in BC emissions factors is considered, BC from ships could represent anywhere between 1.7% and 17% of global diesel source BC emissions, assuming that 2015 diesel source BC emissions are similar to those in Bond et al.'s year 2000 estimates (Bond et al., 2013; Comer et al., in press).

One approach to improving the confidence in BC emission factors is to add to the limited data base; however, interest in real world emissions data from ships has focused on criteria pollutants and not BC. Thus, data on BC emissions from marine engines is generally limited to laboratory testing under controlled conditions (Eyring et al., 2005). Bond et al. (2013) and Petzold et al. (2013) showed that BC emissions varied depending on the measurement method used, while Lack and Corbett (2012) and references therein show that engine load and fuels used also influence BC emission factors. In this research, the focus was on the change in BC emissions with respect to these parameters: measurement method, fuels and engine load.

Marine fuel properties are known as important parameters driving PM mass and BC emission factors. For example, high sulfur, heavy fuel oil (HFO) leads to significant PM mass emissions (Wall et al., 1988; Khan et al., 2012), so environmental agencies require ships to use low sulfur fuels (LSFs) in designated emissions control areas (ECAs) in order to reduce sulfur oxides and sulfur-related PM emissions. Recently, plans were

announced to further limit sulfur emissions that can arise from the use of high sulfur marine fuels (International Maritime Organization (IMO), 2017). The use of LSFs provides reductions in the sulfur-related PM emissions, however, the effect of fuel quality on BC emissions is not clear (Lack and Corbett, 2012). Some studies have suggested that switching to low sulfur heavy fuel oil (LSHFO) could reduce BC emissions due to the reduction in aromatic and long chain hydrocarbon components in the fuel, resulting in lower concentrations of BC particle nuclei (Lack et al., 2011; Lack and Corbett, 2012; Buffaloe et al., 2014). However, several authors found that LSHFO increased BC emissions, while lowering sulfur-related PM emissions (CIMAC, 2012; Aakko-Saksa et al., 2016a; Ristimäki et al., 2010; Sippula et al., 2014). In this case, the authors suggested that metal oxides in the high sulfur heavy fuel oil (HSHFO) catalyzed the oxidation of BC at lower engine loads (Sippula et al., 2014). BC emission factors for low sulfur distillate fuels, however, are consistently lower compared with HSHFO and LSHFO (Aakko-Saksa et al., 2016a; Comer et al., In Press).

The present research study was carried out as part of a broader investigation to improve the confidence in reported BC emission factors with Phase 1 being carried out in the laboratory and Phase 2 making real world emission measurements on ocean going vessels (OGVs). Given the large range in reported BC emission values, the key objective in Phase 1 was to evaluate a number of parameters and learn whether these factors were causative for the large range of reported BC values. These factors included: fuel parameters, engine operating conditions, and BC measurement instruments. The platform for the Phase 1 research was a 2-stroke, high-speed marine engine that was operated with

three different commercial marine fuels at two engine load points (25% and 75%). The three fuels included a low-sulfur content distillate marine (DMA), a low-sulfur residual marine fuel (RMB-30), and a high-sulfur residual marine fuel (RMG-380). Six different BC instruments, based on different measurement principles, were used in the research. The instruments and measurement principles included: 1) light absorption (LA), including photoacoustic spectroscopy (PAS) using a Micro Soot Sensor (MSS), filter smoke number (FSN) using an AVL 415SE-Smoke Meter, an Aethalometer and a multi-angle absorption photometer (MAAP); 2) thermal radiation using laser induced incandescence (LII); 3) thermal-optical using extra-situ and semi-continuous thermal-optical-analysis (TOA). An important outcome of this work was to understand how each instrument performed and to select a subset of instruments for real world measurements on board ships with large, 2-stroke, slow-speed diesel engines. To this end, information from this study was used to guide the planning for real-world tests on two marine vessels, the results of which will be presented in future publications.

5.3. Experimental Approach

5.3.1. Test Engine

The marine test engine was a 2-stroke, high speed, naturally aspirated, compression ignited, Detroit Diesel Model 6-71N, with a cylinder displacement of 7 L, a compression ratio of 18.7:1, a maximum speed of 1,800 revolutions per minute (rpm), a maximum power of 187 kW, a brake mean effective pressure (BMEP) of 641 kPa, and a brake specific fuel consumption (BSFC) of 307 g/kWh (0.505 lb./hp-hr) at 1100 rpm. This engine was initially manufactured in the 1980s time period, and was widely used in marine applications

for fishing and work boats, and as an auxiliary engine on larger vessels. Additional details on the specifications of the engine are provided in the supplementary material. The test engine was selected based on previous experience that this older, 2-stroke engine would produce carbonaceous particulate emissions with a high ratio of organic carbon to elemental carbon (OC/EC ratio) and thus produce similar particulate to that emitted from larger slow speed two stroke main engines for ocean going vessels. The engine was set up with N70, single, large spray pattern port injectors to enable it to burn a range of fuels, from distillate to the dirtiest/cheapest heavy-fuel oil (HFO). N70 injectors, with a single, large spray port, limited coking and plugging of the injection tip during testing. For testing, the engine was mounted and operated on a 600 horsepower (hp) GE DC electric engine dynamometer.

5.3.2. Test Fuels

Three different representative commercial marine fuels with a wide range of properties were tested: a distillate marine A (DMA), a low-sulfur, residual marine B (RMB-30) and a high-sulfur, residual marine G (RMG-380). Some of the main of properties of the test fuels are provided in Table 5-1. This includes fuel sulfur content, density, viscosity, carbon residue, and the Calculated Carbon Aromaticity Index (CCAI). The CCAI is a measure of the ignition quality of residual fuel oil (Sarvi et al., 2008) in diesel engines and is normally a value between 800 and 880. The lower values combust better, and values >880 are above specification. Note that the CCAI is typically a metric for residual fuels, so the value for the DMA fuel was not calculated. CCAI is calculated by:

$$CCAI = D - 140.7 \log(\log(V + 0.85)) - 80.6 - 483.5 \log\left(\frac{t + 273}{323}\right)$$

Where: D= density at 15°C (kg/m³); V= viscosity (cST); and t = viscosity temperature (°C)

Table 5-1 Selected Fuel Properties

Fuel	DMA	RMB-30	RMG-380
Sulfur wt% (ppm)	13	13.2	31,849
Density @ 15°C (kg/L)	0.8309	0.8586	0.9826
Viscosity @ 40°C (cSt)	2.696	-	-
Viscosity @ 50°C (cSt)		13.73	358.9
Micro Carbon Residue (%m/m)	< 0.1	< 0.1	12.84
CCAI_calculated		769	845

The energy content of the DMA fuel, which is similar to No.2 diesel fuel, is estimated to be 45 MJ/kg. The energy contents of the HFO fuels is estimated to be 41 MJ/kg.

The DMA is a low-sulfur distillate fuel similar to No. 2 diesel fuel that is being considered for use for marine engines operated in ECAs. The RMB-30 is a low-sulfur, heavy fuel oil (LSHFO) that is a newer fuel designed to comply with ECA fuel sulfur standards. This fuel combines the performance properties of HFO (e.g., a high flashpoint and low volatility) with a low sulfur content (EPA, 2016). The high-sulfur RMG-380 is comparable to the dirtiest and cheapest fuels often used by large ocean going vessels. Compared with the LSHFO, the RMG-380 viscosity was 100 times higher, and the sulfur level was 1,000 times higher.

The residual fuels were fed from drums heated to 95°C to ensure flow to the engine. Furthermore, the engine was run on DMA fuel at high load for 30 minutes prior to using the RMG-380 to ensure that the piston head temperature was above the fire point, thus serving as a glow plug when introducing the residual fuels. The test fuels are representative of commercial fuels and the broad range of properties enables an analysis of whether those

properties drive BC production and also if they change the nature of the BC and co-emitted species produced such that it influences the different BC measurement technologies.

5.3.3. Test Loads

Testing was conducted using the three fuels at 25% and 75% engine loads with the engine operating at 1100 RPM. The 25% and 75% load points were selected to provide test conditions with different OC to EC ratios. At the 25% load point, the OC/EC ratio was ~9+:1. This OC/EC ratio is similar to the 9:1 ratio that has been seen OGV main engines (Gysel et al., 2017). At the 75% load, the OC/EC ratio was ~1:1, thus allowing a measure of the instruments' response at two very different OC/EC ratios.

5.3.4. Measurement Methods

5.3.4.1. Instruments

BC is defined as a distinct type of solid carbonaceous material, formed primarily in flames, that has a unique combination of physical properties, including strong light absorption, refractory, small and aggregated particles, and resistant to chemical reaction (Bond et al., 2013, Petzold et al., 2013). There are many analytical methods used to measure BC emissions, each relying on one or more of these properties in the detection method. To aid in the interpretation of reported data, Petzold et al. (2013) has suggested the use of terminology which makes clear what type of method has been used. For example, equivalent black carbon (eBC) for light absorption methods, refractory black carbon (rBC) for Laser Induced Incandescence, and elemental carbon (EC) for thermal-optical analysis. It is not clear if any method is considered more accurate or representative of marine BC emissions. In this study, we are investigating whether the use of a broad range of methods

in past studies could have contributed to the large range of emission factors reported in the literature. BC emissions were measured using six instruments that operate on different measurement principles associated with different properties of BC; see Table 5-2. The instruments in this study are widely used, thus allowing an assessment of the potential importance of measurement method on the variability of emission factors reported in the literature.

Table 5-2 Black Carbon Measurement Instruments and Associated Measurement Principles

Instrument	Abbreviation	Model	Measurement Principle	Wavelength (nm)	Report Value	Detection limit ($\mu\text{g}/\text{m}^3$)	Max. Conc. (mg/m^3)
Aethalometer¹	Aethalometer	Magee Scientific AE21	light absorption and scattering	370 and 880	eBC	0.1	0.05
Laser Induced Incandescence²	LII	Artium 300	thermal radiation	N/A	rBC	1	20,000
Multi-Angle Absorption Photometer³	MAAP	Thermo Scientific 5012	light absorption and scattering	670	eBC	0.1	0.05
Micro-Soot Sensor⁴	PAS	AVL 483	light absorption (photoacoustic)	808	eBC	1	50
TOA-Extra Situ⁵	TOA-ES	Sunset Laboratories	thermal-optical		EC	0.3-0.4 $\text{g}/\text{cm}^3/\text{filter}$ loading	
TOA-Semi-Continuous⁶	TOA- SC						
Smoke Meter⁷	FSN Line 1 or FSN Line 2	AVL 415SE	light absorption	420-680	eBC via FSN	20	100

¹Aethalometer, 2016; ²LII, 2016; ³MAAP 2016; ⁴MSS, 2018; ⁵TOA-ES, 2018, ⁶TOA-SC, 2018 ⁷Smoke Meter, 2018.

5.3.4.2. Experimental Layout.

Figure 5-1 provides a schematic of the experimental setup, including the four instrument sampling locations. The schematic also includes the location of a catalytic stripper and sulfur adsorbers that were used for some sample conditioning testing. In this paper, only the results for the bypass (BP) condition (i.e., without the catalytic stripper and sulfur adsorbers) are discussed. The four sampling locations represented 1:1 dilution on stack, and 1:1, 14:1, and 1400:1 dilution after the bypass and sample conditioning. Dilution was necessary for several reasons. First, it mitigates problems with heat, humidity, and lowers the PM concentration to the maximum allowed by the instrument. For example, the MAAP and Aethalometer are designed to measure particle concentrations up to $50 \mu\text{g}/\text{m}^3$ (MAAP 5012 Manual, 2007; Aethalometer Manual, 2005), so these instruments used a dilution of 1400:1. Another important point is that dilution also reduces the vapor pressure of the gaseous materials in the airstream such that when the exhaust is cooled, the partial vapor pressure for sulfuric acid (for example) will not exceed its saturated vapor pressure at that given temperature. This minimizes the potential for artifact condensation. Note that all sample lines were heated up to the point of dilution or the measurement instrument if no dilution was applied (red lines in Figure 1) to reduce condensation of water, semi-volatile and volatile organics.

Different approaches were used for dilution. For the 14:1 dilution, a dilution tunnel with a partial flow dilution sampling system was used with a single venturi following the requirements of the ISO 8178-1 methods (ISO, 1996). Comparisons between FSN at 1:1 on stack and 1:1 dilution sampling points and LII instruments at the 1:1 and 14:1 dilution

sampling points showed good agreement, indicating similar results were seen for different levels of dilution. These results are presented in the Supplementary Material. The dilution air used in this process was pretreated in a unit that included silica gel to remove water, activated carbon to remove hydrocarbons, and a HEPA filter to remove PM. As per ISO-8178-1, the dilution ratio was calculated using raw and dilute concentrations of NO_x and CO₂. This approach allowed the dilution ratio to be calculated by two independent methods. Comparative results met the standard of ISO 8178-1. It should be noted that the LII instrument that we initially placed in the LII #3 position did not work correctly during the testing on the DMA, so the working LII instrument that was in the LII #1 position was swapped to the #3 position for the subsequent testing on the RMG-380 and RMB-30 testing, as the 14:1 dilution point was where most of the more critical instrument comparisons were done.

The special dilution unit for the 1400:1 dilution factor used three dilutors in series. The first stage was a rotating disk dilutor (RDD, DF=10:1), and the second was a mixing dilutor (DF=10:1) that used a rotary vane pump to add filtered air to the RDD output. The final stage used a venturi with a 14:1 dilution ratio. These three stages provided an overall 1400:1 dilution ratio. For the diluted samples, heated lines were not needed after the dilution point because the vapor pressure of water and volatile organics were sufficiently low that condensation was negligible. In order to avoid discrepancies in particle losses between the different instruments at different locations, the residence times of the samples for each BC instrument were matched.

A statistical analysis between instrument, load, and fuel factors was performed by using analysis of variance (ANOVA) methods. The results of these ANOVA analyses are presented in the *Statistical Analysis for BC Emissions for the Load, Fuel, and Instrument Factors* section of the Supplementary Material. The analyses showed that both fuels ($p=0.000$) and engine load ($p=0.000$) had a statistically significant impact on BC emission factors. The primary ANOVA analyses did not show statistically significant differences for the instruments, but there was a statistically significant interaction between the instrument and load factors, indicating that the differences between instruments varied a function of different loads. The results for the different loads and fuels are presented here, while the instrument results are discussed in greater detail in the next section.

The average emission factors over all instruments increased from 0.08 to 1.88 g/kg fuel in going from 25 to 75% load, about 24 times higher. This finding is opposite to the trend that has been reported for medium speed and large slow-speed, turbocharged, marine engines, which represent the majority of marine engines used in ocean-going service. Those engines have shown lower BC emission factors at higher loads (Agrawal et al., 2008a; 2008b; Khan et al., 2012; Khan et al., 2013, Lack and Corbett, 2012; CIMAC, 2012). Lack and Corbett (2012) found that BC emission factors increased by an average factor of 3 in going from 100 to 25%, with increases of up to a factor of 6.5 for loads below 25%. This trend was attributed to the lower fuel consumption at lower loads, and to the fact that at lower loads the engine is operating outside the range where the engine is designed to operate efficiently. Higher emissions at lower load points were also seen in a CIMAC (2012) review, where BC emission factors for a medium speed engine ranged from less

than 0.1 g/kg of fuel to as high as 0.8 g/kg of fuel at 10% load points. They attributed the result to the higher combustion efficiencies at the higher load points. The trend of increasing BC emission factors with increasing engine load in the present study is likely a consequence of using an older, high-speed engine where the residence time for combustion of soot is much shorter compared to medium speed and large slow-speed, turbocharged, marine engines. The test engine in this study was operating at constant speed, so and in order to triple the power output, the input fuel rate was tripled. The older engine used in this study also used a combustion cylinder design that was not improved for soot combustion and burn out as there were no PM standards at that time. While all diesel engines have excess oxygen for combustion, there are localized fuel-rich areas with insufficient air where soot is formed. Combustion design for modern engines aims for very small droplets that readily volatilize and mix with surrounding air to limit soot production and for in-cylinder swirl turbulence and time to burn out the PM. As discussed earlier, the higher speed engine and setup was selected to provide a range of PM characteristics that would be representative of those found in engines, on ocean going vessels, thus enabling a robust comparison of a number of instruments measuring BC emission factors.

In comparing the different fuels, average BC emission factors ranged from 0.13 to 0.82 g/kg fuel for the DMA, from 0.25 g/kg to 1.88 g/kg fuel for the RMB-30, and from 0.08 to 1.12 g/kg fuel for the RMG-380, where the lower and higher values represent the results at the 25% and 75% load points, respectively. At 25% load, the RMG-380 had the lowest emission factor but the DMA was the lowest at 75% load. The RMB-30 – the new low-sulfur HFO with a lower sulfur, viscosity and residual carbon content than the RMG-

380 – showed the highest BC emission factors at both loads. The average results showed increases of about 200% in going from the RMG-380 to RMB-30 fuels at the 25% load, and increases of 97% in going from the DMA to RMB-30 fuels at the 75% load. These differences are important, but were less than the differences seen as a function of different engine loads. The difference of 35.7% between the DMA and RMG-380 fuels at the 75% load point is comparable to the average 30% difference between DMA and RMG-380 found in the literature review by Lack and Corbett (2012).

The results did not show consistent trends in BC emissions as a function of fuel sulfur levels, given that the fuel sulfur levels in the fuels varied from ~13 ppmw to 32,000 ppmw. This finding is not surprising, as BC is primarily formed from the pyrolysis of carbon moieties, and sulfur is not involved in the reaction pathways. The lack of consistent trend for BC emissions as a function of fuel sulfur has also been seen in the literature, with some studies showing higher BC emissions for lower sulfur fuels (CIMAC, 2012; Aakko-Saksa, 2016a; Ristimäki et al., 2010), while others have reported lower BC emissions for LSHFO fuels (Comer et al., In Press; Lack et al., 2011, Lack and Corbett, 2012; Buffalo et al., 2014).

A second fuel factor that could be a primary driver of BC is the fuel oil viscosity, as it is a primary parameter in determining the Sauter mean droplet diameter (Nukiyama and Tanasawa, 1938; Arai et al., 1984). Since the RMG-380 was 25 times more viscous than the RMB-30, the RMG-380 should produce a larger droplet diameter in the combustion chamber and more unburned fuel in the exhaust. Again, the results showed viscosity was not a primary driver of BC emissions. A third parameter investigated was the

resulting carbon residue from pyrolysis of the fuel. Here the RMG-380 with >128 times the propensity to form char on heating as compared with RMB-30 had less BC than the RMB-30. A final parameter was the CCAI. The RMB-30 had a lower CCAI than the RMG-380, indicating that the RMB-30 had better ignition quality and that it should burn more completely. Again, there was more BC with the RMB-30 than with the RMG-380, suggesting that CCAI was not the main factor contributing to BC emissions.

One factor that could have an important impact on BC emissions is the presence of metal oxides from the porphyrins in crude oil. Some have hypothesized that the presence of metals and metal oxides in the HSHFO at lower engine loads may catalyze and enhance the oxidation of BC, which would lead to lower BC emissions for HSHFO (Sippula et al., 2014), consistent with our results. This has been seen in other studies (Sippula et al., 2014; Andreae and Gelencser, 2006). Higher levels of inorganic material in the PM composition in biomass burning studies resulted in TOA-derived EC oxidizing at lower temperatures (Andreae and Gelencser, 2006). In this study, refractory residuals were visually observable on the quartz filters after the NIOSH TOA-ES filter analyses for the RMG-380 samples, but were not visually observed for the other two fuels. There was also some indication of the presence of metals in transmission electron microscope (TEM) images for the RMG-380 fuel, which will be discussed in greater detail elsewhere. The residual was likely a mix of vanadium and nickel oxides from the porphyrins in the crude (Lewan, 1984) that catalyze the oxidation of the EC. Additional analyses of the refractory residual were not available, and further investigation is needed to better understand these results.

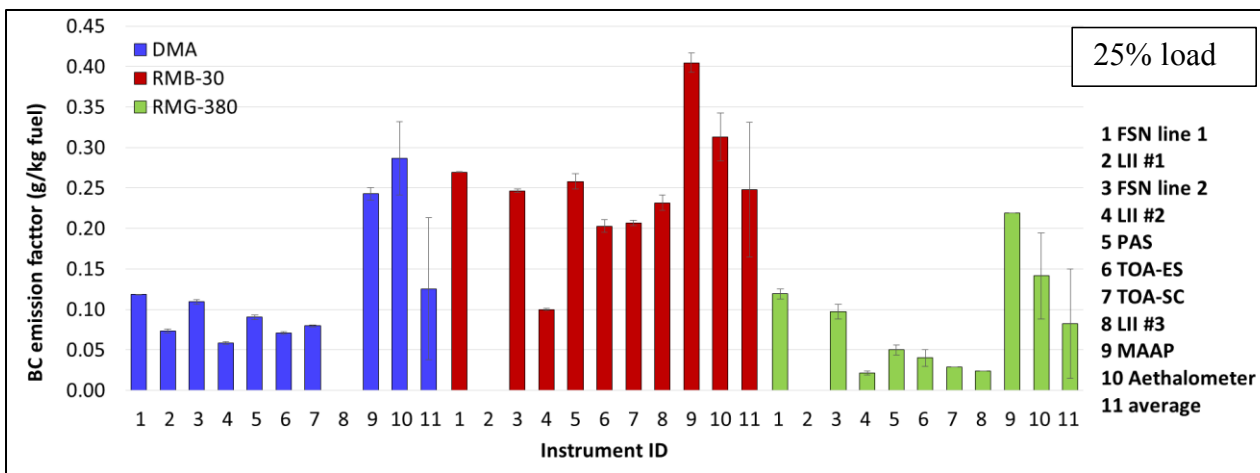


Figure 5-2: Summary of BC Emissions Factors (g/kg fuel) at 25% Load

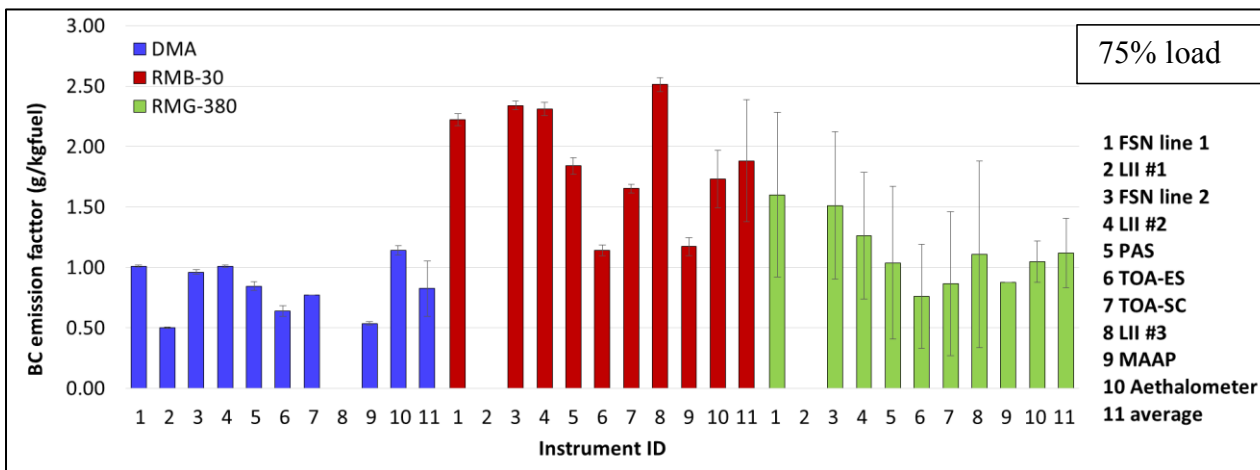


Figure 5-3 Summary of BC Emissions Factors (g/kg fuel) at 75% Load

Although the results show that fuel differences have important impacts on BC emissions, the selected fuel parameters tested in this research did not identify the key parameters or drivers for BC emissions. While this study provided important information about the relationship between fuel properties and BC emissions, future studies are needed and should investigate other fuel parameters as well as the combustion process. The results do suggest that the use of distillate fuels could provide reductions in BC emissions from marine vessels, while LSHFOs could lead to increases in BC emissions.

5.4.2. BC Instrument Comparisons.

The recorded concentration of BC increased for all instruments at higher engine loads, but the increase varied among instruments. In order to get a measure of the variation in values between instruments, we constructed parity plots with the PAS instrument on the x-axis and the other instruments on the y-axis. Additional information on statistical comparisons between BC emission factors for different instruments is provided in the Supplementary Material. The PAS was selected as the basis for comparison for the BC emission factors in this section, since it was incorporated into compliance testing as part of the U.S. EPA's heavy-duty In-Use testing Measurement Allowance Project (Johnson et al., 2011) and in the aviation industry (SAE, 2011, 2013). While we have utilized the PAS as a basis of comparison for these reasons, it should be noted that this is primarily to show the range of BC emissions measurements, rather than to suggest a preference for one instrument above the others.

Values for the slope and intercept of each instrument measured relative to the PAS instrument are shown in Figure 5-4. The data in Figure 5-4 show three clusters of data: one

at lower, medium, and higher BC readings. Values up to 4 mg/m^3 were for 25% load; values near 30 mg/m^3 were the DMA and RMG-380 data for the 75% load; and values between 60 to 80 mg/m^3 were for the RMB-30 fuel and some RMG-380 data for the 75% load. The slopes show similar trends with coefficient of determination, R^2 , values >0.95 for all instruments. The main differences between instruments are the slopes of the regressions themselves, with the slopes being >1 for the FSN and LIIs and <1 for the TOAs and atmospheric instruments (i.e., MAAP and Aethalometer). Additional figures showing the data at the lower concentrations in greater detail are provided in the Supplementary Material in the section *BC mass concentration presented in mass per volume units for the 25% load points*. Some additional analyses of how the slopes for each instrument change when the results for the RMB-30 and RMG-380 fuels are normalized by the DMA results are also presented in the Supplementary Material in the section *BC mass concentrations for the RMB-30 and RMG-380 Fuels Normalized by the DMA Fuels*. This additional analysis shows that most instruments continue to agree with each other as the fuel changes, with the exception of a few instruments.

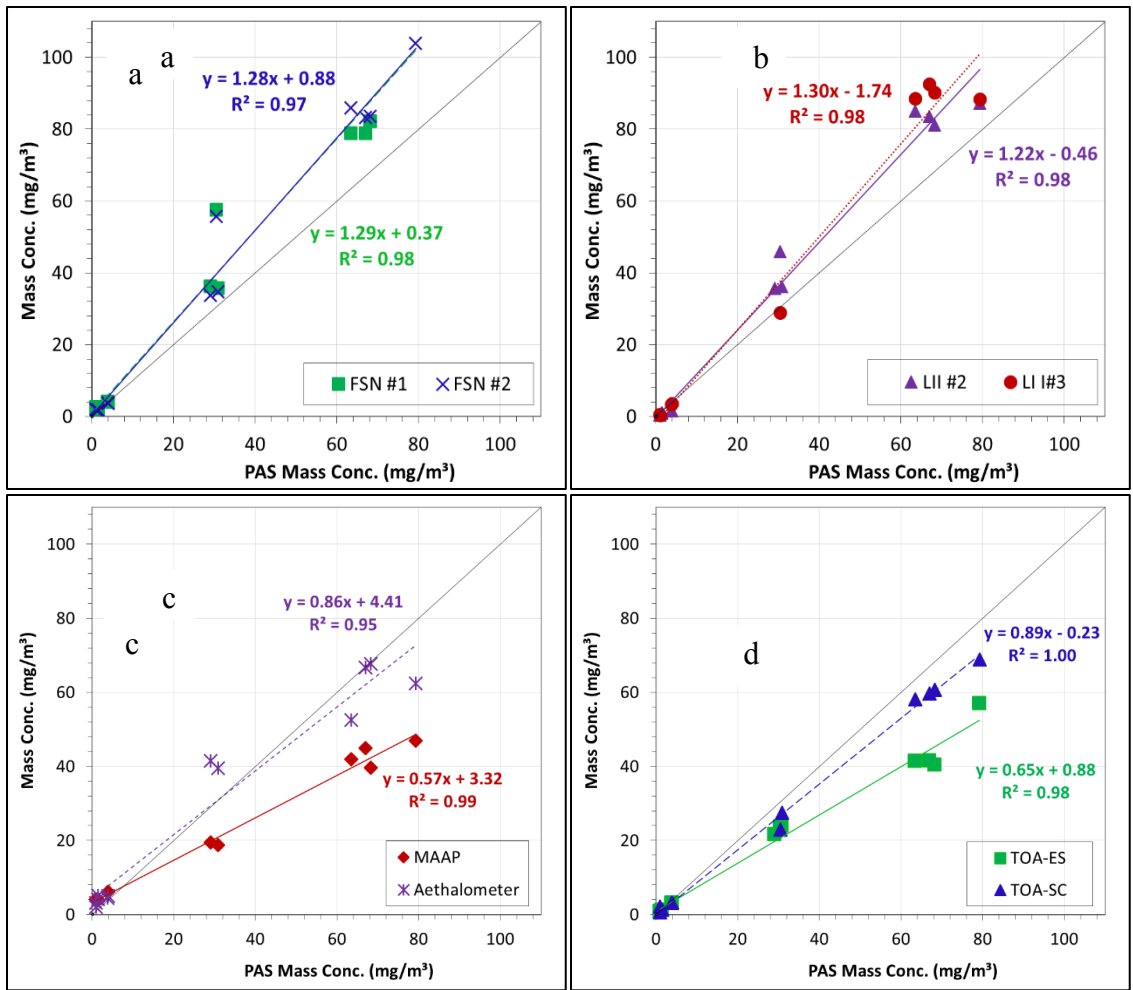


Figure 5-4 Various Instrument Responses with respect to PAS Mass Concentration

The FSN and LII slopes are similar so the instruments responded similarly to BC and had a BC emission factor 1.22-1.29 times that of the PAS instrument (Figure 5-4a and 5-4b). According to the manufacturer, the FSN implemented a thermophoresis loss correction in the Firmware, while the PAS does not correct for thermophoresis loss. The thermophoresis loss correction would contribute to higher readings for the FSN than PAS. The impacts of particle losses were calculated using equation 17 from Shin et al. (2008).

The loss is estimated at 21% to 24% for the PAS, comparable to the differences between the FSN and the PAS.

LII #2 and LII#3 sampled from the DF 1:1 location and the DF 14:1 (diluted) location, respectively. Figure 3b shows that there is a good correlation between the PAS and LIIs, with an R^2 of 0.98 for both LIIs. The slopes of the regression for LIIs range from 1.22 to 1.30, indicating values approximately 22 to 30% higher than those for the PAS. Differences between the two instruments and with the PAS may be due to differences in the calibrations of the two instruments, which may have been calibrated on different particle sources. Another study also found that LIIs measured higher BC values than a PAS (Durbin et al., 2007). While the LII measurement was higher than the PAS at the 75% load point, leading to the higher regression slope, the LII measurements at the 25% load point were lower than those of the PAS, as seen in the Supplementary Material. Another study found lower readings for the LII compared to PAS at ambient level concentrations (Chan et al., 2011). The lower readings at the 25% load point could be related to the high OC content of carbonaceous particles under those conditions. If OC takes the form of a coating on the BC particles this can inhibit the particle heating such that the peak temperature suboptimal for LII detection which can bias readings. High OC content is also linked to lower maturity BC particles with different optical properties than mature BC which can also bias the measurements. In both instances, the bias is towards lower readings.

Of the two commonly used BC instruments developed for ambient air monitoring, the MAAP reported the lowest BC values. Hyvärinen et al. (2013) also found that MAAP readings underestimated BC concentrations, similar to this study, for ambient urban

environments where high concentration levels of BC were found. As shown in Figure 5-4c, BC values for the Aethalometer were on average 86% of those measured by the PAS method. Both ambient instruments are filter-based and known to have measurement errors introduced by light scattering off particles and filter fibers (Weingartner et al., 2003). Also the filter spot change could introduce errors up to 100%, even when corrections are applied (Lack et al., 2015). Some have reported scattering and filter spot change contributed to the lower readings when compared with other instruments (Petzold et al., 2004). Another observation associated with the MAAP and Aethalometer is the relatively larger intercepts of the regressions, as shown in Figure 3c and with more detailed plots in the Supplementary Material in the *BC mass concentration presented in mass per volume units for the 25% load points* section. The MAAP and Aethalometer sampled from the DF 1400:1 location due to their lower concentration ranges. The larger intercepts for BC at the lowest concentration levels for the high dilution could be due to slight offsets in these lower level readings for these instruments relative to the PAS that are multiplied when the exhaust concentrations are corrected for the 1400:1 dilution, as also observed by Aakko-Saksa et al. (2016a, 2016b) and IMO (2016). For the MAAP, the high organic content of the particles at low load could lead to the formation of BC-OC core shell mixtures that can contribute to a lensing effect, leading to higher measured BC concentrations (Lack et al. 2011; Leung et al. 2017; Bhandari et al. 2017). For the Aethalometer, the fact that it is calibrated based on typical atmospheric particles could lead to some of the observed differences, as it may not be properly tuned for the type of particles that were measured in this study. Because of possible errors introduced by dilution methods and the corrections

needed for the light scattering off the particles and the filter, the BC instruments designed for atmospheric air measurements are not recommended for source measurements even with a significant amount of dilution.

The slope for the TOA-ES data plotted against the PAS data is 0.65, suggesting the thermal-optical method measured on average 35% lower EC values than the PAS, as shown in Figure 5-4d. This finding is consistent with the results from several publications (Lack et al., 2011; Kanaya et al., 2008). One possible explanation is that PAS methods overestimate BC concentrations by detecting coatings on the BC particles (lensing effect, e.g., KNOx et al., 2009, Chan et al., 2011). Comparisons can also be made between the TOA-SC and TOA-ES. Both the TOA methods are based on the NIOSH-5040 method, with the TOA-ES method operating with the normal NIOSH-5040 method, while the TOA-SC method used a modified NIOSH method that was designed to be about twice as fast as the regular protocol. As such, a main potential difference of the two instruments are the OC-EC split points. A second important difference is that the semi-continuous TOA had a vapor denuder installed upstream of the instrument to remove organic vapors. As shown in Figure 5-5, the TOA-SC and TOA-ES showed reasonable agreement for Total Carbon (TC) emissions. The higher readings found for the TOA-ES that can probably be attributed to the TOA-SC being equipped with a vapor denuder, which removes some gas-phase organic species that might condense on the filters and contribute to OC readings. Additionally, some small organic particles may be lost via diffusion in the trap. The TOA-SC showed higher EC and lower OC readings than the TOA-ES. The opposite trends seen for the EC and OC readings coupled with the reasonable agreement in TC between the two

measurement methods coincides with the instruments having different OC-EC split points, with the TOA-SC consistently having an earlier split point than the TOA-ES. The results also showed that the position of the OC-EC split point was dependent on the fuel, with the split points for the RMG 380 and DMA fuels being earlier compared to the RMB-30 fuel. This could be due to either a catalytic effect due to the presence of metal oxides or the presence of organics that are not transparent to the red laser monitoring the transmission through the filter. Deeper analysis of this fuel influence on these two TOA instruments will be presented in a subsequent paper where the catalytic stripper and sulfur adsorber results are discussed.

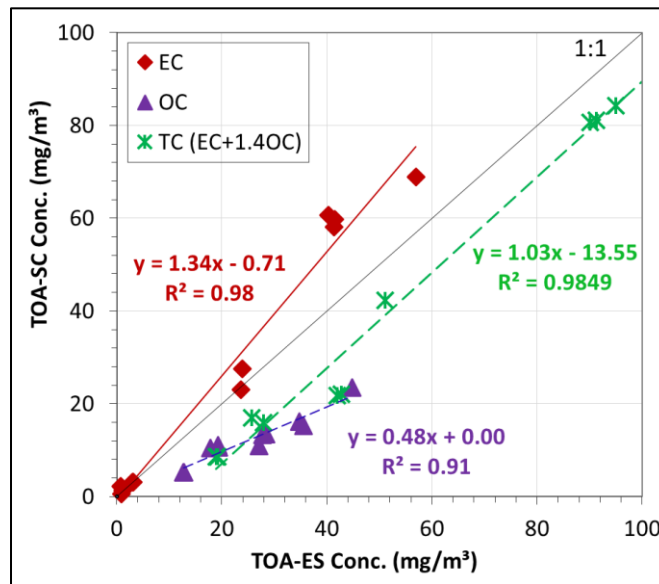


Figure 5-5 Correlations between Two TOA Methods

5.4.3. Particle Size Distributions (PSD).

PSDs collected with a SMPS are shown in Figure 5-6 for each of the test fuels at the 25% and 75% loads. The error bars represent the standard deviation of repeats of test runs at the different conditions. Note that due to the logarithmic scale, the error bars appear

to be larger for the lower error bar than the upper error bar while they are in fact equal. A graph of PSDs on an arithmetic scale is also provided in the Supplementary Material. Generally, the PSDs at the 25% load for all three fuels had higher particle number concentrations than those at 75% loads. The PSDs for the 25% load point are comprised predominantly of small particles with peak particle diameters ranging from 30 nm to 50 nm, with higher concentrations for the DMA and RMG-380 fuels. The PSDs for the DMA and RMB-30 fuels at the 75% load points are dominated by accumulation mode particles, with peak particle diameters ranging from 90 nm to 110 nm. The PSD for the RMG-380 fuel at the 75% load point was bimodal, showing an accumulation mode peak along with a smaller peak ranging from 30 nm to 70 nm in diameter.

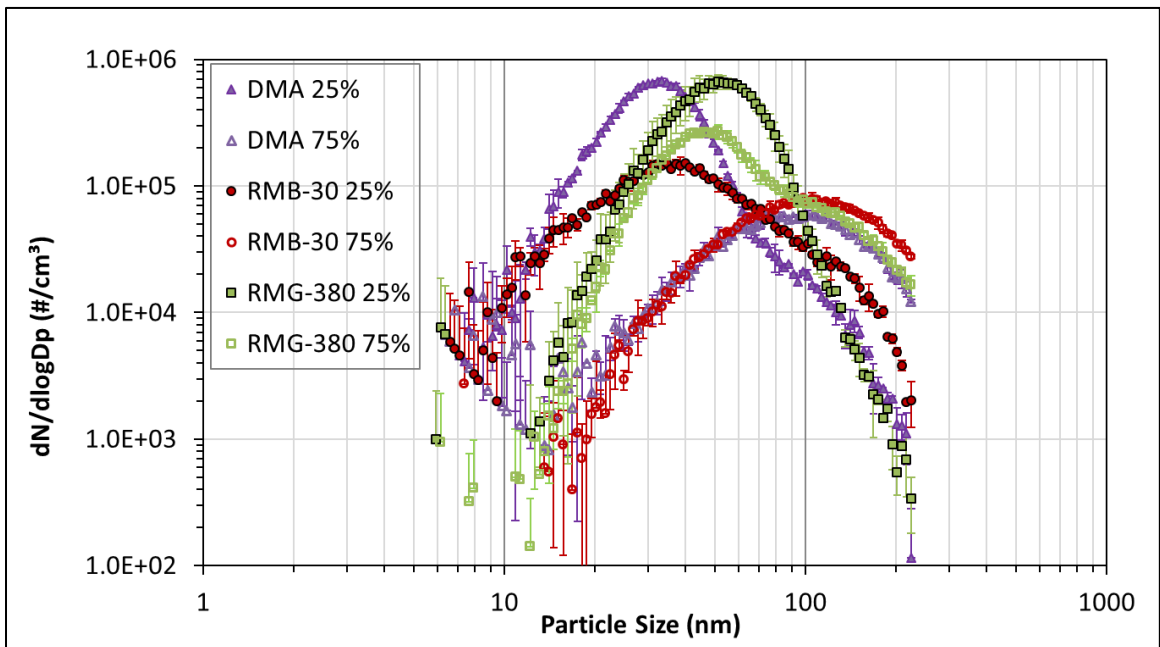


Figure 5-6 Particle Size Distributions for Various Engine Loads and Fuels on a logarithmic scale

Bimodal PSDs for diesel engines burning HFO were observed in several studies, with peaks located in the accumulation mode (0.1-1 μm) and in the coarse mode (1-5 μm)

(e.g., Linak et al., 2000). Since this SMPS measured only up to a diameter of 225 nm, only a single accumulation mode peak, with diameters ranging from 30 nm to 110 nm, could be observed in this study. These values are consistent with the peak diameters of 40 nm - 100 nm previously published (Murphy et al., 2009; Linak et al., 2000; Espinoza, 2014).

The PSDs of the DMA, RMB-30, and RMG-380 at the 25% load had higher number concentrations than at the 75% load. These PSDs at the 25% load had a more pronounced nucleation mode than observed for the 75% load. The PSDs for the RMG-380 at the 75% load showed a bimodal structure and that was shifted toward bigger particles compared to the 25% load, because formation of accumulation mode particles was facilitated as the engine load went up. At the 25% load, a nucleation mode below about 25 nm can be observed, presumably predominantly nucleated by sulfuric acid particles followed by condensation of organics (Lack et al., 2009b). Since the BC mass also increases with engine load, we can infer that the particles in the larger mode include BC particles.

PSD data for LSHFO is scarce in the literature, however, one study conducted by Gysel et al. (2017) measured PSDs from a crude carrier using both RMB-30 and marine gas oil (MGO) in a medium speed 4-stroke diesel engine. The results showed a peak diameter of around 30 nm to 50 nm for RMB-30 and around 20 nm for the MGO, which agrees with the results at the 25% load points in this study. However, the PSDs at the 75% load for the two fuels in the current study showed larger peak diameters than in Gysel et al. (2017). The PSDs of unburned HFO should be larger than 0.5 μm , while the smaller ultrafine mode ($\sim 0.1 \mu\text{m}$) observed in the current study may be due to more efficiently burned HFO (Linak et al., 2000).

5.5. Conclusions and Implications

This study investigated the impacts of measurement method, fuel type, and engine load on BC emission factors from a high-speed, 2-stroke small marine engine operated at two load points with three marine fuels. Six BC analytical methods with different measurement principles were used and the BC emission factors ranged from 0.05 to 1.84 g/kg fuel based on the PAS method for three different fuels and test modes. The instruments all showed increases in BC concentrations at higher loads. At each test point measured values from the different instruments were plotted against values measured with the PAS, and the results showed a good correlation with R^2 values >0.95 . The slope of the regression plots against the PAS values ranged from 0.57 to 1.30, with the slopes being >1 for the FSN and LIIs and <1 for the TOAs and ambient instruments (i.e., MAAP and Aethalometer). The response of the instruments relative to each other was similar after changing fuels, except for a few instruments. This work also provided important information on instrument performance that was subsequently used to plan real-world tests of two OGVs with large, 2-stroke, slow-speed diesel engines, that will be presented elsewhere.

A key finding in this research is that the variations in BC measurement methods, cannot account for the ten-fold range of BC emission factors reported in the literature. As such, other factors, such as engine load, selected fuel properties, and engine characteristics, likely contribute to the large variations in BC emission factors. Load, in particular, had an important impact for this older, small, high-speed engine, with increases greater than a factor of 10 in BC emission factors seen in going from 25% to 75% loads. The observation

of large differences in BC emission factors as a function of load has also been seen in a wider range of studies in the literature, albeit showing trends of higher emissions at lower loads, opposite to the trends seen for the particular engine in this study.

While this study provided important information about the relationship between fuel properties and BC emissions, future studies are needed and should investigate other fuel parameters as well as the combustion processes associated with engines more typically used in modern ocean going vessels. The results do suggest that the use of distillate fuels reduces BC emissions from marine vessels, as distillate fuels generally had lower black carbon emissions. The conventional HFO showed higher emissions than the DMA fuel at the 75% load, similar to the results found in the Lack and Corbett (2012) review of a wider range of studies, but not at the lower 25% load point. The new, low-sulfur residual fuel had the highest BC emissions factor of the three fuels tested, which raises questions as to what the BC emission factors will be when an intermediate fuel oil is made by blending this stream to control sulfur levels. More data need to be collected to ensure that the lower sulfur limits set for fuels lower both sulfur oxides and PM levels as intended in the IMO regulation. Interestingly, the trends in BC emissions did not show consistent trends as a function of some of the most important fuel properties, including sulfur content, viscosity, carbon residue, or the Calculated Carbon Aromaticity Index, so more research is needed to ferret out the primary parameters driving BC production.

The differences in BC emissions as a function of load and fuel type suggest that attention must be given to these parameters in developing test protocols for measuring BC emissions on ocean going vessels. It also suggests that models of marine BC emissions

need to incorporate a broader range of BC emissions factors to account for the range of fuels and loads found in typical in-use operation of marine vessels.

5.6. Acknowledgements

The authors thank the following organizations and individuals for their valuable contributions to this project. We acknowledge funding from the International Council on Clean Transportation. Yue Lin was funded by NSF grant #1233038. We acknowledge the participation of Dr. Gavin McMeeking from Handix Scientific, LLC, and Dr. John Koupal from Eastern Research Group in this program. We acknowledge Dr. Roya Bahreini, Mr. Don Pacocha, Mr. Eddie O'Neal, Mr. Mark Villela, Dr. Lindsay Hatch, Mr. Justin Hernandez Dingle, Mr. Daniel Gomez and Ms. Lauren Aycock of the University of California, Riverside and Mr. David Buote from Environment and Climate Change Canada for their contributions in conducting the emissions testing for this program. We acknowledge AVL for providing the Smoke Meter, the South Coast Air Quality Management District for providing the Aethalometer, and the California Air Resources Board for providing the EEPS.

- Chan, T.W., Brook, J.R., Smallwood, G.J., Lu, G. 2011. Time-resolved measurements of black carbon light absorption enhancement in urban and near-urban locations of southern Ontario, Canada. *Atmos. Chem. Phys.* 11, 10407-10432.
- CIMAC - International Council on Combustion Engines. 2012. Background information on black carbon emissions from large marine and stationary diesel engines-definition, measurement methods, emission factors and abatement technologies, Main, Germany, http://www.cimac.com/cms/upload/workinggroups/WG5/black_carbon.pdf (access 16.12.15).
- Comer, B., Olmer, N., Mao, X., Roy, B., Rutherford, D. 2017. Prevalence of heavy fuel oil and black carbon in Arctic Shipping, 2015 to 2025. The International Council on Clean Transportation (ICCT): Washington, DC, http://www.theicct.org/sites/default/files/publications/HFO-Arctic_ICCT_Report_01052017_vF.pdf (access 17.06.15).
- Comer, B., Olmer, N.S., Mao, X., Roy, B., Rutherford, D. Black carbon emissions and fuel use in global shipping. ICCT, Washington, DC, In Press.
- Corbett, J.J., Winebrake, J.J., Green, E.H., Kasibhatla, P., Eyring, V., Lauer, A. 2007. Mortality from ship emissions: a global assessment. *Environ. Sci. Technol.* 41, 8512-8518.
- Corbett, J.J., Winebrake, J.J., Green, E.H., 2010a. An assessment of technologies for reducing regional short-lived climate forcers emitted by ships with implications for Arctic shipping. *Carbon Manage.* 1, 207-225.
- Corbett, J.J., Lack, D. A., Winebrake, J.J., Harder, S., Silberman, J.A., Gold, M., 2010b. Arctic shipping emissions inventories and future scenarios. *Atmos. Chem. Phys.* 10, 9689-9704.
- Durbin, T.D., Johnson, K., Cocker, D.R., Miller, J.W., Maldonado, H., Shah, A., Ensfield, C., Weaver, C., Akard, M., Harvey, N., Symon, J., 2007. Evaluation and comparison of portable emissions measurement systems and federal reference methods for emissions from a back-up generator and a diesel truck operated on a chassis dynamometer. *Environ. Sci. Technol.* 41, 6199-6204.
- Espinoza, C. 2014. Particle Emissions From Vehicles (SI-PFI and SI-DI) at High Speed and From Large Ocean-Going Vessels, Masters Thesis, University of California at Riverside, College of Engineering, Department of Chemical and Environmental Engineering, December.
- Eyring, V., Köhler, H.W., Van Aardenne, J., Lauer, A. 2005. Emissions from international shipping: 1. The last 50 years. *J. Geophys. Res.* 110, D17305.

- Fuglestad, J., Berntsen, T., Myhre, G., Rypdal, K., Skeie, R.B., 2008. Climate forcing from the transport sectors. *Proc. Natl. Acad. Sci. U.S.A.* 105, 454-458.
- Gysel, N.R., Welch, W.A., Johnson, K., Miller, W., Cocker III, D.R., 2017. Detailed Analysis of Criteria and Particle Emissions from a Very Large Crude Carrier Using a Novel ECA Fuel. *Environ. Sci. Technol.* 51, 1868-1875.
- Kanaya, Y., Komazaki, Y., Pochanart, P., Liu, Y., Akimoto, H., Gao, J., Wang, T., Wang, Z., 2008. Mass concentrations of black carbon measured by four instruments in the middle of Central East China in June 2006. *Atmos. Chem. Phys.* 8, 7637-7649.
- KNOx, A., Evans, G.J., Brook, J.R., Yao, X., Jeong, C.H., Godri, K.J., Sabaliauskas, K., Slowik, J.G., 2009. Mass absorption cross-section of ambient black carbon aerosol in relation to chemical age. *Aerosol Sci. Technol.* 43, 522-532.
- Hyvärinen, A.P., Vakkari, V., Laakso, L., Hooda, R.K., Sharma, V.P., Panwar, T.S., Beukes, J.P., Van Zyl, P.G., Josipovic, M., Garland, R.M., Andreae, M. O. 2013. Correction for a measurement artifact of the Multi-Angle Absorption Photometer (MAAP) at high black carbon mass concentration levels. *Atmos. Meas. Tech.* 6, 81-90.
- International Organization for Standardization (ISO). 1996. ISO8178-2, Reciprocating Internal Combustion Engines: Exhaust Emission Measurement. Part-2: Measurement of Gaseous Particulate Exhaust Emissions at Site, ISO: Geneva, Switzerland.
- International Organization for Standardization (ISO). 2016. Consideration of the Impact on the Arctic of Emissions of Black Carbon from International Shipping: Experience with MAAP measurements. Presented to the IMO, Sub-committee on Pollution Prevention and Response, 4th session, Agenda item 9, PPR 4/9/3, Finland, November, [https://edocs.imo.org/Final Documents/English/PPR 4-9-3 \(E\).docx](https://edocs.imo.org/Final Documents/English/PPR 4-9-3 (E).docx).
- International Maritime Organization (IMO) Website, 2017. [http://www.imo.org/en/OurWork/environment/pollutionprevention/airpollution/pages/sulphur-oxides-\(sox\)---regulation-14.aspx](http://www.imo.org/en/OurWork/environment/pollutionprevention/airpollution/pages/sulphur-oxides-(sox)---regulation-14.aspx) (access 17.05.10).
- Janssen, N.A., Hoek, G., Simic-Lawson, M., Fischer, P., Van Bree, L., Ten Brink, H., Keuken, M., Atkinson, R.W., Anderson, H.R., Brunekreef, B., Cassee, F. R. 2012. Black carbon as an additional indicator of the adverse health effects of airborne particles compared with PM₁₀ PM_{2.5}. *Environ. Health Perspect.* 119, 1691-1699.
- Khan, M.Y., Giordano, M., Gutierrez, J., Welch, W.A., Asa-Awuku, A., Miller, J.W., Cocker III, D.R. 2012. Benefits of two mitigation strategies for container vessels: cleaner engines and cleaner fuels. *Environ. Sci. Technol.* 46, 5049-5056.

- Lack, D. 2015. BC Measurement Overview, and Considerations for a Community Approach to Measurement. Presented at the 2nd Workshop on Marine Black Carbon Emissions. Utrecht, Netherlands, September.
- Lack, D., Lerner, B., Granier, C., Baynard, T., Lovejoy, E., Massoli, P., Ravishankara, A.R., Williams, E. 2008, Light absorbing carbon emissions from commercial shipping. *Geophys. Res. Lett.* 35, L13815.
- Lack, D.A., Cappa, C.D., Langridge, J., Bahreini, R., Buffaloe, G., Brock, C., Cerully, K., Coffman, D., Hayden, K., Holloway, J., Lerner, B., 2011. Impact of fuel quality regulation and speed reductions on shipping emissions: implications for climate and air quality. *Environ. Sci. Technol.* 45, 9052-9060.
- Lack, D.A., Corbett, J.J., 2012. Black carbon from ships: a review of the effects of ship speed, fuel quality and exhaust gas scrubbing. *Atmos. Chem. Phys.* 12, 3985-4000.
- Lewan, M.D. 1984. Factors controlling the proportionality of vanadium to nickel in crude oils. *Geochim. Cosmochim. Acta.* 48, 2231-2238.
- LII 300 Brochure Website*, http://www.artium.com/wp-content/uploads/2017/01/II300_Brochure_Updates_v4.pdf (access 16.09.10).
- Linak, W.P., Miller, C.A., Wendt, J.O., 2000. Comparison of particle size distributions and elemental partitioning from the combustion of pulverized coal and residual fuel oil. *J. Air Waste Manage. Assoc.* 50, 1532-1544.
- MSS 483 Website, <https://www.avl.com/-/mssplus-avl-micro-soot-sensor> (access 18.02.10).
- Multi Angle Absorption Photometer (MAAP) Instruction Manual 5012 Website, 2016. <https://tools.thermofisher.com/content/sfs/manuals/EPM-manual-Model%205012%20MAAP.pdf> (access 16.09.10).
- Murphy, S.M., Agrawal, H., Sorooshian, A., Padró, L.T., Gates, H., Hersey, S., Welch, W.A., Jung, H., Miller, J.W., Cocker III, D.R., Nenes, A., 2009. Comprehensive simultaneous shipboard and airborne characterization of exhaust from a modern container ship at sea. *Environ. Sci. Technol.* 43, 4626-4640.
- Nukiyama, S., and Tanasawa, Y., 1938. An Experiment on the Atomization of Liquid by means of an Air Stream (1. Report), *Transactions of the Japan Society of Mechanical Engineers*, 4 (14), 128-135, <https://doi.org/10.1299/kikai1938.4.128>.
- Peters, G.P., Nilssen, T.B., Lindholt, L., Eide, M.S., Glomsrod, S., Eide, L.I., Fuglestedt, J.S., 2011. Future emissions from shipping and petroleum activities in the Arctic. *Atmos. Chem. Phys.* 11, 5305-5320.

- Petzold, A., Schönlinner, M., 2004. Multi-angle absorption photometry—a new method for the measurement of aerosol light absorption and atmospheric black carbon. *J. of Aerosol Sci.* 35, 421-441.
- Petzold, A., Ogren, J.A., Fiebig, M., Laj, P., Li, S.M., Baltensperger, U., Holzer-Popp, T., Kinne, S., Pappalardo, G., Sugimoto, N., Wehrli, C., 2013. Recommendations for reporting "black carbon" measurements. *Atmos. Chem. Phys.* 13, 8365-8379.
- SAE Aerospace Information Report 6241, 2013. Procedure for the Continuous Sampling and Measurement of Non-Volatile Particle Emissions from Aircraft Turbine Engines, SAE International: Warrendale, PA, USA, <https://saemobilus.sae.org/content/air6241>.
- SAE Aerospace Recommended Practice 1179 Rev D, 2011. Aircraft Gas Turbine Engine Exhaust Smoke Measurement, SAE International, Warrendale, PA, USA, <https://saemobilus.sae.org/content/arp1179>.
- Sand, M., Berntsen, T.K., Seland, Ø., Kristjánsson, J.E., 2013. Arctic surface temperature change to emissions of black carbon within Arctic or midlatitudes. *J. Geophys. Res.: Atmos.* 118, 7788-7798.
- Sarvi, A., Fogelholm, C.J. and Zevenhoven, R., 2008. Emissions from large-scale medium-speed diesel engines: 2. Influence of fuel type and operating mode. *Fuel processing technology*, 89(5), 520-527.
- Shin, W.G., Mulholland, G.W., Kim, S.C., Pui, D.Y.H., 2008. Experimental study of filtration efficiency of nanoparticles below 20 nm at elevated temperatures. *J. Aerosol Science* 39, 488 – 499.
- Sippula, O., Stengel, B., Sklorz, M., Streibel, T., Rabe, R., Orasche, J., Lintelmann, J., Michalke, B., Abbaszade, G., Radischat, C., Groger, T., 2014. Particle emissions from a marine engine: chemical composition and aromatic emission profiles under various operating conditions. *Environ. Sci. Technol.* 48, 11721-11729.
- Smoke Meter Website, <https://www.avl.com/-/avl-smoke-meter> (access 18.02.10).
- TOA-ES website: <http://www.sunlab.com/lab-oc-ec-aerosol-analyzer/>(access 18.02.10).
- TOA-SC website: <http://www.sunlab.com/model-4-semi-continuous-oc-ec-field-analyzer/>(access 18.02.10).
- U.S. Environmental Protection Agency (EPA) Website, 2016. <https://nepis.epa.gov/Exe/ZyPDF.cgi/P100EG0X.PDF?Dockkey=P100EG0X.PDF> (access 16.07.10).
- Wall, J.C., Shimpi, S.A., Yu, M.L. 1988. Fuel sulfur reduction for control of diesel particulate emissions. SAE Tech. Pap. No. 872139. DOI: 10.4271/2006-11- 872139.

- Weingartner, E., Saathoff, H., Schnaiter, M., Streit, N., Bitnar, B., Baltensperger, U., 2003. Absorption of light by soot particles: determination of the absorption coefficient by means of aethalometers. *J. of Aerosol Sci.* 34, 1445-1463.
- Winebrake, J.J., Corbett, J.J., Green, E.H., Lauer, A., Eyring, V. 2009. Mitigating the health impacts of pollution from oceangoing shipping: an assessment of low-sulfur fuel mandates. *Environ. Sci. Technol.* 43, 4776-4782.
- Winther, M., Christensen, J.H., Plejdrup, M.S., Ravn, E.S., Ericsson, O.F., Kristensen, H.O. 2014. Emission inventories for ships in the Arctic based on satellite sampled AIS data. *Atmos. Environ.* 91, 1-14.

5.8. Supporting Information

Table S1: Summary of Engine Operating Conditions for the Test Matrix

Fuel	Load	Engine speed (rpm)	Torque (Nm)	Fuel rate (kg/hr)
DMA	25%	1100	167	10.6
	75%	1100	438	22.4
RMB-30	25%	1100	161	10.3
	75%	1100	438	22.4
RMG-380	25%	1100	146	9.3
	75%	1100	469	23.7

Dilution impact on BC measurements. Since BC instrument comparisons section directly compared results from different dilution levels, it is important to prove that emissions were practically identical at different levels and dilution did not introduce significant errors. Figure S-3 shows the comparisons of BC mass concentrations measured by the same instruments (one FSN with two probes and two LIIs) at different dilution levels. The two FSN probes measured almost identical values at different sample locations with a slope of 1. Figure S-3a shows that the LII #2 with 14:1 dilution measured a little higher, but no significant difference, than the LII #3 with 1:1 dilution. Thus, based on the analysis above, BC emissions measured by the same instruments, but at different stages, were consistent and close enough, which allow the direct comparison of different instruments.

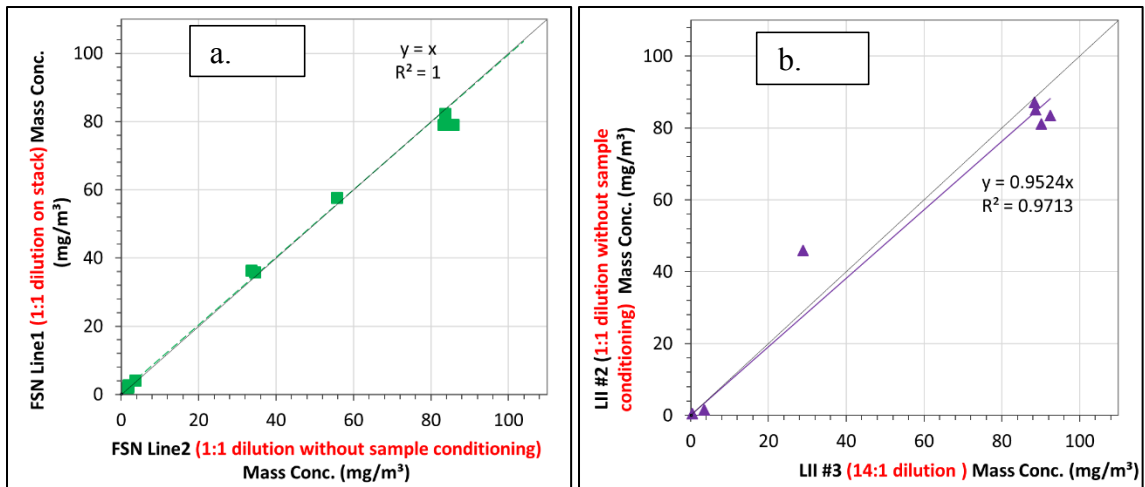


Figure S2: Comparison of the Same Instruments (one FSN with two probes and two LILs) at Different Dilution Levels

Additional BC and Gaseous Emissions Data. Additional information on BC and

NOx emissions is provided in this section. This includes a summary of NOx emissions factors on a g/kg-fuel basis in Table S2, BC emission mass concentrations (g/cm^3) in Table S3, BC emission factors (g/kg fuel) in Table S4, BC emission factors (g/kWh) in Table S5, and plots of BC mass concentrations (g/cm^3) at 25% and 75% load in Figures S4 (a) and (b).

Table S2: Summary of NO_x Emissions Factors on a g/kg-fuel Basis

Fuel	Load	NO _x (g/kg-fuel)
DMA	25%	66.0 ± 1.4
	75%	66.1 ± 0.5
RMB-30	25%	60.1 ± 1.3
	75%	61.4 ± 0.8
RMG-380	25%	n/a
	75%	49.9 ± n/a

Table S3: Summary of BC Emission Mass Concentrations (mg/cm³)

Fuel	Load (%)	On Stack			Group DF 1:1		Group DF 14:1
		FSN line 1		LII #1	FSN line 2		LII #2
DMA	25	2.0 ± 0.0	1.2 ± 0.1	1.8 ± 0.1	0.1 ± 0.0	1.5 ± 0.1	
	75	36.0 ± 0.3	17.8 ± 0.3	34.2 ± 0.7	35.9 ± 0.3	30.0 ± 1.3	
RMB-30	25	4.1 ± 0.0	n/a	3.7 ± 0.0	1.5 ± 0.0	3.9 ± 0.1	
	75	80.0 ± 1.9	n/a	84.3 ± 1.4	83.3 ± 2.0	66.2 ± 2.5	
RMG-380	25	2.7 ± 0.0	n/a	2.0 ± 0.0	0.4 ± 0.0	1.0 ± 0.0	
	75	84.5 ± 38.0	n/a	79.8 ± 34.0	66.6 ± 29.2	54.9 ± 34.5	
Fuel	Load (%)	Group DF 14:1			Group DF 1400:1		
		TOA-ES	TOA-SC	LII #3	MAAP	Aethalometer	
DMA	25	1.2 ± 0.0	1.3 ± 0.0	n/a	4.0 ± 0.1	4.9 ± 0.7	
	75	22.8 ± 1.6	27.5 ± n/a	n/a	19.1 ± 0.5	34.5 ± 3.1	
RMB-30	25	3.1 ± 0.1	3.1 ± 0.0	3.5 ± 0.1	6.1 ± 0.1	5.0 ± 0.5	
	75	41.1 ± 0.6	59.5 ± 1.3	90.4 ± 2.0	42.2 ± 2.7	49.0 ± 8.8	
RMG-380	25	0.8 ± 0.1	1.4 ± n/a	0.5 ± n/a	4.2 ± n/a	4.4 ± 1.1	
	75	40.3 ± 23.6	45.9 ± 32.5	58.6 ± 42.0	47.0 ± n/a	41.4 ± 6.1	

Table S4: Summary of BC Emission Factors (g/kg fuel)

Fuel	Load (%)	On Stack		Group DF 1:1		Group DF 14:1
		FSN line 1	LII #1	FSN line 2	LII #2	PAS
DMA	25	0.12 ± 0.00	0.07 ± 0.00	0.11 ± 0.00	0.06 ± 0.00	0.09 ± 0.00
	75	1.01 ± 0.01	0.50 ± 0.01	0.96 ± 0.02	1.01 ± 0.01	0.84 ± 0.04
RMB-30	25	0.27 ± 0.00	n/a	0.25 ± 0.00	0.10 ± 0.00	0.26 ± 0.01
	75	2.22 ± 0.05	n/a	2.34 ± 0.04	2.31 ± 0.05	1.84 ± 0.07
RMG-380	25	0.12 ± 0.01	n/a	0.10 ± 0.01	0.02 ± 0.00	0.05 ± 0.01
	75	1.60 ± 0.68	n/a	1.51 ± 0.61	1.26 ± 0.52	1.04 ± 0.63
Fuel	Load (%)	Group DF 14:1			Group DF 1400:1	
		TOA-ES	TOA-SC	LII #3	MAAP	Aethalometer
DMA	25	0.07 ± 0.00	0.08 ± 0.00	n/a	0.24 ± 0.01	0.29 ± 0.05
	75	0.64 ± 0.04	0.77 ± n/a	n/a	0.54 ± 0.01	1.14 ± 0.04
RMB-30	25	0.20 ± 0.01	0.21 ± 0.00	0.23 ± 0.01	0.40 ± 0.01	0.31 ± 0.03
	75	1.14 ± 0.04	1.65 ± 0.04	2.51 ± 0.06	1.17 ± 0.08	1.73 ± 0.24
RMG-380	25	0.04 ± 0.01	0.03 ± n/a	0.02 ± n/a	0.22 ± n/a	0.14 ± 0.05
	75	0.76 ± 0.43	0.87 ± 0.60	1.11 ± 0.77	0.88 ± n/a	1.05 ± 0.17

Table S5: Summary of BC Emission Factors (g/kWh)

Fuel	Load (%)	On Stack		Group DF 1:1		Group DF 14:1	
		FSN line 1	LII #1	FSN line 2	LII #2	PAS	
DMA	25	0.05 ± 0.00	0.03 ± 0.00	0.04 ± 0.00	0.02 ± 0.00	0.04 ± 0.00	
	75	0.34 ± 0.00	0.17 ± 0.00	0.32 ± 0.01	0.34 ± 0.00	0.28 ± 0.01	
RMB-30	25	0.11 ± 0.00	n/a	0.10 ± 0.00	0.04 ± 0.00	0.11 ± 0.00	
	75	0.74 ± 0.02	n/a	0.78 ± 0.01	0.77 ± 0.02	0.61 ± 0.02	
RMG-380	25	0.05 ± 0.00	n/a	0.04 ± 0.00	0.01 ± 0.00	0.02 ± 0.00	
	75	0.52 ± 0.22	n/a	0.49 ± 0.19	0.41 ± 0.16	0.34 ± 0.20	
Fuel	Load (%)	Group DF 14:1			Group DF 1400:1		
		TOA-ES	TOA-SC	LII #3	MAAP	Aethalometer	
DMA	25	0.03 ± 0.00	0.03 ± 0.00	n/a	0.10 ± 0.00	0.12 ± 0.02	
	75	0.21 ± 0.01	0.26 ± n/a	n/a	0.18 ± 0.00	0.38 ± 0.01	
RMB-30	25	0.08 ± 0.00	0.09 ± 0.00	0.10 ± 0.00	0.17 ± 0.00	0.13 ± 0.01	
	75	0.38 ± 0.01	0.55 ± 0.01	0.83 ± 0.02	0.39 ± 0.03	0.57 ± 0.08	
RMG-380	25	0.02 ± 0.00	0.01 ± n/a	0.01 ± n/a	0.09 ± n/a	0.06 ± 0.02	
	75	0.25 ± 0.14	0.28 ± 0.19	0.36 ± 0.25	0.28 ± n/a	0.34 ± 0.05	

Statistical Analysis for BC Emissions for the Load, Fuel, and Instrument

Factors. Statistical analyses between the factors of instruments, loads and fuels were performed using analysis of variance (ANOVA) methods. The ANOVA analyses were initially performed using only the primary factors, with the results provided in table S6. The results of the primary analyses in Table S6 show statistically significant differences in BC emission factors for both fuels and loads at greater than a 95% confidence level, with p-values below 0.05 for both factors. These differences are discussed in greater detail in the BC Emissions Factors section in the main text. The primary statistical analysis for the instrument comparisons showed a p-value of 0.117, which is slightly outside of the 0.1 value needed for statistical significance at the 90% confidence. Level.

Table S6: ANOVA testing results

Source	DF	Seq SS	Seq MS	F-Value	P-Value
Instruments	9	1.568	0.1742	1.71	0.117
Fuels	2	3.007	1.5035	14.79	0.000
Loads	1	17.031	17.0311	167.50	0.000
Error	41	4.169	0.1017		
Total	53	25.775			

A second ANOVA analysis was conducted using the primary factors of instruments, loads, and fuels, but also including an instrument by load interaction term. These results are presented in Table S7. This ANOVA analysis similarly shows that there are statistically significant differences in BC emissions as a function of load ($p=0.041$), as discussed in the BC Emission Factors section. The results also showed that statistically

significant interactions for instruments with load and for fuels with load, indicating that the differences between instruments varied as a function of different loads. The differences in fuels are discussed in greater detail in the BC Emissions Factor section.

Table S7: ANOVA testing results

Source	DF	Seq SS	Contribution	Adj SS	Seq MS	F-Value	P-Value
Instrument	9	1.568	6.08%	1.106	0.174	1.01	0.486
Load	1	17.031	66.08%	14.821	17.031	14.99	0.041
Fuel	2	3.007	11.67%	3.007	1.504	1.59	0.387
Fuel* Load	2	2.011	7.80%	1.630	1.005	33.77	0.000
Instrument*Load	9	1.370	5.32%	1.370	0.152	5.79	0.000
Error	30	0.079	3.06%	0.788	0.026		
Total	53	25.775	100.00%				

The differences in BC emission factors for different fuel and instruments were further examined with pairwise t-tests. The t-test results for the different fuels at the 25% and 75% load points are shown in Table S8 (a) and (b). The t-tests show statistically significant differences between fuels at both the 25% and 75% load points, but with different trends at the different load points, with the BC concentrations for the DMA being higher than that for the RMG-380 at the 75% load, while the BC concentrations for the RMG-380 fuel is slightly higher than that for the DMA at the 25% load. The trends between fuels are discussed in greater detail in the BC Emissions Factor section.

The t-test results for the instruments at the 25% and 75% load points are shown in Table S9 (a) and (b) using the PAS as the primary instrument for comparison. The t-tests show statistically significant differences between instruments at both the 25% and 75%

load points, but with different trends at the different load points. These results are discussed in greater detail in the BC Instrument Comparisons section.

Table S8a t-test Comparisons between Fuels at the 25% Load Point

	DMA 25%	RMB-30 25%	RMG-380 25%
FSN line 1	1.96	4.10	2.67
FSN line 2	1.81	3.75	1.97
LII #2	0.08	1.52	0.43
PAS	1.49	3.92	1.01
TOA-ES	1.17	3.08	0.81
TOA-SC	1.32	3.14	1.36
LII #3		3.52	0.49
MAAP	4.00	6.15	4.17
Aethalometer	4.91	5.05	4.36
average	2.09	3.80	1.92
P-Value (DMA vs RMB-30)	0.00		
P-Value (RMG 380 vs RMB-30)		0.00	
P-Value (RMG 380 vs DMA)	0.00		

Table S8b t-test Comparisons between Fuels at the 75% Load Point

	DMA 75%	RMB-30 75%	RMG-380 75%
FSN line 1	35.96	80.03	84.53
FSN line 2	34.17	84.26	79.79
LII #2	35.93	83.25	66.58
PAS	30.02	66.23	54.86
TOA-ES	22.78	41.08	40.30
TOA-SC	27.48	59.48	45.93
LII #3		90.44	58.63
MAAP	19.09	42.23	46.96
Aethalometer	34.50	48.95	41.41
average	29.99	66.22	57.66
P-Value (DMA vs RMB-30)	0.00		
P-Value (RMG 380 vs RMB-30)		0.06	
P-Value (RMG 380 vs DMA)	0.00		

Table S9 (a) t-test Comparisons between Instruments at the 25% Load Point

	load	DMA		RMB-30		RMG-380		P-Value	AVE
Aethalometer	25%	5.40	4.42	5.41	4.69	3.62	5.10	0.00	4.77
MAAP	25%	4.07	3.93	6.21	6.08		4.17	0.00	4.89
FSN line 1	25%	1.95	1.96	4.06	4.13	2.67	2.19	0.04	2.83
FSN line 2	25%	1.76	1.85	3.73	3.76	1.96	1.97	0.14	2.51
PAS	25%	1.45	1.53	3.99	3.85	0.99	1.03		2.14
LII #3	25%			3.59	3.45	0.49	0.46	0.00	2.00
TOA-SC	25%	1.29	1.34	3.15	3.13	2.18	0.55	0.53	1.94
TOA-ES	25%	1.19	1.16	3.13	3.03	0.71	0.91	0.02	1.69
LII #1	25%	1.18	1.25						1.21
LII #2	25%	0.94	0.99	1.52	1.52	0.43	0.44	0.03	0.97

Table S9 (b) t-test Comparisons between Instruments at the 75% Load Point

	load	DMA		RMG-380		RMB-30		P-Value	AVE	
LII #3	75%			28.92	88.35	90.17	88.62	92.52	0.04	77.72
FSN line 2	75%	33.67	34.67	55.75	103.83	83.60	85.88	83.29	0.00	74.50
FSN line 1	75%	36.18	35.74	57.65	111.40	82.19	78.94	78.95	0.01	74.15
LII #2	75%	35.70	36.15	45.95	87.21	81.19	85.06	83.51	0.00	69.84
Aethalometer	75%	41.54	39.55	62.41		67.70	52.61	66.72	0.30	57.80
PAS	75%	29.12	30.91	30.45	79.26	68.23	63.47	66.97		56.55
TOA-SC	75%		27.48	22.98	68.87	60.68	58.07	59.70	0.00	49.63
TOA-ES	75%	21.67	23.89	23.64	56.96	40.36	41.37	41.50	0.00	37.96
MAAP	75%	19.42	18.76	46.96		39.68	42.00	45.00	0.11	38.48
LII #1	75%	18.03	17.61							17.61

BC mass concentration presented in mass per volume units for the 25% load points

The graphs in this section show the lower concentration levels from Figure 4, which represent the 25% load points, in greater detail.

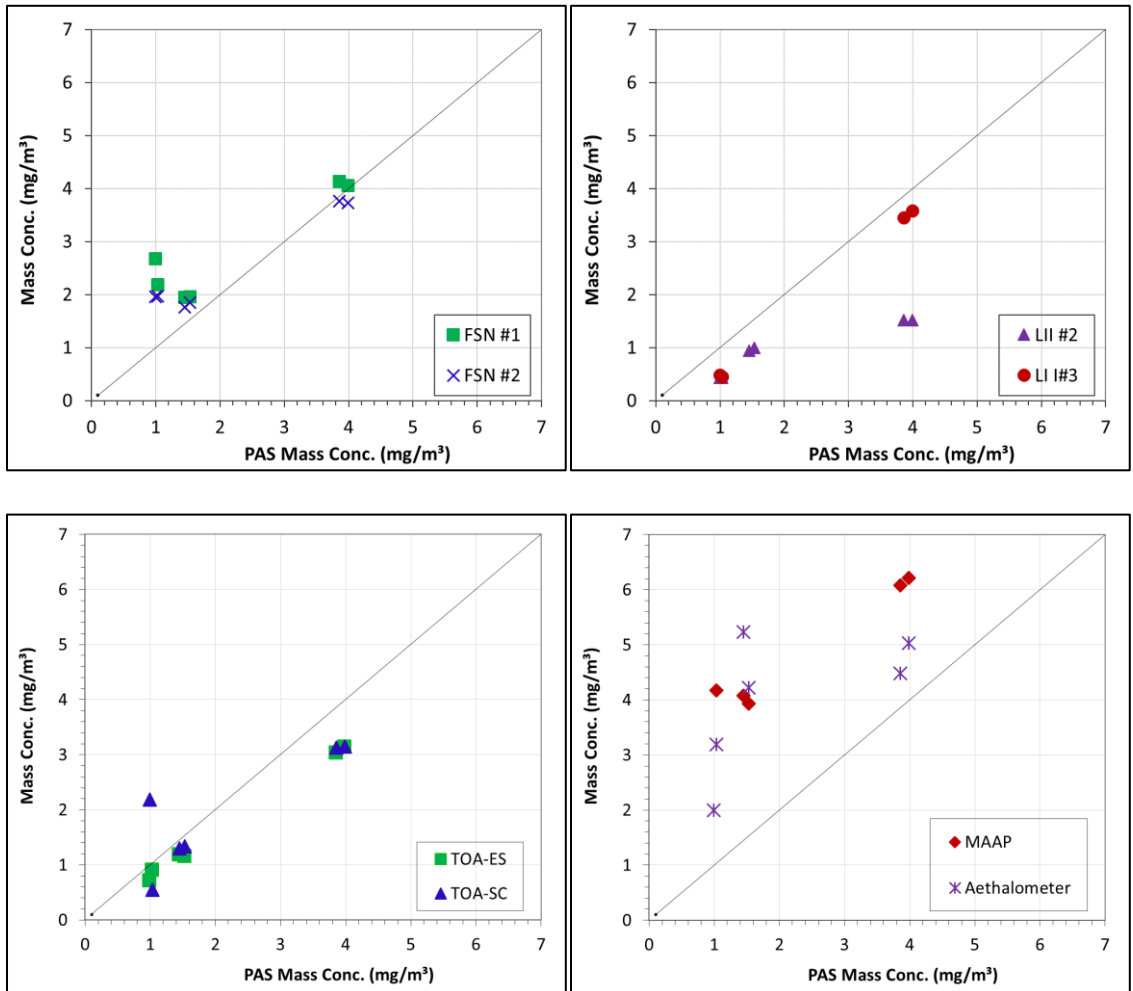


Figure S2: Various Instrument Responses with respect to PAS Mass Concentration at 25% load

6. Black Carbon Measurements from a Marine Engine with Various Fuels: Impacts of Sample Conditioning on Black Carbon Measurement Instruments

6.1. Abstract

This paper describes the impacts of measuring marine engine black carbon (BC) emissions with and without a catalytic stripper (CS) and sulfur absorber unit (S-absorber) sample conditioning (SC) system. The SC was designed to obtain a purer exhaust gas sample to limit interference from gases and non-BC particles. BC was measured using a range of different instruments from a 7 L marine engine with three marine fuels with varying sulfur contents. BC emission factors in the SC mode varied from approximately 0.03 g/kg fuel to 1.36 g/kg fuel based on the photoacoustic spectroscopy (PAS), which was comparable with factors found in the without SC mode, which ranged from 0.05 to 1.84 g/kg fuel. The SC eliminated over 90% of the sulfate for the high sulfur fuel, and between 74 and 95% of the OC for all the fuels, leaving particles composed primarily of EC. The regression analyses between PAS and other five BC methods with different measurement principles showed about with half the instruments below and half above the parity line. These results are similar to the results for the without SC mode, but generally showing a slightly greater spread. The morphology of the particles for the lower sulfur marine fuels for the SC mode showed less densely aggregated, more chain-like structures that appeared to be lighter in color compared to the without SC mode. A key finding in this

research is that the SC improved the comparability of some BC measurements, but only slightly.

6.2. Introduction

Marine vessels emit many types of air and climate pollutants, including black carbon (BC) that is both an air and a climate pollutant (Agrawal et al., 2008; Khan et al., 2012). BC is a distinct type of carbonaceous material that is formed in combustion processes where there is insufficient oxygen (Bond et al., 2013; Petzold et al., 2013). BC is one component of particulate matter (PM) pollution from ships, and it is a significant concern due to its adverse impacts on the air quality (Highwooda and Kinnersleyb, 2005; Janssen et al., 2011). BC can cause cardiovascular and chronic lung disease (Highwooda and Kinnersleyb, 2005; Jansen et al., 2005; Winebrake et al., 2009). Additionally, BC is a climate-warming pollutant that can have a direct warming effect as well as an indirect effect when interacting with clouds (Corbett et al., 2010).

Burning low quality fuels can generate large amounts of PM mass emissions from ships, particularly in the form of sulfates (Agrawal et al., 2008; Khan et al., 2012). This has led to requirements for lower sulfur fuels (LSFs) by the International Maritime Organization (IMO) in certain emissions control areas (ECAs) (IMO, 2008). However, it is still unclear whether LSFs can reduce ship-related BC emissions (Lack and Corbett, 2012; Lack et al., 2011; Buffaloe et al., 2014; CIMAC, 2012; Aakko-Salsa et al., 2016).

BC has the unique physical properties of being refractory up to 4,000K and being ideally light absorbing (Bond et al., 2013, Petzold et al., 2013). Based on these properties, BC can be quantified by using different measurements methods, including light absorption,

thermal radiation, and thermal evolution methods. The differences between these methodologies and instruments are believed to significantly contribute to the wide range of BC emission factors (0.1 g/kg fuel to 1 g/kg fuel) seen in the literature for marine vessels (CIMAC, 2012; Lack et al, 2008; Agrawal et al, 2008; Corbett et al, 2010). In a companion paper to this study, six different BC measurements showed agreement within 43% on average compared to a photoacoustic spectroscopy (PAS) instrument for a 2-stroke marine engine, suggesting that the differences in BC emission factors observed in the literature are probably due to other testing differences, such as engine load, sampling methods, operating conditions or fuels (Jiang et al., 2018). These results still suggest there was need to examine the effects of sample conditioning (SC) and the nature of particle coatings on BC measurements, which is the focus of this research.

One complication in quantifying BC concentrations is that the coatings on the BC particles can enhance the absorption signal (Bond et al., 1999). In general, the term “coatings” is used to refer to these additional compounds covering the BC particles (Schwarz et al., 2008). Some kinds of organic coatings, called brown carbon, also have light absorption ability, while some are non-absorbing particle (Lack and Cappa, 2010; Barnard et al., 2008). Both of these coating types can cause BC measurement uncertainties. The non-absorption particles coatings can enhance the light absorption of BC particles by 50~100% due to light that is refracting like a lens to the BC particles (Lack and Cappa, 2010; Lack, 2015; Bond et al., 2013; Fuller et al., 1999).

In contrast to light absorption techniques, laser-induced incandescence (LII) measures refractory materials to determine BC mass, which is sometimes referred to as

refractory BC (rBC). LII measurements were found to be independent of the characteristics of coatings (as, thickness or material) by several studies (Snelling et al., 2005; Slowik et al., 2007). For thermal-optical-analysis (TOA), which are used to quantify elemental carbon (EC), some studies have shown that coatings can contribute to the measurement uncertainties due to the misidentification of the coating as EC or by lowering the oxidation temperature of EC due to certain inorganic compositions of the coatings (Andreae and Gelencser, 2006; Sippula et al., 2014). However, Kondo et al. (2009) found that less than 10% of the difference in EC mass concentrations was caused by the coatings.

Since coatings contribute to variability in BC measurements, strategies that can be used to remove coatings from BC prior to measurement have been reported to yield better agreements between different BC measurement instruments (Bond et al., 2013; Knox et al., 2009; Kondo et al., 2009). Coatings can be removed using conditioning systems that can be based on evaporation, adsorption, or oxidation principles (Giechaskiel et al., 2014; Bond et al., 2013; Kondo et al., 2009). A thermodenuder is an example of a conditioning system that removes volatile material by heating up the particles and then absorbing the volatile vapors with activated charcoal (Swanson and Kittelson, 2010). A catalytic stripper (CS) is another type of conditioning system that can remove semi-volatile hydrocarbon compounds by catalytic reactions at elevated temperatures with much higher removal efficiencies compared to the conditioning systems based on evaporation or adsorption (Giechaskiel et al., 2014). For a CS, diffusion losses in the channels is the primary mechanism of particle loss (Swanson et al., 2013).

A SC unit, including a CS and two sulfur adsorbers, was designed and constructed for this project. The purpose of the SC was to remove as much of the co-emitted species as possible, yielding a BC particle nearly free of hydrocarbon and sulfurous coatings. This approach would likely achieve BC emissions measurements with a minimum of interference from coatings and allow a truer comparison of the various BC instruments. BC emissions were measured from a 2-stroke marine engine that burned three different marine fuels with varying sulfur content. The fuels included a low sulfur content distillate marine (DMA) and residual marine (RMB-30), and a high sulfur content residual marine (RMG-380). Testing was conducted at 25% and 75% load points with and without SC. A wide range of BC/PM measurement techniques were used to evaluate their measurement effectiveness. BC measurement techniques include: 1) light absorption, including photoacoustic spectroscopy (PAS) using a Micro Soot Sensor (MSS), filter smoke number (FSN) using an AVL 415SE-Smoke Meter, a light-absorption (LA)-Aetholameter and a LA-multi-angle absorption photometer (MAAP); 2) thermal radiation using laser induced incandescence (LII); 3) thermal-optical using integrated and continuous thermal-optical-analysis (TOA). PM measurement techniques are: 1) total PM mass using teflo filters with 47mm diameter 2 μ m pore; 2) particle morphology using a transmission electron microscopy (TEM); 3) particle size distribution using a scanning mobility particle sizer (SMPS). Comparisons were made between the results obtained with and without SC to evaluate the impacts of the SC on BC and other emissions, but only PM/BC is discussed.

6.3. Experimental Approach

6.3.1. Test Engine

The test engine was a 2-stroke 1976 Detroit Diesel Model 6-71N marine engine. The specifications of the engine are provided in the supporting information.

6.3.2. Test Fuels and Loads

Testing was conducted using the three fuels under different engine loads (25%, 50%, and 75%) with and without SC, and three different fuels representing commercially available marine fuels. The characteristics of the test fuels are provided in the supporting information. The effects of SC on BC measurements were investigated by running some tests with and without SC at the 25% and 75% engine load points. The results without SC are discussed in detail in a companion paper on characterizing marine BC measurements methods (Jiang et al., 2018). This paper focuses on the SC mode results in comparison with the without SC results.

6.3.3. Measurement Methods

6.3.3.1. Instruments

This study measured BC emissions using various instruments that employ different measurement principles associated with the unique properties of BC, including strong light absorption, refractory characteristics, and resistance to chemical reaction at normal temperatures (Bond et al., 2013). The instruments that were used and their measurement principles are listed in Table 6-1. Engine emissions were also measured by supporting instruments that were not designed to measure BC specifically, but were useful for providing a more detailed characterization of soot particles emitted. This enables a more

thorough comparison of BC measurement results across instruments. The particle properties they measured are listed in Table 6-2. This included a SPMS and a TEM.

Table 6-1 BC Measurement Instruments Principles

Instrument	Abbreviation	Model	Measurement Principle
Aethalometer	LA- Aethalometer	Magee Scientific AE21	light absorption and scattering
Laser Induced Incandescence	LII	Artium 300	thermal radiation
Multi Angle Absorption Photometer	LA-MAAP	Thermo Scientific 5012	light absorption and scattering
Micro Soot Sensor	PAS	AVL 483	light absorption (photoacoustic)
Semi continuous	TOA-Integrated or TOA- Continuous	Sunset Laboratory	thermal-optical
Smoke Meter	FSN Line 1 or FSN Line 2	AVL 415SE	light absorption

Table 6-2 BC Associated Measurement Principles

Instrument	Abbreviation	Model	Measured Property
Gravimetric PM	PM2.5	Teflon	Total PM mass < 2.5 μm
Scanning Mobility Particle Sizer	SMPS	TSI 3936	particle size distribution
Transmission Electron Microscopy	TEM	FHNW TEM Sampler	particle morphology

The SC unit used in this study included a CS and two sulfur adsorbers. The CS consists of three heated flow-through ceramic monoliths that have platinum and palladium-based washcoats. The operational temperature range is 350°C - 400°C and the maximum operating flow rate is 40 L/min (Swanson et al., 2013). The CS geometry is fixed though

the choice of cell density and physical dimensions, which impacts residence time (about 2s). For a fixed geometry, the operating temperature and flow rate dictate performance, although performance may vary depending on application. Lower flow rates increase the removal of semi-volatile material, but also increase particle losses (Swanson et al., 2013). The oxidation section is followed by two sulfur adsorbers that consist of flow-through ceramic monoliths containing barium. They are designed to capture gas phase SO₃ molecules resulting from the oxidation of SO₂ to SO₃ in the CS, and therefore they were located downstream of the CS. The sulfur absorbing system was operated at around 140°C (98°C to 192°C). When sampling in the without SC mode, the temperature was around 100°C prior to the primary dilution.

6.3.3.2. Experimental Layout

Figure 6-1 provides a graphical representation of the four instrument sampling locations and the measurement instruments at each location, as well as the layout for SC. The four sample locations represented raw exhaust on the stack, 1:1 dilution with and without SC, and 14:1 and 1400:1 dilution with and without SC.

catalyst efficiency could be due to several reasons. It is possible that there may be hydrocarbon adsorption/desorption from surfaces in the SC system or the sample lines downstream of the SC system. Some contribution of OC to the test runs in the SC mode, for example, could be due to desorption of OC that was previously adsorbed on system surfaces or the sample lines downstream of the SC system. The higher temperatures for the SC measurements could also volatilize OC that is not volatilized at the lower temperatures for the without SC measurements. It is also possible that the TOA method may have a residual positive organic artifact as well that makes it difficult to accurately measure the very low levels of OC found for the SC tests.

Another important consideration in sampling PM is the potential for line losses in the sampling system. As EC as measured with and without a SC at a 14:1 dilution ratio, an estimate of the measured system losses can be made. The resulting loss of EC mass based on MSS measurements is provided in Table 3. EC losses ranged from 23.8 to 39.7% depending on the test matrix point. Note that line losses would also be incorporated in the OC removal efficiency results. It is expected that thermophoretic losses that occurred as the sample cools downstream of the SC before measurement or dilution would be the primary source of particle losses (Mulholland, 1989). Diffusion is an additional particle loss mechanism that could also be considered. The results presented in this paper are not corrected for particles losses.

Table 6-3 Particle loss and SC removal efficiencies (based on TOA-Integrated)

Fuel	Load (%)	PM Loss (%)	OC Removal Efficiency (%)	BC Loss based on MSS (%)	Sulfate Removal Efficiency (%)
DMA	25	78.2	80.9	39.7	n/a
	75	53.4	77.6	36.8	n/a
RMB 30	25	89.0	94.7	23.8	n/a
	75	40.3	73.6	26.0	n/a
RMG 380	25	90.7	81.3	38.4	91.6

Note: DMA and RMB-30 were the LSHFO fuels, so the sulfate content wasn't measured in this study.

6.4.2. PM Emission Factors (g/kg fuel)

Figure 3 shows PM mass emission results collected using the SC system mode as well as those collected in a without SC mode on a g/kg fuel basis. The total OC is calculated by using a factor of 1.2 to multiply the OC mass measured by the TOA-Integrated (Shah et al., 2004). Overall, for the without SC mode measurements, a trend of decreasing PM mass as a function of increasing load was seen, with higher PM emissions at the 25% load for all three marine fuels compared to the 75% load. However, the measurements made with the SC showed a totally opposite trend, with higher PM emissions at the 75% load. There were also generally smaller differences in PM emissions between fuels for the SC mode at the same load point.

Figure 6-2 also provides the PM mass compositions. For the without SC mode, PM mass is dominated by organic and EC for the low sulfur fuels (DMA and RMB-30 fuels), and by sulfate for the high sulfur fuel (RMG-380). The PM mass results collected in the SC mode, however, show that OC and sulfate are largely eliminated going through the SC, leaving predominantly EC. EC mass, and correspondingly total PM mass both increase with increasing load for the SC measurements.

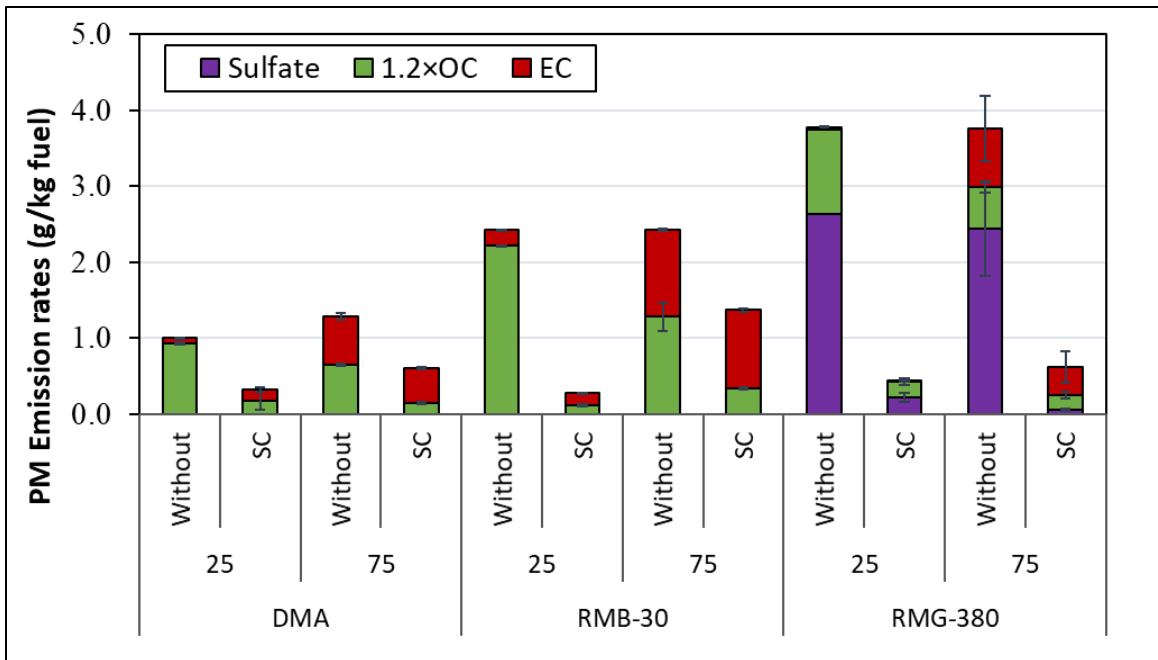


Figure 6-2 PM_{2.5} Composition (based on TOA-Integrated) on a percent of total PM mass basis

6.4.3. BC Emission Factors (g/kg fuel)

The BC emission factors on a g/kg fuel basis in the SC mode are presented based on the dilution at the sampling point in Table 6-4. The BC emission factors without SC are provided in the supporting information. BC emission rates based on the PAS measurements in the SC mode varied from 0.05 g/kg fuel to 0.53 g/kg fuel for the DMA fuel, from 0.20 g/kg fuel to 1.36 g/kg fuel for the RMB-30 fuel, and from 0.03 g/kg fuel to 0.46 g/kg fuel for the RMG-380 fuel. These values are on the same order of magnitude as seen in the literature (CIMAC, 2012; Lack et al, 2008; Agrawal et al, 2008; Corbett et al, 2010). Similar to the PM results in the without SC mode, an increasing trend of BC emission rates with increasing load was seen with the SC. The increasing BC emission factors with

increasing engine load for this naturally aspirated test engine could be due BC created in localized areas of rich combustion at higher loads. Large, turbocharged, in-service marine engines would be less susceptible to localized rich combustion, and hence, it is expected that they would show opposite trends, with lower BC emission factors at higher loads. The RMB-30 fuel, with the lowest sulfur, viscosity and residual carbon content, gave the highest BC emission rates, compared with other two fuels, followed by the RMG-380 fuel with the highest sulfur content. These data indicate that the BC emission factors with this engine and operating conditions were not a strong function of sulfur, viscosity and residual carbon content, as the lowest BC emission rates with the cleanest DMA fuel were similar to those of the dirtiest heavy-fuel oil, RMG-380. For the RMG-380 fuel, the lower BC emission rates could be due to certain metals from the crude that concentrated in the high sulfur fuel oil and that can oxidize part of the BC (Sippula et al., 2014). It was also noted that lower desorption temperatures were found for the RMG-380 fuel in the TOA measurements with some refractory residual left on the filters, which was consistent with the presence of metal oxides on the filter acting as a catalyst. Additional analyses of the refractory residual were not available, and further investigation is needed to better understand these results.

The FSN #1 smoke meter and LII #1 sampled directly from the raw exhaust without a conditioning system. Therefore, the results are not compared with other instruments. It is important to sample from the raw exhaust in order to evaluate the differences in the loads and combustion conditions between tests in the SC and without SC modes, as it is unlikely that complicated dilution systems will be regularly used on vessels when measuring BC.

Note that the LII #1 was only available for the DMA tests. The differences in the FSN #1 results for the without SC and SC modes were within 20% for the same fuel at the same load, except for the RMG 380 fuel at the 75% load, which indicated the relatively stable engine conditions between the without SC and SC tests.

Table 6-4 BC Emission Factors in the SC Mode for the Marine Engine on a g/kg fuel basis

Fuel	Load (%)	On Stack		Group DF 1:1		Group DF 14:1
		FSN line 1	LII #1	FSN line 2	LII #2	PAS
DMA	25	0.15 ± 0.01	0.07 ± 0.01	0.08 ± 0.01	0.05 ± 0.01	0.05 ± 0.00
	50	0.27 ± 0.01	0.18 ± 0.00	0.16 ± 0.00	0.11 ± 0.00	0.13 ± 0.00
	75	0.96 ± 0.01	0.56 ± 0.01	0.70 ± 0.01	0.80 ± 0.03	0.53 ± 0.00
RMB-30	25	0.31 ± 0.03	n/a	0.18 ± 0.01	0.10 ± 0.00	0.20 ± 0.01
	50	0.63 ± 0.01	n/a	0.49 ± 0.02	0.41 ± 0.01	0.42 ± 0.01
	75	2.10 ± 0.07	n/a	1.65 ± 0.06	1.90 ± 0.03	1.36 ± 0.02
RMG-380	25	0.10 ± 0.01	n/a	0.06 ± 0.01	0.02 ± 0.00	0.03 ± 0.00
	50	0.25 ± 0.01	n/a	0.18 ± 0.01	0.09 ± 0.00	0.14 ± 0.01
	75	1.20 ± 0.24	n/a	0.80 ± 0.11	1.13 ± 0.14	0.46 ± 0.05
Fuel	Load (%)	Group DF 14:1			Group DF 1400:1	
		TOA-Integrated	TOA-Continuous	LII #3	LA-MAAP	LA-Aethalometer
DMA	25	0.15 ± 0.13	0.05 ± 0.00	n/a	0.12 ± 0.01	0.18 ± 0.02
	50	0.10 ± 0.00	0.11 ± 0.00	n/a	0.27 ± 0.02	0.29 ± 0.01
	75	0.46 ± 0.02	0.47 ± n/a	n/a	0.29 ± 0.01	0.67 ± 0.05
RMB-30	25	0.16 ± 0.01	0.16 ± 0.00	0.27 ± 0.01	0.19 ± 0.00	0.26 ± 0.03
	50	0.34 ± 0.01	0.32 ± 0.01	0.58 ± 0.00	0.45 ± 0.01	0.46 ± 0.06
	75	1.03 ± 0.02	1.17 ± 0.05	2.06 ± 0.03	0.75 ± 0.12	1.01 ± 0.18
RMG-380	25	0.02 ± 0.00	0.04 ± 0.02	0.02 ± 0.00	0.16 ± 0.17	0.06 ± 0.03
	50	0.08 ± 0.01	0.13 ± 0.01	0.15 ± 0.02	0.38 ± 0.08	0.21 ± 0.04
	75	0.37 ± n/a	0.39 ± 0.07	0.58 ± 0.09	0.49 ± n/a	0.40 ± n/a

6.4.4. BC Instrument Correlations

Regression analyses between the various BC measurement methods and the PAS for the SC mode tests were carried out and results are in Table 6-5 and Figure 6-3. The PAS was utilized, as the reference it has undergone full compliance testing as part of the U.S. EPA's heavy-duty In-Use testing Measurement Allowance program (Johnson et al., 2011) and in the aviation industry (SAE, 2011, 2013). The results of regression analyses were similar to those for the without SC mode, with half of the instruments showing higher readings than PAS and half showing lower readings. One difference is the data for the SC mode showed more variance than that for the without SC mode. Nonetheless, the measured coefficient of determination, R^2 , for the regression analyses between the PAS and all instruments was ≥ 0.94 , except the LA-MAAP was 87%. The slopes for the FSN #2 and the TOA-Continuous, which were closest to the PAS, were 1.21 to 0.83, respectively, but data showed a greater variance compared with the results for the without SC mode (Jiang et al., 2018). The slope between the TOA-Integrated and the PAS was 0.74 for the SC mode, which is closer than the 0.65 slope seen for the without SC mode. Slopes of the LA-MAAP and LA-Aetholameter ranged from 0.50 to 0.69 lower than the PAS.

Table 6-5 Slopes and Intercepts of Instrument Response as a Function of PAS Mass Concentration

Instrument	Sample location	Slope		Intercept		R ²	
		SC	without SC	SC	without SC	SC	without SC
FSN line 2	DF 1:1	1.21	1.29	0.37	0.98	0.97	0.98
LII #2	DF 1:1	1.48	1.22	-0.46	-0.95	0.97	0.99
LII #3	DF 14:1	1.49	1.30	-1.74	-1.33	0.99	0.98
PAS	DF 14:1	-	-	-	-	-	-
TOA-Integrated	DF 14:1	0.74	0.65	0.88	0.32	0.99	0.98
TOA-Continuous	DF 14:1	0.83	0.89	-0.23	0.10	1.00	1.00
LA-MAAP	DF 1400:1	0.50	0.57	3.33	3.95	0.87	0.99
LA-Aethalometer	DF 1400:1	0.69	0.86	4.41	3.30	0.94	0.95

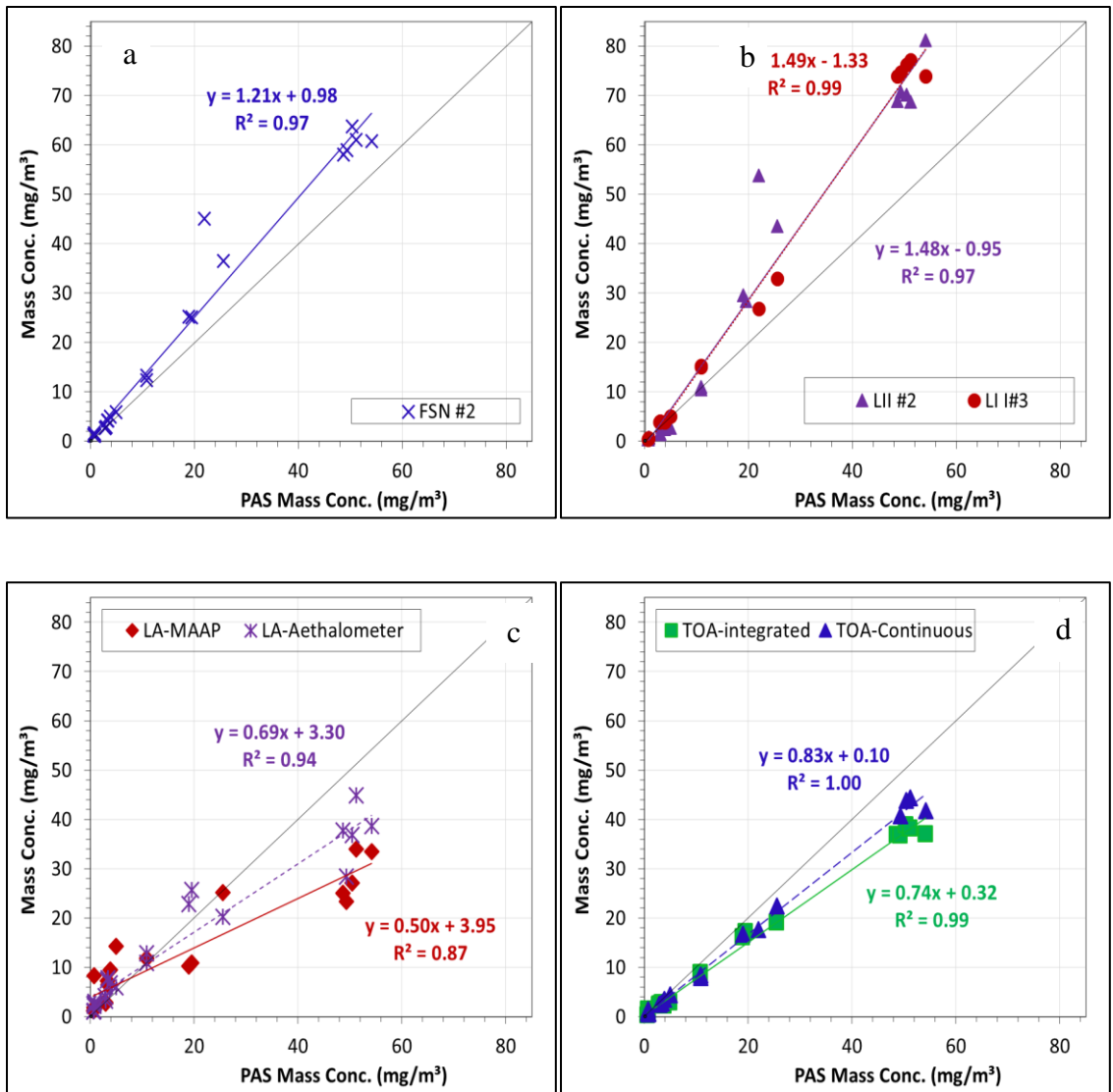


Figure 6-3 Instrument Response as a Function of PAS Mass Concentration for the SC Measurements

Although a better agreement of different instruments was expected after using the SC (Knox et al., 2009; Kondo et al., 2009), both the LA-MAAP and the LA-Aethalometer under the SC modes measured even lower BC mass concentrations relative to the PAS than measured for the without SC modes. Filter-based light absorption methods have uncertainties in measured values due to light scattering particles and filter fibers. The LA-

MAAP is designed with multiple wavelengths to measure both absorption and scattering light, in order to reduce interference from light scattering on the fibrous filters (Petzold and Schönlinner, 2004). Some studies have reported the lower LA-MAAP readings compared with other BC instruments (Hyvarien et al.; Aakko-Saksa et al., 2016; Jiang et al., In Press). With the LA-MAAP instrument the measured slope was 0.50 after the SC and 0.57 without SC. While values trended in the same direction, the difference is only about 12%. One potential explanation for the bigger differences between the LA-MAAP and PAS in the SC mode is associated with the changing of the morphology of BC aggregates when using SC. The BC aggregates looked denser and more spherical for the without SC mode, as shown in Figure 4, which could result in larger scattering signals compared with the SC mode (Kanaya et al., 2008; 2013). The increased scattering signals reduced the absorption signals and caused even lower readings for the LA-MAAP. Similar to the LA-MAAP, the LA-Aetholameter underestimated BC mass concentrations relative to the PAS with a slope of 0.69. The change in the morphology of BC particles may also account for the lower readings of the LA-Aetholameter. Similar to the without SC results, larger intercepts of the regressions were observed for these two ambient measurements in Figure 3c, which may be caused by multiplying slight offset in the zero readings by large dilution factors (1400:1) (Jiang et al., 2018; Aakko-Saksa et al., 2016).

The slope values of 1.48 for the two LIIs observed in this study were higher than the value of 1.25 for the without SC mode (Jiang et al., 2018). The LII is an instrument where the response is independent to the non-refractory coatings of BC particles (Moteki and Kondo, 2007; Slowik et al. 2007). This is because the LII operates at high temperature

and the non-refractory coatings are expected to evaporate during the heating up process (Slowik et al., 2007). The LII mass concentrations for the SC mode were found to be 10% to 24% lower than those for the without SC mode under the same load points in this study, the particle loss calculations suggests this 10% to 24% reduction is probably due to the particle losses through the SC rather than the elimination of the coatings. The organic coatings did contribute to 30% or higher amplified measurements for the PAS for particles with thicker coatings in a previous study (Shiraiwa et al., 2010; Lack et al., 2009). Therefore, the greater differences between the LIIs and PAS may instead be due to a reduction in the PAS enhancement in the SC mode.

The TOA-Integrated had a slope of 0.74 with the R^2 value of 0.99, indicating lower BC concentrations readings than but good correlations with the PAS. Compared with without SC mode, a closer to 1 slope and a higher R^2 value were found from the SC mode, suggesting that a better agreement could be expected between the two instruments after removing the coatings. This is consistent with studies showing the signals of the photoacoustic methods are affected by the coatings (Lack and Cappa, 2010; Bond et al., 2013; Shiraiwa et al., 2010). The TOA-Continuous was found to have the best correlation with the PAS, with a slope of 0.83, which was slightly lower but similar to the slope of 0.89 measured for the without SC mode. The slightly lower slope could be due to the BC particle losses caused by the denuder for the TOA-Continuous in the SC mode. The denuder has a fairly large capacity to provide enough residence time for small particles to diffuse, which may cause particle losses (Giechaskiel et al., 2014).

6.4.5. BC Morphology

Electron microscopy images scanned by TEM are provided in Figure 6-4. The diameters of aggregates for marine fuels in this study were on the order of 50-100 nm, which is much larger than BC particles typically found in ambient air (Li et al., 2003; Bond et al., 2013).

BC particles, based on Bond et al. (2013), are aggregates of spherules that form chain-like structures, as shown in Figure 4. The BC particles for many of the test cases look like aggregates of spherules that are opened and connected in long chains. This includes BC aggregates for both the DMA and RMB-30 fuels collected with and without conditioning, except for the 25% load point for RMB-30. The morphology of the RMG-380 particles were different, being more spherical aggregates at both the 25% and 75% load points for the unconditioned case. At the 75% load point with SC, however, the conditioned particles for the RMG-380 fuel exhibit long chains of spherules, more similar to those observed for the low sulfur fuels. This results indicate that the SC system removes the organic vapors before they have a chance to condense on the aggregates and impact their shape. The morphology of BC at the 25% load point with conditioning for the RMG-380 fuel was more similar to those under the without SC mode, however, with a denser collapsed sphere, but without the coatings that were eliminated by the SC.

The pictures for the without SC mode show some more densely aggregated and darker in color structures compared with the SC mode pictures (e.g., the DMA 75% without SC mode, the RMB-30 75% without SC mode and the RMG-380 75% without SC mode). This is because BC particles tend to collapse into denser clusters when water and organic

vapor condense on them, especially after aging in the atmosphere (Weingartner et al., 1997; Shiraiwa et al., 2007; Bond et al., 2013). For the RMG-380 fuel, the BC particles without conditioning are surrounded by coatings and collapse into denser sphere-like configurations, where it is difficult to distinguish the individual spherules due to the coating.

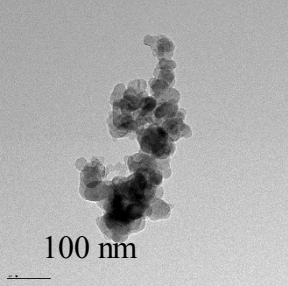
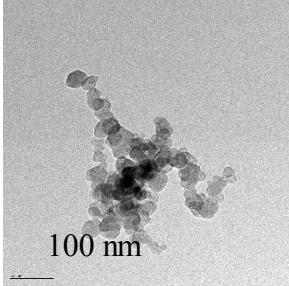
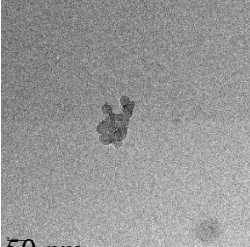
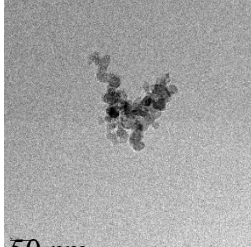
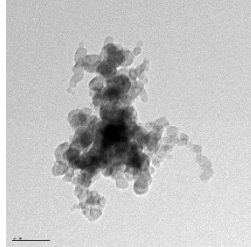
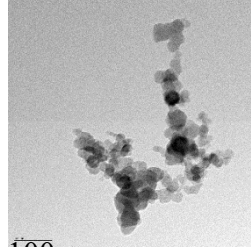
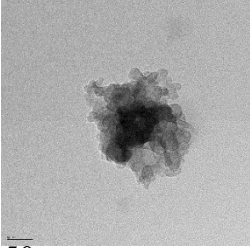
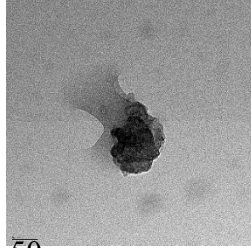
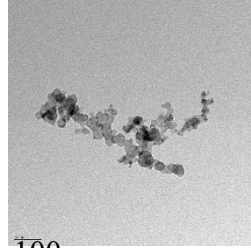
DMA 75% without SC mode		DMA 75% SC mode	
			
RMB-30 25% without SC mode	RMB-30 25% SC mode	RMB-30 75% without SC mode	RMB-30 75% SC mode
			
RMG-380 25% without SC mode	RMG-380 25% SC mode	RMG-380 75% without SC mode	RMG-380 75% SC mode
			

Figure 6-4 Effect of SC on BC Particles

6.4.6. Particle Size Distributions

Particle size distributions (PSDs) measured by a TSI SMPS are provided in Figure 6-5 for the SC mode measurements. The PSDs showed different trends between the 25% load and the 75% load for the three tested fuels, and are discussed separately. For the 75% load point, the PSDs for all three fuels included accumulation mode particles with peak diameters around 90 nm to 110 nm. This is consistent with the more open structure of the aggregates seen in the TEM pictures, and the more solid /EC nature of the particles at the 75% load, as seen in Figure 4. The PSDs for the RMG-380 fuel at the 75% load also showed a peak for nucleation mode particles with diameters around 20 nm to 50 nm.

For the 25% load point for the SC measurements, PSDs showed peaks with smaller diameters. This is consistent with the smaller particles seen in the TEM pictures for the 25% load with SC conditions. The PSD for the DMA fuel was a bimodal, with one higher peak at 10 nm to 20 nm and another wider but smaller peak at 50 nm to 90 nm. This suggests the PSDs are predominantly composed of nuclei mode solid particles. The PSDs for the RMB-30 fuel were dominated by small solid particles with peak particle diameters ranging from 30 nm to 50 nm. For the RMG-380 fuel, only one peak was observed with a diameter around 20 nm - 50 nm, which was consistent with the observations of denser spheres with diameters around 30 nm in Figure 6.

Comparing PSD data for the with and without SC modes shows the peaks were reduced on the order of 10^6 to 10^5 by the SC at the 25% load, which is consistent with the up to 94% OC removal efficiency and 98% sulfate removal efficiency for the SC. For the 75% load, the reductions in the peaks were on the order of 5×10^4 , which was much less

than those for the 25% load. The reason is the particles at the 75% load point are composed more of elemental carbon rather than organic carbon. Thus more particles penetrate the SC system at 75% load as compared with the OC-rich particles generated at 25% load.

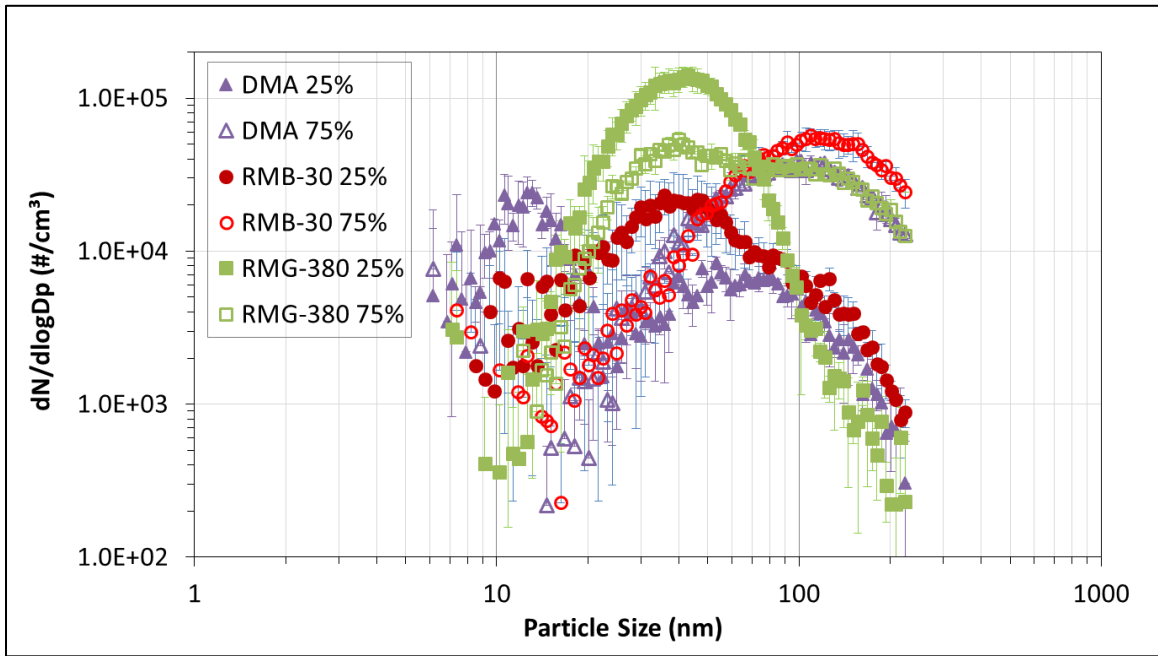


Figure 6-5 Particle Size Distributions from SMPS for the SC Mode

6.5. Conclusion

This study focused on the impacts of SC, as well as fuel types on BC measurement methods from a high-speed, 2-stroke marine engine operated at two load points and with three marine fuels. A wide range of PM/BC measurement techniques were used in this study. Overall, the BC emission rates based on the measured results from the PAS in the SC mode varied from 0.03 g/kg fuel to 1.36 g/ kg fuel. The CS provided over 91% sulfate removal for the high sulfur fuel, and 74 to 95% removal efficiencies of OC for all three fuels. With these reductions, the PM mass after the CS was composed predominantly of EC. The regression analyses were similar to those for the without CS mode, with half of

the instruments showing higher readings than PAS (i.e., the LII and FSN) and half showing lower readings (i.e., the TOA, LA-MAAP, and LA-Aetholameter), but generally showed a slightly greater spread than without CS mode results. The morphology of the particles for the lower sulfur marine fuels for the SC mode showed less densely aggregated, more chain-like structures that appeared to be lighter in color compared to the without SC mode. A key finding in this research is that the SC improved the comparability of some BC measurements, but only slightly.

6.6. Acknowledgements

The authors thank the following organizations and individuals for their valuable contributions to this project. We acknowledge funding from the International Council on Clean Transportation. Yue Lin was funded by NSF grant #1233038. We acknowledge the participation of Dr. Gavin McMeeking from Handix Scientific, LLC, and Dr. John Koupal from Eastern Research Group in this program. We acknowledge Dr. Roya Bahreini, Mr. Don Pacocha, Mr. Eddie O'Neal, Mr. Mark Villela, Dr. Lindsay Hatch, Mr. Justin Hernandez Dingle, Mr. Daniel Gomez and Ms. Lauren Aycock of the University of California, Riverside and Mr. David Buote from Environment and Climate Change Canada for their contributions in conducting the emissions testing for this program. We acknowledge AVL for providing the Smoke Meter, the South Coast Air Quality Management District for providing the Aethalometer, and the California Air Resources Board for providing the EEPS.

6.7. References

- Aakko-Saksa, P., Murtonen, T., Vesala, H., Koponen, P., Nyssönen, S., Puustinen, H., Lehtoranta, K., Timonen, H., Teinilä, K., Hillamo, R., Karjalainen, P., Kuittinen, N., Simonen, P., Rönkkö, T., Keskinen, J., Saukko, E., Tutuianu, M., Fischerleitner, R., Pirjola, L., Brunila, O., and Hämäläinen, E. Black carbon measurements using different marine fuels. Conference paper at the 28th CIMAC World Congress on Combustion Engines, CIMAC Congress 2016a, Helsinki, Finland, Paper No. 68.
- Agrawal, H., Malloy, Q.G., Welch, W.A., Miller, J.W., and Cocker, D.R., 2008. In-use gaseous and particulate matter emissions from a modern ocean going container vessel. *Atmospheric Environment*. 42(21), 5504-5510.
- Andreae, M.O., and Gelencsér, A., 2006. Black carbon or brown carbon? The nature of light-absorbing carbonaceous aerosols. *Atmos. Chem. Phys.* 6(10), 3131-3148.
- Background information on black carbon emissions from large marine and stationary diesel engines-definition, measurement methods, emission factors and abatement technologies, International Council on Combustion Engines (CIMAC): Main, Germany, 2012, http://www.cimac.com/cms/upload/workinggroups/WG5/black_carbon.pdf (access 16.12.15)
- Barnard, J. C., Volkamer, R., and Kassianov, E. I., 2008. Estimation of the Mass Absorption Cross Section of the Organic Carbon Component of Aerosols in the Mexico City Metropolitan Area. *Atmos. Chem. Phys.* 8(22), 6665-6679.
- Bond, T.C., Anderson, T.L., and Campbell, D., 1999. Calibration and intercomparison of filter-based measurements of visible light absorption by aerosols. *Aerosol Sci. Technol.* 30(6), 582-600.
- Bond, T.C., Doherty, S.J., Fahey, D.W., Forster, P.M., Berntsen, T., DeAngelo, B.J., Flanner, M.G., Ghan, S., Kärcher, B., Koch, D., and Kinne, S., 2013. Bounding the role of black carbon in the climate system: A scientific assessment. *J. Geophys. Res.* 118, 5380-5552.
- Buffaloe, G.M., Lack, D.A., Williams, E.J., Coffman, D., Hayden, K.L., Lerner, B.M., Li, S.M., Nuaaman, I., Massoli, P., Onasch, T.B., and Quinn, P.K., 2014. Black carbon emissions from in-use ships: a California regional assessment. *Atmos. Chem. Phys.* 14, 1881-1896.
- Corbett, J.J., Winebrake, J.J., and Green, E.H., 2010. An assessment of technologies for reducing regional short-lived climate forcers emitted by ships with implications for Arctic shipping. *Carbon Manage.* 1, 207-225.

- Fuller, K.A., Malm, W.C., and Kreidenweis, S.M., 1999. Effects of mixing on extinction by carbonaceous particles. *J. Geophys. Res.* 104(15), 941-954.
- Giechaskiel, B., Maricq, M., Ntziachristos, L., Dardiotis, C., Wang, X., Axmann, H., Bergmann, A., and Schindler, W., 2014. Review of motor vehicle particulate emissions sampling and measurement: From smoke and filter mass to particle number. *J. of Aerosol Sci.* 67, 48-86.
- Highwood, E.J., and Kinnersley, R.P., 2006. When smoke gets in our eyes: The multiple impacts of atmospheric black carbon on climate, air quality and health. *Environ. Int.* 32(4), 560-566.
- Hyvärinen, A.P., Vakkari, V., Laakso, L., Hooda, R.K., Sharma, V.P., Panwar, T.S., Beukes, J.P., Van Zyl, P.G., Josipovic, M., Garland, R.M., and Andreae, M.O., 2013. Correction for a measurement artifact of the Multi-Angle Absorption Photometer (MAAP) at high black carbon mass concentration levels. *Atmos. Meas. Tech.* 6(1), 81-90.
- International Maritime Organization (IMO) Website, [http://www.imo.org/en/OurWork/environment/pollutionprevention/airpollution/pages/sulphur-oxides-\(sox\)---regulation-14.aspx](http://www.imo.org/en/OurWork/environment/pollutionprevention/airpollution/pages/sulphur-oxides-(sox)---regulation-14.aspx) (access 17.05.10).
- Janssen, N.A., Hoek, G., Simic-Lawson, M., Fischer, P., Van Bree, L., Ten Brink, H., Keuken, M., Atkinson, R.W., Anderson, H.R. Brunekreef, B., and Cassee, F.R., 2012. Black Carbon as an Additional Indicator of the Adverse Health Effects of Airborne Particles Compared with PM10 PM 2.5. *Environ. Health Perspect.* 119, 1691-1699.
- Jansen, K.L., Larson, T.V., Koenig, J.Q., Mar, T.F., Fields, C., Stewart, J., and Lippmann, M., 2005. Associations between health effects and particulate matter and black carbon in subjects with respiratory disease. *Environ. Health Perspect.* 113(12), 1741-1746.
- Jiang, Y., Yang, J., Gagné, S., Chan, T.W., Thomson, K., Fofie, E., Cary, R.A., Rutherford, D., Comer, B., Swanson, J. and Lin, Y., 2018. Sources of variance in BC mass measurements from a small marine engine: Influence of the instruments, fuels and loads. *Atmospheric Environment*, 182,128-137.
- Johnson, K.C., Durbin, T.D., Jung, H., Cocker III, D.R., Bishnu, D., and Giannelli, R., 2011. Quantifying in-use PM measurements for heavy duty diesel vehicles. *Environ. Sci. Technol.* 45(14), 6073-6079.
- Kanaya, Y., Komazaki, Y., Pochanart, P., Liu, Y., Akimoto, H., Gao, J., Wang, T., and Wang, Z., 2008. Mass concentrations of black carbon measured by four instruments in the middle of Central East China in June 2006. *Atmos. Chem. Phys.* 8(24), 7637-7649.

- Kanaya, Y., Taketani, F., Komazaki, Y., Liu, X., Kondo, Y., Sahu, L.K., Irie, H., and Takashima, H., 2013. Comparison of black carbon mass concentrations observed by multi-angle absorption photometer (MAAP) and continuous soot-monitoring system (COSMOS) on Fukue Island and in Tokyo, Japan. *Aerosol Sci. Technol.* 47(1), 1-10.
- Khan, M.Y., Giordano, M., Gutierrez, J., Welch, W.A., Asa-Awuku, A., Miller, J.W., and Cocker III, D.R., 2012. Benefits of two mitigation strategies for container vessels: cleaner engines and cleaner fuels. *Environ. Sci. Technol.* 46, 5049-5056.
- Knox, A., Evans, G.J., Brook, J.R., Yao, X., Jeong, C.H., Godri, K.J., Sabaliauskas, K., and Slowik, J.G., 2009. Mass absorption cross-section of ambient black carbon aerosol in relation to chemical age. *Aerosol Sci. Technol.* 43(6), 522-532.
- Kondo, Y., Sahu, L., Kuwata, M., Miyazaki, Y., Takegawa, N., Moteki, N., Imaru, J., Han, S., Nakayama, T., Oanh, N.K., and Hu, M., 2009. Stabilization of the mass absorption cross section of black carbon for filter-based absorption photometry by the use of a heated inlet. *Aerosol Sci. Technol.* 43(8), 741-756.
- Lack, D.A., Cappa, C.D., Cross, E.S., Massoli, P., Ahern, A.T., Davidovits, P., and Onasch, T.B., 2009. Absorption enhancement of coated absorbing aerosols: Validation of the photo-acoustic technique for measuring the enhancement. *Aerosol Sci. Technol.* 43(10), 1006-1012.
- Lack, D.A., and Cappa, C.D., 2010. Impact of brown and clear carbon on light absorption enhancement, single scatter albedo and absorption wavelength dependence of black carbon. *Atmos. Chem. Phys.* 10(9), 4207-4220.
- Lack, D.A., Cappa, C.D., Langridge, J., Bahreini, R., Buffaloe, G., Brock, C., Cerully, K., Coffman, D., Hayden, K., Holloway, J., and Lerner, B., 2011. Impact of fuel quality regulation and speed reductions on shipping emissions: implications for climate and air quality. *Environ. Sci. Technol.* 45(20), 9052-9060
- Lack, D.A., and Corbett, J.J., 2012. Black carbon from ships: a review of the effects of ship speed, fuel quality and exhaust gas scrubbing. *Atmos. Chem. Phys.* 12(9), 3985-4000.
- Lack, D. BC Measurement Overview, and Considerations for a Community Approach to Measurement. Presented at the 2nd Workshop on Marine Black Carbon Emissions. Utrecht, Netherlands, September, 2015.
- Li, J., Pósfai, M., Hobbs, P.V., and Buseck, P.R., 2003. Individual aerosol particles from biomass burning in southern Africa: 2, Compositions and aging of inorganic particles. *J. Geophys. Res.: Atmos.* 108(D13).

- Mamakos, A., Khalek, I., Giannelli, R., and Spears, M., 2013. Characterization of combustion aerosol produced by a Mini-CAST and treated in a catalytic stripper. *Aerosol Sci. Technol.* 47(8), 927-936.
- Moteki, N., and Kondo, Y., 2007. Effects of mixing state on black carbon measurements by laser-induced incandescence. *Aerosol Sci. Technol.* 41(4), 398-417.
- Mulholland, G.W., Henzel, V., and Babrauskas, V., 1989. The Effect of Scale on Smoke Emission. *Fire Safety Science.* (2), 347-357.
- Petzold, A., and Schönlinner, M., 2004. Multi-angle absorption photometry—a new method for the measurement of aerosol light absorption and atmospheric black carbon. *J. of Aerosol Sci.* 35(4), 421-441.
- Petzold, A., Ogren, J. A., Fiebig, M., Laj, P., Li, S. M., Baltensperger, U., Holzer-Popp, T., Kinne, S., Pappalardo, G., Sugimoto, N., and Wehrli, C., 2013. Recommendations for reporting "black carbon" measurements. *Atmos. Chem. Phys.* 13, 8365-8379
- SAE Aerospace Recommended Practice 1179 Rev D, Aircraft Gas Turbine Engine Exhaust Smoke Measurement, SAE International, Warrendale, PA, USA, 2011, <https://saemobilus.sae.org/content/arp1179>.
- SAE Aerospace Information Report 6241, Procedure for the Continuous Sampling and Measurement of Non-Volatile Particle Emissions from Aircraft Turbine Engines, SAE International: Warrendale, PA, USA, 2013, <https://saemobilus.sae.org/content/air6241>.
- Schwarz, J.P., Spackman, J.R., Fahey, D.W., Gao, R.S., Lohmann, U., Stier, P., Watts, L.A., Thomson, D.S., Lack, D.A., Pfister, L., and Mahoney, M.J., 2008. Coatings and their enhancement of black carbon light absorption in the tropical atmosphere. *J. Geophys. Res.: Atmos.* 113(D3).
- Sippula, O., Stengel, B., Sklorz, M., Streibel, T., Rabe, R., Orasche, J., Lintelmann, J., Michalke, B., Abbaszade, G., Radischat, C., and Groger, T., 2014. Particle emissions from a marine engine: chemical composition and aromatic emission profiles under Andreae arious operating conditions. *Environ. Sci. Technol.* 48, 11721-11729.
- Shah, S. D., Cocker, D. R., III, Miller, J. W., and Norbeck, J. M., 2004. Emission Rates of Particulate Matter and Elemental and Organic Carbon from In-Use Diesel Engines. *Environ. Sci. Technol.* 38(9), 2544-2550.
- Shiraiwa, M., Kondo, Y., Moteki, N., Takegawa, N., Miyazaki, Y., and Blake, D.R., 2007. Evolution of mixing state of black carbon in polluted air from Tokyo. *Geophys. Res. Lett.* 34(16).

- Shiraiwa, M., Kondo, Y., Iwamoto, T., and Kita, K., 2010. Amplification of light absorption of black carbon by organic coating. *Aerosol Sci. Technol.* 44(1), 46-54.
- Slowik, J.G., Cross, E.S., Han, J.H., Davidovits, P., Onasch, T.B., Jayne, J.T., Williams, L.R., Canagaratna, M.R., Worsnop, D.R., Chakrabarty, R.K., and Moosmüller, H., 2007. An inter-comparison of instruments measuring black carbon content of soot particles. *Aerosol Sci. Technol.* 41(3), 295-314.
- Snelling, D.R., Smallwood, G.J., Liu, F., Gülder, Ö.L. Bachalo, W.D., 2005. A calibration-independent laser-induced incandescence technique for soot measurement by detecting absolute light intensity. *Appl. Opt.* 44(31), 6773-6785.
- Swanson, J., and Kittelson, D. B., 2010. Evaluation of thermal denuder and catalytic stripper methods for solid particle measurements. *J. of Aerosol Sci.* 41(12), 1113–1122.
- Swanson, J., Kittelson, D., Giechaskiel, B., and Bergmann, A., 2013. A Miniature Catalytic Stripper for Particles Less Than 23 Nanometers. *SAE Int. J. Fuels Lubr.* 6(2013-01-1570), 542-551.
- Winebrake, J.J., Corbett, J.J., Green, E.H., Lauer, A., and Eyring, V., 2009. Mitigating the health impacts of pollution from oceangoing shipping: an assessment of low-sulfur fuel mandates. *Environ. Sci. Technol.* 43(13), 4776-4782.

6.8. Supporting Information

Test engine. The test engine is a 2-stroke Detroit Diesel Model 6-71N (naturally aspirated), with an in-line 6 cylinder configuration (7 liters per cylinder), a maximum rated speed of 2300 RPM (range 1100-2300 RPM), a maximum engine power of 187 kW, a brake mean effective pressure (BMEP) of 641 kPa, and an associated rated brake specific fuel consumption (BSFC) of 307 g/kWh (0.505 lb/hp-hr) at 1100 RPM (N70 injectors used during testing). This type of engine is typically used on small vessels or as an auxiliary engine on ocean going vessels (OGVs). OGVs usually switch to auxiliary engines when approaching port or other areas where more maneuvering is required, making the selected test engine relevant for areas where emissions are most often scrutinized. Appendix G provides a more details on the engine used for testing.

Test fuel.

Table S1: Selected Fuel Properties of Three Marine Fuels

Fuel	DMA	RMB-30	RMG-380
Sulfur wt% (ppm)	13	13.2	31,849
Density @ 15°C (kg/L)	0.8309	0.8586	0.9826
Viscosity @ 40°C (cSt)	2.696	-	-
Viscosity @ 50°C (cSt)		13.73	358.9
Micro Carbon Residue (%m/m)	< 0.1	< 0.1	12.84

Instruments. The H-TDMA uses two DMAs. The first DMA, DMA1, works at a constant voltage to extract a monodisperse size cut of the dry aerosol particle distribution from the dilution tunnel at 1400:1. For this study, the particle size selected using DMA1 was 81.3 nm, which is representative of the accumulation particles observed in this study.

The nondispersive particles from DMA1 were put through a stainless steel humidifier chamber, where water was injected to provide a range of higher of relative humidity (RH) levels. Following the humidifier, a second DMA, DMA2, was used to measure the change in particle size characteristics as a function of different humidity levels.

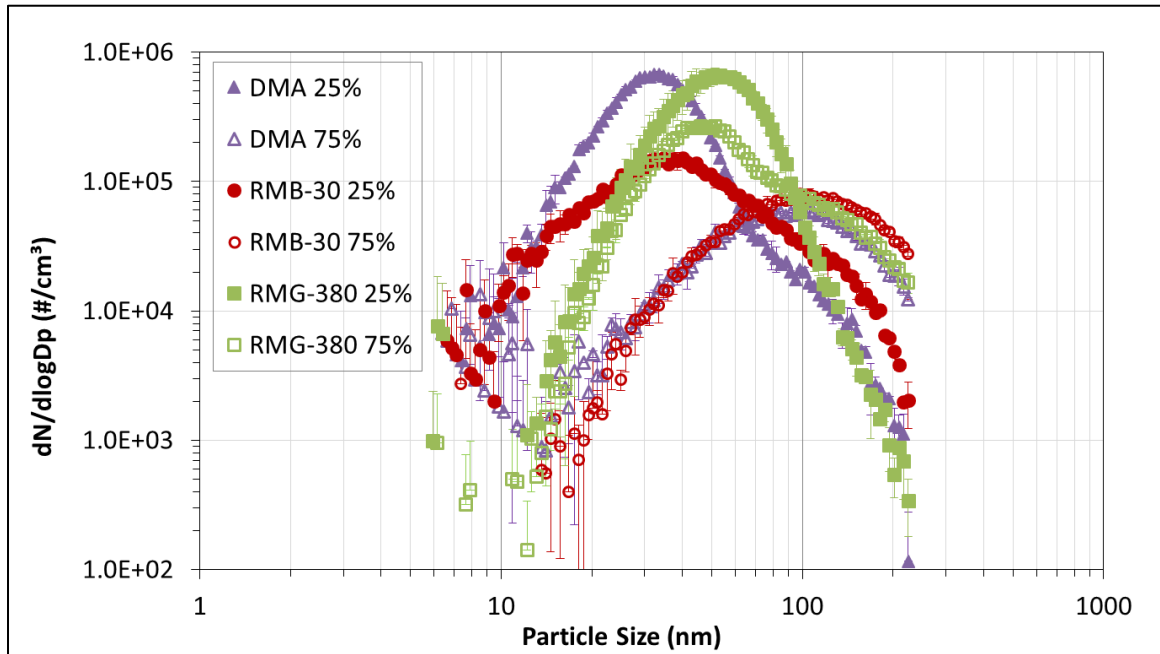
BC emission factors (g/kg fuel).

Table S2: Summary of BC Emission Factors without SC

Fuel	Load (%)	On Stack		Group DF 1:1		Group DF 14:1
		FSN line 1	LII #1	FSN line 2	LII #2	PAS
DMA	25	0.12 ± 0.00	0.07 ± 0.00	0.11 ± 0.00	0.06 ± 0.00	0.09 ± 0.00
	75	1.01 ± 0.01	0.50 ± 0.01	0.96 ± 0.02	1.01 ± 0.01	0.84 ± 0.04
RMB-30	25	0.27 ± 0.00	N/A ± N/A	0.25 ± 0.00	0.10 ± 0.00	0.26 ± 0.01
	75	2.22 ± 0.05	N/A ± N/A	2.34 ± 0.04	2.31 ± 0.05	1.84 ± 0.07
RMG-380	25	0.12 ± 0.01	N/A ± N/A	0.10 ± 0.01	0.02 ± 0.00	0.05 ± 0.01
	75	1.60 ± 0.68	N/A ± N/A	1.51 ± 0.61	1.26 ± 0.52	1.04 ± 0.63
Fuel	Load (%)	Group DF 14:1			Group DF 1400:1	
		TOA-Integrated	TOA-Continuous	LII #3	LA-MAAP	LA-Aethalometer
DMA	25	0.07 ± 0.00	0.08 ± 0.00	N/A ± N/A	0.24 ± 0.01	0.29 ± 0.05
	75	0.64 ± 0.04	0.77 ± N/A	N/A ± N/A	0.54 ± 0.01	1.14 ± 0.04
RMB-30	25	0.20 ± 0.01	0.21 ± 0.00	0.23 ± 0.01	0.40 ± 0.01	0.31 ± 0.03
	75	1.14 ± 0.04	1.65 ± 0.04	2.51 ± 0.06	1.17 ± 0.08	1.73 ± 0.24
RMG-380	25	0.04 ± 0.01	0.03 ± N/A	0.02 ± N/A	0.22 ± N/A	0.14 ± 0.05
	75	0.76 ± 0.43	0.87 ± 0.60	1.11 ± 0.77	0.88 ± N/A	1.05 ± 0.17

Particle size distributions.

Figure S3: Particle Size Distribution from SMPS as a Function of Engine Load Percent for the without SC Mode



7. Conclusions

The main objective of the chapters two to four in this research was to characterize emissions rates of 2010-compliant heavy-duty diesel vehicles (HDDVs) equipped with diesel particulate filters (DPFs) and selective catalytic reduction (SCR) systems. The first phase of this research evaluated emissions rates of five 2012+ model year HDDVs. This phase was critical, as the results showed that the NO_x emission rates of urban driving cycles tested using a chassis dynamometer were higher than the typical certification values based on engine dynamometer testing. The second phase of the research tested two 2010-compliant HDDVs using an engine-dynamometer, a chassis-dynamometer, and on-road testing in order to understand the differences between certification and in-use NO_x emission rates, as well as the factors contributing to these differences and discrepancies. The last phase of this research focused on the development of an Inspection and Maintenance (I/M) program for on-road HDDVs to ensure that the in-use fleet of 2010-compliant HDDVs does not significantly deteriorate over the lifetime of the vehicle. The main objective of chapters five and six in this research was to evaluate the influence of different instrument methods, fuels, loads, and sample conditioning (SC) on black carbon (BC) mass measurements from a small marine engine.

For chapter two, five HDDVs equipped with DPFs for PM emissions control and SCR systems for NO_x emissions control were tested. The vehicles ranged in model year from 2012 to 2015, and were certified to a 0.20 g/bhp-hr NO_x emissions standard, with the

exception of one engine that was certified to a 0.35 g/bhp-hr standard. Each vehicle was tested on UCR's heavy-duty chassis dynamometer over the four phases of CARB's Heavy Heavy-Duty Diesel Truck (HHDDT) cycles, the HHDDT-S cycle, and the UDDS. The key finding from this study was that in-use NO_x emissions can vary significantly depending on the driving cycles and from vehicle to vehicle. The zero mile emission rates (ZMRs) for NO_x ranged from 0.495 to 1.363 g/mi (0.136 to 0.387 g/bhp-hr) for four of the vehicles tested with an average of 0.89 g/mi. These ZMRs were most representative for these low mileage, well maintained heavy-duty vehicles. The ZMRs for heavy-duty vehicles for EMFAC are currently higher at 3.03 g/mi since they incorporate a wider range of vehicles than in the current study with higher mileages, potentially different levels of deterioration, and SCR systems with functionality issues.

Chapter three evaluated two 2010-compliant HDDV engines equipped with DPF and SCR technologies using an engine-dynamometer, a chassis-dynamometer, and on-road testing. The key finding from this study was that in-use NO_x emissions over urban driving cycles for chassis dynamometer, on-road, and engine dynamometer tests were above the 0.2 g/bhp-hr level for both vehicles, with the highest emissions for the chassis dynamometer testing. The NO_x emissions ranged from 0.16 to 1.1 g/bhp-hr over all of the urban test conditions for both vehicles. The results for the freeway/steady state tests were generally lower than those for the urban cycles. For the UDDS, the differences between the tailpipe NO_x emissions could be attributed to several factors, including differences in SCR inlet NO_x temperatures and engine out NO_x emissions. The cycle average SCR efficiencies for both vehicles ranged from 68 to 98%. For inlet SCR temperatures higher

than 250°C, the SCR conversion efficiencies remained consistently high (>80%). At temperatures below 250°C, the SCR efficiencies were generally lower, although this varied from cycle to cycle for both vehicles. For the on-road testing, the results from the Not to Exceed (NTE) analysis showed that the passing rate can vary significantly depending on the tested manufacturers and route selected. The current NTE method has a limitation that it represents only a small percent of real-world operation. The analysis using the Moving Averaging Window (MAW) method incorporated a much greater fraction of in-use operation. The emissions were found to fail the MAW test for a majority of the routes for both vehicles.

Chapter four focused on a heavy-duty (HD) on-road vehicles I/M study. A pilot study was conducted to evaluate methods of emissions measurement that might be used in an I/M program and the potential emissions benefits of I/M repairs. The exploratory pilot program consisted of testing 47 vehicles before and after repair on a chassis dynamometer. The testing included I/M grade emissions analyzers and on-board diagnostics (OBD). The key finding was that vehicles showed good reductions post-repair for NO_x for some of the higher emitting vehicles, but not significant PM reductions. Based on a review of the methods, OBD was selected as the primary methodology of HD I/M, coupled with roadside monitoring with a remote sensing device (RSD). A Mini-PEMS could potentially also be incorporated into a HD I/M program as a verification of the pass/fail determinations.

Chapters five and six investigated the impacts of measurement methods, fuel type, engine load, and sampling condition (SC) on BC emission factors from a high-speed, 2-stroke, small marine engine operated at two load points with three marine fuels. Six BC

analytical methods with different measurement principles were used. A key finding in this research was that variations in BC measurement methods were on the order of a factor of two, and cannot account for the ten-fold range of BC emission factors reported in the literature. The SC improved the comparability of some BC measurements, but only slightly. As such, other factors, such as engine load, selected fuel properties, and engine characteristics, likely contribute to the large variations in BC emission factors in literature studies. Load, in particular, had an important impact for this older, small, high-speed engine, with increases in BC emissions by greater than a factor of 10 in going from 25% to 75% loads. The observation of large differences in BC emission factors as a function of load has also been seen in a wider range of studies in the literature, albeit showing trends of higher emissions at lower loads, opposite to the trends seen for the engine used in this study. While BC emissions were impacted by the fuels used, none of the fuel properties investigated (sulfur content, viscosity, carbon residue and CCAI) was a primary driver for BC emissions. Of the two residual fuels, RMB-30 with the lower sulfur content, lower viscosity and lower residual carbon, had the highest BC emission factors.